An investigation into the role of intercellular adhesion molecule-2 in neutrophil extravasation using an *in vivo* murine model

Krishma Halai

For the degree of

Doctor of Philosophy

Registered at

Barts & The London School of Medicine and Dentistry

Queen Mary, University of London

Centre for Microvascular Research
William Harvey Research Institute
John Vane Science Centre
Charterhouse Square,
London EC1M 6BQ

Acknowledgements

I would firstly like to express gratitude to my supervisors Professor Sussan Nourshargh and Dr Abigail Woodfin for the opportunity to undertake this project at the Centre for Microvascular Research based at the William Harvey Research Institute. This thesis would not have been possible without their patience, support and guidance which I am truly grateful for. I acknowledge the British Heart Foundation (BHF) for providing funds to support this project.

I thank Dr Mathieu Benoit Voisin for his insightful knowledge surrounding key techniques used during the course of the study, Dr Martina Bauer for her expertise in flow cytometry, Dr Natalie McCloskey Mic Res. lab manager and Arif Mustafa BSU technician. I am also very grateful for the support of all my colleagues (past and present) at the Centre for Microvascular Research for their constructive input during various centre meetings. I express my thanks to Michaela Finsterbusch and Shimona Madalli who have not just been colleagues but also great friends who I have shared my journey with. I would also like thank past and present students at William Harvey for creating a fun and pleasant place to work in and for all those strange but wonderful lunch conversations.

Special thanks goes to Krupa, Chandni and Jay who have always been there to listen, helped me to stay positive and unwind after some of those stressful weeks.

Most importantly there are no words to express the love, support and faith I have had from my Mum, Dad and sisters (Prity, Nisha and Mitisha-Tulsi) something that will never be forgotten and am externally grateful for. Last but not least, my little Yash and Tiana what would I have done without you both reminding me about the small but important things in life.

I would like to dedicate this thesis to my late Nana, Parbat Kurji Halaria (Sojitra) and late Baa, Sambai Arjan Halai – જય શ્રી સ્વામીનારાયણ

Abstract

Recruitment of neutrophils into the tissue during inflammation is a crucial component of the immune response. This study aimed to further understand the role of intercellular adhesion molecule-2 (ICAM-2) in this process. Endothelial cell (EC) ICAM-2 has been implicated in neutrophil extravasation however, its precise role in this process is largely unknown. To address this, the current investigation examined the expression and functional role of ICAM-2 in neutrophil-EC interactions *in vivo*.

Analysis of EC ICAM-2 expression was performed in the mouse cremaster muscle using immunofluorescent staining and confocal microscopy. A high EC body expression of ICAM-2 relative to that of EC junctions in post-capillary venules was observed. It was therefore hypothesised that ICAM-2 could potentially be involved in both luminal neutrophil-EC and junctional interactions. This hypothesis was analysed using confocal intravital microscopy (IVM) of cremaster muscles from WT or ICAM-2 KO Lys-eGFP-ki mice (express fluorescent neutrophils) in conjunction with fluorescent labelling of ECs. Neutrophil crawling and transendothelial migration (TEM) dynamics in IL-1β-stimulated post-capillary venules was analysed. A role for ICAM-2 in supporting speed and continuity of crawling and the initiation of TEM was demonstrated. Using functional blocking mAb to MAC-1 in WT and ICAM-2 KOs, the role of ICAM-2 in neutrophil crawling was demonstrated to be governed through a potential interaction with neutrophil MAC-1.

It is therefore possible that non-junctional EC ICAM-2 has important roles in regulating neutrophil polarisation during crawling whilst junctional ICAM-2 mediates the opening of EC junctions and/or influencing the site of 'preferred' TEM. This study provides the first *in vivo* evidence for the ability of ICAM-2 to support neutrophil crawling and the initiation of TEM in IL-1β-induced neutrophil extravasation.

To extend the above findings in a complex vascular injury model, a cremasteric Shwartzman Reaction, amenable to IVM analysis, was also developed as part of this project.

Table of contents

List of figures

Abbreviations

α-SMA	α-smooth muscle actin
Anova	Analysis of variance
APC	Antigen presenting cell
CAMs	Cell adhesion molecules
DC-SIGN	Dendritic cell–specific ICAM-3–grabbing nonintegrin
DNFB	2,4-dinitro-1-fluorobenzene
EAPs	Endothelial proadhesive platforms
EC	Endothelial cell
EGF	Epidermal growth factor
eGFP	Enhanced green fluorescent protein
Erg	Ets related peptide
ERM	Ezrin-Radaxi-Moesin
ESAM	Endothelial cell-selective adhesion molecule
ESL	E-selectin ligand
Ets	E26 transformation specific
F-actin	Filamentous actin
FAK	Focal adhesion kinase
FITC	Fluorescein isothiocyanate
FSC	Forward scatter

GAGs	Glucosaminoglycans
GlyCAM	Glycosylation-dependent cell adhesion molecule
HUVECs	Human umbilical vein endothelial cells
ICAM	Intercellular adhesion molecule
Ig	Immunoglobulin
IL	Interleukin
i.m.	Intramuscular
i.p.	Intraperitoneal
i.s.	Intrascrotal
i.v.	Intravenous
ITIMS	Immunoreceptor tyrosine based inhibitory motifs
IVM	Intravital microscopy
JAM	Junctional adhesion molecule
KO	Knockout
LBRC	Lateral Border recycling compartment
LER	Low expression region
LFA-1	Lymphocyte function-associated antigen-1
LPS	Lipopolysaccharide
LTB_4	Leukotriene B_4
Lys	Lysozyme

mAb	Monoclonal antibody
MAC-1	Macrophage receptor-1
MAdCAM-1	Mucosal addressin cell adhesion molecule
MCP-1	Monocyte chemoattractant protein-1 chemoattractants
MIP	Macrophage inflammatory protein
MRP14	Myeloid-related protein-14
NETS	Neutrophil extracellular traps
PAF	Platelet-activating factor
PBS	Phosphate buffered saline
PE	Phycoerythrin
PECAM-1	Platelet endothelial cell adhesion molecule-1
PFA	Paraformaldehyde
PIP2	Phosphatidylinositol-4, 5-bisphosphate
PI3K	Phosphoinositide 3-kinase
PSGL-1	P-selectin glycoprotein ligand-1
PRR	Pathogen recognition receptors
RANTES	Regulated and normal T cell expressed and secreted
Rho	Ras homology
RFI	Relative fluorescence intensity
ROS	Reactive oxygen species
SSC	Side scatter

SR	Shwartzman Reaction
TNF-α	Tumour necrosis factor-α
TEM	Transendothelial migration
TLRs	Toll-like receptors
VCAM-1	Vascular cell adhesion molecule-1
VE-cadherin	Vascular endothelial cadherin
VLA-4	Very late antigen-4
VOVs	Vesiculo-vacuolar organelles
WT	Wild type

Publications arising from this work

Halai K, Nourshargh S & Woodfin A. (2013) ICAM-2 facilitates neutrophil intravascular crawling dynamics and the initiation of transendothelial migration in vivo. Manuscript submitted to Journal of Cell Science.

Published abstracts

Halai K, Nourshargh S & Woodfin A. (2012) Intercellular adhesion molecule-2 supports neutrophil intraluminal crawling *in vivo*. 2012 workshops. European Journal of Clinical Investigation, 42: 12–88. doi: 10.1111/j.1365-2362.2012.02650.x

Presentations

Halai K, Nourshargh S & Woodfin A. Functional role of ICAM-2 in neutrophil extravasation *in vivo*.

Abstract selected for poster presentation at:

- London Vascular Biology Forum (London, 12th December 2012).
- William Harvey Day (London, 16th October 2012) -*First prize winner*.

Halai K, Nourshargh S & Woodfin A. Intercellular adhesion molecule-2 supports neutrophil intraluminal crawling *in vivo*.

Abstract selected for oral presentation at:

- William Harvey Research Institute Annual Review (London, 11th July 2012).
- UK Adhesion Society (Sheffield, 17th April 2012).
- 46th Annual Scientific Meeting of the European Society for Clinical Investigation (Budapest, 22nd-24th March 2012).

Halai K, Nourshargh S & Woodfin A. Expression and functional role of endothelial ICAM-2 in leukocyte transmigration.

Abstract selected for poster presentation at:

- London Vascular Biology Forum (London, 7th December 2011).
- William Harvey Day (London, 19th October 2011).

Statement of originality

The approach and experiments presented here are novel. The author has personally undertaken all the work described here, unless stated otherwise.

CHAPTER 1: General introduction

1.1 Inflammation

Inflammation is a physiological process crucial for the body's immune response to harmful stimuli, such as pathogens (e.g. viruses, bacteria, fungi or parasites), damaged cells or other irritants. It serves to eliminate the initial cause of tissue injury and remove necrotic cells and debris which have formed as a result. The host immune response is mediated by the innate and the adaptive systems. The innate system is the first line of defence and has a vital role in initiating subsequent adaptive immune response by distinguishing between self and harmful foreign material. The innate immune response consists of neutrophils and macrophages which have the ability to kill and engulf bacteria. The adapted immune response processes the pathogen through highly specialised T and B lymphocytes. This latter phase ultimately stimulates cell death and the development of memory to specific pathogens. Upon complete removal of the pathogen and the immune cells involved the inflammatory response comes to an end (Serhan et al., 2008). In some cases when this response becomes uncontrollable and/or is inappropriately triggered it can harm the host and develop into pathological inflammation. This uncontrolled immune response is an underlying cause and/or effect of numerous diseases such as vasculitis, atherosclerosis, arthritis, sepsis, ischemia-reperfusion injury and is also a component of cancers. Inflammation can therefore occur throughout the body and is exhibited in and/or is a cause of a wide range of different pathological conditions. The fundamental mechanisms of this response are however consistent in all inflammatory reactions and remain of immense interest to researchers seeking to unravel the associated mechanisms.

An inflammatory response is characterised by swelling/odema (*tumour*) caused by the increase in vascular permeability, vasodilatation and leukocyte migration, redness

(*rubor*) as a result of increased blow flow, pain (*dolor*) due to the increased sensitivity of neurones and release of neuropeptides in addition to the pressure exerted by edema, heat (*calor*) caused by the increase in blood flow and an increase in the metabolic rate and lastly can be associated with loss of function (*function laesa*). These effects are caused by the co-ordinated response of local inflammatory mediators on blood vessels, leukocytes and plasma components and the activation of several pathways including the complement system, coagulation, fibrinolysis, arachidonic acid pathway, kinin metabolism and the generation of free radicals.

1.1.1 Innate immunity

Upon initial encounter of foreign antigens the innate immune response primes or prepares the adaptive immune response. Neutrophils and classical monocytes (Geissmann et al., 2008) are the first cells to be recruited to the tissue. In humans they form the most abundant subsets of leukocytes in the blood circulation and hence are readily available to be activated and recruited. Tissue resident leukocytes such as macrophages differentiated from non-classical monocytes, and dendritic cells differentiated from classical monocytes exist at sites underlying the epithelial barrier (Geissmann et al., 2008) where they engulf pathogens and have the ability to generate inflammatory mediators such as cytokines, chemokines and chemoattractants which act to recruit other immune cells to the specific site of infection. Identification of the two monocytes subets is now well accepted and are defined by the different levels of surface protein they express, divergent differiation pathways and their fate (Geissmann et al., 2008).

Key cytokines involved in innate immunity include tumour necrosis factor-α (TNF-α) and interleukin-1β (IL-1β) which act predominately on leukocytes and endothelial cells (ECs) respectively. Chemokines such as CCL2/monocyte chemoattractant protein-1 (MCP-1) and CXCL8/interleukin 8 (IL-8) and lipid chemoattractants including leukotriene B_4 (LTB_4) and platelet-activating factor (PAF) are in general

thought to guide and attract leukocytes to specific sites of inflammation (Ley et al., 2007; Mantovani et al., 2011). These inflammatory mediators together with the changes that occur in the blood flow in turn upregulate and/or redistribute EC adhesion molecules e.g. E-selectin, intercellular adhesion molecule-1 (ICAM-1), junctional adhesion molecule-C (JAM-C) as well as activating various integrins that are expressed on leukocytes. Collectively, these events promote leukocyte adhesion to the vascular wall and initiate leukocyte extravasation into the tissue.

Once neutrophils are recruited to the site of inflammation they degranulate specific peptides such as lytic enzymes, potent anti-microbial and cytotoxic mediators. Reactive oxygen species (ROS) which are present in cytoplasmic granules also help kill the pathogen. In addition to this, neutrophils have the ability to produce various cytokines, chemokines and chemoattractants which stimulate the activation of ECs and the recruitment of more cells. Neutrophils interact with pathogens via pattern recognition receptors (PRRs). The PRRs (e.g. toll-like receptors (TLR) and formyl methionine peptide receptors) are expressed on the surface of neutrophils, monocytes and macrophages, component of the innate immune response that can engulf and kill pathogens (Figure 1.1) (Geissmann et al., 2008). The complement system consisting of several serum proteins can also recognise pathogens. This pathway can therefore assist in combating the pathogen and can relay information to the adaptive immune system. Neutrophils are also known to form neutrophil extracellular traps (NETs) which help localise, engulf and destroy the pathogen through respiratory burst induced by rapid ROS production (Figure 1) (Brinkmann et al., 2004). Once components of the innate system cells are recruited and the pathogen is localised and engulfed the adaptive system is activated.

1.1.2 Adaptive immunity

The adaptive immune system consisting of T and B cells (also known as T and B lymphocytes) process the pathogen resulting in the elimination of the harmful stimuli. Lymphocytes develop memory to the pathogen in order to generate more

efficient response upon subsequent exposure to that particular pathogen. Macrophages together with dendritic cells initially present antigens to cells of the adaptive immune system (T and B cells). For this to take place antigen presenting cells (APCs) must migrate to lymphoid tissues to encounter T and B cells, and this occurs via the active and dynamic movement of cells from the extravascular tissue (site of injury) into local lymph vessels. Once the cells are in the lymphoid tissue they can encounter and activate T or B cells initiating a slower but highly specific adaptive immune response (Figure 1.1). Initially the APC presents the antigen to T cells where the antigen is processed through the formation of an immunological synapse which induces intracellular signalling leading to immune priming and apoptosis, a process usually termed cellular immunity. Alternatively macromolecular antigens are recognised by immunological antibodies which are mediated by B cells and referred to as humoural immunity. The development of highly specialised T and B cells takes several days to occur and the feature of pathogen memory by lymphocytes allows a quicker and more efficient response upon subsequent exposure to the same pathogen. More importantly it also allows the body to recognise significantly more pathogens through the highly complex process of genetic recombination.

A high concentration of toxic mediators are released during both innate and adaptive immunity therefore this process has to be effectively controlled to ensure elimination of the pathogen with minimal damage to the host. When these responses are excessive and/or inappropriately triggered it can lead to and/or exacerbate numerous pathological conditions. For this reason there is now much interest in the resolution phase of inflammation, the series of responses that promote tissue healing through the action of numerous endogenous anti-inflammatory mediators (e.g. resolvins) that assist in controlling inflammation (Serhan et al., 2007). Inflammation can be classified into an acute or chronic response. An acute inflammatory response usually occurs immediately after an encounter with a pathogen or tissue injury and lasts for a short time period (minutes to days) and is generally characterised by neutrophil infiltration and plasma exudation. Chronic inflammation is longer lasting (days to years) and primarily involves macrophages, monocytes and lymphocytes and this

response can typically occur during autoimmune diseases. This type of inflammation is associated with a significant amount of pain due to sustained inflammation over longer time periods and the release of neuropeptides which increases the sensitivity of sensory nerves (Brain, 1997). As uncontrolled inflammation is the underlying cause and/or effect of many diseases, it is important to understand this process in more detail. Investigating the early stages of leukocyte recruitment from the blood into the tissue, which initiates this whole process, can help enhance our understanding of inflammatory reactions and potentially identify targets for novel anti-inflammatory drugs.

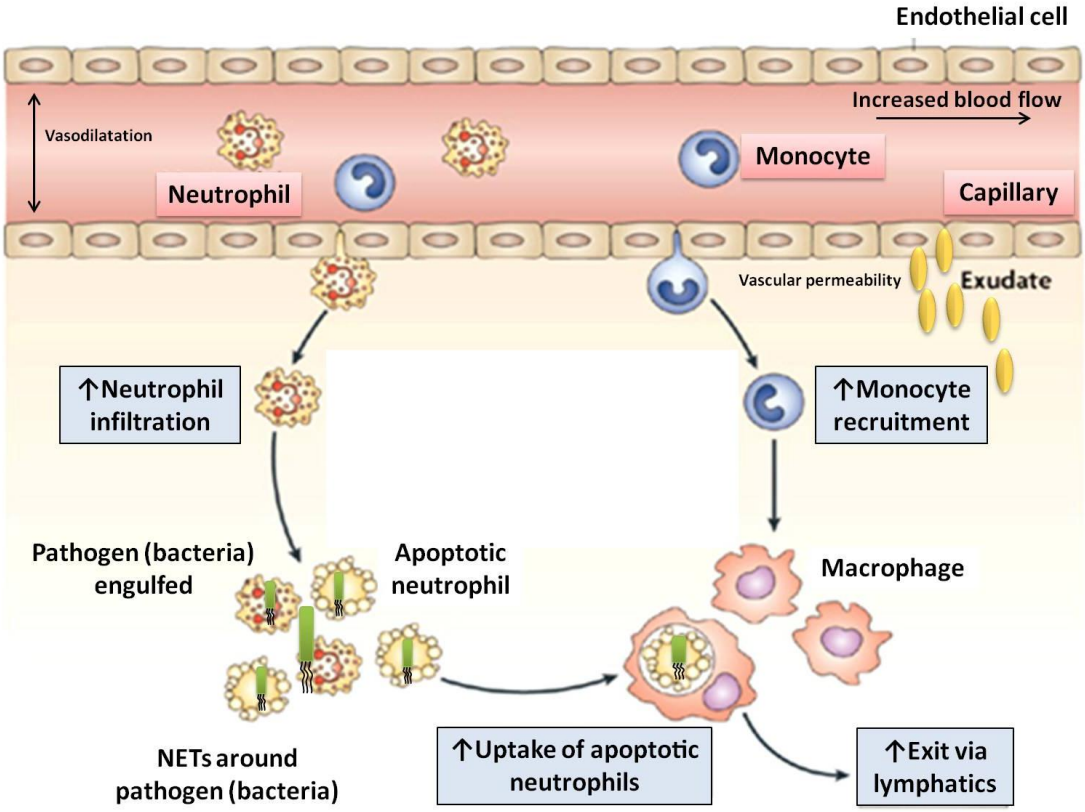

Figure 1.1: Key vascular processes that occur during inflammation.

During an inflammatory response an increase in neutrophil and monocyte recruitment, vasodilatation, increased blood flow and vascular permeability are seen. The pathogen (e.g. bacteria shown in green) is engulfed and killed using toxic granules present inside the cytoplasm. Macrophages phagocytose the apoptotic neutrophil and promote phagocyte exit from the tissue via the lymphatics where it presents the antigen to lymphocytes in lymphatic tissues. Diagram adapted from Serhan et al., 2008.

1.2 Leukocyte extravasation

Leukocyte extravasation is a multistep process by which leukocytes are recruited from the blood circulation to the extravascular space where they accumulate, identify and engulf the invading pathogen. For this to occur leukocytes free flowing in blood at high shear rates must be effectively slowed down in order to establish strong interactions with ECs lining the vascular lumen (Ley et al., 2007). This process is required to enable leukocytes to breach the barriers of the vessel wall and is largely dependent on a series of specific, dynamic and overlapping adhesive interactions between activated leukocytes and components of the vessel wall.

1.2.1 Vessel wall barrier

ECs line the lumen of the vessel wall and are the first barrier through which leukocytes must penetrate to reach the extravascular tissue. This monolayer is in direct contact with the blood. ECs can be continuous and non-fenestrated (e.g. brain, skin, heart and lung vasculature), fenestrated (e.g. in capillaries of endocrine glands and kidney glomeruli) or alternatively can have a discontinuous pattern as found in the liver. ECs have a role in mediating blood pressure through regulating vascular tone although these processes are largely mediated by vascular smooth muscle cells. The contacts between two ECs determines the degree of tightness and hence this layer also controls vascular permeability and leukocyte TEM.

Each EC is connected to adjacent cells through interendothelial junctions (Figure 1.2) forming structures known as tight junctions consisting of JAMs, occludin, and claudins and adherens junctions consisting of VE-cadherin and catenins (Dejana, 2004). Tight junctions reduce vascular leakage and are closely associated with the actin cytoskeleton and hence also involved in cell polarity. Adherens junctions are important for the regulation of structural integrity, and also interact with the actin cytoskeleton. There are also gap junctions formed by the connexin family, which are

essential for communication and the formation of molecular pores, although they are not considered to be involved in leukocyte migration (Dejana, 2004).

Molecules well known to be involved in leukocyte migration directly are also part of tight/adherens junctions. These molecules include platelet endothelial cell adhesion molecule (PECAM-1), ICAM-2, CD99, CD99L2 and endothelial cell-selective adhesion molecule (ESAM) (Figure 1.2). These protein-protein interactions collectively maintain vascular integrity, regulate permeability and also enable inter-endothelial communication (Dejana, 2004). For leukocytes to transmigrate through this barrier the junctional cell-cell contacts must be overcome in a highly regulated manner through the sequential interaction of activated leukocyte and ECs. These interactions are collectively known as the leukocyte adhesion cascade.

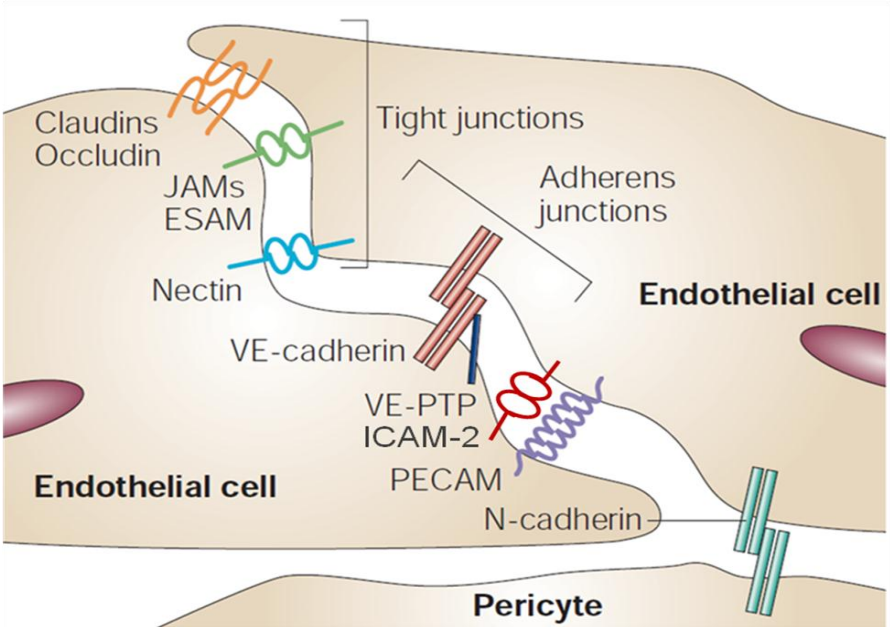

Figure 1.2: Junctional contacts between two endothelial cells.

Endothelial cell-cell junctional interactions are formed of tight junctions composed of junctional adhesion molecules (JAMs), occludin, and claudins, and adherens junctions composed of VE-cadherin and catenins. Diagram adapted from Dejana, 2004.

1.3 Leukocyte adhesion cascade

The initial model of the leukocyte adhesion cascade consisted of three stages; leukocyte rolling, activation and firm adhesion. In more recent years extra steps have been defined and the full cascade currently consists of the following; leukocyte tethering (capture), rolling, slow rolling, firm adhesion (arrest), spreading (polarisation), crawling, transendothelial migration (TEM) (transcellular or paracellular) and transmigration through the pericyte sheath and basement membrane (Figure 1.3) (Ley et al., 2007). Each stage is mediated by several adhesion molecules which are described in Figure 1.3. The key stages involved in this process are described in more detail below.

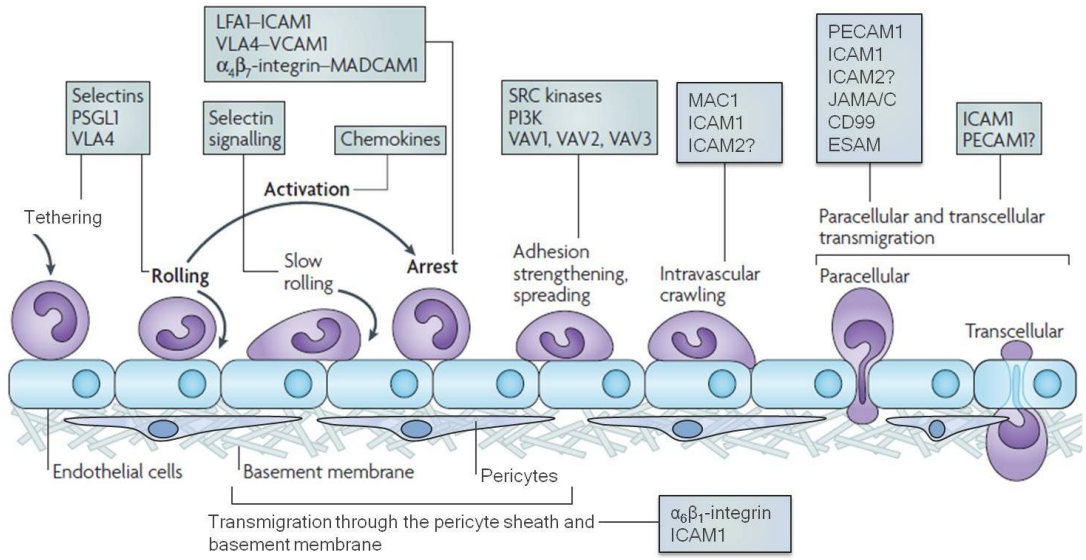

Figure 1.3: Leukocyte adhesion cascade.

Key endothelial adhesion molecules and the leukocyte ligands that are involved at each distinct stage are shown. These include selectin and integrin mediated rolling, integrin mediated firm adhesion, spreading involving various signalling moclules such as VAV PI3K and SRC, ICAM-1 mediated intravascular crawling, PECAM-1, JAMs, CD99 and ESAM mediated transendothelial migration and finally ICAM-1 and integrin mediated transmigration through the pericyte sheath and basement membrane. Diagram adapted from Ley et al., 2007.

1.3.1 Leukocyte tethering and rolling

Leukocyte tethering and rolling describes the transient adhesive interactions between leukocytes and ECs lining blood vessels. This process brings the fast flowing circulating leukocytes in direct contact with ECs which only occurs in response to inflammatory stimuli. During an inflammatory response EC activation by inflammatory mediators (e.g. endotoxins, cytokines) results in an increase in the expression of selectins such as P-selectin (CD62P) and E-selectin (CD62E), and CAMs such as intercellular adhesion molecules-1 (ICAM-1) and vascular cell adhesion molecule-1 (VCAM-1) on the intravascular EC surface. There are in fact 3 different types of selectins and are all important for leukocyte tethering and rolling. L-selectin (CD62L) which is constitutively expressed on circulating leukocytes, P-selectin which is stored in granules of platelets and ECs and are rapidly mobilised when activated and E-selectin which is expressed on activated ECs.

Selectins are type 1 transmembrane glycoproteins with a N-terminal C-type lectin domain which is more than 60% identical across all three subtypes, an epidermal growth factor (EGF) -like domain followed by a variable series of short consensus repeats composed of complementary regulatory-like modules (Bevilacqua and Nelson, 1993; Ridger et al., 2008). Selectins have a transmembrane domain and a short cytoplasmic tail linking to the cytoskeleton. The number of consensus repeats in each selectin is different. The lectin domain is a carbohydrate portion considered to be the site which binds to several ligands such as P-selectin glycoprotein ligand-1 (PSGL-1), glycosylation-dependent cell adhesion molecule (GlyCAM-1), mucosal addressin cell adhesion molecule (MAdCAM-1), E-selectin ligand-1 (ESL-1) and CD44. All selectin ligands are fucosylated carbohydrate structures containing sulfated-sialyl-Lewis^{x}, which is a tetrasaccharide carbohydrate recognised by the lectin domain of selectin (Bevilacqua and Nelson, 1993; Zarbock et al., 2011). Among these ligands PSGL-1 expressed on leukocytes and ECs is the major ligand of all three selectins (Figure 1.3).

A key feature of selectins is their unique ability to transiently bind to their ligands under high shear rate. This feature is required for leukocyte capture, and enables subsequent strengthening of leukocyte-EC interactions (Ley et al., 2007; Ridger et al., 2008). These bonds are initially relatively weak and involve rapid dissociation followed by the formation of new bonds. L-selectin is considered to be involved in the very early stages, and unlike P-selectin and E-selectin expression which increases during inflammation, L-selectin is shed from leukocytes following their activation by chemoattractants (e.g. IL-8, C5a and PAF). L-selectin interaction with PSGL-1 is also involved in leukocyte-leukocyte interaction and enforces secondary leukocyte recruitment (Ley et al., 2007). P-selectin is preformed and rapidly mobilised (5-10 minutes) from Weibel-Palade bodies during EC activation and it is crucial for tethering as well as rolling. Of interest the role of platelet P-selectin has also been shown to support platelet-leukocyte interactions (Gawaz et al., 2005). E-selectin requires *de novo* synthesis via transcriptional up-regulation and hence peaks around 4-6 hours and is important for rolling although more recently its sequential interactions with PSGL-1, ESL-1 and CD44 has been shown to be involved in tethering, rolling and slow rolling respectively (Hidalgo et al., 2007) (Figure 1.4). It should be noted, however, that rolling can still occur in the absence of P-selectin/PSGL-1 (Ridger et al., 2005) and that the molecules involved in tethering, rolling and slow rolling are likely to have overlapping and redundant roles.

Ligand bound selectins and EC bound chemokines trigger downstream signalling pathways within leukocytes which results in the activation, clustering and the conformational change of key leukocyte surface proteins called integrins which are discussed in more detail in Section 1.3.2. Up-regulating and activating integrins promotes interactions with their key ligand ICAM-1 on activated ECs. This process leads to slow rolling and hence increases leukocyte proximity to ECs inducing further up-regulation and activation of integrins. In addition to the selectins, VCAM-1 interaction with the integrin very late antigen-4 (VLA-4, $\alpha_4\beta_1$, CD49d/CD29) also supports this process and could be involved in selectin independent rolling. Eventually leukocyte motility slows down considerably, and stronger interactions

form resulting in greater exposure of leukocytes to chemokines (e.g. MCP-1, IL-8, RANTES and MIP-1α/β) that eventually results in leukocyte adhesion.

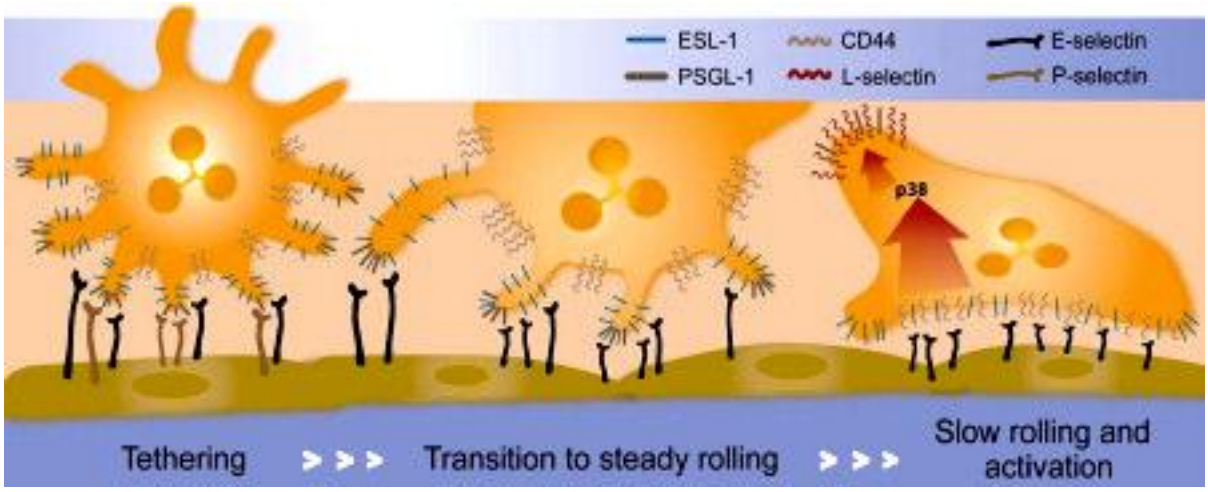

Figure 1.4: Selectin mediated leukocyte tethering, rolling, slow rolling and activation.

PSGL-1 is a key ligand for P-selectin and E-selectin. More recently E-selectins has been shown to exhibit a sequential interaction with PSGL-1, ESL-1 and CD44, mediating tethering, rolling and slow rolling, respectively. Diagram from Hidalgo et al., 2007.

1.3.2 Leukocyte adhesion

Leukocyte adhesion is a rapid process mediated by EC associated chemokines and chemoattractants, and marks the point at which the leukocyte has strong interactions with the EC layer. Whilst tethering and rolling is mediated in general by selectins, adhesion is predominately mediated by chemokines which activate key integrins on the surface of leukocytes which in turn bind to EC proteins such as ICAM-1 and VCAM-1 (Ley et al., 2007).

Integrins are a large group of type 1 transmembrane polypeptide receptors. Each integrin consists of one α and β chain that are non-covalently bound with a large glycosylated extracellular domain, a hydrophobic transmembrane portion and a small cytoplasmic tail (Figure 1.5) (Shattil et al., 2010). There are currently at least 24 different subtypes of integrins that exist (formed from 18 different α and 8 β subunits) however three particular subtypes are most widely implicated in leukocyte-EC interactions. These are, β_1-integrin VLA-4, and β_2-integrins lymphocyte function-associated antigen-1 (LFA-1, $\alpha_L\beta_2$, CD11a/CD18) and macrophage receptor 1 (MAC-1, $\alpha_M\beta_2$, CD11b/CD18). These integrins are commonly found on most leukocytes (Hogg et al., 2011; Huttenlocher and Horwitz, 2011). Whilst LFA-1 and MAC-1 are well known to bind to ICAM-1 and ICAM-2, VLA-4 is known to bind to VCAM-1 during leukocyte recruitment.

The α and β domains of integrins contain seven and four repeated homologous domains on the N terminus respectively (Figure 1.5). The α subunit is a C2-type Ig-like domain, which contains an 'I' or 'A' domains (~200 amino acids located between the second and third domain) in the extracellular portion which forms the metal ion-dependent ligand binding domain (Hogg et al., 2011; Ley et al., 2007). The β subunit consists of a similar 'I'-like domain, PSI (for plexins, semaphorins and integrins) domain followed by four tandem EGF-like repeats (Figure 1.5). The cytoplasmic portions for both subunits are small, however the β unit is slightly longer and is generally considered to be essential for focal adhesion and cell spreading through inside-out signalling via proteins such as talin (Kinashi, 2005; Shattil et al., 2010). Alterations in their structural conformation and clustering of heterodimers into oligomers regulate their binding and activation properties which are also generally induced by inside-out signalling. These events are highly complex whereby the affinity and avidity of integrins for their ligands are altered. Whilst low affinity integrins have a more folded extracellular portion, high affinity integrins have an extended extracellular domain (Figure 1.5) (Hogg et al., 2011; Ley et al., 2007). Conformational change in the large extracellular domain exposes the ligand binding site and thus stimulates outside-in signalling. Integrin membrane clustering also

occurs and facilitates protein interactions between the cytoplasmic domains (Kinashi, 2005; Shattil et al., 2010). The bi-directional integrin signalling is key to numerous cellular process such as cell polarity, cytoskeletal structure, gene expression, cell survival and proliferation (Kinashi, 2005; Shattil et al., 2010). After such functions integrins are known to be recycled.

Upon ligand interaction of integrins, leukocyte-EC interactions become stronger, and hence can be further activated by chemokines and chemoattractants that are immobilized and presented on luminal surface of ECs by GAGs which bind to G-protein coupled receptors (GPCRs) on leukocyte (Ley et al., 2007). This also induces inside-out signalling which can subsequently lead to the conformational change and clustering of integrins (Ridger et al., 2008). Of interest, platelets are also known to adhere to ECs and leukocytes during this cascade and may also be involved in recruiting and/or stabilizing leukocyte adhesion. Once leukocytes have firmly adhered, the interaction is further strengthened through integrin mediated outside-in signalling and consequently further phenotypic and physiological changes within leukocytes occur leading to leukocyte spreading or polarization and crawling (Ley et al., 2007).

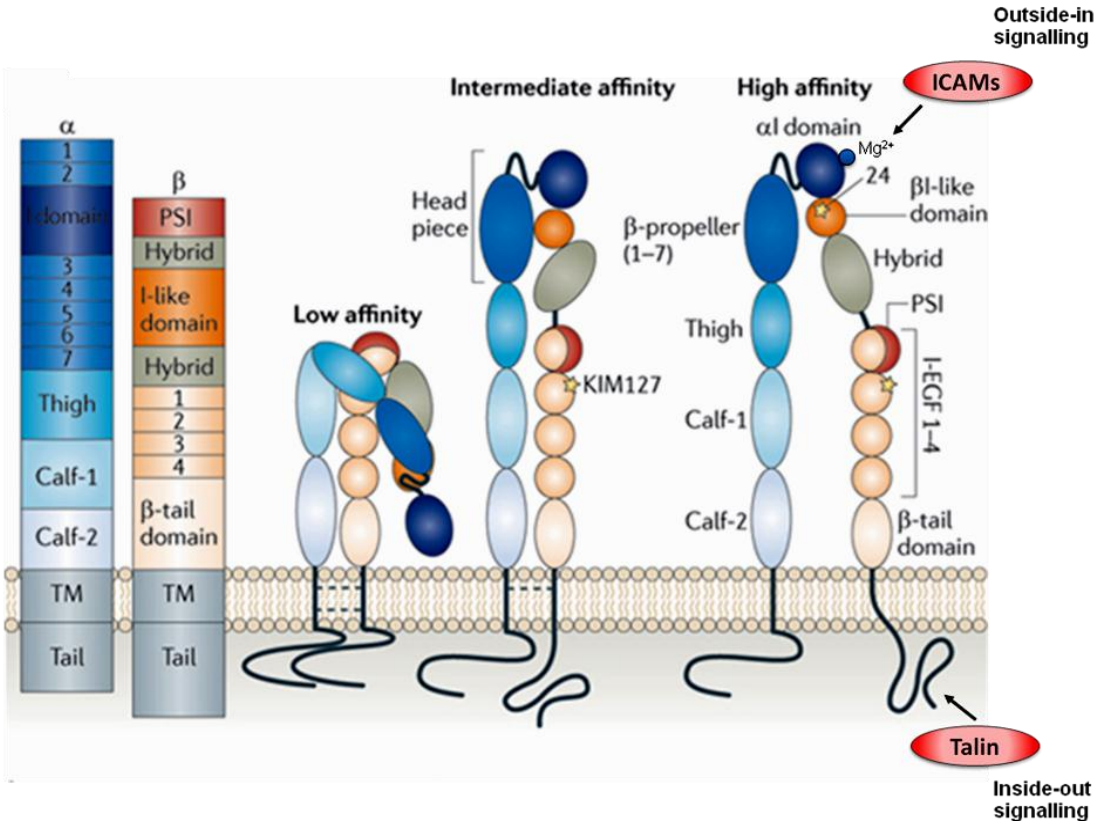

Figure 1.5: The structure and conformational changes of integrins.

As an example the structure of lymphocyte function-associated antigen-1 (LFA-1, $\alpha_L\beta_2$) is shown. Integrins are composed of an α and β subunit. The α unit is slightly longer in the extracellular portion and the β unit is slightly longer in the cytoplasm portion. In low affinity forms, extracellular regions of the α- and β-subunits are folded whereas in the higher affinity forms this region is extended. The α subunit contains an I domain where extracellular ligands such as the CAMs interact, inducing outside-in signalling. The β subunit contains an I-like domain, however its functions are not fully understood. Inside-out signalling generally occurs through proteins such as talin interacting with the cytoplasmic portion of the β unit. Diagram adapted from Hogg et al., 2011.

1.4 Leukocyte polarization and crawling

Leukocyte polarisation and crawling describes the shape change that occurs within leukocytes and the motion by which leukocytes move to a specific site on the EC layer to undergo TEM. Although leukocyte polarisation is likely to occur during leukocyte rolling, it is more commonly associated with the crawling stage. Polarisation describes the rearrangement of proteins within the cell creating a leading (front) end and trailing (back) end. Almost all leukocytes undergo crawling which suggests that the initial site of adhesion is not ideal to support TEM and may require further activation of EC and/or leukocytes. Furthermore as crawling has been shown to occur perpendicular and against the direction of blood flow (Phillipson et al., 2009), it is well accepted that this is an active process rather than due to passive movements as a result of the high shear rates of blood flow. In order for leukocytes to crawl the cell must undergo spreading or polarisation. This includes extension of leukocyte protrusions via active reorganization of actin cytoskeleton, forming a protrusive leading edge called pseudopodia (Figure 1.6). These can be large and broad (lamellipodia) or thin (filopodia) and these structures are formed on the closest side to the chemoattractant (Huttenlocher and Horwitz, 2011) (Figure 1.6). The lamellipodia has 'dendritic' like filamentous actin (F-actin) which extend based on directional cues, in contrast filopodia display long parallel bundles and are sensors to the local environment and hence may not be essential for chemotaxis (Ridley, 2003). On the opposite side of the leading edge a contracting trailing end called the uropod is formed. These distinct structures have been characterised as having different intracellular protein localisation however there is very little information with regards to the mechanism that determains the type of protrusions formed and whether these different types of protrusions can form simultaneously. It is also unknown whether different types of potrusions are dependent on the type of stimuli.

The crawling process involves key molecular actin machinery. Actin is regulated through co-ordinated signalling events which cause cell polarisation, protrusion,

adhesion formation, rear retraction and de-adhesion (Figure 1.6). Local activation of signalling proteins at the leading edge, for example Cdc42-Par6-atypical protein kinase C (aPKC) pathway, Rac and PIP_3 polarizes cellular structures such as the microtubule organizing centre (MTOC), Golgi complex and nucleus (Figure 1.6). Rac/Cdc42 and WASP/WAVE signalling together with actin-binding proteins underlie the mechanisms associated with the organisation and polymerisation of the actin (Ridley, 2003). The interaction of Rho and Rac ensures that whilst Rac activity increases at the leading edge, Rho activity is inhibited at that site. In this situation, Rho activity is stimulated at the sides and uropod, whereas Rac-induced protrusions are inhibited in these areas. De-adhesion at the rear has also been suggested to involve Rac (Ridley, 2003) therefore indicating that Rho and Rac activity and regulation is far more complex. After cell protrusions are established they are further strengthened via molecules such as talin, which bind to integrins as described previously (Section 1.3.2) and stimulates inside-out signalling involving phosphatidylinositol 3-kinase (PI3K) (Figure 1.5). These adhesive interactions are transient and are followed by de-adhesion which in turn are followed by new adhesions at the leading edge, responses associated with focal adhesions and focal adhesion kinases (FAKs).

Different types of focal adhesions exist, nascent adhesions, focal complexes and focal adhesions (Huttenlocher and Horwitz, 2011). Nascent adhesions and focal complexes are small dot-like adhesions located on leading edge protrusions and are known to support actin polymerisation (Huttenlocher and Horwitz, 2011). Focal adhesions are more well known and are composed of integrin clusters located in the middle part of the cell and on actin filament bundles (Huttenlocher and Horwitz, 2011). Focal adhesions in particular, regulate the turnover of adhesion and de-adhesions (Ridley, 2003). This also occurs at the trailing edge and involves weakening of the integrin/cytoskeletal linkage possibly through the cleavage of talin and a deactivation of integrins via conformational changes to a low affinity state. Relative to the leading edge, the events that occur at the trailing edge are less well understood however it is known that mechanisms that occur in the latter region are

often linked to Rho/ROCK signalling whilst myosin II sustains cell polarity during rear retraction (Huttenlocher and Horwitz, 2011; Ridley, 2003; Rottner and Stradal, 2011). Rear retraction and de-adhesion is associated with Rho family of proteins as well as FAK, Src, ERK and Ca^{2+} influx.

The mechanisms that occur at the leading and trailing edge take place in a highly regulated manner causing leukocytes to migrate in response to directional cues (e.g. gradients of chemokines) and adhesion molecules (Phillipson et al., 2006; Sumagin et al., 2010). The leading and trailing edges are formed to assist leukocyte locomotion/crawling towards preferential EC sites which can support TEM. As the leading edge extends forward the uropod de-adheres, creating a millipede-like movement. Integrins have key roles in the crosstalk between the cell membrane and the cytoskeleton and these interactions are crucial to this process. Key linkage molecules that exist between the actin cytoskeleton with cell surface integrins are talin, vinculin and α-actinin, although the precise ligand interactions are unclear as these linkage proteins can all also bind to actin directly, as well as to integrins. The short transient occurrence of protrusions, adhesions, and de-adhesions in a coordinated fashion, sustains cell polarity which is the key to efficient leukocyte crawling.

In neutrophils, cellular polarisation and crawling has been linked to MAC-1/ICAM-1 interactions whereas adhesion is considered to be mediated by LFA-1/ICAM-1 interactions (Ley et al., 2007; Phillipson et al., 2006; Sumagin et al., 2010). MAC-1 is stored in secretory secondary and tertiary granules and is readily mobilised following neutrophil activation (Zarbock and Ley, 2008). There is also some data that suggests that LFA-1 engagement results in MAC-1 up-regulation and is involved in stages following LFA-1-mediated adhesion. Further studies using confocal microscopy have shown although MAC-1 expression is homogenous on the cell surface, its activity is more pronounced at the leading edge of the cell (Hidalgo et al., 2009), and could therefore mediate dynamic adhesions and de-adhesions between

leukocytes and ECs during leukocyte crawling. This could be regulated by conformational changes in the structure of MAC-1, which alters ligand affinity states, and has been linked to inside-out signalling via linkage proteins such as talin (Figure 1.5) (Ridley, 2003). These linkage molecules provide communication between the cell membrane and the cytoskeleton, hence inducing focal adhesions (integrin clustering), and thereby supports neutrophil crawling.

The crawling of different leukocyte subsets has been shown to be dependent on slightly different molecules. For example LFA-1 is known to be crucial in lymphocyte crawling (Shulman et al., 2009) whereas MAC-1 is known to be important in neutrophil crawling (Ley et al., 2007; Phillipson et al., 2006; Sumagin et al., 2010). Interestingly monocyte and T cell crawling have also been linked to ICAM-2 which is discussed in more detail in Section 1.8. Recent data highlights the involvement of ICAM-1 clustering (Sumagin and Sarelius, 2010), VAV-1 (Rho family guanine exchange factor) (Phillipson et al., 2009) and JAM-A (Weber et al., 2007) although very little is known about the mechanisms by which these molecules are involved in leukocyte polarisation and/or crawling. Whether this is a random process or an inherent response remains unclear and whether crawling is chemotactic, chemokinetic, haptotactic or mechanotactic (driven by mechanical forces) is still poorly understood. The redundant, co-operative and multiple overlapping functions of several proteins that regulate leukocyte polarisation and crawling clearly demonstrate that these events are highly complex and the mechanisms and pathways involved are only just being identified.

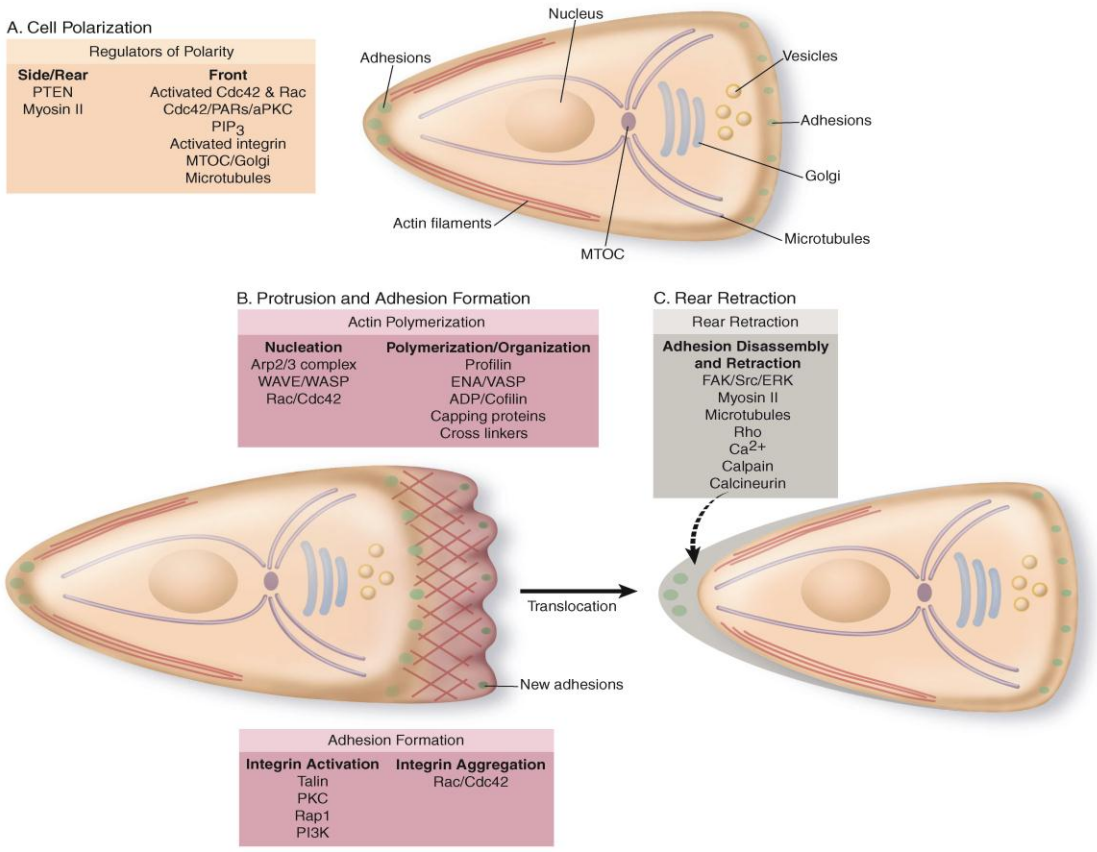

Figure 1.6: Leukocyte polarisation and crawling.

(**A**) Cell polarity involves the rearrangement of proteins at the front (leading edge), the back (trailing edge) or the sides of the cell in response to chemotactic agents. Cdc42 along with PKC reorganises specific proteins toward the leading edge, controls the organization of microtubules and regulates the localization of microtubule organising centre (MTOC) and golgi apparatus. (**B**) Protrusions and adhesion formation is required for the movement of the cell. This requires WASP/WAVE proteins (targets of Rac and Cdc42 and other signalling pathways) which regulates the formation of actin branches through actin polymerisation. Protrusions are stabilized by the formation of integrin dependent adhesions. Integrins are activated by talin binding and through PKC-, Rap1-, and PI3K-mediated pathways. (**C**) Rear retraction occurs though de-adhesion which is mediated by several signalling pathways such as Src/FAK/ERK, Rho and myosin II. Collectively these events induce a millipede-like cell movement on activated ECs. Diagram from Ridley, 2003.

1.5 Leukocyte transendothelial migration

Intravascular crawling is followed by leukocyte interactions with the site of TEM. Leukocyte interactions with ECs during crawling trigger the expression of various inflammatory adhesion molecules, mediators and intracellular signalling events that initiate and/or facilitate leukocyte passage through the endothelium. This is an active process where *in vitro* studies based on clustering of adhesion molecules generates endothelial proadhesive platforms (EAPs), docking structures or transmigratory cups (Carman and Springer, 2004), regions that are considered to be 'equipped' for TEM (Figure 1.7). The existence of locations particularly permissive to TEM, or 'transmigratory portals', have variously been suggested to be at tricellular EC junctions which are most abundant at the convergence of two vessels (Burns et al., 1997; Sumagin and Sarelius, 2010), ICAM-1 enriched regions (Sumagin and Sarelius, 2010), or identified by chemotactic gradients (Burns et al., 1997; Massena et al., 2010; Sumagin and Sarelius, 2010). It is also known that invasive leukocyte protrusions may seek out permissive areas and actively force leukocytes to squeeze through the distinct barriers of the vascular wall (Figure 1.7). Leukocyte TEM occurs via paracellular (between two EC junctions) or transcellular (through the body of an EC) migration (Figure 1.7 and 1.8) and two distinct mechanisms have been proposed (Nourshargh et al., 2010).

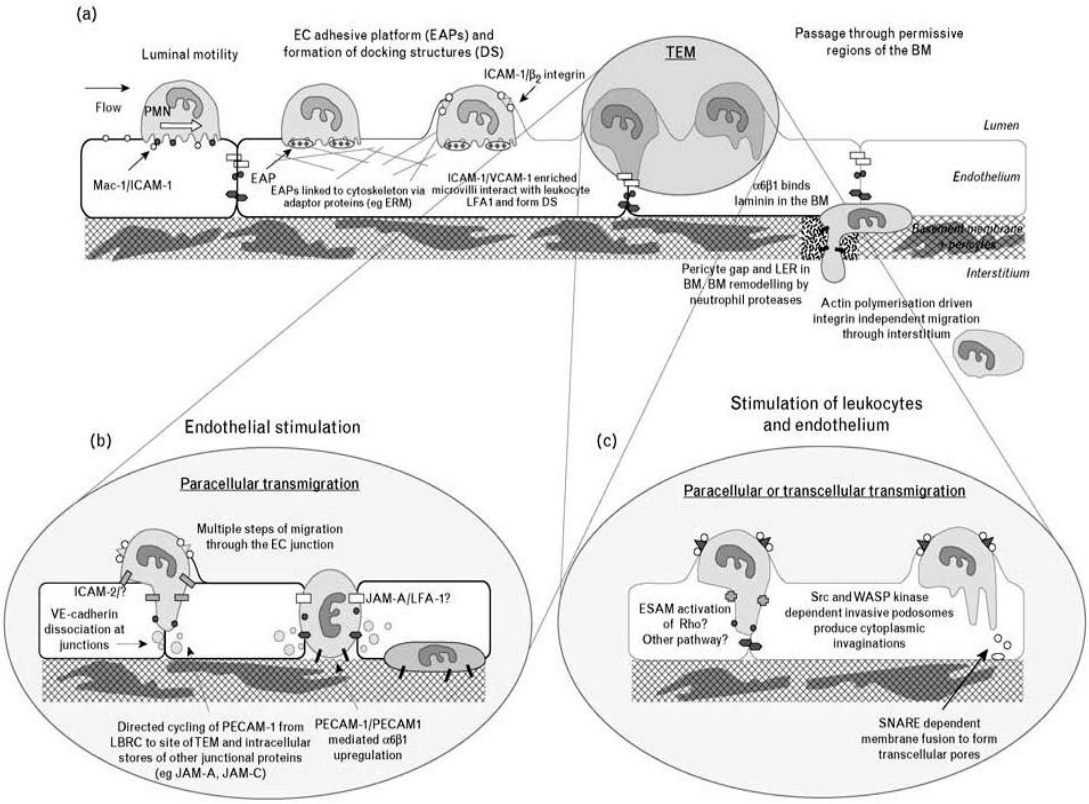

Figure 1.7: Leukocyte crawling and transmigration through the vessel wall.

Intraluminal leukocyte crawling mediated via MAC-1/ICAM-1 allows the cell to reach a specific region of the vessel wall usually between two adjacent ECs (paracellular). The formation of docking structures (DS) and endothelial adhesive platforms (EAPs) is known to influence the site at which leukocytes begin to transmigrate through. Once the leukocyte has penetrated the EC layer it migrates through the gaps between pericytes and areas which have low expression regions (LERs) of proteins in the basement membrane. Diagram from Woodfin et al., 2010.

1.5.1 Paracellular TEM

Paracellular TEM described the movement of leukocyte between adjacent ECs. In order for paracellular TEM to occur protein-protein interactions between two ECs need to be overcome. Adherens junctional interactions involving VE-cadherins are

crucial to this process, due to their fundamental role in maintaining EC-EC contacts as previously discussed (Section 1.2.1). During paracellular TEM, this interaction is breached through cytoskeletal contraction with ECs induced by intracellular Ca^{2+} flux which activates myosin light chain kinase leading to the phosphorylation of numerous signalling molecules (Nourshargh et al., 2010). This results in a reduction in EC-EC interactions allowing leukocyte protrusions to access areas between two adjacent ECs. Consequently this permits endothelial junctional molecules to interact with their leukocyte ligands. Other junctionally expressed proteins (e.g. JAM-A, JAM-C) can be cleaved and/or undergo resdistribution away from junctions, events that also reduce the barrier function of EC-EC contacts. More recently a distinct vesicle-like interconnected membrane compartment called the lateral border recycling compartment (LBRC) situated beneath EC borders has been shown to be involved in the recycling of EC membranes which facilitates leukocyte TEM (Mamdouh et al., 2003; Mamdouh et al., 2008). This compartment contains PECAM-1, CD99 and JAM-A which is trafficked to the site of TEM by kinesin (Mamdouh et al., 2008). These events occur in a highly regulated and selective manner ensuring that a tight seal of the EC membrane around the leukocyte is maintained.

ICAM-2, JAMs and PECAM-1 are heavily implicated in TEM. Each of these molecules display a distinct and sequential role at specifics stages (Woodfin et al., 2009). ICAM-2 expressed on ECs has been demonstrated to mediate luminal stages of TEM, supporting the movement of cells from the vascular lumen to junctional regions (Figure 1.7). JAM-A interaction appears to support the migration of leukocytes between two ECs (Figure 1.8). Other JAM members such as JAM-B and JAM-C are also concentrated at tight junctions and are appear to support this process (Figure 1.8). EC JAMs can interact in a homophilic manner with adjacent ECs or in a heterophilic manor with various integrins such LFA-1 for JAM-A, VLA-4 for JAM-B and MAC-1 for JAM-C. Furthermore some JAMs also interact with each other such as JAM-B and JAM-C (Weber et al., 2007). The role of JAMs in regulation of TEM is highly complex and has been reviewed by Weber et al., (2007). After JAM-A interactions, EC PECAM-1 interacts with PECAM-1 expressed on leukocytes

resulting in induced expression and activation of leukocyte laminin receptors (integrin $\alpha_6\beta_1$) (Dangerfield et al., 2002). This allows leukocytes to transmigrate through the pericyte sheath and the vascular basement membrane (Nourshargh et al., 2010). The involvement of ICAM-2, JAM-A and PECAM-1 in transmigration has been demonstrated to occur only if the EC is directly activated whereas direct stimulation of leukocytes overrides the requirements for these proteins in some models (Woodfin et al., 2009).

Leukocyte TEM can also occur independently of ICAM-2, JAM-A and PECAM-1 as induced by different stimuli or in the context of recruitment of different leukocyte subsets. Other molecules implicated in TEM include CD99 and CD99L2 (Bixel et al., 2010). The mechanisms through which thee molecule mediates TEM are not fully understood although CD99 and CD99L2 have been demonstrated to have roles at a later stage to PECAM-1 (Bixel et al., 2010). Other endothelial junctional molecules implicated in TEM include ESAM found on ECs and platelets but again full details of how this molecule regulates TEM remains to be elucidated. The involvement of these EC proteins are considered to be a dynamic process, some involving the LBRC which has been shown to express PECAM-1, JAM-A and CD99. Several forms of paracellular migration have also been reported; normal TEM (i.e. luminal to abluminal), hesitant TEM (i.e. luminal to abluminal but also showing several back and forward oscillations within the junction) and reverse TEM (i.e. abluminal to luminal) which has been linked to the loss of EC JAM-C (Woodfin et al., 2011). These multiple forms of TEM add further layer of complexity to this field.

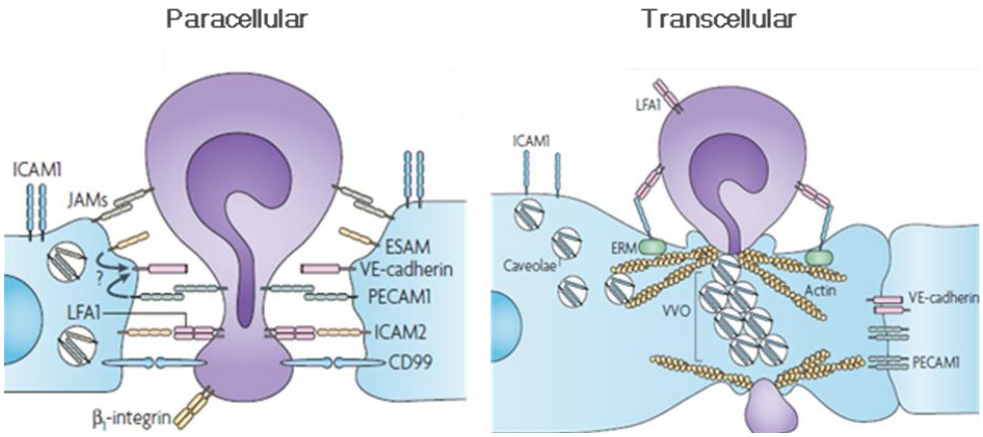

Figure 1.8: Molecules supporting leukocyte paracellular and transcellular TEM.

Proposed molecular pathways involved in TEM between adjacent ECs (paracellular) and through cell body of EC (transcellular). Diagram from Ley et al., 2007.

1.5.2 Transcellular TEM

Although paracellular migration occurs more frequently, it is now known that transcellular migration can also take place (Feng et al., 1998; Feng et al., 2002). Transcellular TEM describes the movement of leukocytes directly through the body of thin EC layers (Figure 1.8). In most models studied this represents approximately 10-30% of all transmigration events (Ley et al., 2007). One study has demonstrated that inhibiting the ability of leukocytes to crawl to the site of 'preferred' TEM enhanced transcellular TEM (Phillipson et al., 2006). Other studies have seen an increase in transcellular event following N-formyl-methionyl-leucyl-phenylalanine (FMLP) stimulation (Feng et al., 1998). However, the concept of transcellular TEM is still novel and there are various discrepancies in the literature regarding the associated mechanisms.

It is generally considered that transcellular TEM involves many of the proteins implicated in paracellular TEM as some of these are also expressed in non-junctional areas (e.g. PECAM-1). Transcellular TEM is initiated by insertion of leukocyte membrane protrusions into ECs (Carman and Springer, 2008). Leukocyte protrusive structures can bind to ICAM-1 clusters which form EC transmigratory cups that embrace the leukocyte and encapsulates it with EC membrane (Carman and Springer, 2008). As well as ICAM-1, these structure have been demonstrated to also involve VCAM-1 and is thought to be dependent on LFA-1 and VLA-4 (Carman and Springer, 2004) however it should be noted that the mechanism and the existence of transmigratory cups *in vivo* still remains to be established. During transcellular TEM VCAM-1, ICAM-1 and CD99 concentrate at sites called the vesicular vacuolar organelles (VVOs) (Ley et al., 2007). VVOs are located in close proximity to intercellular junctions and consist of continuous membrane layers at the site of EC pore formation, which connects to F-actin providing additional membrane during leukocyte TEM (Figure 1.8) (Nourshargh et al., 2010). Similarly, other studies have suggested that PECAM-1 within the LBRC is involved in this process, again by providing additional membrane which is enriched with JAM-A, PECAM-1 and CD99 (Mamdouh et al., 2003; Mamdouh et al., 2008). As this route of TEM very rarely occurs and given that there are some reports that have suggested that this route takes slightly longer, this mechanism of TEM may therefore be a 'back up' response which occurs more frequently when paracellular events are restricted (e.g. the ECs of the blood brain barrier due to tight EC-EC interactions) (Phillipson et al., 2006).

1.6 Transmigration through the pericyte sheath and the basement membrane

Once leukocytes have penetrated the EC layer, they must overcome the next barrier which is the pericyte sheath and the basement membrane (Figure 1.3). Pericytes are elongated cells which have many protrusions that are directly in contact with ECs.

They are situated around the endothelium and are embedded within the basement membrane. The basement membrane is predominately composed of collagen type IV and laminin interconnected to other extracellular matrix protein components. Transmigration through this layer appears to take much longer (>5-15 minutes) than the time taken to breach the EC layer (~6 minutes) (Ley et al., 2007). This reflects the relative difference in barrier strength and/or how dynamically the barrier can respond to the migration of leukocytes in comparison to that of ECs and more importantly highlights the fact that different mechanisms and interactions are mediating these events. A limited number of studies have investigated the profile and mechanism, of leukocyte migration through the pericyte and basement membrane, partially due to current experimental limitations in isolating and culturing pericytes, and therefore it is poorly understood. A recent development in this area has been the identification of regions within the basement membrane that contain a lower expression of various basement membrane components such as, laminin-8, laminin-10 and collagen IV (Voisin et al., 2010). These sites have been termed low expression regions (LERs) and appear to be regions preferentially used by migrating leukocytes to exit venular walls (Voisin et al., 2010) (Figure 1.7). The pericyte layer contains gaps between adjacent cells that are aligned with LERs, providing a more permissive route for migrating leukocytes (Voisin et al., 2010). Recent studies in our group have indicated that pericyte gaps enlarge during TEM, a response that may additionally facilitate leukocyte transmigration (Proebstl et al., 2012). It was also found that leukocytes exhibit abluminal crawling on the pericyte sheath within the vessel wall, a process that was demonstrated to be mediate via ICAM-1 (Proebstl et al., 2012).

In conjunction with the morphological changes within this layer, specific adhesive interactions also appear to occur. As mentioned previously homophilic PECAM-1 interactions can lead to the up-regulation of β_1-integrins (e.g. $\alpha_6\beta_1$) which bind to laminin and thereby facilitate migration of leukocytes through this layer (Dangerfield et al., 2002). Together the LERs, pericyte gaps and various integrin interactions provide a mechanism by which leukocytes can pass through the pericyte layer and

basement membrane, and enter the extravascular tissue as guided by chemokines and chemoattractant gradients formed at the core of the inflammatory site.

1.7 Key endothelial cell proteins involved in leukocyte extravasation

1.7.1 PECAM-1

PECAM-1 is widely expressed on immune cells which originate from hematopoietic stem cells, such as neutrophils, monocytes, platelets and lymphocytes (DeLisser et al., 1997). It is also highly expressed on vascular ECs with pronounced expression at EC junctions. It is commonly associated with leukocyte TEM, angiogenesis, thrombosis, permeability and exhibits key signalling properties (Privratsky et al., 2010). PECAM-1 has been demonstrated to bind to PECAM-1, $\alpha_v\beta_3$-integrin, GAGs, CD38 and CD117. This molecule can also undergo inside-out signalling whereby shear stress, inflammatory mediators and ligation of various immune receptors can result in multiple functions governed by changes in its expression and/or phosphorylation status (Privratsky et al., 2010). As a result of intense research there is currently a significant body of information regarding the structure and function of PECAM-1 in inflammation (Privratsky et al., 2010).

PECAM-1 (CD31) is a 130 kDa type 1 transmembrane protein part of the immunoglobulin (Ig)-like superfamily and is well known for its role in leukocyte TEM. It is composed of a large extracellular domain containing six N-terminal Ig-like domains encoded by single exon, a transmembrane domain and a large cytoplasmic tail (Figure 1.9) (DeLisser et al., 1997; Privratsky et al., 2010). The first Ig-like domain is crucial for homophilic ligand interaction whereas domain 5 and 6 are implicated in heterophilic binding (Woodfin et al., 2007). The cytoplasmic domain contains residues that are important in cell signalling such as palmitoylation sites (important for apoptosis), docking structures and phosphorylation sites including immunoreceptor tyrosine based inhibitory motifs (ITIMs) (Figure 1.9). The

two cytoplasmic ITIMs are known to contain 2 tyrosine residues at position 663 and 686 (Figure 1.9). Upon ligand interaction these residues are phosphorylated and undergo downstream signalling events involving proteins containing Src homology 2 (SH-2). Downstream signalling results in various cellular responses such as up-regulation and activation of integrins, increase in permeability, PECAM-1 recycling (Mamdouh et al., 2008), cell motility and contractility and cell survival (Woodfin et al., 2007).

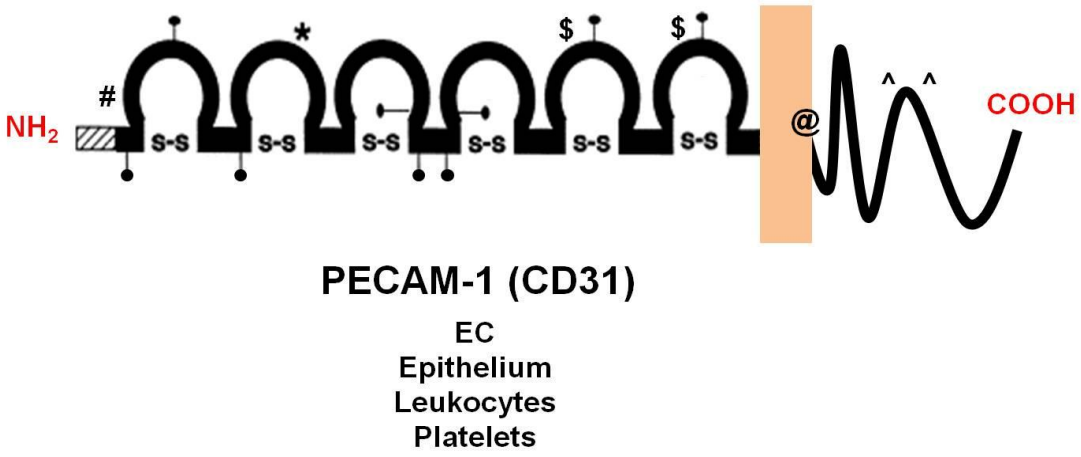

Figure 1.9: Structure of PECAM-1.

PECAM-1 is a 130 kDa transmembrane glycoprotein protein belonging to the Ig-like super family of adhesion molecules. It consists of extracellular domain containing 6 Ig-like domains, a transmembrane domain and a cytoplasmic tail. Key components of PECAM-1 have been shown; S-S disulfide bridges, * heparin binding sequence, • N-linked glycosylation sites, $ heterophilic binding, # homophillic binding, @ important residues for localisation and ^ ITIMs. Diagram adapted from DeLisser et al., 1997.

1.7.2 PECAM-1 in leukocyte transmigration

Using *in vitro* migration assays through endothelial monolayers, Muller et al., (1993) were the first to show a function for PECAM-1 in leukocyte transmigration. This role was further confirmed using various *in vivo* models such as the rat peritonitis model (Vaporciyan et al., 1993). The first direct evidence for the involvement of PECAM-1 in the leukocyte adhesion cascade came from intravital microscopy (IVM) studies where its role in leukocyte migration was demonstrated (Wakelin et al., 1996). Since these initial studies research has focused on understanding the regulation and mechanisms behind the functions of PECAM-1 in more depth. It is well accepted that PECAM-1 exerts its role in this context in a homophilic manner where EC PECAM-1 interacts with leukocyte PECAM-1. However, heterophilic interactions have also been reported such as interactions with CD177, a molecule detected on a subset of neutrophils (Sachs et al., 2007). Other more controversial heterotypic ligands are $\alpha_v\beta_3$-integrin, GAGs and CD38 present on lymphocytes although the precise function of these interactions are largely unknown. Studies by Mamdouh et al., (2003) have suggested a novel mechanism of PECAM-1 mediated leukocyte TEM involving the LBRC which provides a means of recycling proteins between the vesicle and the EC border (Mamdouh et al., 2003; Mamdouh et al., 2008). During leukocyte TEM the recycled PECAM-1 is directed to EC junctional areas where leukocytes are transmigrating. This source of PECAM-1 has been shown to support both paracellular and transcellular TEM (Mamdouh et al., 2009; Mamdouh et al., 2003) and provides novel insights into the regulation of PECAM-1 expression. Whilst of great interest, this mechanism has been based on *in vitro* assays and the existence of LBRCs *in vivo* is yet to be defined.

Other *in vivo* studies have demonstrated that the functional role of PECAM-1 during leukocyte TEM is dependent on the inflammatory stimulus, as IL-1β but not TNF-α-induced leukocyte transmigration is reduced in PECAM-1 KO mice (Thompson et al., 2001). This study also indicated that PECAM-1 has a transient role in mediating transmigration. Furthermore, the site of leukocyte arrest in PECAM-1 deficient mice (as shown by electron microscopy) was found to be between ECs and the

perivascular basement membrane (Figure 1.3) suggesting a key role for PECAM-1 at this stage. As mentioned previously, subsequent studies have suggested that leukocyte and EC PECAM-1 interaction upregulates key laminin receptors such as β_1-integrins (e.g. $\alpha_6\beta_1$), required for neutrophil transmigration through the perivascular basement membrane (Dangerfield et al., 2002).

1.7.3 JAM family

The JAMs are type 1 transmembrane proteins and are part of the Ig-like superfamily. JAMs consist of two groups, the classical members JAM-A, -B and –C and the other subgroup consists of ESAM, coxsackie adenovirus receptor (CAR), JAM-4 and JAM-like (JAM-L) protein (Dejana, 2004; Ebnet et al., 2004; Weber et al., 2007). Although these molecules (apart from JAM-4) have been reported to be involved in leukocyte migration, the classical JAMs have received most attention in recent years.

The classical JAMs are members of the Cortical Thymocyte markers for *Xenopu* (CTX) family, and are well known to be constitutively expressed at EC junctions (Ebnet et al., 2004; Weber et al., 2007). They are composed of an extracellular portion containing two N-terminal Ig domains incorporating disulphide bonds through conserved cysteine residues, a single transmembrane segment and a 40 amino acid cytoplasmic tail which has PDZ domain binding motifs (Figure 1.10). JAMs are known to exhibit homophilic and heterophilic binding to various integrins as well as other JAM family members. In addition to their EC junctional expression, JAM-A and JAM-C are known to be expressed on different leukocyte subsets and JAM-A is also found on platelets. During leukocyte migration some JAM members (e.g. JAM-A and JAM-C) have been shown to redistribute away from EC junctions (Weber et al., 2007) and thereby support leukocyte adhesion as well as TEM, although the mechanism by which this occurs is yet to be established.

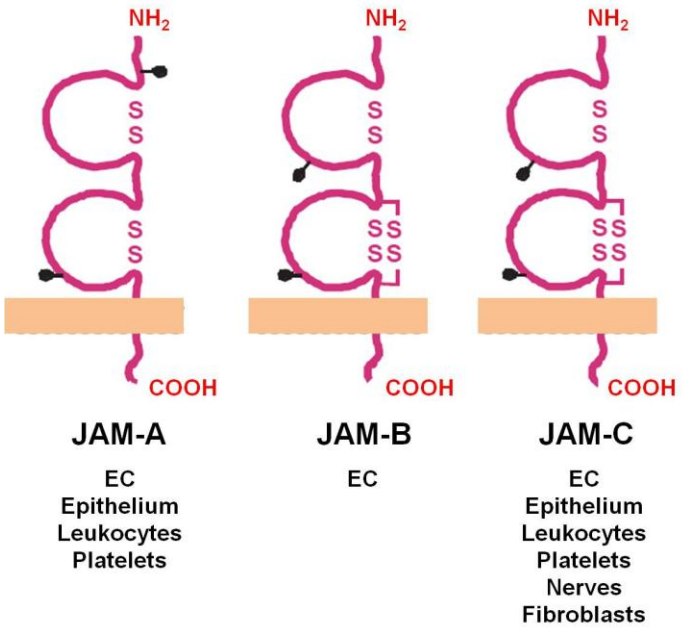

Figure 1.10: Structure of classical JAMs.

JAMs are transmembrane glycoprotein proteins belonging to the Ig-like super family of adhesion molecules. They consist of extracellular domain containing 2 Ig-like domains, a transmembrane domain and a cytoplasmic tail. JAM-A, B and C are sub grouped into the CTX family and are strongly implicated in leukocyte migration. Key components of JAMs have been shown; S-S disulfide bridges and • N-linked glycosylation sites. Diagram adapted from Ebnet et al., 2004.

1.7.4 JAMs in leukocyte transmigration

JAM-A binds to leukocyte LFA-1 and is expressed on ECs, leukocytes and platelets. Its expression on ECs is known to be redistributed, cleaved or upregulated upon inflammation in some *in vitro* models (Weber et al., 2007). It has also been specifically implicated in leukocyte extravasation at the level of the EC, proximal to that of PECAM-1 (which is at the level of the basement membrane) (Woodfin et al., 2009). Like PECAM-1 its role is dependent on the direct activation of ECs (Woodfin

et al., 2009). Leukocyte JAM-A has also been implicated in leukocyte directional motility through regulating the activity of the actin cytoskeleton (Dejana, 2004).

JAM-B binds to VLA-4 on leukocytes, JAM-C on leukocytes and ECs and JAM-B on ECs. Interestingly it has a higher affinity for JAM-C than JAM-B. JAM-B expression is confined to ECs and has been detected in Peyer's Patches, lymph nodes, heart, brain and testes. It has been shown to have a role in leukocyte recruitment in various inflammatory models (Cunningham et al., 2002; Lamagna et al., 2005; Ludwig et al., 2005; Ludwig et al., 2009). Direct evidence for the role of JAM-B at specific stages of leukocyte extravasation comes from the use of a murine cutaneous IVM model where fluorescently labelled lymphocytes were injected in mice along with an anti-JAM-B antibody (mAb) (Ludwig et al., 2009). This study reported that anti-JAM-B treatment reduces T-lymphocyte rolling however, the authors also found that JAM-B had tissue-specific roles. The function of JAM-B in leukocyte recruitment is also found to be independent of JAM-C (Ludwig et al., 2005), however the mechanisms through which this protein regulates leukocyte migration are only just emerging and require further investigation.

Lastly JAM-C has roles independent to that of JAM-B as it can also bind to leukocyte MAC-1 and EC JAM-C. JAM-C is expressed on ECs, smooth muscle cells, fibroblast, nerves and testis. Its expression on ECs is known to be redistributed away from junctions upon inflammation and has been implicated in leukocyte extravasation using several models. More recently it has been directly linked to polarised neutrophil migration during paracellular TEM (Woodfin et al., 2011) although further studies are required to fully understand its role in this process.

1.7.5 ICAMs family

The ICAMs are type 1 transmembrane proteins part of the Ig-like superfamily, and are well known for their ability to bind to integrins. There are currently five members of this family: ICAM-1, -2, -3, -4 and -5. ICAM-1 has been most widely studied and has key roles in leukocyte extravasation along with ICAM-2. ICAM-3 is known to be involved specifically in dendritic cell migration where as ICAM-4 is implicated in some erythrocyte functions (e.g. in sickle cell anaemia) and ICAM-5 has been shown to have key roles in the development of neurones (Hayflick et al., 1998; Heping Yang, 2012; Toivanen et al., 2008). Each protein consists of 2-9 C-type Ig-like domains and is capable of binding to integrins and inducing numerous cellular events. As the current investigation focuses on leukocyte migration and very little is known about ICAM-3 only ICAM-1 and ICAM-2 will be discussed in detail below.

1.7.6 ICAM-1

ICAM-1 is constitutively expressed on ECs at low levels and is highly upregulated upon inflammation peaking at around 4-6 hours. ICAM-1 is also expressed on various leukocyte subsets and can be found in a soluble form in plasma of patients with cardiovascular disorders (Lawson and Wolf, 2009). ICAM-1 is known to be involved in APC/T cell interactions and signalling and is a key protein involved in leukocyte transmigration (Albelda et al., 1994; Hayflick et al., 1998).

ICAM-1 (CD54) is a 90-110 kDa protein (depending on its glycosylation status) and is well known for its ability to bind to key integrins. It is composed of an extracellular domain containing five N-terminal Ig-like domains, a transmembrane domain and a cytoplasmic tail (Figure 1.11) (Toivanen et al., 2008). The three Ig-like domains are crucial for heterophilic ligand interaction, whereas the cytoplasmic domain contains residues that are important in cell signalling which enables it to have a close interaction with the cytoskeleton (Figure 1.11). ICAM-1 has binding

affinity for the β_2-integrins LFA-1 and MAC-1 on leukocytes, fibrinogen, rhinoviruses and *Plasmodium falciparum*-infected erythrocytes. ICAM-1 also undergoes inside-out signalling where it can bind to adaptor proteins such as ERM, talins and kindlins to regulate its affinity and avidity for its ligand.

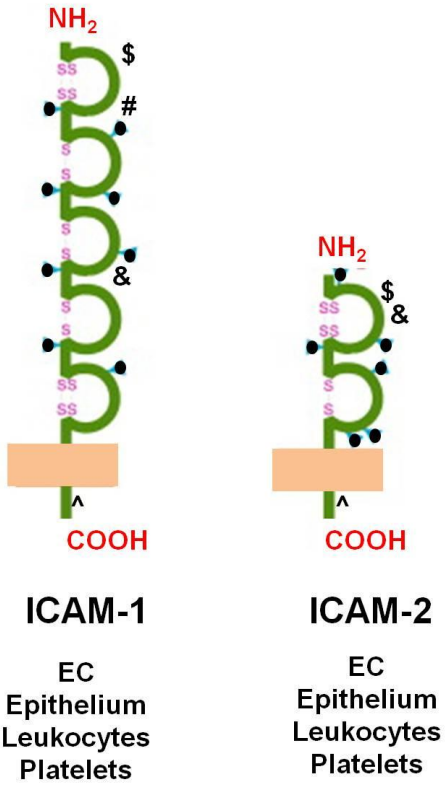

Figure 1.11: Structure of ICAM-1 and ICAM-2.

ICAMs are transmembrane glycoproteins belonging to the Ig-like super family of adhesion molecules. ICAM-1 and ICAM-2 are strongly implicated in leukocyte migration. They consist of extracellular domain containing 5 or 2 Ig-like domains, a transmembrane domain and a cytoplasmic tail. Key components of ICAM-1 and ICAM-2 have been shown; S-S disulfide bridges, • N-linked glycosylation sites, $ LFA-1 binding, & MAC-1 binding and # fibrin(ogen) binding. Diagram adapted from Toivanen et al., 2008.

1.7.7 ICAM-1 in leukocyte transmigration

The role of ICAM-1 at specific stages of the leukocyte adhesion cascade has been studied for many years and it has been implicated in all key stages of this process. It has been described as a molecule that supports slow rolling (Ley et al., 2007) or the transition between rolling and adhesion however it is most well known to mediate adhesion. Almost no leukocyte transmigration occurs if the function of this molecule is inhibited in a wide range of *in vitro* and *in vivo* models, confirming its key role in this process. It is now becoming clear that ICAM-1/LFA-1 interactions are involved in adhesion where as ICAM-1/MAC-1 interactions are involved in leukocyte crawling (Phillipson et al., 2006; Sumagin et al., 2010). Heterogeneous ICAM-1 expression on ECs during inflammation has been linked to leukocyte crawling and ICAM-1 clustering is deemed to influence the 'preferred' sites of leukocyte TEM (Sumagin and Sarelius, 2010). Furthermore transmigratory cups containing F-actin surrounded by various integrin and adaptor proteins are also enriched with ICAM-1 (Carman and Springer, 2004). This occurs through the activation of ICAM-1 which induces Ca^{2+} influx activating signalling pathways such as p38, Rho and MECS. These signalling pathways regulate cell polarisation and facilitate migration of leukocytes through ECs by destabilising endothelial junctional bonds (Ridley, 2003). Recently ICAM-1 has been found on pericytes and was demonstrated to be involved in abluminal neutrophil crawling between ECs and the pericyte sheath (Proebstl et al., 2012).

Another key area of research focuses on the co-operative and redundant roles of ICAM-1 relative to that of ICAM-2. At present the results from the literature imply that these molecules have distinct and overlapping functions that can be co-operative or redundant in some cases depending on the inflammatory model and the subset of leukocyte. There is data to suggest that only in the absence of functional ICAM-1, ICAM-2 is involved in TEM of T cells (Reiss et al., 1998). In support of this study a different group has also shown that ICAM-1 has a co-operative role with ICAM-2 in lymphocyte migration across lymph nodes however this study also demonstrated that ICAM-1 has ICAM-2-independent roles in lymphocyte migration to inflamed tissues

(Lehmann et al., 2003). A more recent study showed that T cell polarization and crawling under physiological shear flow is supported by EC ICAM-1 and in its absence, by EC ICAM-2 (Steiner et al., 2010) although ICAM-2 can only partially compensate for the lack of ICAM-1 in these early stages (Boscacci et al., 2010). Studies by Issekutz et al (1999) showed an additive reduction of neutrophil extravasation when ICAM-1 and ICAM-2 were both blocked however they found no effect when ICAM-2 alone was inhibited. Collectively these studies demonstrate that ICAM-1 and ICAM-2 exhibit some co-operative roles which seem to be largely dependent on the experimental model and/or the subtype of leukocyte being investigated.

1.8 ICAM-2

ICAM-2 (CD102) is a 55 kDa protein and is well known for its role in leukocyte recruitment through binding to key leukocyte integrins. More specifically it has been shown to have extracellular binding affinity to the integrins LFA-1 (Li et al., 1993; Staunton et al., 1989) and MAC-1 (Xie et al., 1995), VLA-4 (Seth et al., 1991) and DC-SIGN (Geijtenbeek et al., 2000). ICAM-2 is composed of an extracellular domain containing two N-terminal Ig-like domains, a transmembrane domain and a short 28 amino acid cytoplasmic tail (Figure 1.11) (Staunton et al., 1989). Domain 1 consists of 85 amino acid residues, and has a disulphide bond creating a compact, flat structure. It has a highly conserved glutamine residue at position 37 which is crucial for interacting with LFA-1 (Casasnovas et al., 1997). Domain 2 is much larger and is positioned so that the functional N-terminal faces away from the cell membrane (Casasnovas et al., 1997). ICAM-2 has many structural similarities to ICAM-1 specifically, the two Ig domains of ICAM-2 have a 35% homology to that of ICAM-1. However as ICAM-2 has a smaller N-terminal relative to ICAM-1 it is believed to have restricted accessibility for ligands. For this reason LFA-1 is thought to have a much lower affinity for ICAM-2 relative to that of ICAM-1. Like most Ig-like

proteins it is secured by disulphide bridges and consists of numerous glycosalytion sites (Figure 1.11). LFA-1 and MAC-1 bind to the first Ig domain and precise site of DC-SIGN binding to ICAM-2 is currently unknown, although this is thought to be the primary ligand for ICAM-2 due to its high affinity for ICAM-2 (Geijtenbeek et al., 2000). It has also been demonstrated to bind in *trans* in a homophilic manner (Huang et al., 2005). ICAM-2 can form intracellular interactions with ezrin (Heiska et al., 1996; Yonemura et al., 1998) and α-actinin (Heiska et al., 1996) which implies it has a key role in intiating intracellular signalling.

Based on the high basal expression of ICAM-2 and the fact that this protein remains unchanged during inflammation, ICAM-2 was initially deemed more relevant in lymphocyte recirculation. There is now however strong evidence for a role of ICAM-2 in leukocyte transmigration (Huang et al., 2006; Woodfin et al., 2009). There are also some studies that have indicated that ICAM-2 could be involved in other cellular processes such as apoptosis (Helander et al., 1996; Perez et al., 2002), angiogenesis (Huang et al., 2005), immune cell activation (Carpenito et al., 1997)(Carpenito et al., 1997; Carpenito.C et al., 1997), signalling (Perez et al., 2002; Yonemura et al., 1998), osteoclastogensis (Li et al., 2012), transepithelial migration (Gerwin et al., 1999; Porter and Hall, 2009) and surveillance in pancreatic carcinogenesis (Hiraoka et al., 2011) although these areas are poorly understood. Exciting data demonstrating ICAM-2 transfection using adenovirus vector might be an effective form of gene therapy(Carpenito.C et al., 1997) for peritoneal metastasis of gastric cancer due to its involvement in recruiting immune cells to the site (Tanaka et al., 2004) has been shown. Additionally high gene expression of ICAM-2 in patients with acute conary syndrome has also been reported (Glogowska-Ligus et al., 2012) and a suppression of metasis potential in ICAM-2 expressing neuroblastoma cells *in vivo* (Feduska et al., 2013). These studies provide further indications that the specific functions of ICAM-2 are poorly understood and require further investigations.

1.8.1 ICAM-2 expression

ICAM-2 is constitutively expressed on ECs and is not generally thought to be regulated during inflammatory responses (de Fougerolles et al., 1991), although there are some reports of a down regulation in expression (Godwin et al., 2004; McLaughlin et al., 1999; McLaughlin et al., 1998). In more clinical models there appears to be an up-regulation of ICAM-2 (Alizadeh et al., 2000; Bernstein et al., 1998; Gerwin et al., 1999; Hiraoka et al., 2011; Renkonen et al., 1992) although this could be linked to its expression on epithelial cells (Porter and Hall, 2009) rather than ECs. It is also known to be expressed on neutrophils (Sundd et al., 2012), monocytes (de Fougerolles et al., 1991), T cells (de Fougerolles et al., 1991), eosinophils (Gerwin et al., 1999), natural killer cells (Helander et al., 1996; Somersalo et al., 1995), platelets (Diacovo et al., 1994; Kuijper et al., 1998) and synovial cells (Singh et al., 2006). ICAM-2 is constitutively expressed at much higher levels than ICAM-1 (15-fold) on ECs under basal conditions and unlike ICAM-1 which is well known to be highly inducible by various inflammatory stimuli (e.g. IL-1β and TNF-α) ICAM-2 is not. Although ICAM-2 is highly conserved, its expression is found to be variable across species and therefore it's function may also vary in this respect (Godwin et al., 2004).

1.8.2 ICAM-2 in leukocyte transmigration

Despite the fact that both ICAM-1 and ICAM-2 were cloned just over 20 years ago (Horley et al., 1989; Staunton et al., 1989), relative to ICAM-1 very little is known about the functions of ICAM-2. ICAM-2 was initially heavily implicated in the recruitment of lymphocytes (Boscacci et al., 2010; Lehmann et al., 2003; Steiner et al., 2010; Reiss et al., 1998) however to date it has now been linked to the recruitment of neutrophils (Hobden, 2003; Huang et al., 2006; Issekutz et al., 1999; Sundd et al., 2012; Woodfin et al., 2009), monocytes (Schenkel et al., 2004), eosinophils (Gerwin et al., 1999), natural killer cells (Somersalo et al., 1995) and dendritic cells (Geijtenbeek et al., 2000). Very few studies have however have attempted to elucidate the mechanisms through which ICAM-2 supports leukocyte

extravasation. Those studies which have addressed this question have shown that ICAM-2 is implicated in natural killer cell polarisation during crawling, a process which maybe regulated by F-actin polymerisation at the leading edge (Somersalo et al., 1995). Other studies have demonstrated a role for EC ICAM-2 in monocyte 'locomotion' on human umbilical vein endothelial cells (HUVECs) through its interaction with β_2-integrins (Schenkel et al., 2004) and in lymphocyte polarisation and crawling in a blood brain barrier model *in vitro* (Steiner et al., 2010). The latter role was suggested to occur co-operatively with that of ICAM-1 and this property has been confirmed in numerous other studies (Boscacci et al., 2010; Huang et al., 2006; Lyck et al., 2003; Steiner et al., 2010). A recent report has identified a role for neutrophil ICAM-2 in stabilising rolling through interactions with neutrophil LFA-1 (Sundd et al., 2012). However the majority of reports that have linked ICAM-2 to leukocyte extravasation consider this phenomenon to be mediated by EC ICAM-2 (Boscacci et al., 2010; Schenkel et al., 2004; Steiner et al., 2010; Woodfin et al., 2009). ICAM-2 is specifically considered to be involved in regulating neutrophil transmigration into the tissue, but not adhesion *in vivo* (Huang et al., 2006; Woodfin et al., 2009) however the ligand and the precise mechanisms by which it contributes to neutrophil extravasation are largely unknown, and these questions form the focus of the present investigation.

1.9 Aims and hypothesis

At present little is known about the functional role of ICAM-2 in acute inflammation and this was further investigated in the current study. It was hypothesised that ICAM-2 supports neutrophil extravasation via mechanisms occurring prior to the completion of TEM. The overall aim of this study was therefore to investigate the involvement of ICAM-2 in regulating neutrophil extravasation *in vivo* by addressing the following key objectives:

1.9.1 Investigate the cellular distribution of ICAM-2 expression

To date no study has investigated the possibility of EC ICAM-2 redistribution during inflammation. Therefore post-capillary venules of the mouse cremaster muscle and the ear dermal vasculature were analysed for the precise sub-cellular location of ICAM-2 within individual ECs. Using the cremasteric tissues a more detailed analysis of the expression of ICAM-2 was carried out under control and inflamed conditions to examine potential changes in expression of ICAM-2. ICAM-2 expression on different blood leukocyte subsets was also studied.

1.9.2 Anaylse the functional role of endothelial ICAM-2 in neutrophil-EC interactions during neutrophil extravasation

To elucidate the specific function of ICAM-2 during inflammatory conditions *in vivo*, neutrophil-EC interactions were investigated in IL-1β-stimulated mouse cremaster muscles. Using confocal IVM of mice expressing eGFP in neutrophils (Lys-eGFP-ki mice), and *in vivo* EC labelling, neutrophil crawling and TEM dynamics were quantified in both WT and ICAM-2 deficient mice.

1.9.3 Examine the potential neutrophil ligand for ICAM-2 that supports neutrophil-EC interactions

ICAM-2 is well known to interact with β_2-integrins. The function of ICAM-1, MAC-1 and ICAM-2 in IL-1β-stimulated neutrophil-EC interactions were analysed using confocal IVM. Using this approach, the potential interaction of EC ICAM-2 with

neutrophil MAC-1 was investigated. The contribution of ICAM-1 in this model was examined to account for any ICAM-1 dependent MAC-1 functions.

1.9.4 Develop a cremasteric Shwartzman reaction model.

To enable the possibility of extending the above investigations of IL-1β-induced inflammation to a more complex, pathologically relevant model, a cremasteric Shwartzman reaction IVM model was developed as part of this work. This response shows neutrophil recruitment, formation of microthrombi and haemorrhage, and can be used in future work for investigating the role of ICAM-2 as well as other adhesion molecules in these responses by IVM.

CHAPTER 2: Materials and methods

2.1 Animals and reagents

2.1.1 Animals

Male mice (20–25g) of several different genotypes were used in this study. All mice, including genetically modified animals, were on a C57BL6 background. Wild-type (WT) C57BL/6 mice were purchased from Charles River Laboratories (Margate, United Kingdom), and ICAM-2 KO mice (Gerwin et al., 1999) were a gift from Prof. Britta Engelhardt (Theodor Kocher Institute, University of Bern, Switzerland). For live imaging WT or ICAM-2 KO mice with eGFP gene knocked-in (ki) to the lysozyme M (Lys) locus (Lys-eGFP-ki) resulting in exhibition of eGFP in myelomonocytic cells (Faust et al., 2000) were used. This genotype of mouse expresses high levels of eGFP in neutrophils and a lower level in monocytes. No differences in neutrophil responses have been reported using either the homozygous or heterozygous Lys-eGFP-ki mice in our model, however only mice heterozygous for Lys-eGFP-ki were used in the present study. ICAM-2 KO x Lys-eGFP-ki mice were generated in-house for this study by interbreeding the ICAM-2 KO mice with Lys-eGFP-ki mice, yielding animals deficient in ICAM-2 (homozygous) with eGFP positive neutrophils and monocytes (heterozygous). C57BL/6 mice in which the gene for eGFP has been knocked-in to the CX3CR1 locus (CX3CR1-eGFP-ki), resulting in the expression of eGFP in all monocytes (as well as in natural killer cells and some T cells) but not in neutrophils obtained from the European Mutant Mouse Archive (Orleans, France) were also used. No differences in leukocyte transmigration using heterozygous CX3CR1-eGFP-ki mice compared to WT have been reported. However, homozygous mice CX3CR1-eGFP-ki mice have shown some differences in leukocyte migration compared with WT, therefore only mice heterozygote for CX3CR1-eGFP-ki were used during the course of this study. All animals were housed in individually ventilated cages and animal facilities were regularly monitored for health status and infections. All *in vivo* experiments were

performed under the UK legislation for the protection of animals, and animals were humanely killed by cervical dislocation in accordance with UK Home Office regulations.

2.1.2 Antibodies

All monoclonal antibodies (mAbs) used during the course of this study were raised against mouse proteins. Anti-ICAM-2 mAb (3C4; rat IgG2a), isotype control mAbs (rat IgG2a and rat IgG2b) were obtained from Serotec (Kidlington, United Kingdom). Anti-ICAM-1 mAb (YN-1; rat IgG2b), anti-PECAM-1 mAb (C390; rat IgG2a), APC-labelled anti-CD115 (AF598; rat IgG2a), Alexa Fluor 647-labelled anti-CD3 (17A2; rat IgG2B), anti-VE-cadherin (BV14; IgG2b) and anti-integrin alpha IIb (CD41)-phycoerythrin (PE) (MWReg30; rat IgG1) was from eBiosciences (Hatfield, United Kingdom). Anti-MAC-1 (M1/70; rat IgG2b), Alexa Fluor 488-labelled anti-ICAM-2 (3C4; rat IgG2a), PE-labelled anti-GR1 (Ly-6 G/Ly-6 C) (RB6-8C5; rat IgG2b) and PE-Cy7-labelled anti-B220 (RA3-6B2; rat IgG2a) was purchased from Biolegend (Cambridge, United Kingdom). Anti-CD16/CD32 (2.4G2, rat IgG2b) was from BD Pharmingen (Oxford, United Kingdom). Anti-α-smooth muscle actin (α-SMA)-Cy3 (1A4; mouse) was from Sigma (Saint Louis, USA). Monoclonal antibody Alexa Fluor conjugation kits were from Invitrogen (Paisley, United Kingdom). The following antibodies were conjugated in-house; anti-PECAM-1 (CD31) mAb, anti-ICAM-2 mAb, anti-ICAM-1, anti-VE-cadherin and appropriate isotype controls. All mAb given *in vivo* had low endotoxin levels based on the manufactures data sheets.

2.1.3 Inflammatory stimuli

Recombinant mouse interleukin-1β (IL-1β) was purchased from R&D systems (Abingdon, United Kingdom). Lipopolysaccharide (LPS) from E.coil 011:B4 was obtained from Sigma-Aldrich (Dorset, United Kingdom).

2.1.4 Other Miscellaneous reagents

Triton X-100, Tyrode's salts and Dextran fluorescein isothiocyanate (FITC) (Molecular weight: 150,000 ~ 85 Angstroms (8.5nm) were purchased from Sigma-Aldrich (Dorset, United Kingdom). Ketamine (Ketaset) was from Fort Dodge Animal Health Ltd (Southampton, United Kingdom) and Xylazine (Rompun) was from Bayer (Newbury, United Kingdom).

2.2 Flow cytometry

Flow cytometry was used to establish the percentage of circulating blood leukocytes in WT and ICAM-2 KO mice and expression of ICAM-2 on different leukocyte subsets. Blood samples were collected from unstimulated WT and ICAM-2 KO mice by cardiac puncture following cervical dislocation. This procedure was carried out by cutting through the ribcage to gain access to heart directly. Blood was removed using a needle and syringe containing 50µl of 0.5M Ethylenediaminetetraacetic acid (EDTA) solution. Approximately 0.5-1 ml blood per animal was withdrawn from the right ventricle in each animal. Blood cells were washed by centrifuging the sample at 300g for 5 mins at 4°C, removing the serum supernant and, resuspending in PBS.

2.2.1 Total leukocyte counts

Total live cell counts were performed with a Neubauer haemocytometer (Optik Labor, Germany) using 0.4% trypan blue (Sigma) and expressed as cells/ml. Trypan blue is a dye that enables identification of dead cells, which are permeable to the dye and appear blue under light microscopy. Viable cells exclude the dye and appear colourless and refractile under phase contrast. A 1:1 dilution of the cell suspension in trypan blue was used for cell counts. Approximately 10µl of the mix was loaded onto the haemocytometer and the cells were viewed under a microscope (Olympus BH2-RFCA) at 100 X magnification.

2.2.2 Staining of ICAM-2 in different leukocyte subsets

Unspecific Fc-receptor mediated mAb binding was blocked by incubating 50µl of the washed blood cells with 0.5µg Fc block for 15 mins on ice. Each sample was labelled with a mixture of fluorescently conjugated antibodies or their specific isotype control. Antibody mixture was made up to 50µl using FACs buffer (PBS and 1% heat inactivated goats serum) and samples were stained for CD115, Gr-1, B220 and ICAM-2 or CD3, Gr-1, B220 and ICAM-2. Samples were incubated for 30 mins at 4°C in the dark with the mAb solution. Blood cells were then pelleted by centrifugation at 300g for 5 min at 4°C to remove unbound mAb, and the cell pellet was resuspended in 500µl ACK lysis buffer (150mM NH_4Cl, 1 mM $KHCO_3$, 0.1 mM EDTA, pH 7.3.) at room temperature for 5 mins, to lyse the erythrocytes. After lysis, cells were spun again under the same conditions, resuspended in 200µl FACS-PBS buffer (1% goat serum in PBS) to obtain a uniform suspension of single cells. Data acquisition was performed using FACS-calibur flow cytometer (Beckson Dickinson, Oxford, UK) with CellQuest software (Beckson Dickinson). 20,000 leukocytes were acquired per sample and analysed using FlowJo 7.6.1. ICAM-2 KO blood samples acted as the control for ICAM-2 staining. Unstained and single stained samples for all markers were carried out in every experiment to detect background staining of leukocytes (auto-fluorescence).

2.2.3 Identification of leukocyte subsets

Back gating from single stained antibodies confirmed which subsets were leukocytes in the forwards and side scatter plots. During data analysis leukocyte populations were gated out based on forward scatter (FSC) and side scatter (SSC) (Figure 2.1A). Neutrophils and the two monocyte subsets (classical and non-classical) were distinguished by Gr-1 labelling intensity versus CD115 intensity after removing B220 negative cells to exclude B cells (Figure 2.1D). Neutrophils were identified as a Gr-1 high and CD115 negative population, classical monocytes were identified as Gr-1 low and CD115 positive cells and non-classical monocytes were Gr-1 and CD115 positivity (Figure 2.1D). B cells and T cells were identified by B220 and

CD3 expression respectively (Figure 2.1B and C). Total neutrophil, classical and non-classical monocyte, B cell, and T cell numbers were calculated by multiplying the percentage of leukocytes (derived from flow cytometry) by total leukocyte count (derived by trypan blue staining). These different leukocyte subsets were then analysed for ICAM-2 expression where the percentage of ICAM-2 positive cells and the relative fluorescent intensity (RFI) of each leukocyte subset analysed was determined (Figure 2.2).

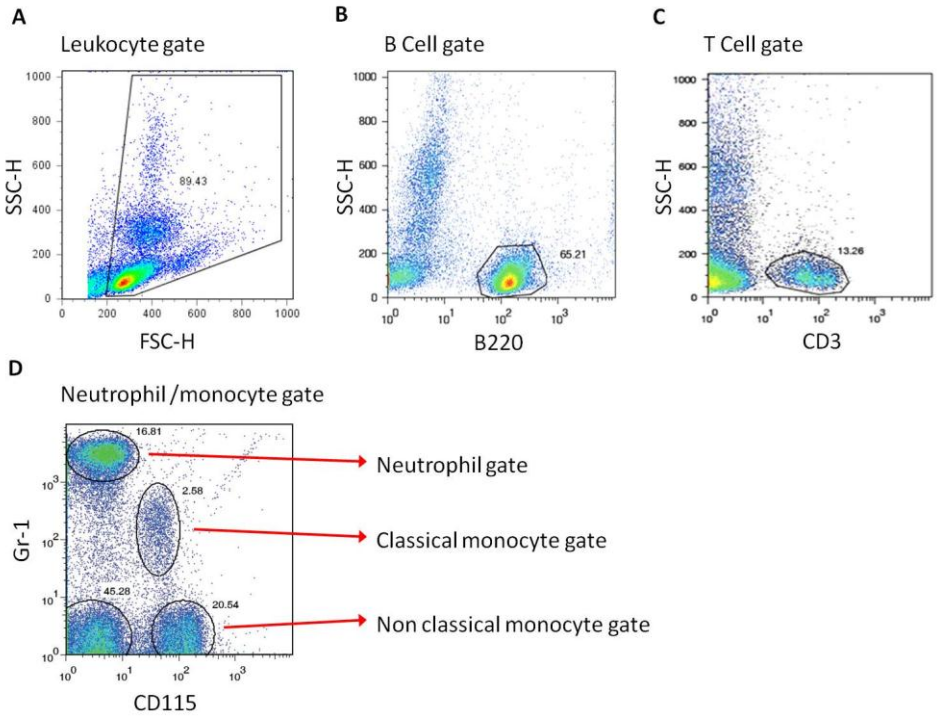

Figure 2.1: Representative flow cytometry plots demonstrating the gating strategies for identification of leukocytes subsets.

(**A**) Leukocytes were identified based on the FSC/SSC scatter. (**B**) B220 positive B cell population. (**C**) CD3 positive T cell population (**D**) Gr-1 high neutrophils, Gr-1 high and CD115 positive classical monocytes and Gr-1 low and CD115 positive non-classical monocyte populations. Double negative population represent lymphocytes.

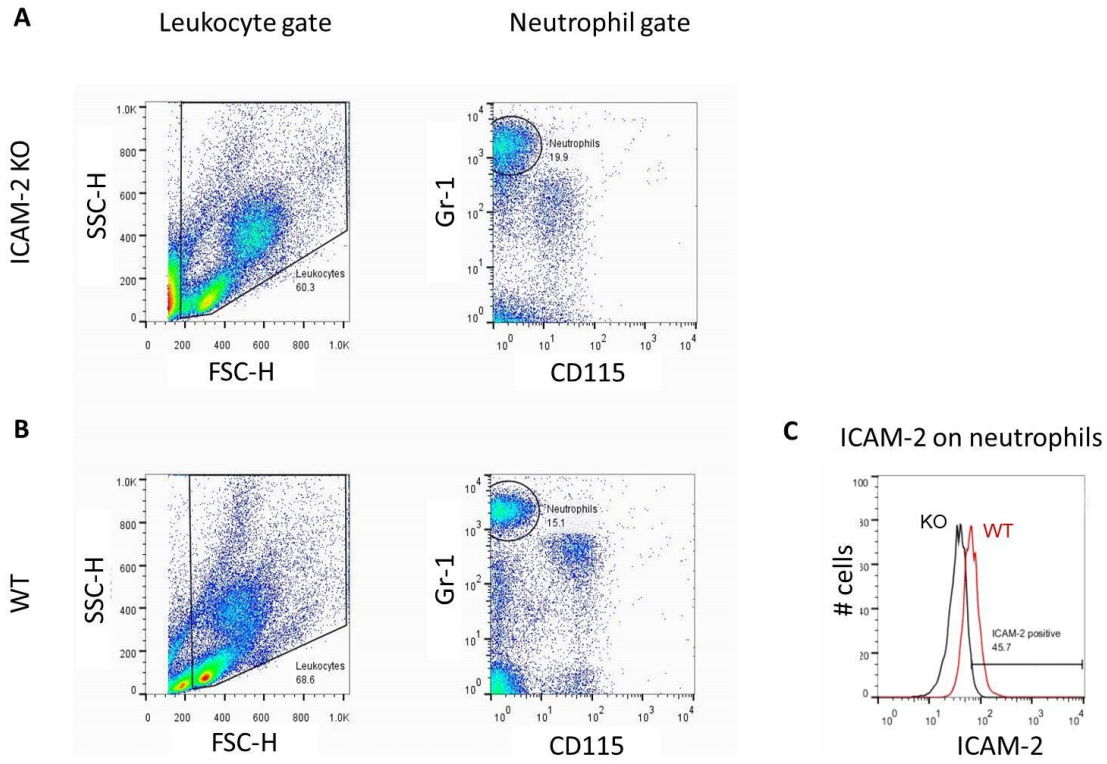

Figure 2.2: Representative flow cytometry plots demonstrating gating strategies for identification of ICAM-2 expression on neutrophils.

Neutrophils were identified based on the surface expression Gr-1 in both (**A**) ICAM-2 Kos and (**B**) WTs. (**C**) The percentage of neutrophils which stained positive for ICAM-2 was determined in WTs (red line). Gating strategies were based on negative control samples taken from ICAM-2 KO mice (black line). The RFI of fluorescently labelled ICAM-2 in each leukocyte subset was also determined.

2.3 Cremaster muscle

The functional role of ICAM-2 in various vascular responses was predominately investigated using a mouse model of cremasteric IVM. This method enables direct

visualisation of vascular processes in real time *in vivo*. Brightfield and confocal IVM were used during the course of the study. Brightfield IVM was used to measure leukocyte rolling flux, adherent and transmigrated leukocytes. Confocal IVM was used to quantitatively analyse EC expression and distribution of adhesion molecules, subset of recruited leukocytes (intravascular and extravascular), the dynamics of leukocyte-EC interactions, leukocyte TEM dynamics, leukocyte-platelet interactions and vascular perfusion. This was carried out using fluorescent immunolabelling of specific proteins, in conjunction with genetically modified mice which express endogenous eGFP in specific cells. In some studies pre-treatment with functional blocking antibodies and/or inflammatory stimuli was carried out. Specific details of immunolabelling and pre-treatment are described in the relevant sections.

2.3.1 Cremasteric muscle dissection

For all IVM studies mice were anesthetized by intraperitoneal (i.p.) injection of Ketamine (100 mg/kg) and Xylazine (10 mg/kg) and maintained at 37°C on a custom-built, heated microscope stage. The cremaster muscle is a thin layer of striated muscle that surrounds the testicle (Figure 2.3). It is commonly used for IVM because of the thin translucent nature of this tissue which allows direct visualisation of the microvasculature *in vivo*. To isolate this tissue, a midline incision was made in the scrotum making sure not to damage the underlying tissues and testis (Figure 2.3B). The testicles were gently drawn out by separating the underlying connective tissue from the cremaster muscle. The distal end of the cremaster muscle was pinned to the viewing column of the microscope stage to keep the cremaster muscle exteriorised (Figure 2.3C). An incision was made along the centre of the muscle, ensuring that the main artery and venule going into and out of the tissue was kept intact (Figure 2.3D). The cremaster muscle was then opened and pinned flat over the viewing window. The connective tissue attaching the testis to the cremaster muscle was then cut to enable the testes to be laid toward the side so that the entire cremasteric microvasculature could be clearly observed (Figure 2.3D). The cremaster muscle was kept moist with continous flow of warm Tyrodes buffered solution. Care was taken to ensure limited contact between the dissecting instruments and the

cremaster muscle throughout surgery. The cremaster muscles were then ready to be viewed under a microscope (confocal or brightfield) for detailed analysis of vascular responses.

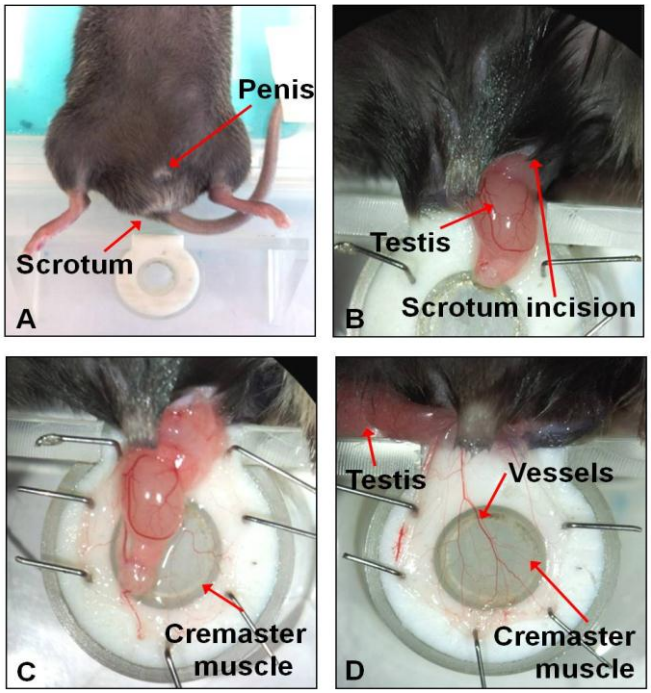

Figure 2.3: Surgical exteriorisation of the mouse cremaster muscle.

The cremaster was exteriorized (**A,B**) and pinned out flat over the optical window (**C**). The mesentary connecting testis and the cremaster muscle was cut and the testis moved out of the field of view (**D**). The microscope stage was kept at a constant temperature and was superfused with Tyrode's solution to keep the tissue moist throughout surgery.

2.4 Endothelial protein expression and distribution

2.4.1 Whole mount cremasteric immunostaining

The vascular expression profile of VE-cadherin, PECAM-1 and ICAM-2 was initially investigated by immunofluorescent staining and confocal microscopy of whole mount murine cremaster muscle and ears. WT mice were injected intravenously (i.v.) with a blocking mAb directed against ICAM-2 (3mg/kg). After 10 min animals were killed by cervical dislocation. Cremaster muscles were dissected from the mouse (Figure 2.3) and pinned out on a piece of wax. In some experiments the vasculature of the ear was also used. Tissues (cremaster and ear) were fixed in 4% PFA for 30 mins at 4°C. Immunofluorescent staining of whole mounted tissues was then performed. Tissues were permeabilised after fixation with blocking buffer (0.5 % Triton X-100 and 10 % foetal calf serum and 10 % goat serum in PBS) for 2 hour, at room temperature on a gentle rotator. Tissues were then incubated with appropriate secondary mAb for anti-ICAM-2 mAb for 2 hours in the dark. Tissues were washed 3 times with PBS on a shaker and re-blocked in PBS containing 20% serum with purified rat IgG2a for 1 hour. The tissues were finally incubated with two endothelial markers (anti-PECAM-1 conjugated to Alexa Fluor 488 mAb and anti-VE-cadherin conjugated to Alexa Fluor 647 mAb) for 24 hours in the dark. After a final PBS wash, the tissues were mounted on glass slides and viewed under a confocal microscope. Analysis of the distribution of ICAM-2 on different parts of the vascular tree was carried out using Imaris (Bitplane, Zurich, Switzerland) 3D analysis software.

2.5 Intravital microscopy

2.5.1 Pre-treatments and *in vivo* labelling

In some studies live confocal IVM was used to analyse EC expression of ICAM-2 in unstimulated (saline) or IL-1β-stimulated cremaster muscles. Animals were sedated via intramuscular (i.m.) injection of 1 ml/kg anaesthetic (40 mg/kg Ketamine and 2 mg/kg Xylazine in saline) and were subsequently subjected to intrascrotal (i.s.) injection of IL-1β (50 ng/400μl saline) in order to stimulate an inflammatory response. Control animals were given saline (i.s.) alone. Saline or IL-1β injections were given in conjugation with a non-blocking anti–mouse Alexa Fluor 647–labelled PECAM-1 mAb (2μg/mouse) and an anti–mouse Alexa Fluor 488–labelled ICAM-2 mAb (4μg/mouse) in order to quantitatively analyse the relative distribution patterns of PECAM-1 (a well-established EC junctional marker) and ICAM-2. In some experiments an anti–mouse Alexa Fluor 555–labelled ICAM-1 mAb (4μg/mouse) was also administered. 4 hours after i.s. injections, the cremaster muscles were prepared for confocal IVM as described previously.

2.6 Confocal microscopy

Tissues were viewed using a Leica SP5 confocal microscope with a 20× water-dipping objective (NA 1.0) (Figure 2.4). *Z*-stack images of 3-5 post-capillary venules per cremaster, with a diameter of 25–45μm, good blood flow and few branches were selected for analysis (3-4 mice per group). Images of half vessels were acquired by sequential scanning of the 488 and 633nm channels at a resolution of 1024 × 512 pixels in the *x*-*y* plane and 0.5μm steps in *z*-direction corresponding to a voxel size of 0.23 × 0.23 × 0.49μm in *x*-*y*-*z* respectively. Microscope settings were optimised to exclude signal from non-specific binding of mAb using isotype control labelled

tissues, or tissues from mice genetically deficient for the protein of interest. Quantification of the expression and distribution of ICAM-2 on venular ECs was carried out using Imaris 3D analysis software.

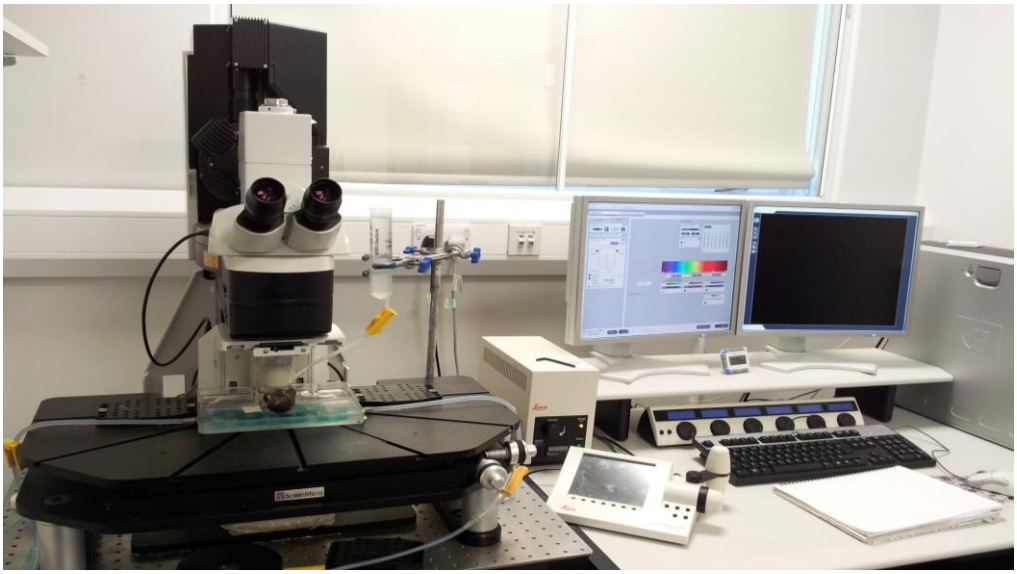

Figure 2.4: Leica SP5 confocal microscope incorporating a 20× water-dipping objective (NA 1.0) fitted with 561, 488 and 633 nm lasers.

Mice were placed on a heated stage and the cremaster muscle was exteriorized and superfused with Tyrodes buffered solution. Z-stack images of vessels were acquired and reconstructed in to 3D models using Imaris software.

2.6.1 Quantifying vascular distribution of proteins

Vascular distribution of ICAM-2 was deternained through the creation of an isosurface using Imaris software. An isosurface is a two dimensional object built on the surface of a 3D object (i.e. the vessel) based on it's intensity in the selected fluorescent channel. The fluorescent intensity of the selected channel can then be specifically quantified within the isosurface. This enables the expression of the protein of interest, in this case ICAM-2, within a known structure (PECAM-1

expressing endothelial cells) to be quantified. This software module is able to identify voxels belonging to an object in a single fluorescent channel. The criterion for the identification is the grey value for the voxel hence is able to distinguish between high and low intensites. An isosurface of the whole vessel was created (as previously described in Proebstl et al., 2012) using the PECAM-1 channel, and the fluorescence intensity of Alexa Fluor labelled PECAM-1 and ICAM-2 within this surface was quantified (Figure 2.5). This analysis determines the intensity of ICAM-2 staining within the PECAM-1 positive areas. A differential analysis of the intensity of EC junctional and non-junctional expression levels was carried out by creating isosurfaces with threshold settings on either high intensity PECAM-1 at the EC junctions, or on the low intensity PECAM-1 staining on the EC bodies (Figure 2.6). The intensity of both proteins within these regions was determined. The expression and distribution of ICAM-1 was also determined using the same method.

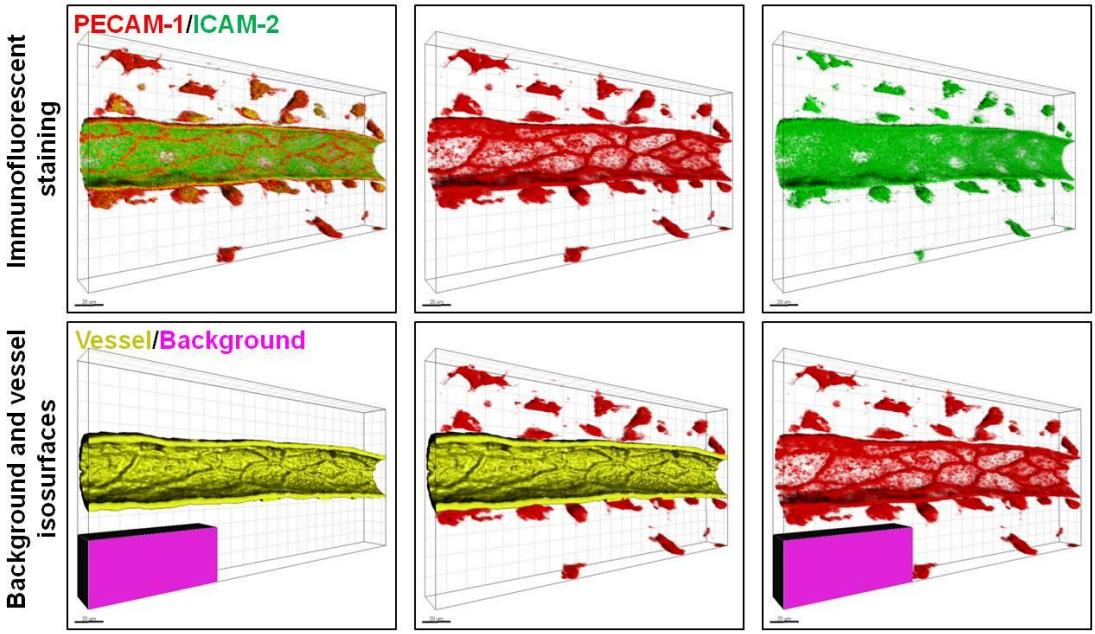

Figure 2.5: Whole vessel isosurfaces based on the immunostained PECAM-1 using Imaris software.

Isosurfaces were constructed using intensity thresholding on PECAM-1 in post-capillary venules. PECAM-1 (red/yellow) and ICAM-2 (green) labelling intensity within these isosurfaces could then be quantified. The background intensity was subtracted by creating an isosurface on an area devoid of venules (pink).

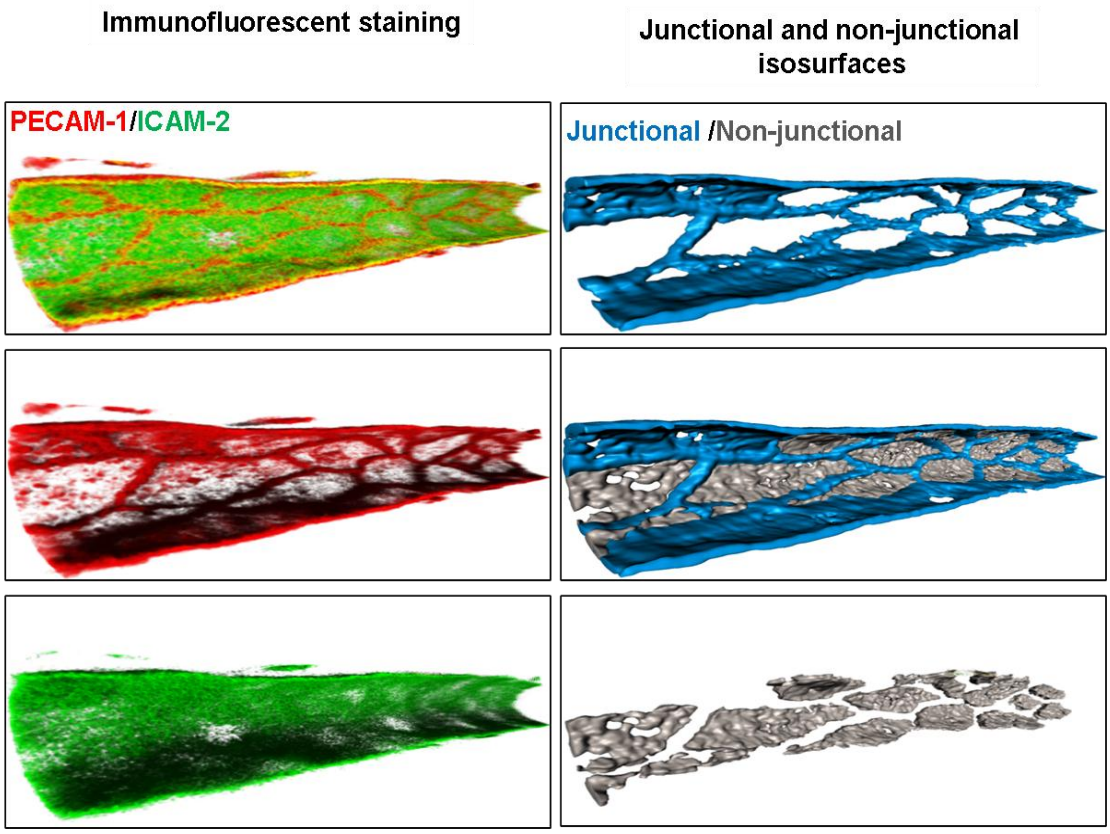

Figure 2.6: EC junctional and non-junctional isosurfaces based on the intensity of immunostained PECAM-1.

Isosurfaces were constructed using intensity thresholding on PECAM-1 high EC junctions, and PECAM-1 low cell bodies in post-capillary venules. The intensity of PECAM-1 (red/blue) and ICAM-2 (green/grey) within these isosurfaces could then be quantified.

2.6.2 Luminal neutrophil-EC interactions *in vivo*

To understand the role of ICAM-2 in neutrophil recruitment luminal leukocyte-EC interactions were analysed using confocal IVM. Cremaster muscles of WT or ICAM-2 KO x Lys-eGFP-ki mice were stimulated with saline or IL-1β, co-administered with a non-blocking Alexa Fluor 555–labelled PECAM-1 mAb (2 μg) in order to visualize the endothelium. For ICAM-2–, ICAM-1– and MAC-1–blocking

experiments the blocking mAb, or rat IgG2a (anti–ICAM-2 isotype) or rat IgG2b (anti–ICAM-1/MAC-1 isotype) control mAb, were administered (i.v. 3mg/kg) 15 minutes before IL-1β stimulation. To analyse the effect of the blocking anti–ICAM-2, anti–ICAM-1 and anti–MAC-1 mAbs confocal images of 3-5 post-capillary venules per cremaster muscle were taken at the end of the experiment (~4 hours after i.s. injections), and intravascular and extravascular leukocytes were quantified (Figure 2.7). In order to observe firmly adherent neutrophil crawling and neutrophils which eventually undergo TEM the cremaster muscles were prepared for confocal IVM 2 hours after IL-1β stimulation and observed for a further 2 hours.

Cremaster muscles were viewed using a Leica SP5 confocal microscope incorporating a 20× water-dipping objective (NA 1.0). *Z*-stack images of 1-2 post-capillary venules per cremaster with a diameter range of 20–45 μm, with good/fast blood flow (based on observation of the flow by transmitted light where vessels with reduced or slow blood flow have a 'granular' appearance as the individual erythrocytes become visible) and few branches, were selected for analysis. Images of selected vessels were acquired every 30 seconds for approximately 30-40 minutes per vessel for a further 2 hours. This was carried out by sequential scanning of the 488 and 561 nm channels at a resolution of 1,024 × 350 pixels in the *x*-*y* plane and 0.9 μm steps in *z*-plane corresponding to a voxel size of 0.41 × 0.41 × 0.99 μm in *x*-*y*-*z*, respectively. Confocal images were acquired using a resonance scanner of 8,000 Hz, and acquisition of a single *z*-stack of ~60 images routinely took ~30 seconds. As previously stated Lys-eGFP-ki mice express endogenous eGFP on monocytes as well as neutrophils. As the aim of these experiments was to examine neutrophil recruitment dynamics confocal settings were optimised to ensure capturing of neutrophils only. This was possible due to the high eGFP intensity of neutrophils relative to monocytes (Woodfin et al., 2011). Additionally an IL-1β mediated response after 4 hours is known to be primarily a neutrophillic response (Thompson et al., 2001).

2.6.3 Reconstruction of confocal images into four-dimensional confocal IVM

Post-acquisition sequential *z*-stacks were analysed using Imaris software. This software allows for 3D reconstruction of the vessel with high spatial and temporal resolution. As full *z*-stacks were acquired every 30 seconds 3D video models were obtained (4D). For most preparations tissues were stable and movement from the heartbeat did not interfere with image acquisition. Slower movements from muscular contraction-relaxation occasionally resulted in movement of the vessel of interest in *x*-*y*-*z* plane, and a drift-correction algorithm was applied during the 3D reconstruction stage by the Imaris software. The resulting 4D confocal IVM video models were analyzed offline using Imaris, which renders the optical sections of half vessels into 3D video models, thereby enabling the dynamic interactions between luminal EC and leukocytes to be observed, tracked and analyzed (Figure 2.8, Movie 1). All images and videos show half vessels to enable clear visualization from only one luminal or abluminal side of the vessel wall. Using this technique luminal neutrophil crawling and TEM profile and dynamics were quantified.

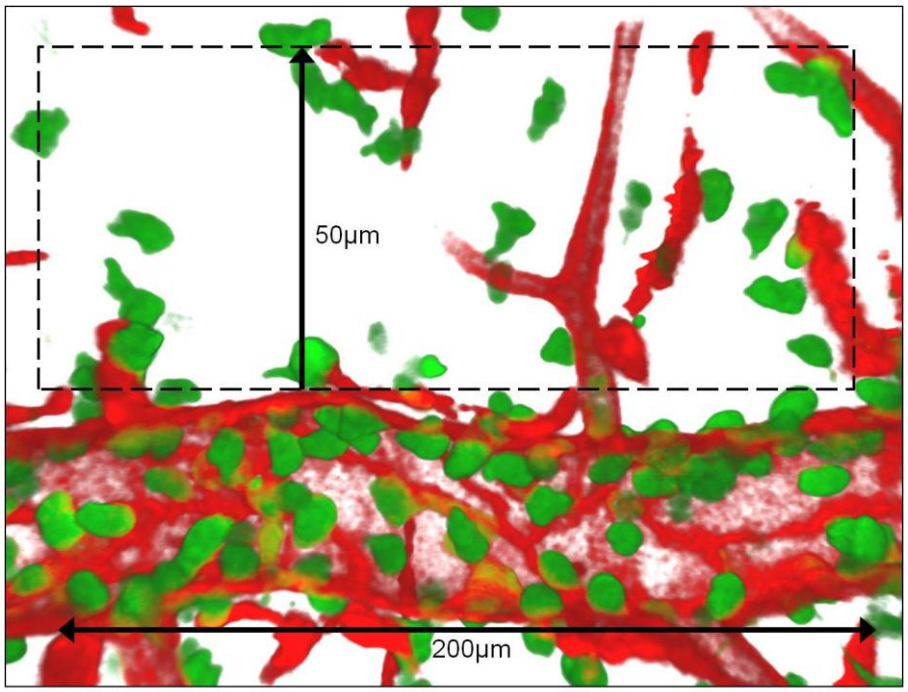

Figure 2.7: Quantification of intravascular and extravascular neutrophils.

Confocal image of a cremasteric post-capillary venule (red, endothelial cells, PECAM-1 staining) from an IL-1β-stimulated cremaster muscle. Neutrophils (green, Lys-eGFP-ki) which were observed in the lumen of the vessel were counted over a 200µm vessel length. Neutrophils that have transmigrated into the tissue on one side of the vessel, in a 50x200µm^2 away from the vessel were counted.

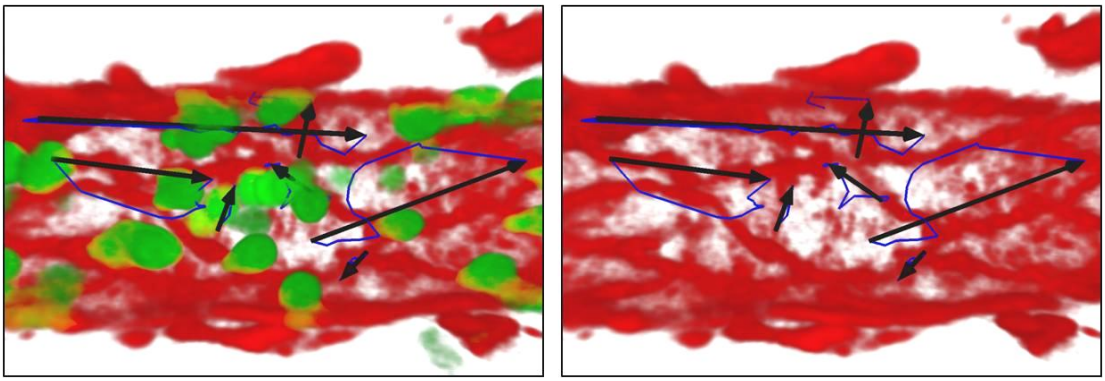

Figure 2.8: Quantification of luminal neutrophil crawling.

Confocal image of a cremasteric post-capillary venule (red, endothelial cells, PECAM-1 staining) showing individual neutrophil (green, Lys-eGFP-ki) crawling tracks (blue) which were clearly observed and tracked for 5 or more frames (>2.5 minutes). Crawling neutrophils were defined as any neutrophils which had a displacement (black arrows) of more than 5µm (approximately half of neutrophil diameter).

2.6.4 Analysis of luminal neutrophil crawling dynamics

For each image sequence neutrophil crawling within the lumen were analysed in terms of their location and dynamics. Approximately 70 crawling neutrophils were analysed from 3–8 mice per group. Specific parameters were established for recording the profile and dynamics of leukocyte luminal crawling on the endothelium. Only neutrophils which could be tracked for 5 or more frames (which corresponds to >2.5 minutes) were quantified. Stationary neutrophils were defined as any neutrophil which had a displacement less than 5µm (approximately half of its diameter). Any neutrophils which had a displacement of more than 5µm over the period of observation was defined as crawling. On average approximately 10 neutrophils per venule were tracked. The percentage of stationary and crawling neutrophils per venule was determined. Individual luminal neutrophil crawling paths were tracked manually using Imaris and the following parameters were quantified: (a) observed duration of crawling (minutes), (b) speed of crawling (µm/minute), (c)

distance crawled (μm), (d) total displacement (i.e., length in micrometers of the shortest distance between the first and last track point), (e) crawling displacement direction relative to blood flow, (f) crawling straightness (ratio of crawling displacement length to crawling length) and (g) crawling speed variation (ratio of the crawling speed standard deviation to the crawling speed mean value).

This imaging system allows neutrophils at various stage of the leukocyte-adhesion cascade to be tracked. However as a single *z*-stack takes 30s only cells which remained adherent (for 30s or more) were fully acquired and appeared spherical in 3D. Rolling neutrophils which move at high speeds appeared as small thin discs and so were excluded from crawling analysis. In this model only a small percentage of crawling cells were observed to undergo TEM, irrespective of the genotype of the mouse. This is due to the technical limitations involved in tracking an individual neutrophil from initial adhesion to TEM in a limited time period and in a small field of view of each vessel. Only neutrophils that were observed to crawl and were not stationary (5μm displacement over the period of observation) were included in the analysis of crawling parameters. The crawling behaviour of neutrophils which were later observed to undergo transmigration was also analysed in isolation from all other crawling cells and various crawling parameters as stated previously were analysed.

2.6.5 Continuity of neutrophil crawling

Two distinct types of neutrophil crawling behaviour were routinely observed; 'continuous crawling' and 'discontinuous crawling'. Neutrophils were classified as exhibiting continuous crawling if they were mobile for the duration of observation. Discontinuous crawling was defined as neutrophils exhibiting crawling behaviour with periods of immobility lasting 5 frames or more (i.e. 2.5 minutes or more) during the period of observation. Immobility was defined by a cell displacement of less than half the diameter of a cell (~5μm). The percentage of 'continuous' and 'discontinuous' crawling neutrophils per venule was quantified along with various crawling dynamic parameters.

2.6.6 Direction of neutrophil crawling relative to blood flow

Neutrophil crawling directionality in relation to blood flow was analysed. Directionality was defined by the overall movement of the neutrophil from the start to end position (displacement direction) of a given neutrophil crawling track. Each crawling displacement track (Figure 2.8) was categorised as crawling in the direction of blood flow or against blood flow within a 45 degree angle either side of the blood flow direction, or perpendicular to the blood flow again within a 45 degree angle either side of the direction directly (Figure 2.9).

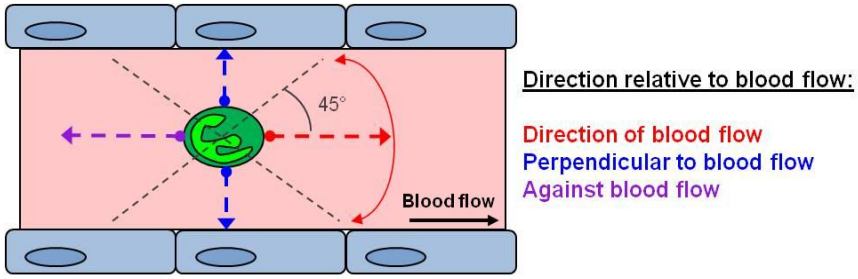

Figure 2.9: Quantification of neutrophil crawling direction relative to blood flow.

Schematic diagram representing how neutrophil crawling displacement was classified into crawling in the direction of blood flow (red), perpendicular to blood flow (blue) or against blood flow (purple).

2.6.7 Analysis of leukocyte transendothelial migration dynamics

In order to investigate the role of ICAM-2 in the migration of neutrophils through the EC barrier only neutrophil TEM events clearly visible for the complete duration of TEM were analysed. The frequency of neutrophil paracellular TEM events were quantified by the occurrence of EC junctional disruption, visualised by the occurrence of transient pores in EC layer during a TEM event as previously

described (Woodfin et al., 2011). The association of such events with bicellular EC contacts or at EC junctions between multicellular (three or more) ECs was noted and quantified. Secondly transcellular TEM events were identified as transmigrating cells associated with the occurrence of transient pores within the EC body visualised by disruption of the diffuse cell body PECAM-1 labelling, but not associated with disruption of EC junctions. Lastly the duration for which the neutrophils were in contact with an EC junction before commencing paracellular TEM (pre-TEM) and the duration of paracellular TEM was analysed (Figure 2.10). It should be noted that transcellular events were excluded during the analysis of TEM duration as they were infrequently observed. The start of TEM was defined as the time when a leukocyte protrusion was inserted into the EC junction and the formation of an EC pore. The end of TEM was defined as the time at which the leukocyte was no longer in contact with the abluminal side of the endothelium.

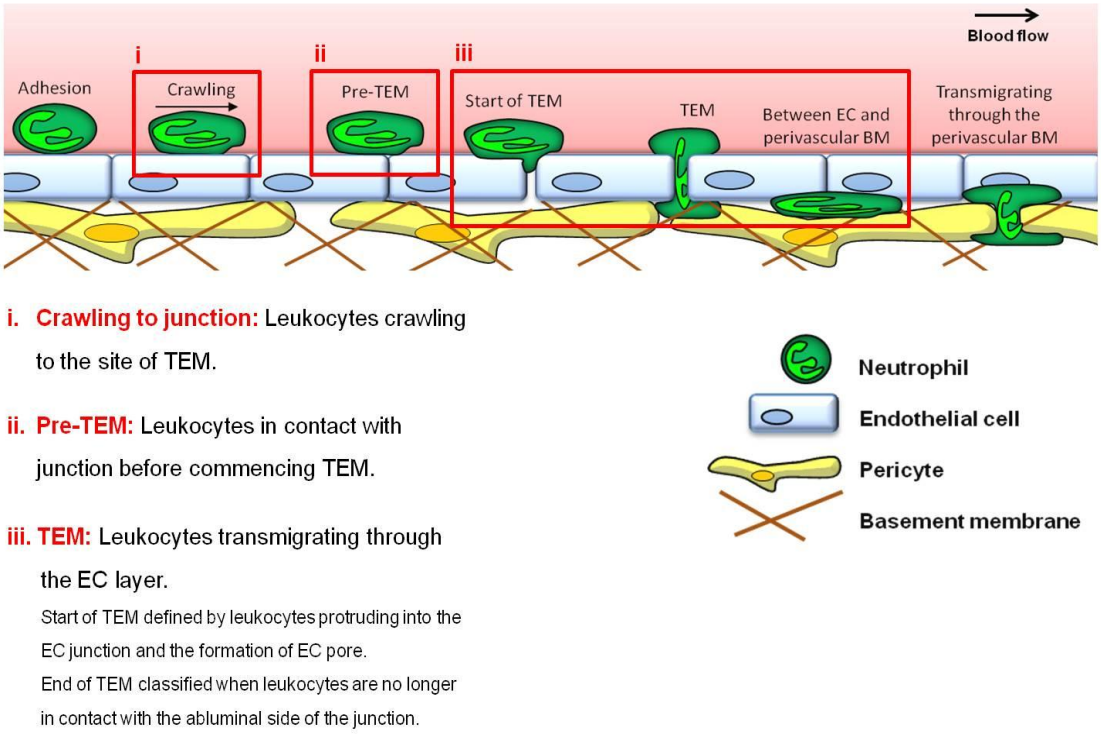

Figure 2.10: Quantification of neutrophil transendothelial migration dynamics.

Stages leading up to TEM and TEM were categorized into 3 stages in order to analyse the dynamics of leukocyte TEM. (i) Crawling to the site of TEM, (ii) Contact with the junction before commencing TEM (pre-TEM), (iii) Paracellular transmigration through the EC layer. TEM initiated by the first cell protrusions into the endothelial junction and the formation of transient pore in the EC, and transmigration through the EC until the cell is no longer in contact with the abluminal side of the junction.

2.7 Development of a cremasteric Shwartzman Reaction model

The Shwartzman Reaction (SR) is a process which describes the body's reaction to particular toxic reagents and has been likened to, or claimed to manifest in, clinical disorders. This includes sepsis, vasculitis and various other conditions which have an underlying inflammatory component (Hjort and Rapaport, 1965). Classically it can

be elicited experimentally via two LPS doses 24 hours apart and is characterised by leukocyte recruitment, thrombus formation and haemorrhage. SR is commonly induced in dermal models. As part of the present project a SR was established for the first time in the cremaster model to enable direct visualisation of vascular responses in real time.

A classical local SR was elicited by two LPS injections 24 hours apart. 30ug of LPS (from E.coil 011:B4) was injected i.s. (Hickey et al., 1998) to prime the endothelial cells for a reaction. 24 hours later 150µg of LPS was administered i.v. (Figure 2.11). Control animals were treated with saline. 2 hours post-i.v. injection the cremaster muscle was exteriorised as previously described (Figure 2.3), and observed using brightfield or confocal microscopy.

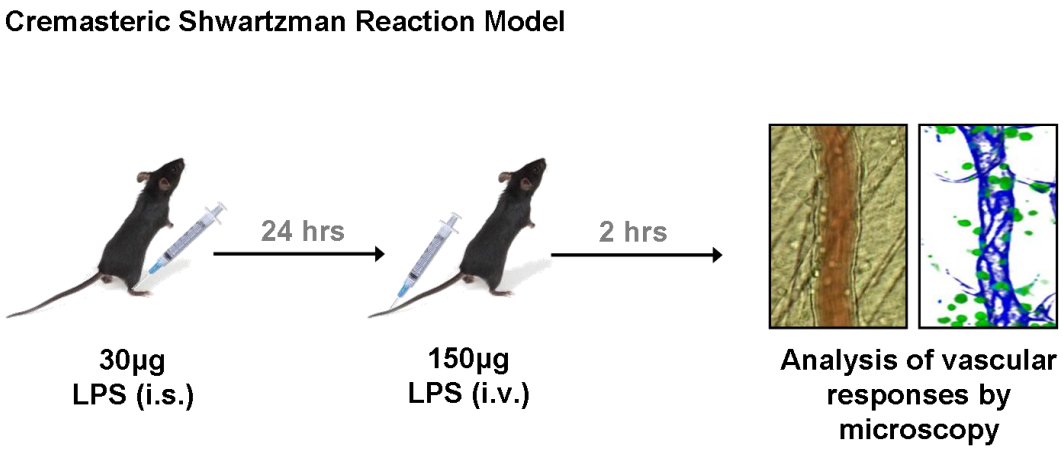

Figure 2.11: Schematic diagram illustrating the experimental protocol for mouse cremasteric Shwartzman Reaction model *in vivo*.

Mice were given an i.s. injection of LPS (30µg) to prime the endothelial cells for a reaction. 24 hours later they were administered with an i.v. injection of LPS (150µg) and the cremaster muscle was exteriorized and vascular responses were analysed by brightfield and confocal microscopy.

2.7.1 Analysis of leukocyte adhesion and transmigration

Cremaster muscles were viewed using an upright brightfield microscope (Carl Zeiss, Welwyn Garden City, United Kingdom) incorporating a 20×water-dipping objective (NA 1.0). A JVC colour video camera was used to acquire the image onto a monitor (Figure 2.12A). 3-4 post-capillary venules per cremaster which were 20-40µm in diameter with good/fast blood flow (based on observation of the flow by transmitted light where vessels with reduced or slow blood flow have a 'granular' appearance as the individual erythrocytes become visible) and few branches were selected for analysis. Frequency of rolling leukocytes was quantified by counting the number of rolling leukocytes that passed a given point in 60 seconds. Firmly adherent leukocytes were defined as leukocytes which were stationary for at least 30 seconds, and the number of adherent cells was quantified in a 500µm long section of each venule. Transmigrated leukocytes in the perivascular region, 50µm each side of the 500µm length vessel were also analysed. In some experiments using confocal microscopy analysis, transmigration 0-50 and 50-100µm into the perivascular tissue from one side of the vessel length was also analysed (Figure 2.12B).

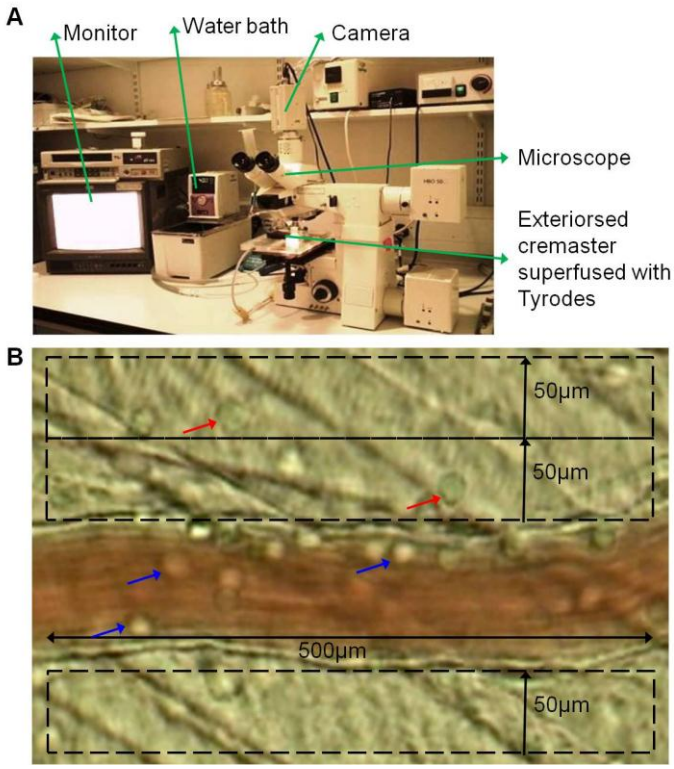

Figure 2.12: Leukocyte adhesion and transmigration as observed by brightfield intravital microscopy.

(**A**) Image shows the different components used for brightfield IVM. Mice were placed on a heated stage and the cremaster muscle was exteriorized and kept moist with Tyrodes buffered solution. A 20 × water-dipping objective connected to a camera and projected on monitor where leukocyte responses were analyzed. (**B**) Brightfield image showing an inflamed post-capillary venule. Leukocytes which were adherent for more than 30 second in the lumen of the vessel (blue arrows) was counted over a 500µm length. Leukocytes that have transmigrated into the tissue, 50µm either side from the vessel were counted over a length of 500µm.

2.7.2 Characterisation of the SR using Lys-eGFP-ki mice and CX3CR1-eGFP-ki mice

To characterise the SR response within the cremaster muscle the subtype of leukocytes recruited during this reaction was determined through live confocal IVM using Lys-eGFP-ki mice (expressing GFP in neutrophils and monocytes) (Faust et al., 2000), and CX_3CR1-eGFP-ki mice (expressing GFP in monocytes and dendritic cells) (Jung et al., 2000). A SR was stimulated in the cremaster muscle and prepared for confocal IVM as previously described. Anti–mouse Alexa Fluor 647–labelled PECAM-1 mAb (i.s.) was used as a marker for endothelial cells lining the vessel. 3-4 post-capillary venules were selected and viewed using a Leica SP5 confocal microscope as previously described. Live images were acquired through sequential scanning of different lasers (488 nm, 561 nm and 633 nm) at a resolution of 512 x 512 pixels corresponding to a voxel size of approximately 0.7 x 0.7 x 0.9 μm in the *x-y-z* planes, respectively. Acquired *z*-stack images were reconstructed and analysed in 3D using Imaris. The number of intravascular leukocytes in each venule was analysed. The number of transmigrated leukocytes in the perivascular region, 0-50μm and 50-150μm away from the venule was also analysed.

2.7.3 Live immunofluorescent analysis of microthrombi formation

Platelet-vessel wall interactions in SR-induced inflammation were investigated. Platelets were labelled i.v. with anti–mouse phycoerythrin (PE) labelled CD41 mAb (0.1μg/g) (Falati et al., 2006). Anti–mouse Alexa Fluor 647–labelled PECAM-1 mAb was used to label vessels (i.s.). 2 hours after the induction of the SR the cremaster muscle was prepared for confocal IVM as previously described and imaged, using a Leica SP5 confocal microscope as previously described. Venules of 300μm in length ranging from 5μm to 60μm in diameter were selected. Live images were acquired through sequential scanning of different lasers (488 nm, 561 nm and 633 nm) at a resolution of 920 x 312 pixels corresponding to a voxel size of approximately 0.7 x 0.7 x 0.9 μm in the *x-y-z* planes. Using Leica LAS AF Lite (2.1.1 build) software the mean fluorescent intensity of immunostained stained CD41

and PECAM-1within the vessel region was determined by dividing the pixel sum of each channel by the area of the whole venule. The ratio of the mean intensity of fluorescently labelled CD41 to PECAM-1 was calculated as a measure of microthrombi and/or platelet-vessel wall interactions. Vessels which had microthrombi would have fluorescently labelled platelets adhering to the endothelium and therefore have a higher ratio of CD41 intensity to PECAM-1 intensity.

2.7.4 Quantification of vascular perfusion in the SR

Vessel perfusion was investigated using dextran-fluorescein isothiocyanate (FITC) to fluorescently label all perfused vessels. 2 hours after the induction of the SR, the cremaster muscle was prepared for confocal IVM as previously described. Intrascrotal anti–mouse Alexa Fluor 647–labelled PECAM-1 mAb was used to label all vessels. 500μg dextran-FITC was administered through the carotid artery in order to label only perfused vessels. Five standard regions per cremaster were selected and live images were acquired through sequential scanning 488, 561 and 633 nm laser, at a resolution of 920 x 312 pixels corresponding to a voxel size of approximately 0.7 x 0.7 x 0.9 μm in the *x-y-z* planes, respectively. Using Leica LAS AF Lite software mean fluorescent intensity of immunostained stained dextran and PECAM-1 was determined by dividing the pixel sum by the area of the whole venule. The ratio of the mean intensity of fluorescently labelled dextran to PECAM-1 was calculated as a measure of vascular perfusion. Vessels which were perfused would have fluorescently labelled dextran and therefore have a higher ratio of fluorescent intensity.

2.8 Statistics

All results are presented as mean plus or minus standard error of the mean (SEM). Statistical significance was assessed by the unpaired two-tailed Student t test or by one-way or two-way analysis of variance (Anova) with the Newman-Keuls multiple comparison test. P values below 0.05 were considered significant (GraphPad Prism 4 software). Further statistical advise from a statiscian was sought with regards to the appropreaite minimum n numbers (i.e. number of mice) to be used which will give meaanifull data given the ethical implications of using mice.

CHAPTER 3: Expression profile of ICAM-2 *in vivo*

3.1 Introduction

ICAM-2 is an adhesion molecule well known to have a high, constitutive expression on vascular ECs. Expression of ICAM-2 on high endothelial venules (lymph node, tonsil), sinus lining cells in the spleen, capillary ECs in the lung, Kupffer's cells and sinus lining cells in the liver and ECs of the glomerulus and intertubular spindle cells in the kidneys has been previously reported (de Fougerolles et al., 1991). In contrast to the closely related adhesion molecule ICAM-1, ICAM-2 is not upregulated upon stimulation with pro-inflammatory cytokines such as IL-1β and TNF-α. In fact, ICAM-2 has be demonstrated to be expressed 10-fold higher than that of ICAM-1 at a basal level (de Fougerolles et al., 1991) and for this reason ICAM-2 has been considered to be an adhesion molecule involved in homeostatic processes, such as re-circulation and homing of lymphocytes. More recently, with the development of more sensitive techniques, the expression of ICAM-2 has been found to be regulated in some inflammatory reactions. Specifically, in IL-1β and TNF-α-stimulated HUVECs, ICAM-2 has been reported to be downregulated in both a protein and transcriptional level by up to 50% in comparison to basal levels (McLaughlin et al., 1999; McLaughlin et al., 1998). Subsequent *ex vivo* studies by the same group confirmed ICAM-2 downregulation in ECs from human mammary arteries and demonstrated an ERG transcription factor dependent expression (McLaughlin et al., 1999). In most studies however ICAM-2 expression has been demonstrated to remain unchanged on vascular ECs during cytokine induced inflammation (de Fougerolles et al., 1991;Hobden, 2003). *In vitro* studies ICAM-2 has been localized to EC junctions (McLaughlin et al., 1998) suggesting a role for this adhesion molecule in leukocyte TEM. Indeed ICAM-2 supports leukocyte extravasation into tissues, but the expression pattern of EC ICAM-2 in post-capillary venules under basal conditions is different to that of other junctional proteins involved in TEM. Most notably ICAM-2 was observed to have a high heterogenic expression across the vascular lumen as

well at EC junctions (Woodfin et al., 2009), an expression profile that was further investigated as part of this project.

In addition to ECs, ICAM-2 is also expressed on epithelial cells (Carreno et al., 2002; Porter and Hall, 2009), neutrophils (Sundd et al., 2012), monocytes (de Fougerolles et al., 1991), T cells (de Fougerolles et al., 1991), eosinophils (Gerwin et al., 1999), natural killer cells (Helander et al., 1996; Somersalo et al., 1995), platelets (Diacovo et al., 1994; Kuijper et al., 1998) and synovial cells (Singh et al., 2006). The relative amount of ICAM-2 surface expression on different leukocyte subsets seems to be variable and it is well known that a much lower expression is evident on leukocytes in comparison to ECs (de Fougerolles et al., 1991; Gerwin et al., 1999; Sundd et al., 2012). Some studies have indicated no expression on neutrophils (de Fougerolles et al., 1991) whilst other groups have demonstrated clear neutrophil ICAM-2 expression (Sundd et al., 2012). It should be noted however, that these two latter studies use cells from different species to analyses the expression of ICAM-2 and this may account for the differences seen. As the focus of the present study is related to the role of ICAM-2 in neutrophil transmigration using a murine model, ICAM-2 expression on different leukocyte subsets from the mouse blood circulation was also investigated.

Although both EC and leukocyte ICAM-2 expression has previously been demonstrated, further investigations are required to understand the regulation and distribution of these expressions in the context of neutrophil transmigration. This chapter aims to investigate the expression profile of ICAM-2 throughout the EC vasculature, as well as on specific leukocyte subsets. In order to investigate the possibility of EC ICAM-2 redistribution upon inflammation, which may support neutrophil transmigration, the sub-cellular localisation of EC ICAM-2 under basal conditions was compared with that after IL-1β stimulation. This was carried out in comparison with other well-established markers of EC junctions such as PECAM-1 and VE-cadherin. These objectives were addressed by immunolabelling and confocal

microscopic analysis of the mouse cremaster muscle, a tissue that was subsequently used for investigations into the role of ICAM-2 in neutrophil trafficking. For comparison, key findings in the cremaster muscle were also investigated in the dermal (ear) vasculature. The expression profile of ICAM-2 on different leukocyte subtypes in the blood circulation of naïve WT mice was also examined using flow cytometry as part of this study.

3.2 Results

3.2.1 Distribution of ICAM-2 in the vasculature

The expression profile of EC ICAM-2 on the vasculature of the murine cremaster muscle was analysed. This tissue was utilised due to its thin and transparent nature, rendering it highly amenable for high resolution immunofluorescence staining and confocal microscopy. Initially the characteristics of different types of blood vessels in the cremasteric vasculature were investigated. As a key aim of this work was to analyse the distribution of ICAM-2 in relation to its expression at EC junctional and non-junctional regions, well-known EC junctional molecules PECAM-1 and VE-cadherin were also stained and their specificity was confirmed using their respective isotype control mAb (Figure 3.1). The α-SMA mAb was used to visualise the vasculature, and discriminate between arterioles and venules. This staining is routinly carried out within our group and the pattern of expression was expected and are confident that the expression is specific based on a strain of mice which have eGFP expression in the α-SMA gene (see Proebstl al., 2012 for further details). High amounts of ICAM-2 were found in ECs surrounding post-capillary venules, arterioles and lymphatic's (Figure 3.2A). Identification of different sections of the vascular tree was based on the morphology of vessels and ECs as shown by the well established EC junctional markers VE-cadherin and PECAM-1. Specifically, venules commonly

displayed multiple meandering vascular branches with rounded cobblestone ECs, whereas arterioles displayed fewer branches which were straighter and had elongated ECs (Figure 3.2). Lymphatic vessels were blunt ended and had ECs with oak leaf morphology. The EC layer within these vessels was thinner and arranged in a more irregular fashion than that of venules and arterioles whereby a single EC was not clearly visible (Figure 3.2A). In arterioles and post-capillary venules VE-cadherin was almost entirely localised at the endothelial junctions, where as PECAM-1 was strongly enriched at the junctions but also showed a low homogeneous expression on the EC body. In agreement with previous studies, high ICAM-2 expression was seen at EC junctions and with high heterogeneous expression on the EC body (Woodfin et al., 2009) (Figure 3.2A).

Vascular labelling of PECAM-1 is well established in this tissue, however ICAM-2 labelling required significant optimisation. In preliminary experiments several labelling protocols were carried out in conjunction with tissues from ICAM-2 KO mice to confirm specificity of the mAb employed as well as the staining protocols (Figure 3.2B).

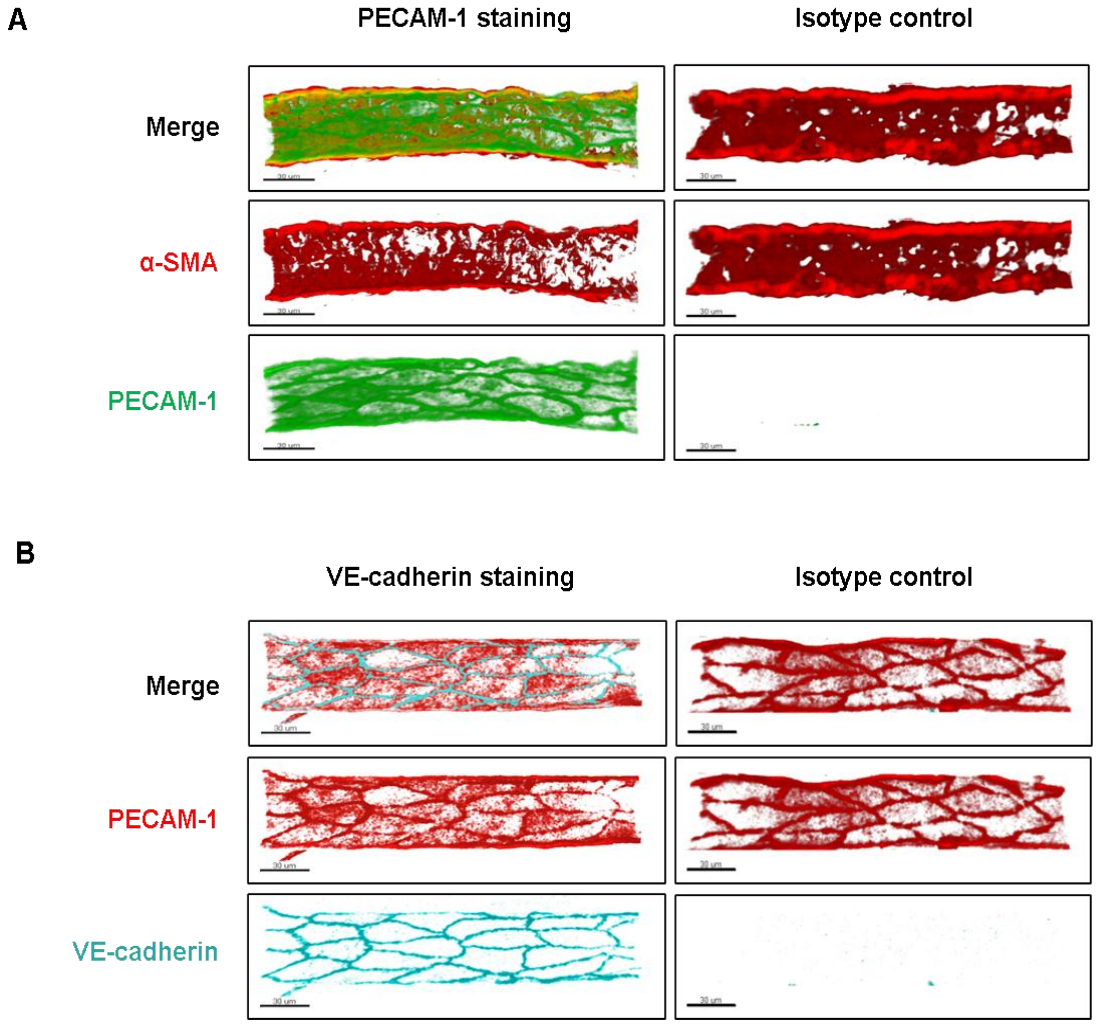

Figure 3.1 : Endothelial junctional expression of PECAM-1 and VE-cadherin in the mouse cremasteric vasculature.

(**A**) Whole mount tissues were stained with fluorescent secondary mAb directed against α-SMA (red) and PECAM-1 (green) or (**B**) PECAM-1 (red) VE-cadherin (blue). Samples were observed using Leica confocal microscope. Representative images of half venules were generated using Imaris software. Specificity of anti-PECAM-1 mAb and anti-VE-cadherin mAb was confirmed in cremaster muscles stained with the respective isotype control. Scale bar represents 30µm.

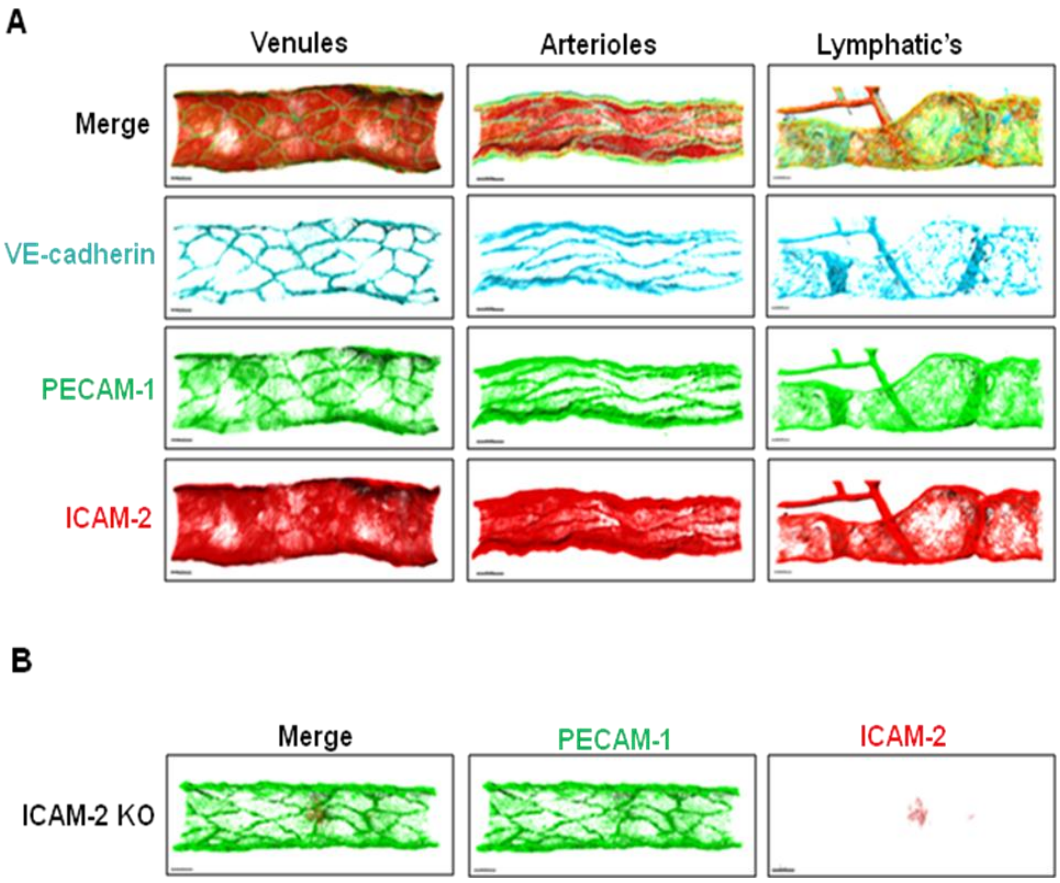

Figure 3.2: Endothelial cell expression of ICAM-2 in the mouse cremasteric vasculature.

(**A**) Mice were injected with 3mg/kg anti-ICAM-2 (3C4) mAb intravenously. After 10 mins cremaster muscles were dissected away from mice and fixed in PFA. Whole mount tissues were stained with fluorescent secondary mAb directed against ICAM-2 (red). Tissues were washed, re-blocked and stained for PECAM-1 (green) and VE-cadherin (blue) using directly conjugated mAbs. Samples were observed using Leica confocal microscope. Representative images of half venules were generated using Imaris software (n=3). (**B**) Specificity of the anti-ICAM-2 mAb binding was confirmed in immunostainings carried out in cremaster muscles from ICAM-2 KO mice. Scale bar represents 20µm.

3.2.2 Localisation of ICAM-2 on venular endothelial cells

As the principal aim of the overall study was to understand the role of ICAM-2 in neutrophil extravasation, in the present section a detailed analysis and quantification of EC ICAM-2 expression on post-capillary venules was conducted. The i.v. method of staining previously used (Figure 3.2) required a significant amount of mAb and hence the staining method employed for ICAM-2 was further optimised. Taking into account that EC PECAM-1 is routinely stained locally *in vivo* (i.s.) within our group (Woodfin et al., 2011), and is very reliable and uses significantly less mAb, it was considered that this mode of staining could also be effective for labelling EC ICAM-2. This method of staining produced results comparable to that noted previously with i.v. mAb in terms of distribution within cremasteric vasculature as well as localisation on ECs. With this approach, the sub-cellular distribution of venular EC ICAM-2 and PECAM-1 was compared in unstimulated and IL-1β-stimulated tissues. Image stacks of PECAM-1- and ICAM-2- labelled venules of both small (20-40μm) and large (40-70μm) vessels were rendered into 3D models using Imaris (Figure 3.3). Intensity thresholding was used to build an isosurface on the whole vessel (Chapter 2, Figure 2.5). The mean intensity of fluorescently labelled PECAM-1 and ICAM-2 was determined 4 hours after saline or IL-1β administration. No differences were detected in EC PECAM-1 expression between saline and IL-1β pre-treatment or between WT and ICAM-2 KO mice (Figures 3.3 and 3.4). Additionally, the size of venules had no impact on the fluorescent intensity of PECAM-1. Similarly EC expression of ICAM-2 remained unaffected after IL-1β stimulation, and again no differences in ICAM-2 expression were detected between small and large venules in this tissue (Figures 3.3 and 3.4). It should be noted that the fluorescent intensity quantified in these experiments are controlled for between experiments through several ways. Firstly confocal microscope settings were kept largely constant and are based on control images (i.e. stainings from isotype control tissues or tissues from mice lacking that protein). Secondly the fluorescent intensity values given are the mean value within the isosurface, therefore are internally controlled for the volume

of tissue/vessel wall analysed and most importantly the background fluorescent intensity of each channel was substracted from each image (Chapter 2, Figure 2.5).

The sub-cellular distribution of EC PECAM-1 and ICAM-2 on post-capillary venules was quantitatively analysed. This was carried out using Imaris software, where again the intensity thresholding was used to build an isosurface. This time an isosurface was created on the high intensity PECAM-1 corresponding to EC junctions or the low intensity PECAM-1 corresponding to EC bodies or EC 'non-junctional' regions (Chapter 2, Figure 2.6). The mean intensity of PECAM-1 and ICAM-2 within these two surfaces in unstimulated and IL-1β-stimulated tissues was determined. PECAM-1 expression was found to be significantly higher at EC junctions than on the EC body, while the mean intensity of fluorescently labelled ICAM-2 was not different in these two regions (Figure 3.5). This distribution of EC ICAM-2 was also seen in post-capillary venules in the ear dermal microvasculature (Figure 3.7). It should be noted that a different method was used for labelling the ear dermal vasculature. Specifically the i.v. method of labelling ICAM-2 was carried out within the ear (Figure 3.7), a protocol that gave similar results to that previously obtained in the cremaster muscle (Figure 3.2). Of note, the i.v. method of labelling ICAM-2 within the cremaster muscle showed a comparable distribution of ICAM-2 to that detected by the i.s. method of labelling (Figure 3.3).

In the cremaster muscle neither PECAM-1 or ICAM-2 showed differences in their respective distribution or fluorescent intensity following IL-1β stimulation (Figures 3.3, 3.4 and 3.5). Analysis of neutrophil responses (rolling, adhesion and transmigration), by brightfield microscopy confirmed a neutrophil response after IL-1β stimulation in comparison to saline controls (Figure 3.6). Of importance i.s. administration of directly labelled anti-PECAM-1 and anti-ICAM-2 mAb did not inhibit leukocyte transmigration (Figure 3.6B). As a non-function blocking mAb to PECAM-1 and very low doses of anti-ICAM-2 mAb were employed. As a positive control ICAM-2 KO mice were also used in thes experiments (Figure 3.6) where no difference in leukocyte adhesion is seen after IL-1β stimulation however a significant

reduction in leukocyte transmigration is seen in IL-1β stimulation ICAM-2 KO mice when compared to WT controls.

Clearly it is not possible to make inferences about the absolute levels of these proteins in comparison to each other, due to possible differences in mAb affinity or avidity as well as epitope access, but the presence of substantial amounts of ICAM-2 on the EC body suggests that it may have a function beyond its accepted role in leukocyte transmigration.

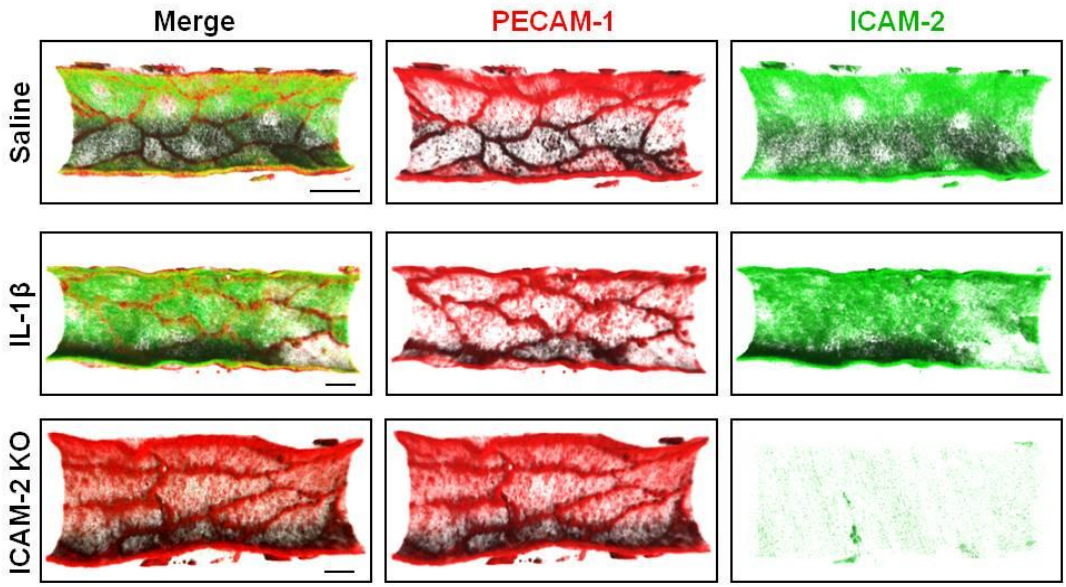

Figure 3.3: Distribution of endothelial ICAM-2 on post-capillary venules in IL-1β-stimulated mouse cremasteric vasculature.

Mice were injected with IL-1β (50ng/400µl, i.s.) or saline and fluorescently conjugated anti-ICAM-2 (3C4) (green) and anti-PECAM-1 (C390) (red) mAbs (i.s.) for 4 hours (n=3 mice, 3-5 vessels/cremaster). Cremaster muscles were prepared for confocal IVM and live images of samples were observed using a confocal microscope. Representative images of half venules were generated using Imaris

software. The specificity of binding of anti-ICAM-2 mAb was confirmed in cremaster tissues from ICAM-2 KO mice. Scale bar represents 20µm. NB- In these experiments tissues were also staining for ICAM-1 results are presented in chapter 6.

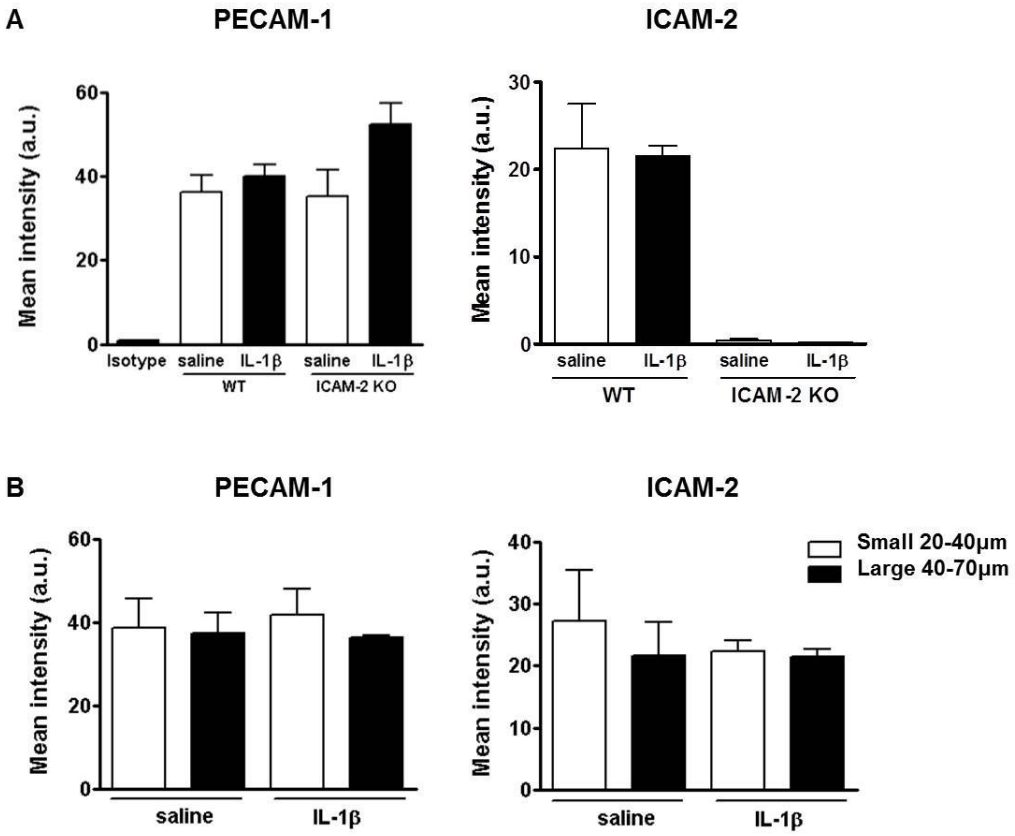

Figure 3.4: Quantification of mean fluorescence intensity of total endothelial PECAM-1 and ICAM-2 on post-capillary venules in IL-1β-stimulated mouse cremaster muscles.

Isosurfaces were built on the EC layer (Chapter 2, Figure 2.5) and the mean fluorescent intensity of total EC (**A**) PECAM-1 and ICAM-2 was determined in saline and IL-1β (50ng/400µl, i.s.) -stimulated tissues from WT and ICAM-2 KO mice. (**B**) Small (20-40µm in diameter) and large (40-70µm in diameter) venules from saline and IL-1β-stimulated WT mice were individually grouped. Each bar represents the mean fluorescence intensity per mouse (n=3 mice, 3-5 vessels/cremaster). NB- In these experiments tissues were also staining for ICAM-1 results are presented in chapter 6.

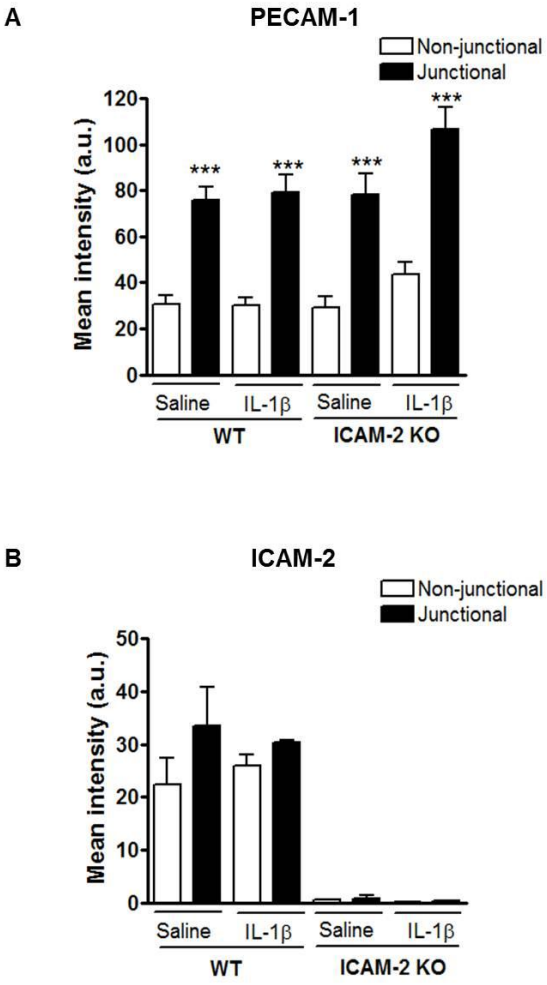

Figure 3.5: Quantification of the distribution of endothelial PECAM-1 and ICAM-2 on post-capillary venules in IL-1β-stimulated mouse cremaster muscles.

Isosurfaces were built on the EC non-junctional and junctional regions (Chapter 2, Figure 2.6). Using WT and ICAM-2 KO mice the mean fluorescent intensity of (**A**) PECAM-1 and (**B**) ICAM-2 4 hours after saline and IL-1β (50ng/400µl, i.s.) stimulation was determined. Results are presented as mean ± SEM for each mice (n=3 mice, 3-5 vessels/cremaster). Significant differences were assessed using one way Anova between saline and IL-1β groups indicated by asterisks (***P < 0.001). NB. ICAM-2 KO treated with IL-1β group n=1 mice. NB- In these experiments tissues were also staining for ICAM-1 results are presented in chapter 6.

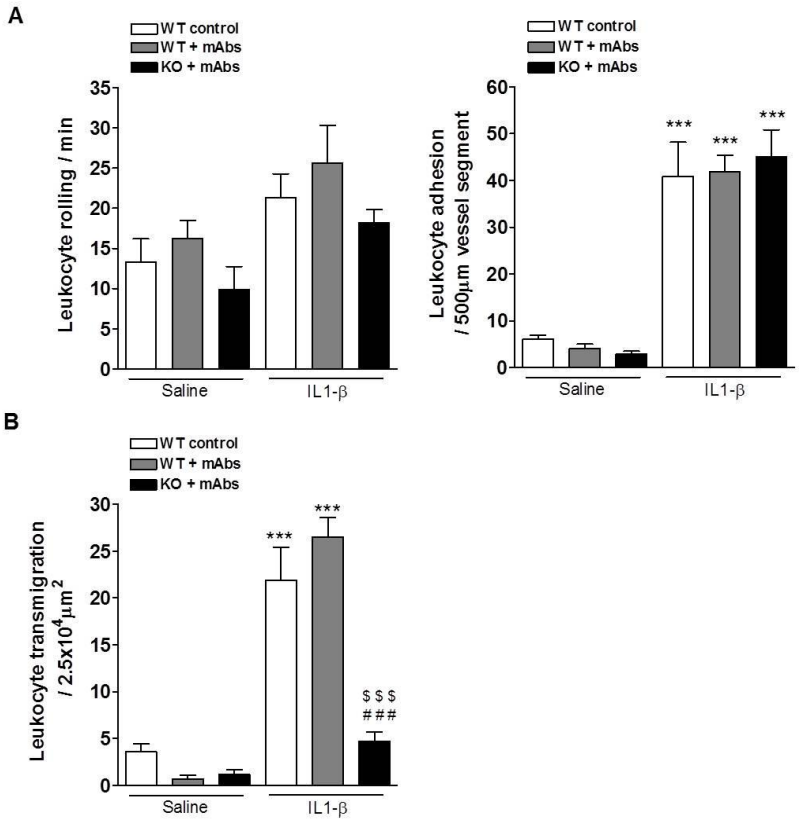

Figure 3.6: Effect of *in vivo* labelling of ICAM-2 on leukocyte responses in IL-1β-stimulated cremaster muscles.

WT and ICAM-2 KO mice were injected with saline or IL-1β (50ng/400µl, i.s.) for 4 hours. Fluorescently conjugated mAbs to PECAM-1 (2µg/mouse) and ICAM-2 (4µg/mouse) were co-administered via i.s. injection. Cremaster muscles were exteriorised and leukocyte responses were analysed by brightfield IVM. (**A**) The number of rolling leukocytes past a fixed point per minute, adherent leukocytes per 500 µm length vessel and (**B**) transmigrated leukocytes per $2.5x10^4\mu m^2$ were analysed. Results are presented as mean ± SEM for each mice (n=3 mice, 3-5 vessels/cremaster). Significant differences were assessed using one way Anova between saline and IL-1β groups are indicated by asterisks (***P < 0.001). Additional statistical comparisons between WT control and ICAM-2 KO groups are indicated by hash symbols (###P < 0.001). Comparisons between WT + fluorescent mAb administration and ICAM-2 KOs groups are indicated by dollar symbols ($$$P < 0.001).

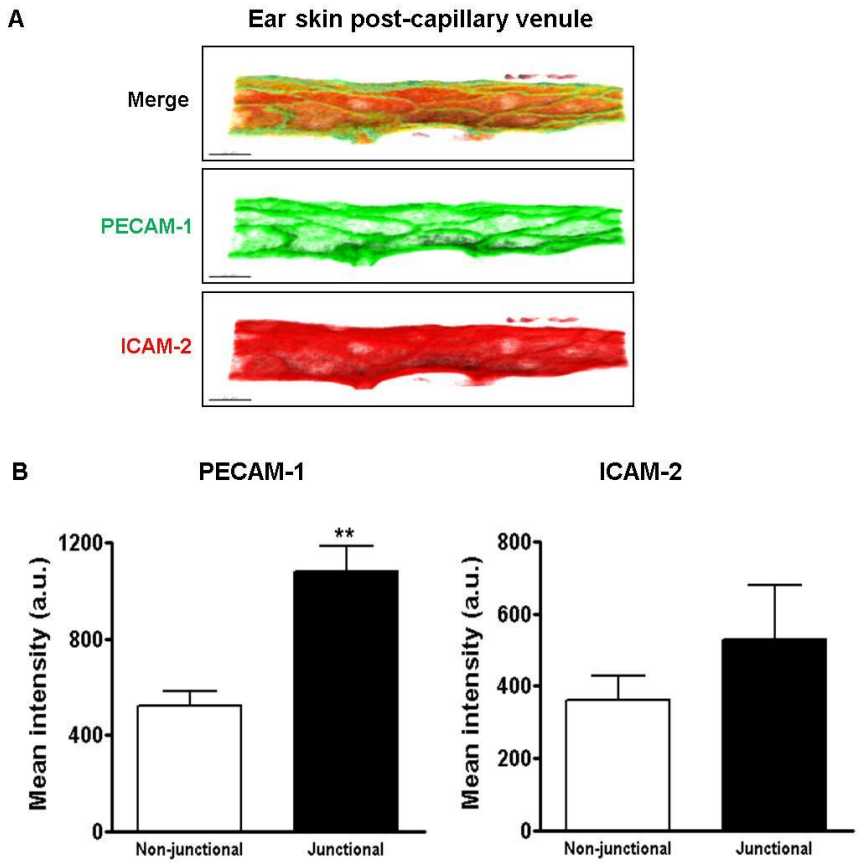

Figure 3.7: The distribution of endothelial PECAM-1 and ICAM-2 on post-capillary venules in the ear dermal vasculature.

(**A**) Mice were injected with 3mg/kg anti-ICAM-2 (3C4) mAb i.v. Ears were dissected away from mice and fixed in PFA. Whole mount tissues were stained with a fluorescent secondary mAb direct against ICAM-2 (red) and PECAM-1 (green). Images were captured using a confocal microscope. Representative images of half venules were generated using Imaris software. Scale bar represents 20µm. (**B**) Region of interest was built on the EC non-junctional and junctional regions, and the mean fluorescence intensity of PECAM-1 and ICAM-2 in these regions was determined. Results are presented as mean ± SEM for each mice (n=3 mice, 3-5 vessels/cremaster). Significant differences between groups were assessed using an unpaired t-test.

3.2.3 Leukocyte ICAM-2 expression

Previous studies have highlighted a role for ICAM-2 during leukocyte extravasation and this role was linked to the expression of ICAM-2 on EC. ICAM-2 is however also expressed on leukocytes. To date the expression of ICAM-2 on lymphocytes and NK cells is well established but the expression of ICAM-2 on neutrophils is currently inconsistent. Earlier data has highlighted that ICAM-2 is not expressed on neutrophils (de Fougerolles et al., 1991) however more recently using cells from the mouse blood and bone marrow, ICAM-2 on neutrophils has been demonstrated (Sundd et al., 2012). ICAM-2 has also been shown to undergo homophillic interactions (Huang et al., 2005) and therefore it is possible that neutrophil ICAM-2 may interact with EC ICAM-2 during neutrophil extravasation. Further examination of the expression of ICAM-2 on different leukocyte subsets could provide additional insights into the mechanism by which ICAM-2 exerts its function during neutrophil extravasation.

Peripheral blood leukocytes from WT mice were analysed for surface expression of ICAM-2 using flow cytometry. Leukocytes were fluorescently stained for specific markers in order to distinguish different leukocyte subsets. For this purpose, fluorescent mAbs directed against Gr-1, CD115, B220 and/or CD3 were used. Based on current literature, Gr-1 positive and CD115 negative leukocytes corresponds to neutrophils. Gr-1 positive and CD115 positive cells corresponds to classical monocytes and Gr-1 negative and CD115 positive corresponds to non-classical monocytes. Lastly, CD3 and B220 positive leukocytes correspond to T cells and B cells respectively. For gating strategies of different leukocyte subsets and ICAM-2 expression see method section (Chapter 2, Figure 2.1 and 2.2). The results confirmed that almost all B and T cells, and 70-80% of all classical and non-classical monocytes stained positive for surface ICAM-2 expression (Figure 3.8 and 3.9A). In contrast, only 20% of Gr-1 high neutrophils stained positive for ICAM-2. The RFI of AlexaFlour-488 labelled anti-ICAM-2 mAb on different leukocyte subsets confirmed

that B cells and classical monocytes have the highest expression of ICAM-2 followed by T cells and non-classical monocytes (Figure 3.9B). Neutrophils however displayed the least expression of ICAM-2 with a very low average RFI (Figure 3.8B). Therefore the data presented here confirms that only a small portion of neutrophils express ICAM-2 at relatively low level in comparison to other leukocyte subsets. Furthermore, ICAM-2 was not detectable on neutrophils using confocal microscopy suggesting that neutrophils express a relatively low levels of ICAM-2 in comparison to that observed on ECs.

In initial flow cytometry studies, each stained population was back gated on to the forward and side scatter (indicating size and granularity respectively) to ensure gating of all leukocyte subsets. These studies also help optimised flow cytometry settings and compensation. Antibody specificity was determined by using isotype controls. In all experiments unstained and single stained blood samples were used in addition to blood samples from ICAM-2 KO mice, confirming anti-ICAM-2 mAb specificity.

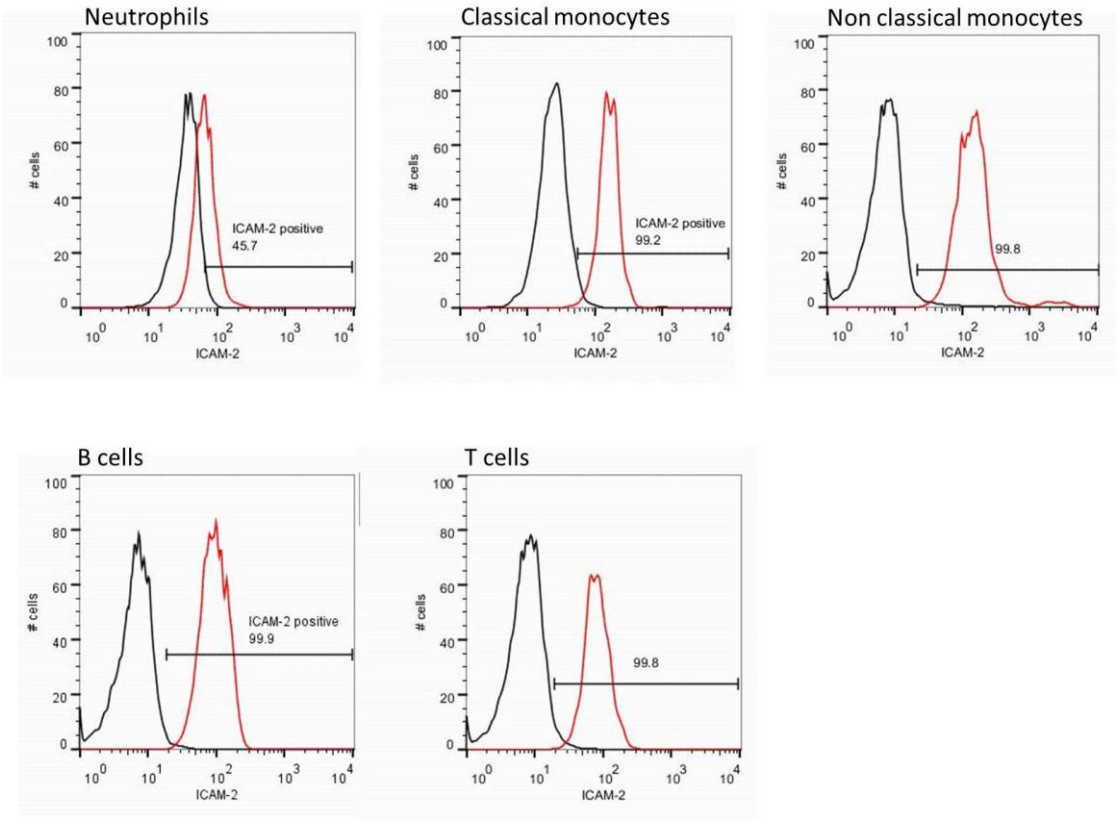

Figure 3.8: Representative flow cytometry plots demonstrating the expression of ICAM-2 in different leukocyte subsets.

Surface ICAM-2 expression of different mouse blood leukocyte subsets was determined by flow cytometry. The percentage of neutrophils, classical and non-classical monocytes and T and B cells which stained positive for ICAM-2 (red line) was determined (see Chapter 2, Figure 2.1 and 2.2 for leukocyte subset gating strategies). The RFI of fluorescently labelled ICAM-2 in each leukocyte subset was also determined. Gating strategies were based on negative control samples taken from ICAM-2 KO mice (black line).

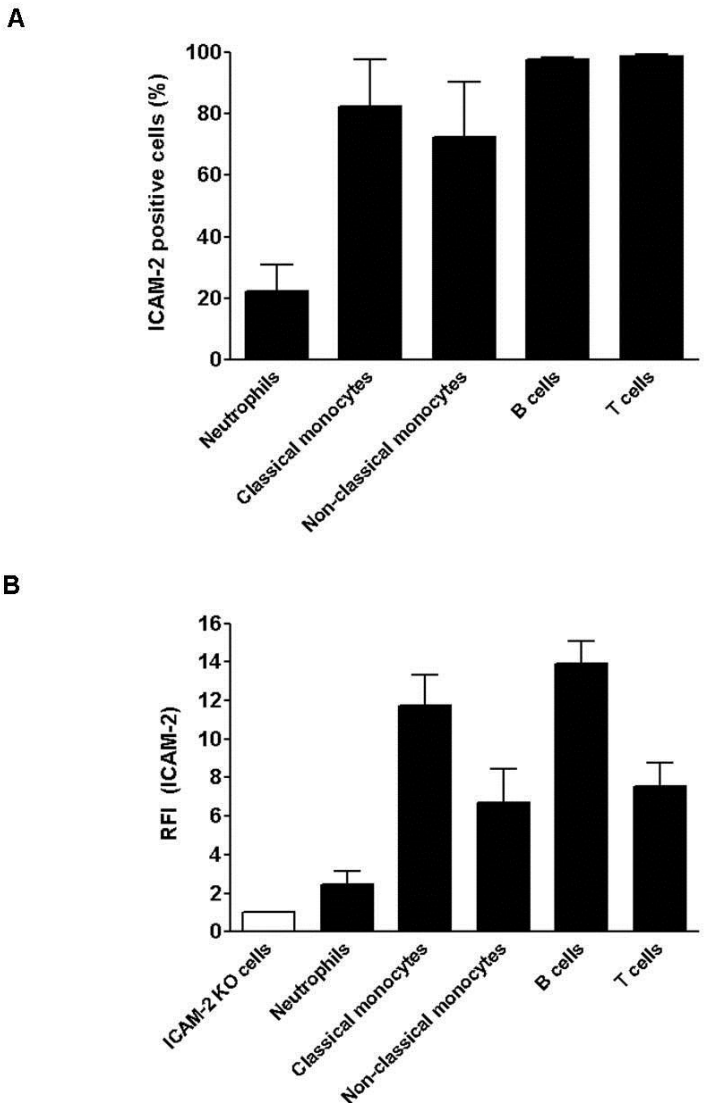

Figure 3.9: Expression of ICAM-2 in different leukocyte subsets from the mouse blood circulation.

Surface ICAM-2 expression of different mouse blood leukocyte subsets was determined by flow cytometry. (**A**) The percentage of neutrophils, classical and non-classical monocytes and T and B cells which stained positive for ICAM-2 was determined (Chapter 2, Figure 2.1 and 2.2). (**B**) The RFI of fluorescently labelled ICAM-2 in each leukocyte subset was also determined. Gating strategies were based on negative control samples taken from ICAM-2 KO mice. Results are presented as mean ± SEM for each mice (n=3 mice).

3.3 Discussion

In this chapter the expression of ICAM-2 was investigated on mouse ECs *in vivo* as well as on leukocytes. For this purpose the cremaster muscles for EC analysis and circulating blood for leukocyte anaylsis were used. The cremaster muscle is a thin, translucent and highly vascularised tissue. These characteristics enable immunostaining and direct visualisation using confocal microscopy, and thus permit detailed analysis of the exact distribution pattern of EC ICAM-2 relative to that of more established molecules such as PECAM-1 and VE-cadherin. In previous studies the expression pattern of ICAM-2 was reported to be different to that of PECAM-1 and JAM-A under basal conditions (Woodfin et al., 2009). The present findings expand on this observation through detailed quantification of EC ICAM-2 expression under control and inflamed conditions. Additionally as there is little information regarding the relative expression of ICAM-2 on different leukocyte subsets this was also further examined.

To extend our understanding of the expression pattern of EC ICAM-2, cremaster muscles were immunostained and analysed by confocal microscopy. In line with previous studies ICAM-2 was found to be expressed on ECs of arterioles, post-capillary venules, large venules and lymphatics in the cremaster muscle under basal conditions. The high basal expression of ICAM-2 has been suggested to be involved in EC-EC contacts (Huang, 2004), lymphocyte recirculation (Boscacci et al., 2010), monocyte patrolling (Schenkel et al., 2004) and in angiogenesis (Huang et al., 2005). Although ICAM-2 supports leukocyte extravasation during inflamed conditions the expression pattern of EC ICAM-2 on post-capillary venules was found to be distinct to other junctional proteins implicated in leukocyte transmigration. In the present study quantitative analysis of ICAM-2 localisation within ECs demonstrated a high heterogenic expression on the vascular lumen as well as at EC junctions. In contrast PECAM-1 was highly localised at EC junctions with a faint and diffuse cell-body expression. The distribution pattern of ICAM-2 and PECAM-1 detected in the

cremaster muscle under basal conditions was also demonstrated in the ear vasculature suggesting that this expression could be applicable to other vascular beds. The distinct expression of ICAM-2 compared to that of PECAM-1 further suggests that these molecules may have different functional roles. It has been demonstrated in prior studies from our group that ICAM-2, PECAM-1 and JAM-A have sequential non-redundant roles, and these roles appeared to be dependent on direct EC activation (Woodfin et al., 2009). From this study it was suggested that ICAM-2 has an early role during TEM whilst JAM-A was involved once the leukocyte was within the EC junction and PECAM-1 was involved when the leukocyte was on the abluminal side of the vessel. Taking this into account as well as the high EC body and junctional expression of ICAM-2, it is possible that ICAM-2 may have dual roles in leukocyte extravasation, namely luminal leukocyte-EC interactions as well as in TEM itself. It is also possible that the distribution of EC ICAM-2 may change during inflammation and this was further examined.

ICAM-2 is commonly compared to ICAM-1 as they belong to the same family of proteins. Whilst ICAM-1 is highly inducible by a wide range of inflammatory stimuli (Sumagin and Sarelius, 2010) ICAM-2 is not. In the present study, using immunostaining and confocal microscopy to analyse the mouse cremaster muscle, no effect on the total expression of EC ICAM-2 was detected in these vessels after IL-1β stimulation. This is in line with numerous studies, however using IL-1β stimulated HUVECs and human mammary arteries a down regulation in ICAM-2 has been reported (McLaughlin et al., 1999;McLaughlin et al., 1998). The differences seen between the findings of the present work and the work of McLaughlin et al., (1998) may be due to the latter study using ECs lining the arteries. No observable differences between venules and arterioles in the mouse cremaster muscle were however noted in the present study. Additionally McLaughlin et al., (1998) examined ICAM-2 expression using human cells in an *in vitro* system, suggesting possible differences between species (Godwin et al., 2004) and/or experimental conditions and this maybe the cause for these inconsistencies. Of interest ICAM-2 expression in pigs is similar to that of mice in that it is not downregulated upon stimulation with

TNF-α or IL-1β (Godwin et al., 2004). Variation in expression of ICAM-2 in different species is understudied and requires further investigation. It is important to note that the purpose of ICAM-2 down regulation on human and not in mice ECs is unknown, but could be related to the fact that ICAM-1 and ICAM-2, in some experimental conditions, have been shown to be functionally redundant (Lehmann et al., 2003).

Although total vessel ICAM-2 expression remains unchanged after IL-1β stimulation in our model, it is possible that ICAM-2 may undergo redistribution within individual ECs to support leukocyte TEM. This hypothesis was postulated in the light of recent findings that JAM-C redistributes away from EC junctions in inflammation (Scheiermann et al., 2009; Woodfin et al., 2011). In the present model no effect on ICAM-2 localisation within individual ECs was found in response to IL-1β stimulation. Nevertheless, it is possible that using a more complex inflammatory stimulus such as a combination of TNF-α and IFNγ, or alternatively I/R injury to induce neutrophil recruitment, a redistribution of ICAM-2 away from junctions may occur.

In contrast to the general consensus regarding the expression of ICAM-2 in inflammatory conditions, in the mucosal layer of the ileum from patients with Crohn's disease, an increase in ICAM-2 expression was detected using immunohistochemistry (Bernstein et al., 1998), although a similar study found very little change (Vainer and Nielsen, 2000). ICAM-2 expression in whole lung tissue from ovalbumin treated mice also demonstrated an up-regulation of ICAM-2 mRNA (Gerwin et al., 1999). It is likely that ICAM-2 up-regulation demonstrated in these experiments is in fact located on the epithelium rather than on the endothelium. In support of this, intraepithelial precursor lesions from patients with pancreatic cancer were found to have an upregulated ICAM-2 expression (Hiraoka et al., 2011). In human samples of malignant lymph nodes (lymphoma) an increase in ICAM-2 expression was also evident (Renkonen et al., 1992). It is therefore likely that when

lymphocyte infiltration is more dominant or alternately when the epithelium is stimulated an up-regulation in ICAM-2 expression occurs. This may reflect a different functional role for ICAM-2 under these circumstances. In the current study using a relatively simple acute model, no up-regulation or change in distribution of ICAM-2 expression on ECs were detected. It still remains to be elucidated whether more aggressive inflammatory stimuli would result in alterations in EC ICAM-2 expression *in vivo*. Collectively the data on EC ICAM-2 expression reported in the current study suggests that ICAM-2 may have dual roles in luminal neutrophil-EC interactions as well as in TEM, and this possibility was studied in subsequent chapters.

The stimulus used (IL-1β i.s.) in the current study predominately recruits neutrophils at a 4 hour time point (Thompson et al., 2001; Woodfin et al., 2011). For this reason detailed quantification of leukocyte ICAM-2 expression was carried out in order to understand the relative importance of EC versus neutrophil ICAM-2. Neutrophils (Sundd et al., 2012), monocytes (de Fougerolles et al., 1991), T cells (de Fougerolles et al., 1991), eosinophils (Gerwin et al., 1999) and natural killer cells (Helander et al., 1996; Somersalo et al., 1995) have all been previously shown to express ICAM-2. To date no studies have reported an increase in ICAM-2 expression on leukocytes in inflammation or upon activation. It is known that there is high ICAM-2 expression on ECs relative to that on leukocytes and the major focus of many previous studies investigating ICAM-2 function has been on the role of EC ICAM-2 rather than that on leukocytes. In the present study immunostaining of ICAM-2 (via i.v. and i.s. administration) and confocal analysis of IL-1β-stimulated cremaster muscles showed no evidence of neutrophil ICAM-2. In contrast, using flow cytometry analysis of whole mouse blood, neutrophil ICAM-2 expression was detected and this is in line with a recent report (Sundd et al., 2012), although a much higher relative fluorescent intensity was reported in that study. The current data suggests that ICAM-2 expression on neutrophils is relatively low in comparison to that of ECs and other leukocyte subsets. Flow cytometry analysis of mouse blood leukocytes under basal conditions confirmed that almost 100% of T and B cells were ICAM-2 positive. In

comparison approximately 80% of classical and non-classical monocytes were ICAM-2 positive. In contrast only 20% of all neutrophils expressed ICAM-2 and was expressed at relatively very low levels. For this reason homophilic interactions for ICAM-2 are also unlikely to occur during neutrophil extravasation. These results collectively suggest that the role of ICAM-2 in neutrophil extravasation is due to its expression on ECs rather than on neutrophils. The latter is further supported by earlier work in which WT bone marrow leukocytes transferred into ICAM-2 KO animals did not restore the observed defect in IL-1β-stimulated extravasation (Woodfin et al., 2009). Taking this into account, the data suggests that in the mouse cremaster muscle the defect in leukocyte extravasation seen after IL-1β stimulation when ICAM-2 is not functional, is likely to be a result of the loss of EC ICAM-2 as opposed to leukocyte ICAM-2.

Collectively the results from this chapter quantitatively demonstrate the expression of ICAM-2 within the mouse vasculature as well as on different leukocyte subsets. On post-capillary venules, a high heterogenic ICAM-2 expression was evident on the EC body as well at EC junctions. In contrast PECAM-1 was highly localised at EC junctions with a faint and diffuse cell-body expression. This expression pattern of EC ICAM-2 and PECAM-1 was demonstrated in the mouse cremasteric and ear skin vasculature. The total expression and localisation of ICAM-2 was unaffected by IL-1β stimulation, therefore discounting the possibility of both up-regulation and/or redistribution upon IL-1β-induced inflammation. In addition, as EC ICAM-2 expression is significantly higher than that detected on leukocytes, it is highly likely that the deficiency in leukocyte extravasation seen in ICAM-2 KO mice after IL-1β stimulation (Huang et al., 2006; Woodfin et al., 2009) is due to loss of EC ICAM-2 rather than leukocyte ICAM-2. These findings extend previous works on the expression profile of ICAM-2 *in vivo* and suggests a possible role for ICAM-2 in neutrophil-EC interactions in addition to its role in TEM.

CHAPTER 4: Role of ICAM-2 in luminal neutrophil-endothelial cell interactions

4.1 Introduction

ICAM-2 is has been shown to support neutrophil extravasation into the tissue, however, the mechanism by which it mediates this response is currently unknown. The previous chapter focussed on investigating the localisation of ICAM-2 to gain further insights into its functions. These studies demonstrated that ICAM-2 has relatively high heterogeneous basal EC expression at non-junctional regions in comparison to junctional regions between adjacent ECs. This EC ICAM-2 distribution was in contrast to that observed for PECAM-1, a well-established endothelial junctional molecule which is known to support neutrophil migration into the extravascular tissue via mediating neutrophil TEM (Privratsky et al., 2010). More specifically, PECAM-1 displayed a high EC junctional expression and a relatively low homogeneous EC non-junctional expression. The distinct expression of ICAM-2 compared to PECAM-1 suggests that these molecules may have functionally different roles. A role for ICAM-2 at early stages of TEM was suggested (Huang et al., 2006; Woodfin et al., 2009) however to date no studies have directly reported the mechanism or stage by which EC ICAM-2 is involved in neutrophil extravasation.

The high basal expression of ICAM-2 is likely to be due to its role in EC to cell contacts (Huang, 2004), lymphocyte recirculation (Boscacci et al., 2010), monocyte patrolling (Schenkel et al., 2004) and its role in angiogenesis (Huang et al., 2005), all which have been previously demonstrated. Under inflammatory conditions, ICAM-2 is likely to have different functions. Trafficking of neutrophils (Hobden, 2003; Huang et al., 2006; Issekutz et al., 1999; Woodfin et al., 2009), eosinophils (Gerwin et al., 1999), monocytes (Schenkel et al., 2004), T cells (Boscacci et al., 2010; Lehmann et al., 2003; Lyck et al., 2003; Reiss et al., 1998; Steiner et al., 2010),

dendritic cells (Geijtenbeek et al., 2000; Helander et al., 1996; Wethmar et al., 2006) and the activation of natural killer cells (Helander et al., 1996) have all been shown to be, at least in part, dependent on the presence of functional ICAM-2. However very few studies have investigated the precise stage by which it regulates this process. A recent study has confirmed a role for neutrophil ICAM-2 during rolling through the formation of 'slings' using bone marrow derived neutrophils in *in vitro* microfluidic perfusion assays (Sundd et al., 2012). However they also show that in the mouse bone marrow, neutrophils have a higher RFI of immunostained ICAM-2 than that detected in blood circulation and therefore may reflect differences in the role of immature bone marrow neutrophils. The low expression of ICAM-2 on neutrophils which was confirmed in Chapter 3 and earlier work showing that WT bone marrow leukocytes transferred into ICAM-2 KO animals did not restore the observed defect in IL-1β-stimulated neutrophils extravasation (Woodfin et al., 2009), together with numerous other reports on the role of EC ICAM-2 in leukocyte recruitment (Boscacci et al., 2010; Schenkel et al., 2004; Steiner et al., 2010), the focus of the present study was on EC ICAM-2 function. With the use of real time microscopy, previous reports have suggested a role for EC ICAM-2 during T cell adhesion, polarisation and possibly TEM (Boscacci et al., 2010; Steiner et al., 2010) as well as in monocyte crawling (Schenkel et al., 2004). A study by Phillipson et al (2006), reported that a functional blocking mAb to ICAM-2 had no effect on the total percentage of adherent neutrophils that crawled, however whether ICAM-2 affected the dynamics of crawling was not documented.

Taken together the distinct expression pattern of EC ICAM-2 in comparison to that of PECAM-1, and the fact that several different inflammatory models have clearly shown a role for ICAM-2 in neutrophil migration into the tissue which seems to be at a stage post-adhesion but prior to TEM, it was hypothesised that ICAM-2 may mediate luminal neutrophil-EC interactions during crawling. The studies presented in the current chapter therefore aimed to investigate the precise function of ICAM-2 in mediating neutrophil extravasation by examining its potential role in neutrophil crawling. This objective was addressed through the use of the cremasteric confocal

IVM model. Using this technique neutrophil migration dynamics were investigated in the vasculature from WT and ICAM-2 KO mice. Collectively the results obtained provide further insights into the role of ICAM-2 in neutrophil extravasation during inflammation.

4.2 Results

4.2.1 ICAM-2 contributes to neutrophil extravasation but not initial adhesion

ICAM-2 has been shown to support neutrophil extravasation, and this study aimed to elucidate the mechanism by which this occurred. Previous work using transmitted light IVM has shown that in the absence of functional ICAM-2, IL-1β stimulation elicits normal levels of neutrophil adhesion, but reduced neutrophil extravasation (Huang et al., 2006; Woodfin et al., 2009). Initial studies sought to confirm these findings using a 4D confocal IVM model.

Mice expressing eGFP under the lysozyme promoter (Lys-eGFP-ki), which exhibit endogenous fluorescent neutrophils, and to lesser extent monocytes, were employed in this study (Faust et al., 2000). These animals were crossed with mice deficient in ICAM-2 to produce a strain of ICAM-2 KO animals with eGFP positive neutrophils and monocytes. The vasculature of the cremaster muscle was labelled via an i.s. injection of fluorescently tagged anti-PECAM-1 mAb (clone 390, which is a non-function blocking mAb). This labelling technique has been shown to have no impact on normal leukocyte responses (Woodfin et al., 2011). Cremaster muscles were subjected to 2 hours stimulation with IL-1β (i.s.) after which the cremaster muscles was exteriorised following anaesthesia. Sequential images of venules were captured using *in vivo* confocal microscopy for approximately a further 2 hours. The number

of extravasated neutrophils was taken from the final time point of live imaging experiments (~ 4 hours after initial IL-1β i.s. injections). Post-acquisition the images were analysed using the 4D modelling software Imaris and the numbers of intravascular and extravascular cells were quantified (Figure 4.1A).

The leukocyte subtype recruited in this model was neutrophils as the eGFP monocytes in Lys-eGFP-ki mice which exhibit lower level of eGFP fluorescence in comparison to neutrophils were excluded from the analysis (Woodfin et al., 2011). IL-1β stimulation was used as an acute inflammatory stimulus which is primarily neutrophil driven at the 4 hour time point (Thompson et al., 2001; Woodfin et al., 2011), hence the analysis represents acute neutrophillic inflammation.

In both WT and ICAM-2 KO Lys-eGFP-ki mice, IL-1β stimulation elicited a significant increase in intravascular neutrophils (Movies 1 and 2), but no difference between WT and KO mice were seen (Figure 4.1). In contrast while WT animals exhibited a significant increase in extravascular neutrophils following IL-1β stimulation (Movie 2), those lacking ICAM-2 showed a substantial reduction in extravasation following IL-1β compared to WT, and did not exhibit a response significantly different to saline treatment (Figure 4.1). The defect in neutrophil recruitment seen in the ICAM-2 KO mice was not due to a reduction in the number of circulating leukocytes in the blood. This was illustrated by taking blood samples from both mouse strains staining them with trypan blue. Trypan blue enables easy identification of dead cells which take up the dye and appear blue with uneven cell membranes. In comparison, viable cells repel the dye and appear colourless and refractile under phase contrast. Using this technique the total blood leukocytes/ml was determined. Both WT and ICAM-2 KO mice had approximately 2.5×10^6 leukocytes per ml, indicating no differences in bone marrow mobilisation of leukocytes between both strains (Figure 4.2A).

To further ensure normal percentages of different leukocytes subsets within the blood circulation, the percentage of different leukocyte subsets was determined by flow cytometry. Leukocyte subsets were identified based on the surface expression of specific markers as mentioned previously. All percentages were comparable to that detected in published data (Gerwin et al., 1999). Specifically, 25% of leukocytes were neutrophils in both WT and ICAM-2 KO mice (Figure 4.2B) and classical monocytes and non-classical monocytes represented 4.5% and 5% of leukocytes respectively in WT mice with no differences being detected in ICAM-2 KO animals (Figure 4.2C). Furthermore, B cell (40%) and T cell (19%) percentages of total leukocytes were also comparable in both mouse strains (Figure 4.2D). Together the results indicate no defect in the total numbers and the relative percentages of circulating blood leukocyte subsets in ICAM-2 KO mice suggesting that the reduced number of tissue infiltrated neutrophils was due to a defect in neutrophil extravasation.

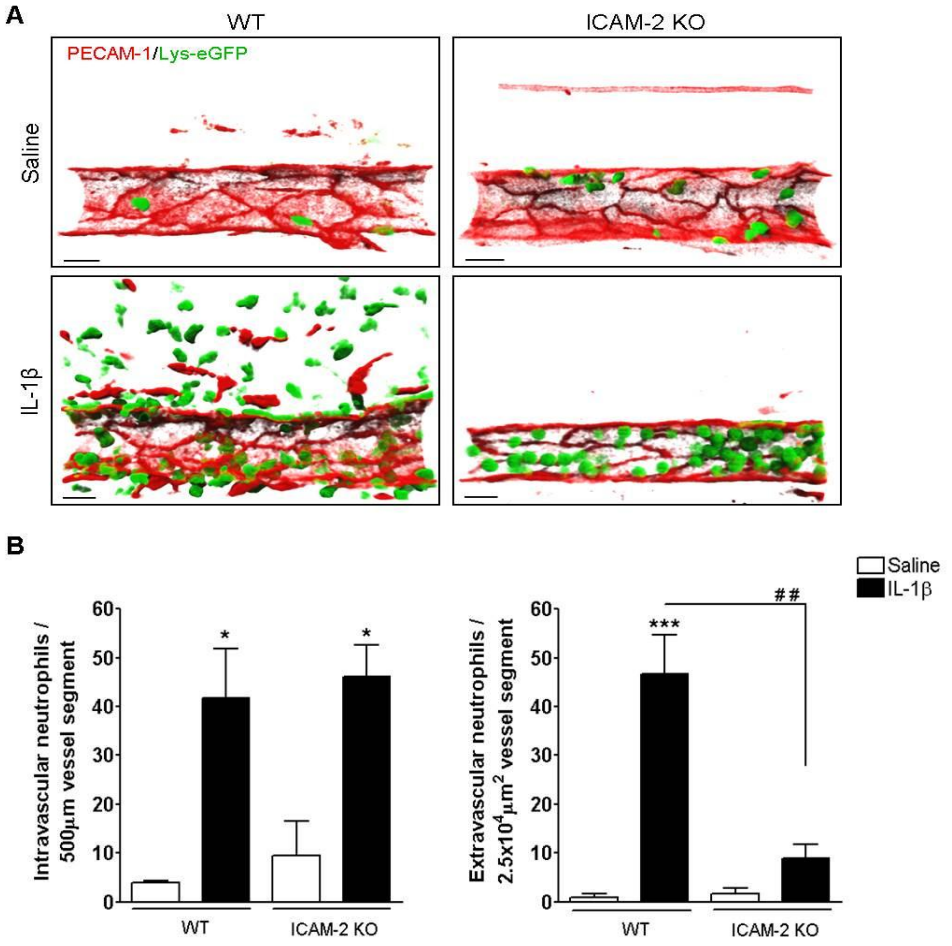

Figure 4.1: IL-1β-induced inflammation in WT and ICAM-2 KO cremasteric post-capillary venules.

Cremasteric confocal IVM of WT or ICAM-2 KO Lys-eGFP-ki mice stimulated with i.s. IL-1β (50 ng/mouse) or saline for 2 hours. (**A**) Representative images of post-capillary venules where PECAM-1 (i.s. labelling *in vivo*) are shown in red and neutrophils (Lys-eGFP-ki mice) are in green. (**B**) Quantification of intravascular and extravascular neutrophils in WT and ICAM-2 KO mice after saline or IL-1β stimulation. N = 3-7 animals per group, 3-5 vessels per cremaster. Error bars show SEM. Statistically significant (Anova) differences between IL-1β or saline stimulated tissues are indicated by asterisks, *P<0.05 and ***P<0.001. Differences between WT and KO responses are indicated with hash symbols ## P<0.01.

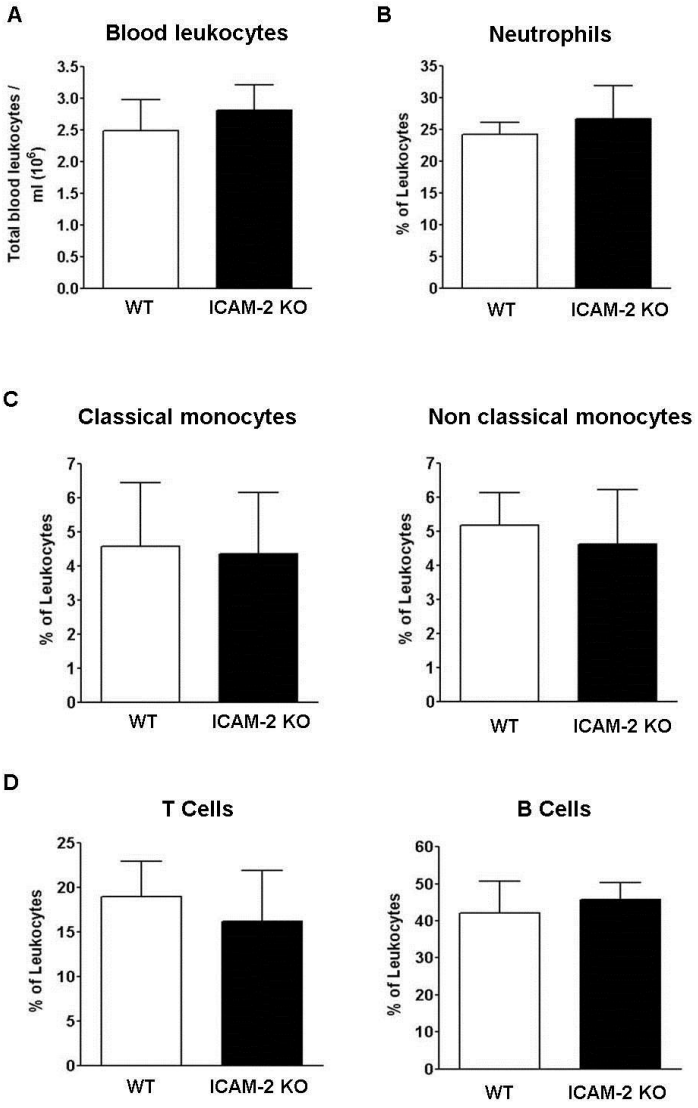

Figure 4.2: Circulating blood leukocyte numbers in WT and ICAM-2 KO mice.

(**A**) Total blood leukocyte numbers were determined by trypan blue and counted using a Neubauer haemocytometer. (**B**) Neutrophils, (**C**) monocytes and (**D**) lymphocytes as percentage total of leukocytes present in the blood circulation was determined by flow cytometry. Neutrophils were classified by Gr-1 staining. Classical monocytes were Gr-1 and CD115 positive where as non-classical monocytes were negative for Gr-1 and positive for CD115 staining. T cells corresponded to cells which were positive for CD3 staining. B cells corresponded to cells which were positive for B220 staining. Results are presented as mean ± SEM for each mice (n=3 mice).

4.2.2 Luminal crawling of neutrophils under basal conditions

The expression pattern of EC ICAM-2 suggests it may have a role in luminal neutrophil-EC interactions. In order to investigate this hypothesis, luminal neutrophil crawling dynamics were analysed initially under basal conditions in the mouse cremaster muscle using *in vivo* confocal imaging. The cremasteric vasculature of WT or ICAM-2 KO mice expressing eGFP in neutrophils was labelled with fluorescent anti-PECAM-1 mAb (i.s.) as described in Chapter 2. Labelled tissues were exteriorised after 2 hours, and selected post-capillary venules were imaged at 30 second intervals for a further 2 hours (approximately 30-40 minutes per vessel). Post-acquisition the sequential image stacks were converted into dynamic 3D models (an example of uninflamed vs inflamed vessel is shown in Movies 1 and 2 respectively), and the migratory crawling behaviour of individual cells was tracked and quantified using Imaris (Movie 3). Still images of the dynamic movement of an individual crawling neutrophil are shown in Figure 4.3.

Using this technique all neutrophils which were able to be tracked for at least 5 frames (2.5 minutes) was analysed (Figure 4.3). Under basal conditions WT and ICAM-2 KO mice had a low average number of quantifiable neutrophil crawling events per venule (Figure 4.4A), this is most likely due to the low number of adherent neutrophils seen in response to saline treatment (Figure 4.1B) and hence fewer cells progressing to the crawling stage. Of the few cells which were tracked after saline treatment, various neutrophil crawling dynamics were analysed. In WT mice neutrophil crawling speed was 9.4 ± 1.0 μm/min (n=13 cells, from 4 vessels in 3 mice), duration was 9.8 ± 2.1 min and length covered was 90.5 ± 18.1 μm (Figure 4.5). In ICAM-2 KO mice these neutrophil crawling dynamics were slightly reduced, however this was not significantly different (Figure 4.4) and may reflect the low number of cells available to analyse. Overall no conclusions can be made on the role of ICAM-2 in mediating neutrophil crawling under basal conditions.

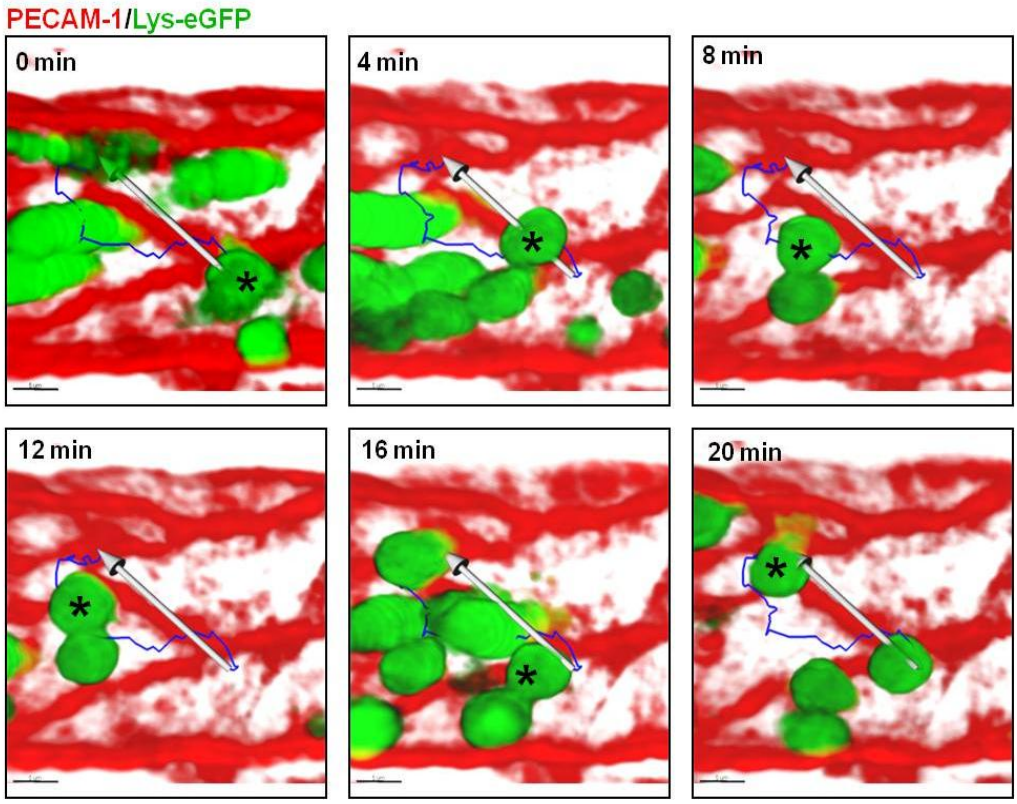

Figure 4.3: Intraluminal neutrophil crawling on endothelial cells lining post-capillary venules as analysed by 4D confocal IVM.

Representative images of cremasteric post-capillary venules from Lys-eGFP-ki mice as investigated by confocal IVM. High magnification images acquired at indicated time points illustrating the time course of an individual crawling neutrophil which could be tracked for at least 5 frames (2.5 minutes) as indicated by the asterisks. The blue line shows the entire crawling track and the white arrow shows the track displacement of the highlighted neutrophil. Scale bar represents 5 µm. (Movie 3).

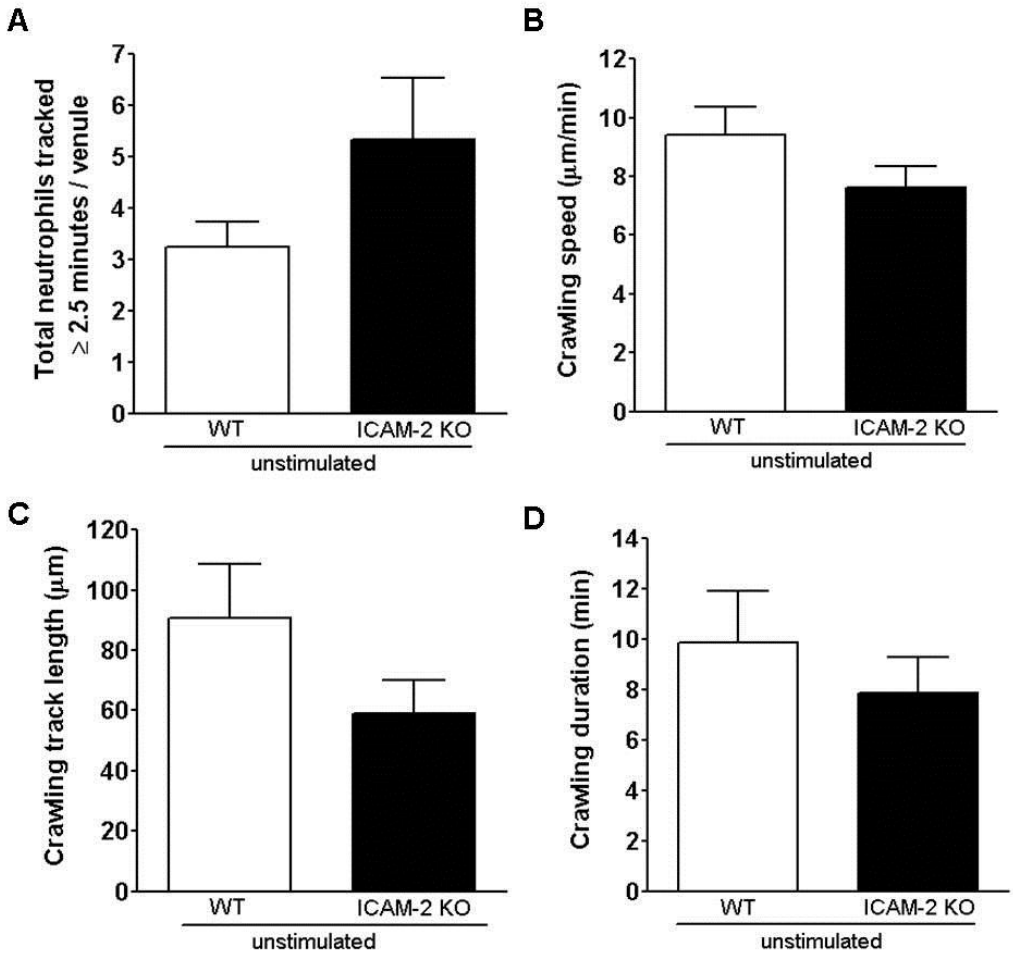

Figure 4.4: Neutrophil crawling dynamics under basal conditions in WT and ICAM-2 KO mice.

Cremasteric confocal IVM of WT or ICAM-2 KO Lys-eGFP-ki mice stimulated with i.s. saline for 2 hours. Various parameters relating to crawling dynamics were quantified using Imaris. (**A**) The total number of luminal neutrophils which were observable for at least 5 frames (2.5 minutes) or more was analysed. The mean total (**B**) speed, (**C**) duration and (**D**) track length of luminal crawling cells in WT and ICAM-2 KO mice under unstimulated conditions. N=13-16 cells, from 3-4 vessels in 3 mice per group. Error bars show SEM. (Movie 1).

4.2.3 IL-1β stimulates neutrophil luminal crawling in the cremaster muscles from WT and ICAM-2 KO mice

Using the technique detailed above, neutrophil crawling dynamics was analysed in cremasteric venules post-IL-1β in WT and ICAM-2 KO mice. After IL-1β stimulation the total number of clear events analysed per venule increased to approximately 10 cells irrespective of genotype (Figure 4.5A). As expected from the intravascular data (Figure 4.1), no difference in the number of adherent neutrophils was detected between WT and ICAM-2 KO mice after IL-1β stimulation. Interestingly, it was found that after IL-1β stimulation, a small subset of neutrophils did not exhibit crawling and appeared to undergo only slight movements for the duration of the observation period. These cells were classified as 'stationary neutrophils' and were defined as neutrophils which were able to be tracked and displayed immobility of crawling as quantified by a displacement less than 5 μm (approximately half of the cell diameter) for the duration of observation (Figure 4.6 and Movie 3). Crawling cells were defined as neutrophils which were able to be tracked for at least 5 frames (2.5 minutes) and displayed a crawling displacement of at least 5 μm for the duration of the observation period. These definitions were used to quantify the percentage of adherent cells which crawled in WT and ICAM-2 KO mice after IL-1β stimulation. In line with published data in both WT and ICAM-2 KO mice the vast majority of adherent cells exhibited crawling behaviour (Phillipson et al., 2006). However as mentioned previously, a small reduction in crawling frequency in the ICAM-2 deficient group was seen (95.6 ± 3.4 % WT and 80.4 ± 4.7 % ICAM-2 KO, n=10 venules, 76-81 cells form 6-7 mice, Figure 4.5B).

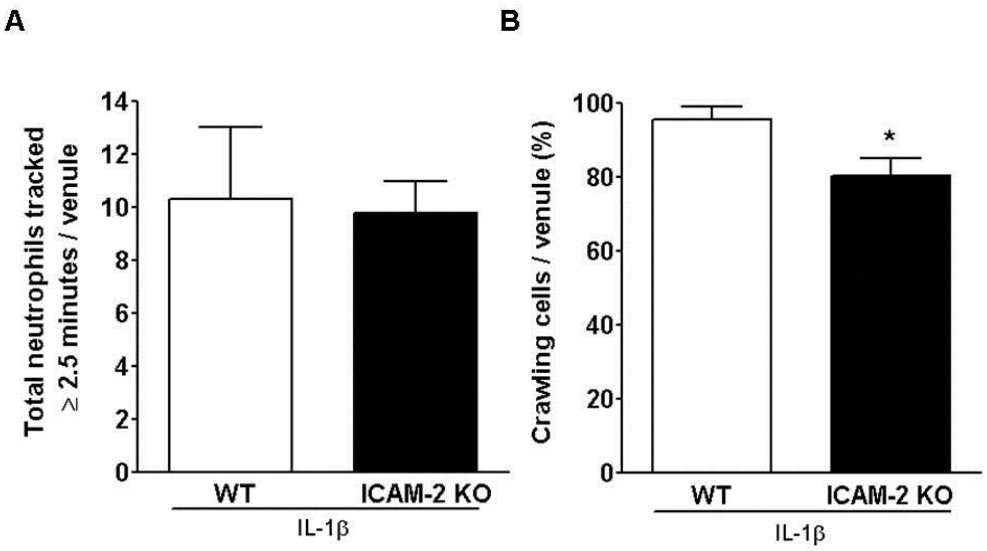

Figure 4.5: IL-1β-stimulated neutrophil crawling in WT and ICAM-2 KO mice.

Cremasteric confocal IVM of WT or ICAM-2 KO Lys-eGFP-ki mice stimulated with i.s. IL-1β (50 ng/mouse) for 2 hours. Various parameters relating to crawling dynamics were quantified using Imaris. (**A**) The total number of luminal neutrophils which were observable for 2.5 minutes or more was analysed. (**B**) The percentage of adherent neutrophils which exhibited crawling motility with a displacement of more than 5μm was quantified, per venule, in WT and ICAM-2 KO. N = 76-81 cells from 10 vessels in 6-7 animals per group. Error bars show SEM. Statistically significant (T-test) differences between WT and ICAM-2 KO data are indicated by asterisks *P< 0.05. (Movie 2).

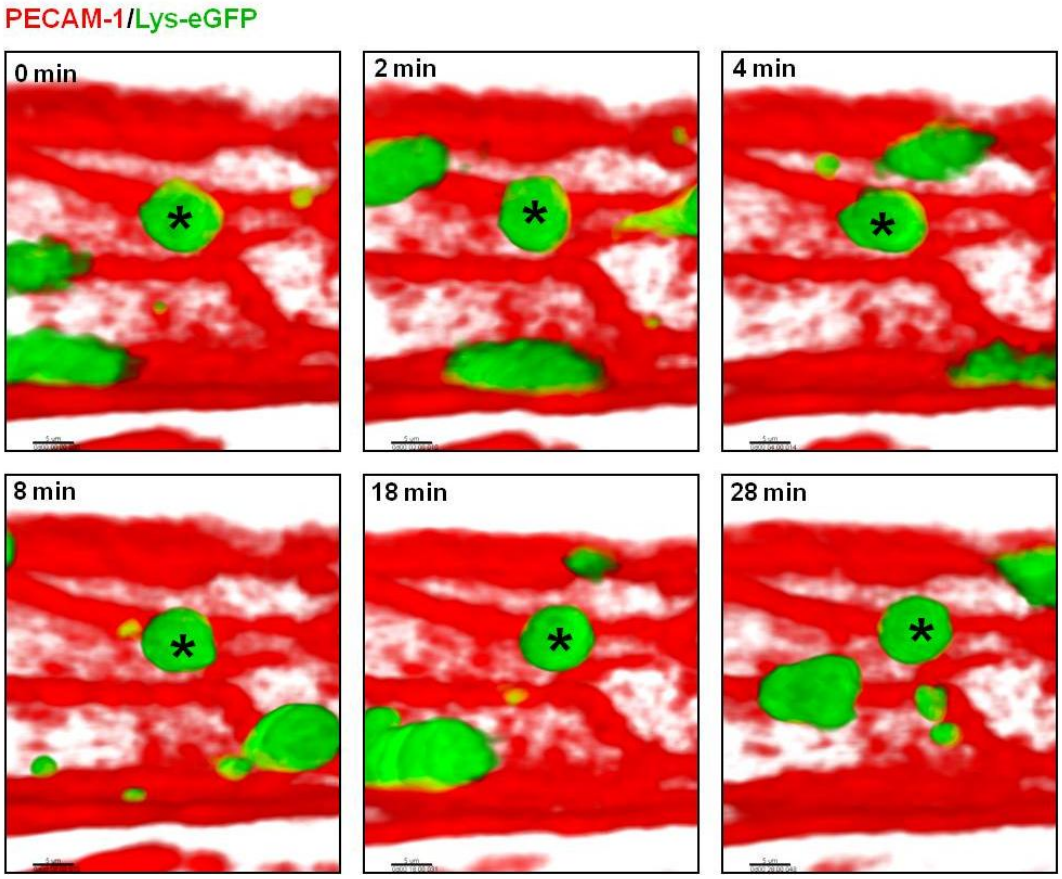

Figure 4.6: Intraluminal stationary neutrophil as analysed by 4D confocal IVM.

Representative images of cremasteric post-capillary venules from Lys-eGFP-ki mice as investigated by confocal IVM. High magnification images acquired at indicated time points illustrating the time course of an individual stationary neutrophil indicated by the asterisks. Stationary (or immobile) neutrophils as defined by a displacement less than 5 µm for the duration of observation. Scale bar represents 5 µm. (Movie 4).

4.2.4 ICAM-2 supports luminal neutrophil crawling dynamics in IL-1β-stimulated inflammation

Using the detailed *in vivo* system, individual crawling neutrophils were tracked and a number of migratory parameters quantified in WT and ICAM-2 KO cremaster muscles post-stimulation with IL-1β. All data presented is the mean of 76-81 cells, from 10 venules, from 6-7 mice. A significant reduction ($P<0.001$) in mean neutrophil crawling speed was detected in ICAM-2 KO mice (6.3 ± 0.3 μm/min, n= 81 cells) in comparison to WT (10.4 ± 0.5 μm/min, n= 76 cells) (Figure 4.7A). Interestingly the variability in crawling speed was considerably higher in the ICAM-2 KO mice as compared to WT (Figure 4.7B). The crawling speed variability of each track was calculated by dividing the crawling speed standard deviation by the crawling speed mean value. The length and duration of observed neutrophil crawling cells was significantly different in these two strains of mice. Whilst the crawling length was slightly reduced in the ICAM-2 KO mice (Figure 4.7C), the duration of crawling was approximately 4 minutes longer than that detected in WT controls (9.4 ± 0.9 min in WT, 13.1 ± 1.1 min in ICAM-2 KO) (Figure 4.7D). No difference between the two strains was detected in neutrophil crawling displacement (the distance between the first and the last point) and straightness (displacement/total crawling track length) of crawling (Figure 4.8). The net neutrophil crawling displacement direction relative to blood flow was also analysed. Each crawling displacement vector was classified as crawling in the direction of blood flow, perpendicular to or against blood flow and the specific criteria was based on angles from the direction of blood flow (Figure 4.9A). In both groups the net crawling displacement direction relative to blood flow was predominately in the direction of blood flow (52.5 ± 5.6 % in WT, 67.5 ± 4.9 % in ICAM-2 KO), while 34.7 ± 7.0 % of neutrophils in WT, 25.7 ± 4.9 % of neutrophils in ICAM-2 KO crawled perpendicular to the flow of blood. Approximately 10% of neutrophils crawled against the flow of blood in both mouse strains (Figure 4.9).

These data indicate that ICAM-2 is essential for supporting efficient luminal crawling with respect to speed, duration and distance and this may facilitate the identification of sites permissive for TEM thus reducing the total duration of crawling time and increasing the crawling speed in WT mice.

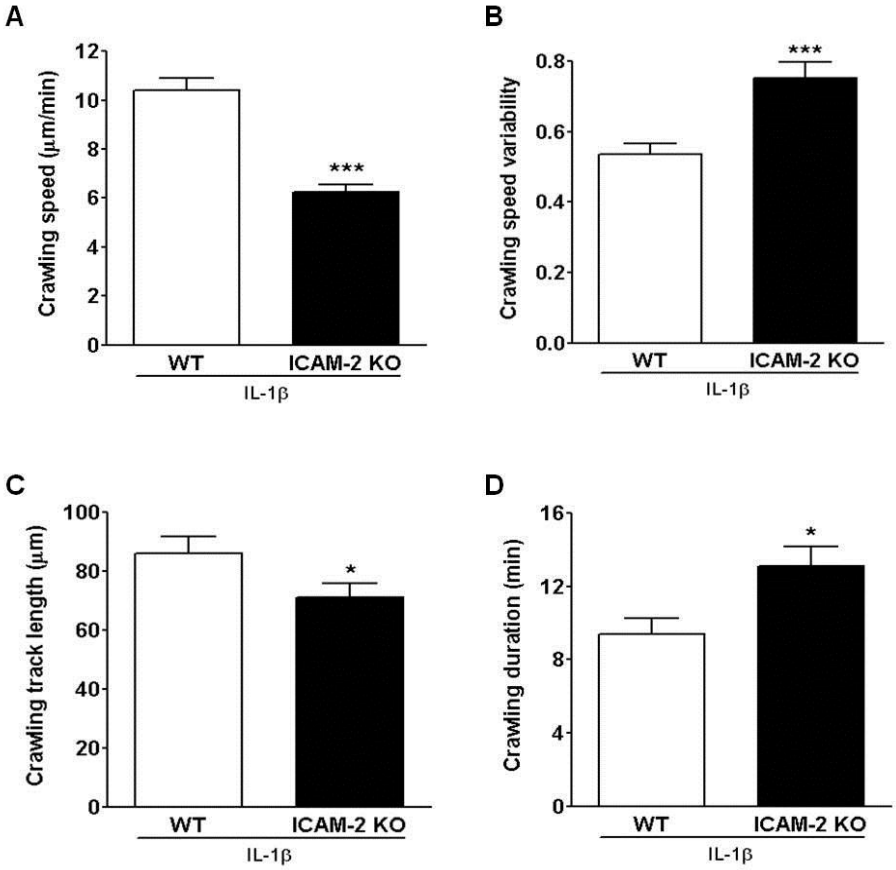

Figure 4.7: IL-1β-stimulated neutrophil crawling dynamics in WT and ICAM-2 KO mice.

Cremasteric confocal IVM of WT or ICAM-2 KO Lys-eGFP-ki mice stimulated with i.s. IL-1β (50 ng/mouse) for 2 hours. Various parameters relating to crawling dynamics were quantified using Imaris. The mean total (**A**) speed (**B**) speed variability (**C**) track length and (**D**) duration of crawling in WT and ICAM-2 KO venules was quantified. N = 76-81 cells from 10 vessels in 6-7 animals per group. Error bars show SEM. Statistically significant (T-test) differences between WT and ICAM-2 KO data are indicated by asterisks *P< 0.05, ***P< 0.001.

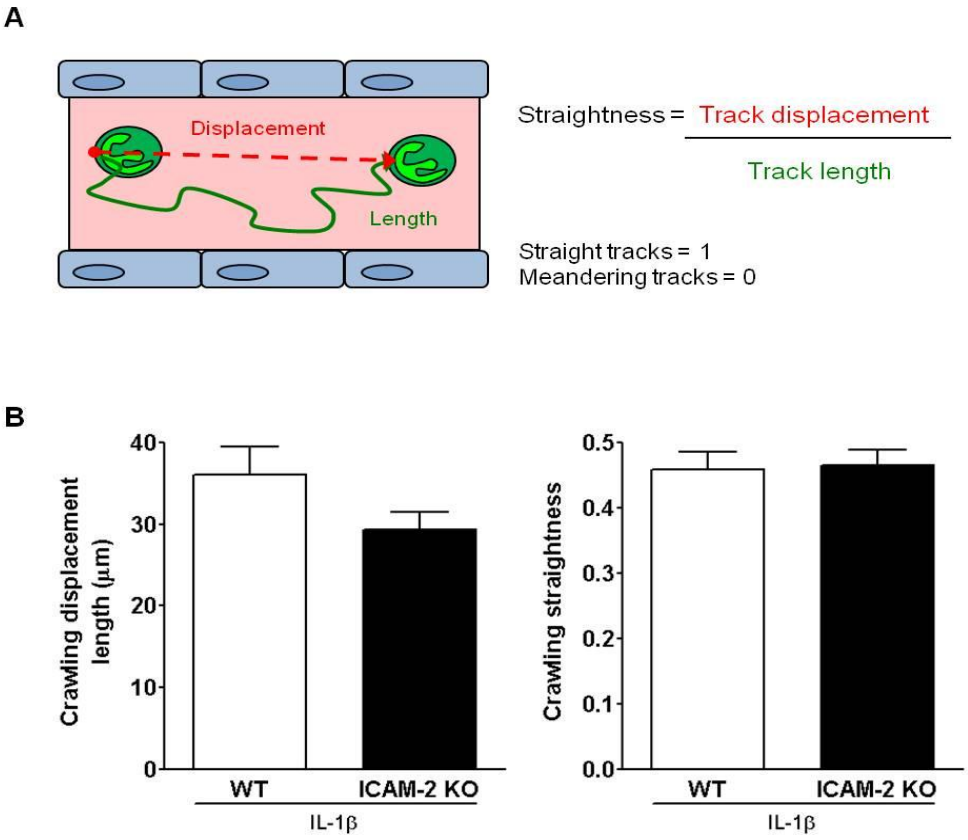

Figure 4.8: Neutrophil crawling displacement and straightness after IL-1β stimulation in WT and ICAM-2 KO mice.

Cremasteric confocal IVM of WT or ICAM-2 KO Lys-eGFP-ki mice stimulated with i.s. IL-1β (50 ng/mouse) for 2 hours. Various parameters relating to crawling dynamics were quantified using Imaris. (**A**) Diagram showing how neutrophil crawling displacement (dashed red line) and straightness was determined. Neutrophil crawling straightness is calculated by the track displacement divided by the total track length (green line). The mean total (**B**) displacement and straightness of crawling in WT and ICAM-2-KO venules was quantified. N = 76-81 cells from 10 vessels, in 6-7 animals per group. Error bars show SEM.

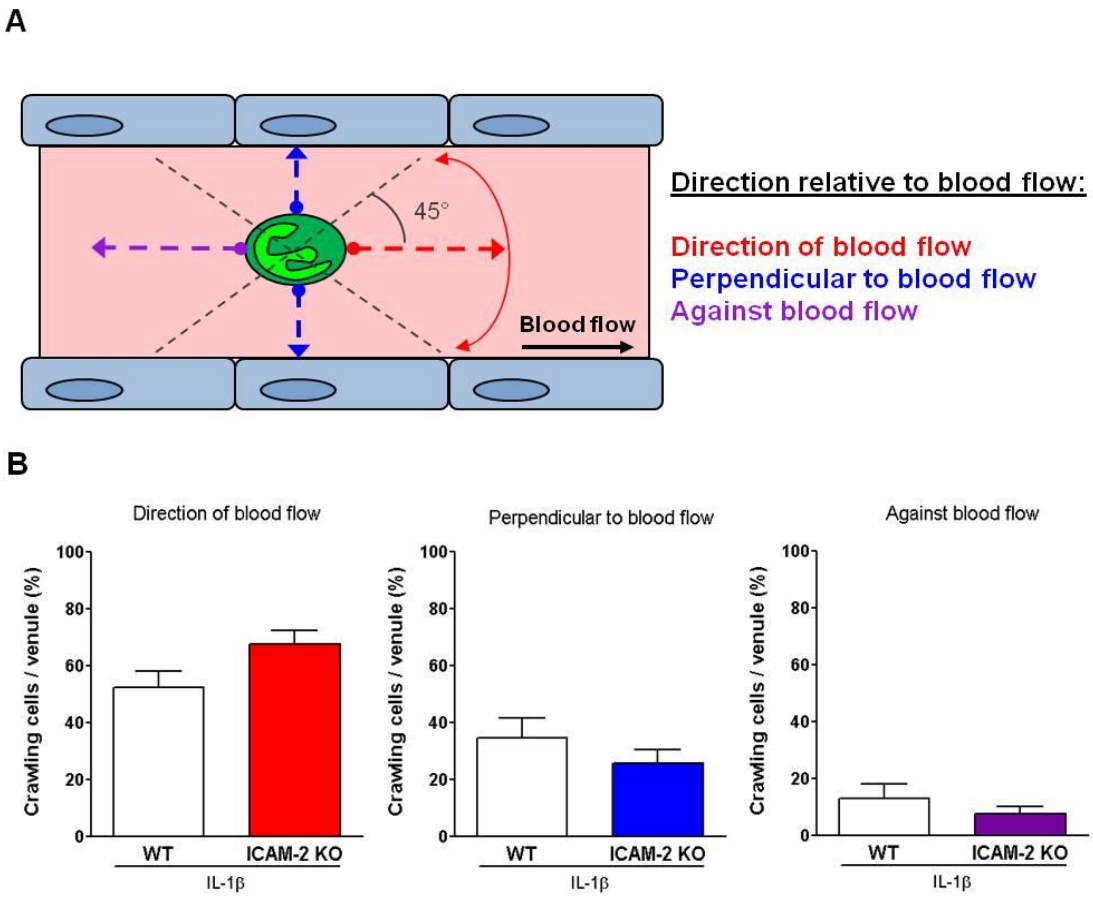

Figure 4.9: Neutrophil crawling displacement direction relative to blood flow in IL-1β-stimulated WT and ICAM-2 KO mice.

Cremasteric confocal IVM of WT or ICAM-2 KO Lys-eGFP-ki mice stimulated with i.s. IL-1β (50 ng/mouse) for 2 hours. Various parameters relating to crawling dynamics were quantified using Imaris. (**A**) Diagram showing how neutrophil crawling displacement direction relative to blood flow was determined. Dotted lines show the regions which were classified as crawling with blood flow, perpendicular to blood flow and against blood flow. (**B**) The percentage of neutrophil crawling displacement direction that was in the direction of blood (red), perpendicular to blood flow (blue) or against blood flow (purple) was determined. N= 76-81 cells from 10 vessels, in 6-7 animals per group. Error bars show SEM.

4.2.5 Neutrophils exhibit two distinct types of crawling behaviour

In ICAM-2 KO animals the mean neutrophil crawling speed was reduced, and in addition to this there was a greater variability in crawling speed of individual cells. The behaviour of individual cells was examined in more detail, and it was observed that while some cells exhibited continuous crawling behaviour, in that they were mobile for the full duration of tracking, other cells exhibited periods of immobility for at least 5 frames (2.5 minutes) during the observation period. These behaviours are now referred to as 'continuous' (Figure 4.10, Movie 5) and 'discontinuous' (Figure 4.11, Movie 6) crawling. Neutrophils were classified as exhibiting 'continuous' crawling if they were mobile for the duration of the observation period.

Examples of the speed of different neutrophil crawling behaviours (i.e. continuous or discontinuous) throughout their tracks are shown in Figure 4.12A. All crawling behaviours were highly variable with respect to speed throughout the duration of crawling. Whilst, the continuous crawling cells displayed generally high speeds, stationary neutrophils had speeds which remained below 2 μm/min throughout the duration of observation (Figure 4.12A). Stationary cells (or immobile cells) did not have a speed of 0 μm/min as these cells displayed very slight movements which were likely to be a result of shear flow of blood or due to small movements of the cremaster muscle itself. In contrast discontinuously crawling neutrophils exhibited speeds similar to that of continuously crawling cells however they also exhibited periods of immobility which had a speed comparable to that of stationary neutrophils (Figure 4.12A). The average duration of the periods of immobility in cells categorised as discontinuously crawling was 6.8 minutes, demonstrating that the definition of immobility (for 5 frames or 2.5 minutes or more) was a true characteristic and the strict categorisation of cells in terms of duration was not a restricting factor. On average there was approximately 2 periods of immobility in any discontinuously crawling cell, and during this period no evidence of EC junctional

disruption (pore formation), or neutrophil protrusions into EC junctions was evident. Crawling behaviour at junctional and non-junctional EC regions was determined in both continuously and discontinuously crawling neutrophils to understand these behaviours in more detail. The results indicated no differences in the crawling speed of neutrophils at EC junctional and at non-junctional regions. There was a significant reduction in the mean crawling speeds between continuous and discontinuous crawling irrespective of its location on EC (Figure 4.12B). The neutrophil crawling dynamics between these two behaviours in WT and ICAM-2 KO was subsequently analysed in more detail.

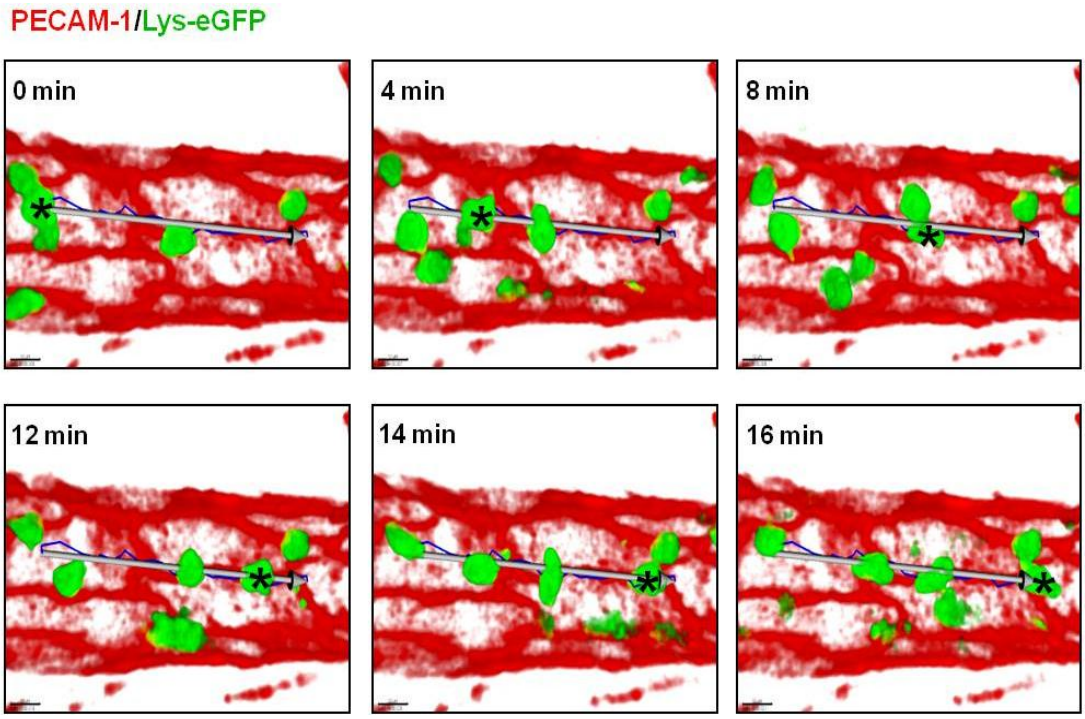

Figure 4.10: Continuously crawling neutrophil in the venular lumen.

Time sequence of neutrophil crawling in the cremasteric post-capillary venules from Lys-eGFP-ki mice as investigated by confocal IVM. High magnification images acquired at indicated time points illustrating the time course of a continuously crawling neutrophil as indicated by the asterisks. The blue line shows the entire crawling track and the white arrow shows the track displacement of the highlighted neutrophil. Scale bar represents 10 μm. (Movie 5).

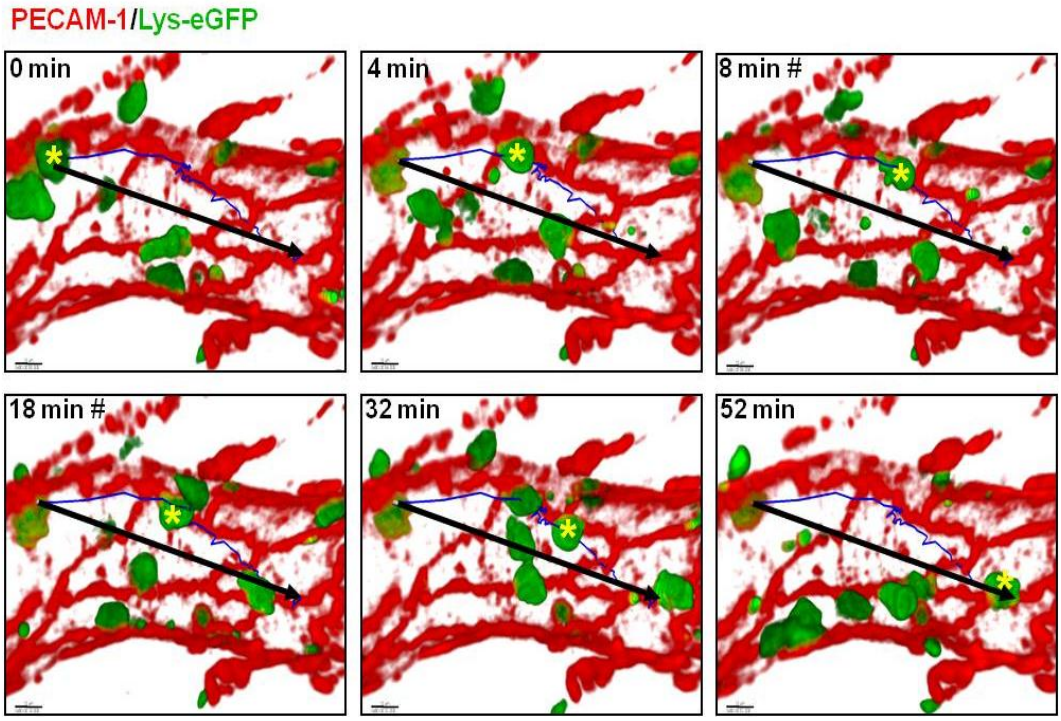

Figure 4.11: Discontinuously crawling neutrophil in the venular lumen.

Time sequence of neutrophil crawling in the cremasteric post-capillary venules from Lys-eGFP-ki mice as investigated by confocal IVM. High magnification images acquired at indicated time points illustrating the time course of a discontinuously crawling neutrophil as indicated by the asterisks. Time points which are followed by hash symbol represents the period of immobility. The blue line shows the entire crawling track and the black arrow shows the track displacement of the highlighted neutrophil. Scale bar represents 10 μm. (Movie 6).

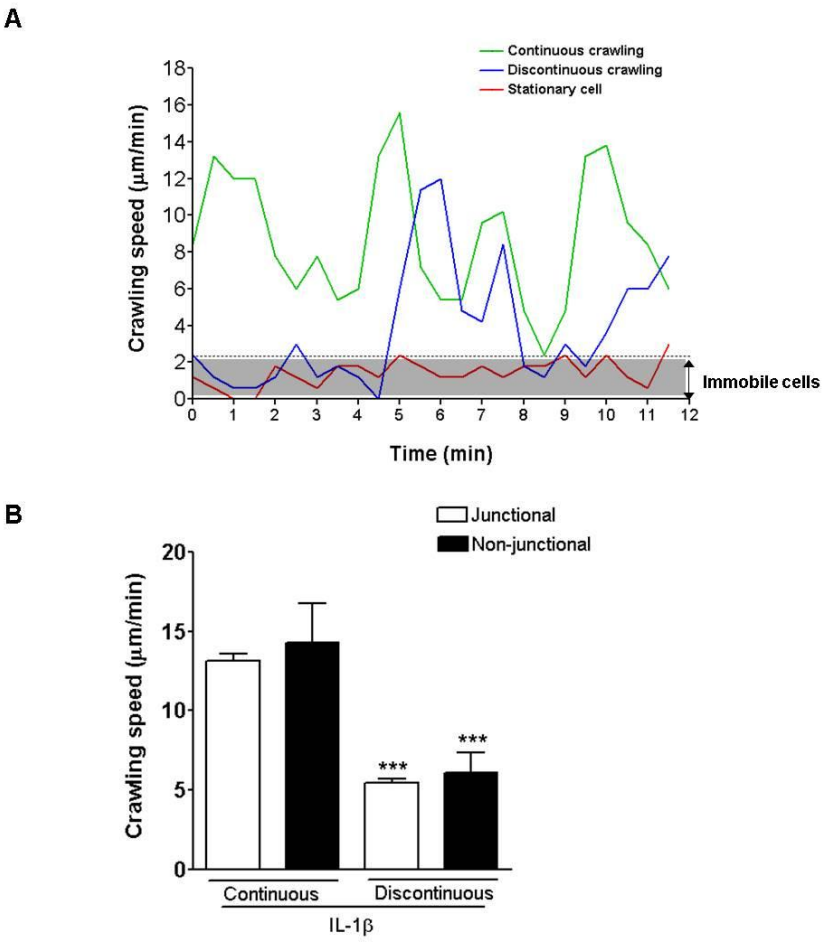

Figure 4.12: Neutrophil crawling speed of individual cells.

Cremasteric confocal IVM of WT Lys-eGFP-ki mice stimulated with i.s. IL-1β (50 ng/mouse) for 2 hours. (**A**) The speed of an individual cell exhibiting continuous, discontinuous and stationary crawling behaviours over time. (**B**) The mean speed of continuous and discontinuous crawling cells when in contact with EC junctions and non-junctional regions. N = 76-81 cells from 10 vessels, in 6-7 animals per group. Error bars show SEM. Statistically significant (Anova) differences between respected behaviours continuous and discontinuous data are indicated by asterisks ***P< 0.001.

4.2.6 Dynamic profile of continuously and discontinuously crawling neutrophils in WT and ICAM-2 KO mice

Each crawling track from WT and ICAM-2 KO mice, following IL-1β stimulation, was classified as showing 'continuous' or 'discontinuous' crawling, and the frequency of each behaviour per venule was determined. In WT mice the majority of crawling cells showed continuous crawling (87.2 ± 5.6 %) (Figure 4.13), while in the ICAM-2 KO animals there was a shift towards discontinuous crawling (51.5 ± 8.8 %) (Figure 4.13). This represents a 41.5 % reduction in continuous crawling ($P < 0.01$, n=10) in ICAM-2 KO vessels. In order to further understand the differences between continuous and discontinuous crawling behaviours in more detail in the two mouse strains, the crawling dynamics were determined. Neutrophils exhibiting discontinuous crawling phenotype were found to have a significantly reduced crawling speed, high speed variation and an increased duration of luminal crawling in both WT and ICAM-2 KO animals (Figure 4.14). This group of cells also had a tendency towards a lower straightness score than continuously crawling cells in both mouse strains (Figure 4.15B). The differences seen are likely to be due to the immobile periods in discontinuously crawling cells where small movements within a restricted area was seen.

Both groups contained some cells showing discontinuous crawling, and these cells had a mean reduction in crawling speed compared to the continuously crawling cells (Figure 4.14A). Although this behaviour was more frequently observed in the ICAM-2 KO animals (Figure 4.13B), this did not however fully account for the overall reduction in crawling speed in ICAM-2 KO as compared to WTs (Figure 4.7A). This is because when comparing continuously crawling cells between the two mouse strains there was still a reduction in crawling speed in the ICAM-2 KO mice and a small reduction in crawling length (Figure 4.14A and C). Furthermore, there was also a trend towards a reduction in crawling displacement in discontinuous crawling WT

mice only, although this difference was not significant (Figure 4.15A) due to the very few discontinuously crawling cells noted in WT mice were seen.

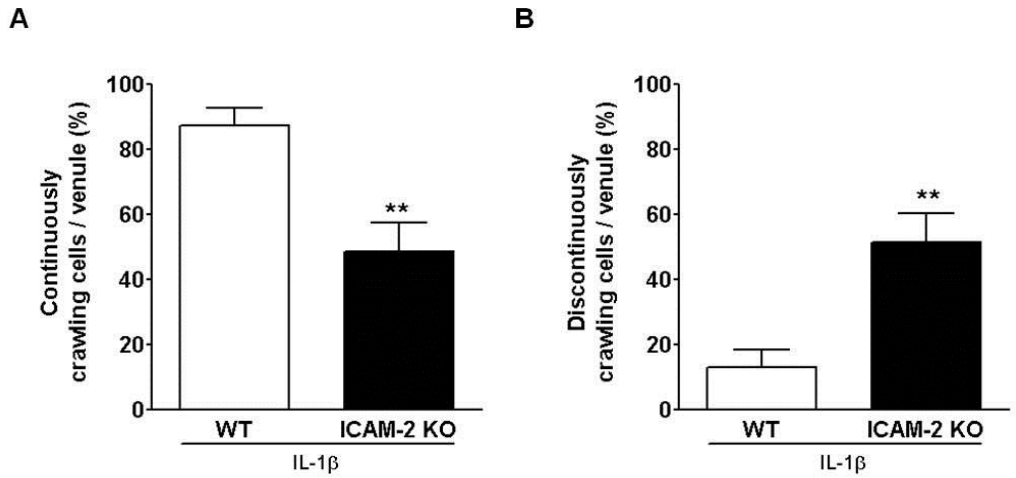

Figure 4.13: The frequency of continuously and discontinuously crawling neutrophils in IL-1β-stimulated WT and ICAM-2 KO venules.

Cremasteric confocal IVM of WT or ICAM-2 KO Lys-eGFP-ki mice stimulated with i.s. IL-1β (50 ng/mouse) for 2 hours. The percentage of (**A**) continuously and (**B**) discontinuously crawling neutrophils per venule was quantified. N = 76-81 cells from 10 vessels, in 6-7 animals per group. Error bars show SEM. Statistically significant (T-test) differences between WT and ICAM-2 KO data are indicated by asterisks **P< 0.01.

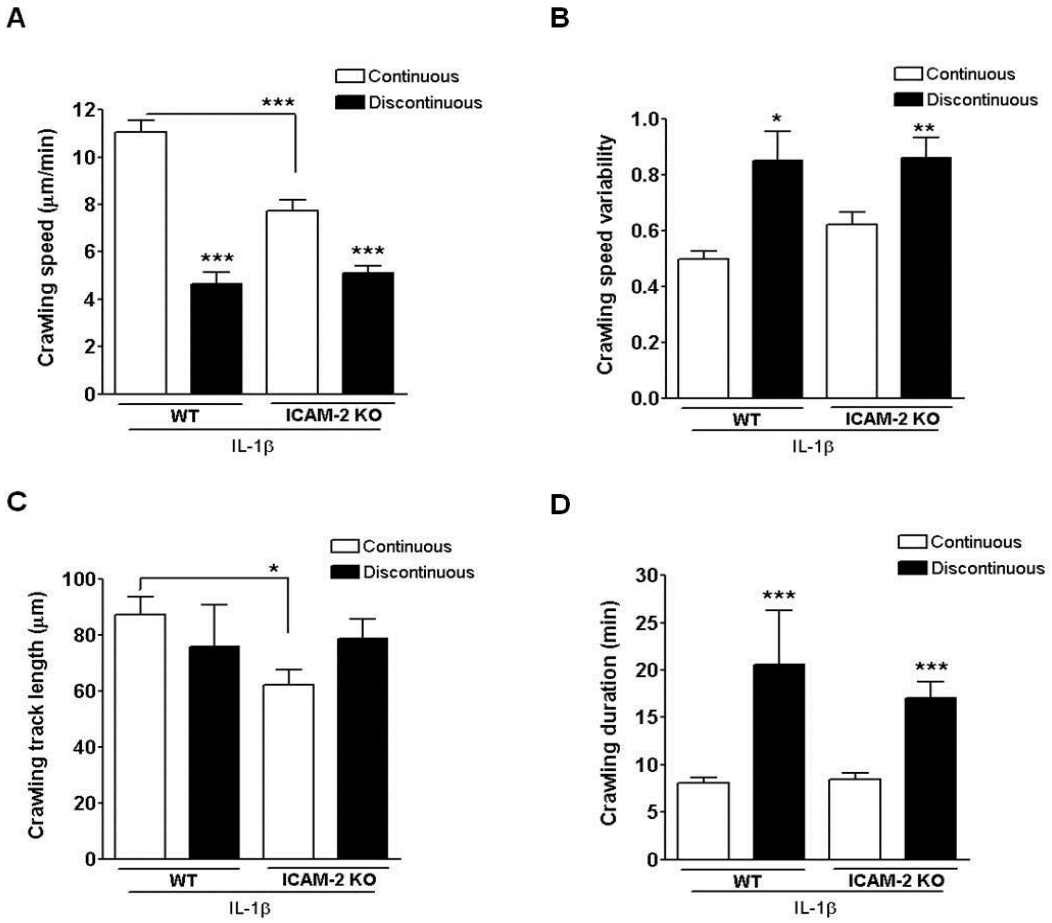

Figure 4.14: Continuous and discontinuous crawling dynamics in IL-1β-stimulated WT and ICAM-2 KO mice.

Cremasteric confocal IVM of WT or ICAM-2 KO Lys-eGFP-ki mice stimulated with i.s. IL-1β (50 ng/mouse) for 2 hours. The mean total (**A**) speed (**B**) speed variability throughout the duration (speed standard deviation divided by the mean speed) (**C**) length (**D**) duration of crawling in WT and ICAM-2 KO venules was quantified. N = 76-81 cells from 10 vessels, in 6-7 animals per group. Error bars show SEM. Statistically significant (Anova) differences between continuous and discontinuous data are indicated by asterisks *P< 0.05, **P< 0.01, ***P< 0.001. Differences between WT and ICAM-2 KO mice are indicated with lines.

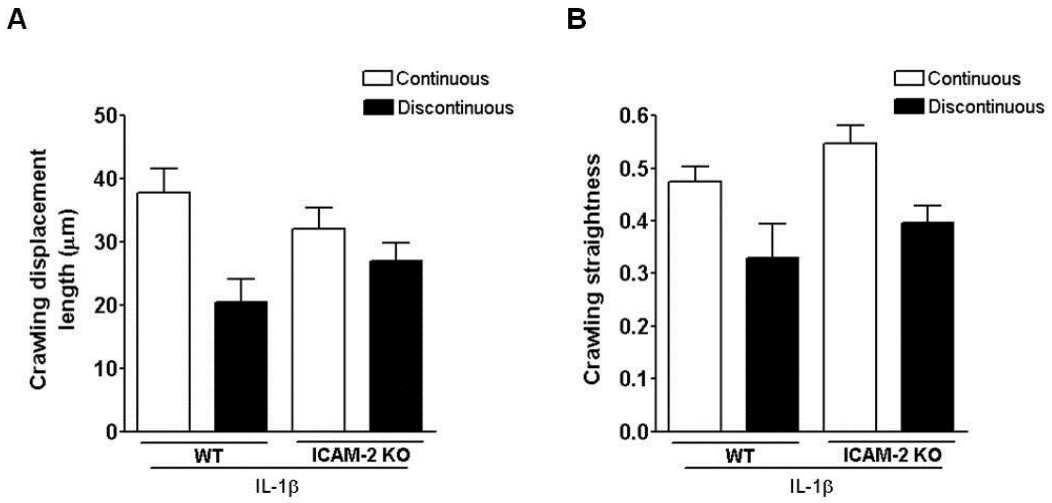

Figure 4.15: Continuous and discontinuous crawling displacement and straightness in IL-1β-stimulated WT and ICAM-2 KO mice.

Cremasteric confocal IVM of WT or ICAM-2 KO Lys-eGFP-ki mice stimulated with i.s. IL-1β (50 ng/mouse) for 2 hours. The mean total (**A**) displacement (**B**) straightness of crawling in WT and ICAM-2 KO venules was quantified (for definitions see Figure 4.8). N = 76-81 cells from 10 vessels, in 6-7 animals per group. Error bars show SEM.

4.2.7 Association of periods of immobility during discontinuous crawling with EC junctions

To understand discontinuously crawling neutrophils in more detail the site of immobility during these periods were examined. As this behaviour was predominantly seen in ICAM-2 KO mice, and these mice also had a significant reduction in the number of neutrophils in the extravascular tissue, it was hypothesised that the periods of immobility seen in this type of crawling could reflect failed attempts of neutrophils to initiate TEM. Therefore the possibility that periods of immobility were associated with EC junctions was investigated.

To investigate this hypothesis the location of all periods of immobility in WT and ICAM-2 KO vessels was analysed and identified as being directly on top of a junction, partially in contact with a junction or not in contact with a junction (Figure 4.16B and C). The location of normally adherent/crawling cells was also analysed at two time points using the first and last time frame of each confocal image sequences acquired (Figure 4.16).

The percentage of immobility located directly on EC junctions, partially on EC junctions or at EC non-junction sites were analysed in IL-1β-stimulated venules from WT and ICAM-2 KO mice (Figure 4.17). The results showed that almost all immobile cells were in contact with a junction and more than 80% of these neutrophils were predominately found directly on top of EC junctions (Figure 4.17). Crawling/adherent cells within the same vessel were also predominately in contact with a junction however only 60% were directly on top of EC junctions (Figure 4.17). More interestingly there was a significant difference between crawling/adherent cells and immobile cells classified as directly on EC junctions indicating that immobile cells had a greater association with EC junctions in comparison to that of adherent/crawling cells. No difference was seen between WT and ICAM-2 KO mice.

In order to determine if these trends were an active association of normally crawling cells with junctions rather than a result of the morphology of the vessel wall (or distribution of endothelial junctions), *in silico* experiments were carried out. Using the same vessels the distribution of EC junctions were masked, and neutrophil sized spots were randomly distributed across the vessel (Figure 4.16D and E). The PECAM-1 labelling was then revealed and the location of the randomly placed spots was quantified in the same way. Using this system although approximately 90% of randomly allocated spots were in contact with the junction, only 32% of the spots were directly associated with a junction (Figure 4.17). The results overall showed an

increase in adherent/crawling cells and immobile cells associated directly with EC junctions compared to that of randomly placed spots suggesting that this association was not chance occurrence due to EC morphology. There was an increase in random cells which were partially on junctions therefore any association of cells classified as 'partially' on EC junction was due to EC morphology. Together, the data indicates that the association of adhesion and to a greater extent the periods of immobility in discontinuous crawling neutrophils is associated with neutrophils being positioned directly on top of EC junctions regardless of the EC morphology.

Collectively, the data presented in this chapter show that in the absence of functional ICAM-2 there is a reduction in both crawling continuity and speed, and an increase in speed variation and duration after IL-1β stimulation. Therefore, ICAM-2 supports the efficient crawling of neutrophils in IL-1β-induced inflammation. Furthermore periods of immobility that occurred during discontinuous crawling appeared to be directly associated with EC junctions. It is therefore possible that as discontinuous crawling occurs more frequently in stimulated ICAM-2 KO mice, ICAM-2 may also have additional roles in the opening of EC junctions.

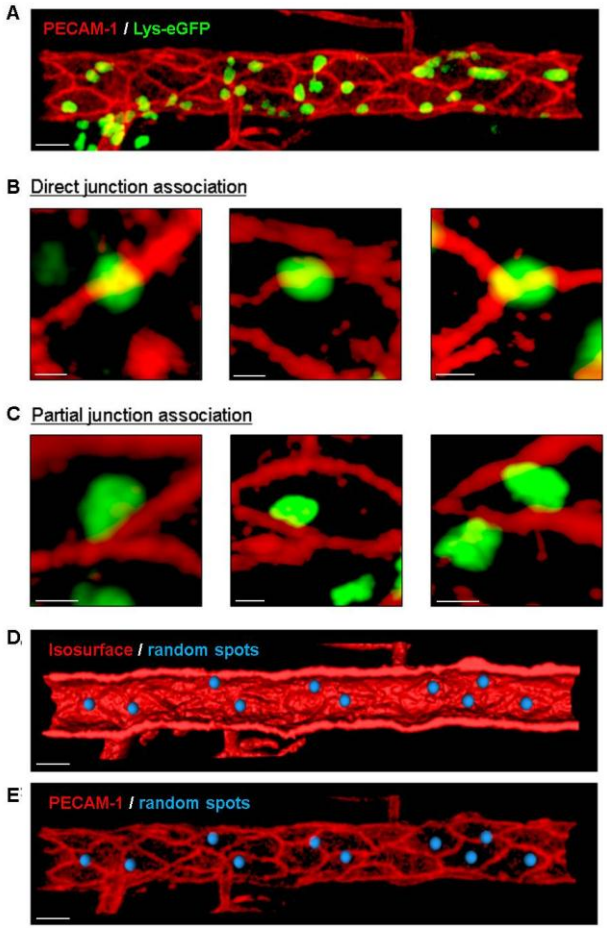

Figure 4.16: Analysing the association of the period of immobility in discontinuous crawling behaviour with EC junctions.

An example confocal image of the cremasteric post-capillary venule from Lys-eGFP-ki mice. High magnification images illustrate the analysis of association of neutrophil adhesion and the periods of immobility in discontinuous crawling with EC junctions. (**A**) Example of an inflamed venule exhibiting PECAM-1 (red) and Lys-eGFP/neutrophils (green). The location of the crawling neutrophils in relation to EC junctions was quantified at two time points. (**B**) Examples of neutrophils directly and (**C**) partially in contact with EC junctions. (**D**) An isosurface was created on the vessel in order to mask the location of EC junctions, and 10 simulated cells (blue dots) were randomly placed on the vessel. (**E**) The isosurface was removed, and the location of the simulated cells was quantified.

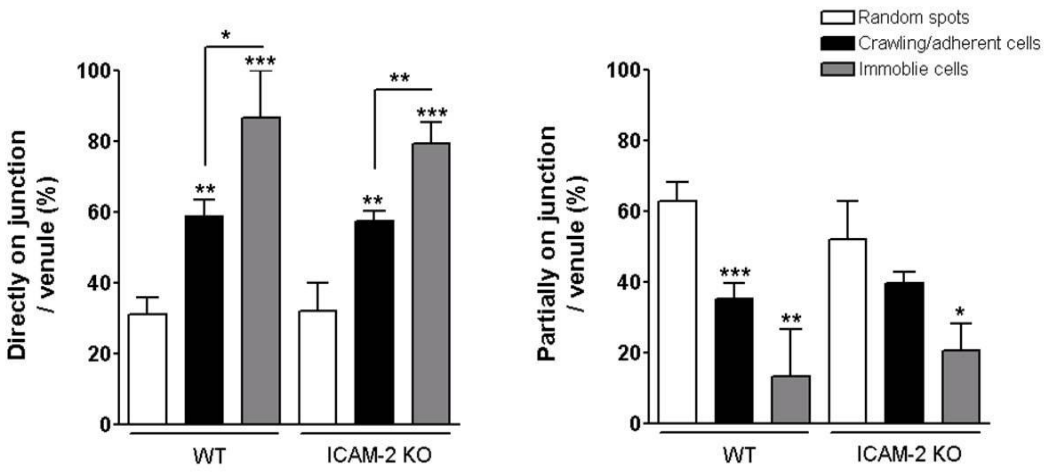

Figure 4.17: Association of periods of immobility in discontinuous crawling behaviour with EC junctions.

The percentage of cells and 10 random spots directly and partially associated with EC junctions per venule in IL-1β-stimulated WT and ICAM-2 KO mice. The location of the crawling/adherent neutrophils in relation to EC junctions was quantified at two time points. N = 10 vessels in 6-7 animals per group. Error bars show SEM. Statistically significant differences from respective random group is indicated by asterisks *P< 0.05, **P< 0.01, ***P< 0.001. Differences between crawling/adherent cells and immobile cells are indicated with lines.

4.3 Discussion

The role of endothelial proteins in leukocyte extravasation has been the subject of intense study for many years, but many details of the molecular mechanisms supporting extravasation remain unknown. Whilst the contribution of ICAM-2 is one of the more neglected areas in this field, it has been shown to be involved in neutrophil extravasation at a stage after the initial adhesion of cells to the vessel wall (Huang et al., 2006; Woodfin et al., 2009). Previous studies of fixed tissues have also identified sequential and non-redundant roles for ICAM-2, JAM-A and PECAM-1 during paracellular migration (Woodfin et al., 2009). The work presented in this chapter has employed a recently developed *in vivo* confocal imaging system (Woodfin et al., 2011) in order to investigate the role of ICAM-2 in the dynamics of neutrophil extravasation in greater detail. As expected in unstimulated conditions only a few neutrophils were present in both WT and ICAM-2 KO mice. Under basal conditions the very few cells that did adhere and exhibit crawling displayed no dynamic differences between WT and ICAM-2 KO mice in terms of crawling speed, duration and length. Further analysis into the role of ICAM-2 in crawling dynamics was therefore carried out in IL-1β-stimulated tissues.

A significant increase in neutrophil adhesion was detected after IL-1β stimulation, hence a higher number of crawling events were able to be tracked and analysed. Almost all luminally adherent neutrophils exhibited some crawling, with a small reduction in the percentage of crawling cells in ICAM-2 KO mice. This latter reduction is in contrast to previously published findings (Phillipson et al., 2006) and this difference is likely to be a result of variations in the inflammatory stimuli, definition of non-crawling cells and/or imaging system employed. Alternatively it could be possible that in the present study the adherent or stationary neutrophils observed could be crawling in a discontinuous manner, with long stationary periods that lasts the whole period of observation.

A number of parameters relating to neutrophil crawling dynamics were quantified in WT and ICAM-2 KO animals after IL-1β stimulation. A significant reduction in crawling speed was observed in the ICAM-2 KO vessels, while the variability of crawling speed of individual cells was increased. The duration of observed crawling was also increased in the ICAM-2 KOs, although it is important to remember that this value refers to the duration of crawling observed within approximately 30 minute imaging period, not the absolute duration of crawling between initial adhesion and TEM or detachment of neutrophils from the luminal EC back into the blood circulation. Furthermore the following parameters relate to a time for which each cell was observed during a limited 30-40 minute observation period, and within an approximately 300 μm long vessel segment in the field of view. In many cases cells which were already adherent at the beginning of observation were still exhibiting luminal crawling at the end of the observation period, or simply crawled out of the field of view, and as such their ultimate fate was undetermined.

The small increase in the number of stationary neutrophils, the reduction in crawling speed and the increased variability in the crawling speed in the ICAM-2 KO vessels prompted further investigations of the behaviour of individual cells. It was observed that some cells had a discontinuous crawling pattern, with periods of immobility. The frequency of continuously and discontinuously crawling cells was quantified in each genotype. In WT animals ~90% of crawling cells exhibited a continuous crawling behaviour, but in the ICAM-2 KO animals there was a shift towards a more discontinuous crawling phenotype (~50%). In both genotypes the continuously crawling cells had a shorter duration of crawling. The increased frequency of discontinuous crawling only partially accounts for the overall reduction in mean crawling speed in the ICAM-2 KOs, as even within the continuously crawling populations there was a significant reduction in speed in the ICAM-2 deficient animals, indicating that ICAM-2 supports both the speed and continuity of crawling.

The mechanisms by which ICAM-2 supports neutrophil crawling speed and continuity are currently unknown, although ICAM-2 has also previously been implicated in the luminal locomotion of T cells (Steiner et al., 2010) and monocytes (Schenkel et al., 2004). With respect to T cells, continuous crawling has been demonstrated on primary mouse brain microvascular ECs (pMBMECs), where it was found that a majority of cells exhibited continuous crawling with only a small proportion showing stationary behaviour (Steiner et al. 2010). This is in line with the crawling behaviours noted for neutrophils in the present *in vivo* study. In the same study, discontinuous crawling of T cells which was termed 'recurrent arrest' was observed. This behaviour was evident only when both ICAM-1 and ICAM-2 were genetically deleted, which differs from the current study on neutrophils. This highlights that different subsets of leukocytes employ different EC junctional proteins during the crawling stage. It should be noted however that no information on the dynamics of 'recurrent arrest' was documented and so it is not clear as to whether 'recurrent arrest' behaviour is similar to the discontinuous crawling reported in this study.

Discontinuous type of crawling occurred for longer time periods at a reduced mean speed which was highly variable. There was on average 2 periods of immobility which lasted 6.8 minutes. This strengthens the criteria used for defining neutrophil discontinuous crawling (immobility for at least 5 frames which represents 2.5 minutes). The location at which discontinuously crawling cells exhibited periods of immobility was investigated, and compared to a random selection of other adherent/crawling cells within the same vessels at a fixed time point, and with randomly placed simulated cells. The periods of immobility were found to occur directly at EC junctions (80%) indicating that these neutrophils may have been trying to transmigrate through these sites and when they are unable to do so they resume crawling. The high frequency of adherent/crawling cells which were found associated with junctions is in line with previous reports (Wojciechowski, 2005), although this earlier work did not differentiate between cells which were directly on top of a junction from those which had partial contact. It is therefore possible that the

immobile cells were at a stage where they were unable to undergo transmigration. However no evidence of junctional disruption or neutrophil protrusions was seen and as neutrophils undergo TEM quite rapidly once they are at a 'permissive' EC junction it is possible that a defect in the opening of EC junctions and/or guidance to EC junctions may have occurred under these circumstances.

Further studies are required to establish the fate of discontinuously crawling neutrophils in our model. It is possible that neutrophils that crawl in a discontinuous manner detach from the EC and go back into the blood circulation thereby resulting in a reduction in TEM and therefore a reduction in neutrophils in the extravascular tissue. There is however an *in vitro* study that has shown a greater detachment of leukocytes on immobilised ICAM-2 (Steiner et al., 2010) although this study was carried out with T cells and therefore generalisation of responses from one leukocyte subset to another should be avoided due to their different functions (Sumagin et al. 2010). It is also possible that when ICAM-2 is not functional, TEM could occur at a later time point.

ICAM-2 has the ability to form homophillic interactions in *trans* (Huang et al., 2005) however in Chapter 3 ICAM-2 was shown to be expressed by only a small percentage of neutrophils at lower levels in comparison to other leukocyte subsets investigated and to a far greater extent the vascular ECs. Whilst not conclusive, the data suggests that neutrophil ICAM-2 is unlikely to support the functions reported in the present study. The role of EC ICAM-2 is likely to be mediated by ligation of a leukocyte ligand, subsequent outside-in signalling, and the activation/stabilisation of leukocyte locomotive machinery via pathways involving Rac, Cdc42 and WAVE/WASP. The current literature provides evidence for the ability of ICAM-2 to bind to key leukocyte integrins LFA-1, MAC-1 and VLA-4 (Li et al., 1993; Seth et al., 1991; Staunton et al., 1989; Xie et al., 1995) and some of these integrins are well known to be involved in luminal leukocyte crawling (Phillipson et al., 2006; Sumagin et al., 2010). Although the involvement of integrins is generally thought to

be mediated via their interaction with ICAM-1, it is well documented that ICAM-2 can interact with β_2-integrins and these interactions could also mediate the crawling process. Of relevance to the current study, the role of EC ICAM-2 in neutrophil migration has been suggested to occur via neutrophil LFA-1 (Issekutz et al., 1999). The function of ICAM-2 in this context was however only evident when ICAM-1 was also blocked, where an additive inhibitory effect on neutrophil migration was seen when both proteins were functionally blocked relative to ICAM-1 blockade alone. This study was carried out using an *in vitro* HUVECs model, and any differences in the role of ICAM-2 with that presented in the current chapter could be a result of different experimental models used.

It is possible that ICAM-2 has two distinct roles in neutrophil extravasation as it is expressed on the EC non-junctional and junctional sites. EC non-junctional ICAM-2 is involved in the 'efficient' continuity of crawling whereas EC junctional ICAM-2 could be associated with the opening of EC junctions. Neutrophil ligands and the ability of ICAM-2 to regulate TEM and EC junctional pore opening (which maybe occurring during the periods of immobility in discontinuous crawling cells) will be further investigated in subsequent chapters.

In summary although ICAM-2 does not have important roles in the frequency of initial adhesion and crawling of neutrophils, it has a significant impact on the speed, duration and continuity of crawling in IL-1β-stimulated inflammation in the mouse cremaster muscle. The high frequency of discontinuous crawling behaviour in stimulated ICAM-2 KO mice could be a result of a defect in the opening of EC junctions and/or guidance to sites permissive for transmigration. These findings extend previous works on the functional role of ICAM-2 by dissecting the precise stage at which it mediates neutrophil extravasation *in vivo*. Further studies are required to establish whether ICAM-2 has a role in neutrophil TEM and understand the leukocyte ligands with which it interacts.

CHAPTER 5: Role of ICAM-2 in neutrophil transendothelial migration

5.1 Introduction

Previously presented data has demonstrated a luminal expression of ICAM-2 in post-capillary venules in two different vascular beds (Chapter 3). This expression pattern has been linked to the efficient crawling of neutrophils within the lumen in IL-1β-stimulated inflammation (Chapter 4). It is therefore believed that efficient crawling facilitates effective neutrophil extravasation by enabling cells to locomote to sites permissive for TEM. ICAM-2 is also however expressed within EC junctions, and is generally considered to be a junctional molecule, so a possible role for this protein in supporting TEM directly was investigated as part of the current chapter.

Studies by Steiner et al., (2010) found that the lack of endothelial ICAM-1 and ICAM-2 reduced T cell TEM across the mouse BBB (pMBMECs) *in vitro* to a greater extent than conditions where ICAM-1 function alone was inhibited. Interestingly no effect on TEM was evident in this model when ICAM-2 function alone was impaired, suggesting a synergistic role for these ICAMs in diapedesis of T cells. Numerous other studies have however found a role for ICAM-2 in extravasation of neutrophils (Hobden, 2003; Huang et al., 2006; Issekutz et al., 1999; Woodfin et al., 2009), eosinophils (Gerwin et al., 1999), monocytes (Schenkel et al., 2004), and dendritic cells (Geijtenbeek et al., 2000; Helander et al., 1996; Wethmar et al., 2006) however whether it has a role in TEM directly is unknown. Earlier work within our group has shown that in IL-1β-stimulated whole mount cremaster muscles, neutrophil TEM occurs through JAM-A interactions at the level of the EC and PECAM-1 interactions at the level of the basement membrane (Woodfin et al., 2009). In relation to this ICAM-2 interactions were suggested to play a role at an earlier stage than JAM-A at the level of the EC lumen before entering the EC

junction as investigated by fixed tissue confocal analysis. The work presented in the current chapter aims to extend these findings by analysing the role of ICAM-2 in the dynamics of neutrophil TEM using real time, high resolution confocal IVM imaging.

In Chapter 4 two distinct types of neutrophil crawling behaviour in response to IL-1β were quantified. These behaviours were termed continuous crawling which was predominantly found in WT mice, and discontinuous crawling which was more frequently observed in ICAM-2 KO mice. As the periods of immobility in discontinuous crawling were primarily located directly on EC junctions (Chapter 4), it was hypothesised that these immobile periods could represent failed attempts to initiate neutrophil TEM. Analysis of TEM dynamics in the present chapter may also provide further insights into this hypothesis.

5.2 Results

5.2.1 IL-1β-stimulated ICAM-2 KO mice display a reduction in neutrophil TEM

In addition to the EC non-junctional expression, ICAM-2 is also expressed at EC junctions however the role of ICAM-2 at stages prior to TEM and TEM itself has not been investigated directly. The dynamics of neutrophil TEM in ICAM-2 KO mice was therefore examined to further understand the role of ICAM-2 in neutrophil extravasation. In the current study the location and dynamics of TEM was examined using 4D confocal IVM of IL-1β-stimulated cremaster muscles from WT and ICAM-2 KO mice, which expressed endogenous eGFP in their neutrophils. EC junctions were labelled with fluorescent non-function blocking anti-PECAM-1 mAb in order to visualise neutrophil EC junctional interactions as previously described (Chapter

2). Images of venules were captured over a 30-40 minute period and sequences of these images were reconstructed into 3D models of half venules using Imaris software. This technique allowed direct visualisation of TEM events in real time and the number of TEM events per 30 minutes per venule were quantified. TEM events were classified as neutrophils migrating through the EC layer from the luminal to the abluminal side and in most cases clear neutrophil protrusions into the EC layer and formation of EC junctional pores was evident (Movies 3, 7, 8, 9). The results showed that ICAM-2 KO mice had a significant reduction in the frequency of TEM (5.5 ± 2.1 TEM events, per 30 minutes, per venule, n=12 vessels from 6 mice) in comparison to WTs (22.18 ± 4.6 events, per 30 minutes, per venule, n=10 vessels from 7 mice) (Figure 5.1A). This was in line with results from Chapter 4 (Figure 4.1) where neutrophil extravasation was significantly reduced in ICAM-2 KO mice 4 hours after IL-1β. Furthermore, as several neutrophils were observed to sequentially transmigrate through the same EC junctional pore, the frequency of pore formation per 30 minutes per venule was also quantified. In WT mice 15.6 ± 3.3 EC junctional pores (per 30 min, per venule) was observed, suggesting that a small proportion of neutrophils observed do follow other neutrophils and use pre-existing pores to transmigrate. Significantly fewer EC junctional pores (4.7 ± 1.8 pores per 30 min, per venule) were detected in ICAM-2 KO mice (Figures 5.1B) compared to WTs (15.6 ± 3.3 pores).

The route of neutrophil TEM was also quantified and each event was defined as following a paracellular (Movies 7 and 8) or transcellular (Movie 9) non-junctional route (Figure 5.2). In both WT and ICAM-2 KO mice more than 90% of neutrophil TEM events occurred via the paracellular route (Figure 5.3). Of these events there was an equal prevalence of bicellular TEM (TEM through the junction between 2 adjacent ECs, Movie 7) and multicellular TEM (TEM through the junction between 3 or more ECs, Movie 8) in both groups (Figures 5.4 and 5.5). Collectively ICAM-2 deficiency reduces the number of neutrophil TEM events whilst the number of adherent and crawling cells within the vessel remains normal. However, no significant differences were observed in relation to the route of TEM.

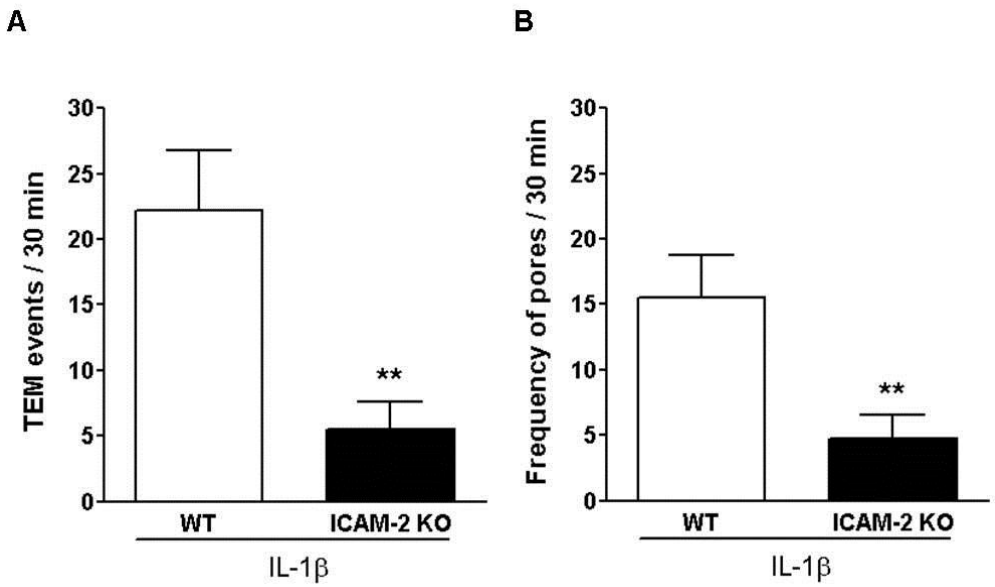

Figure 5.1: Frequency of IL-1β-stimulated TEM events in ICAM-2 KO and WT mice.

Cremasteric confocal IVM of WT or ICAM-2 KO Lys-eGFP-ki mice stimulated with i.s. IL-1β (50 ng/mouse) for 2 hours. (**A**) The frequency at which cells were seen to progress to TEM following IL-1β-stimulation was quantified and is shown as the frequency per 30 minutes, the standard period of observation, per venule. (**B**) The frequency at which neutrophils were seen to produce transient EC pores as a consequence of TEM was also quantified per 30 minutes (per venule). Bars represent mean ± SEM per venule (n = 10 vessels from 6-7 mice per group). Statistically significant (T-test) differences between WT and ICAM-2 KO data are indicated by asterisks **P< 0.01. (Movies 3, 7, 8, 9).

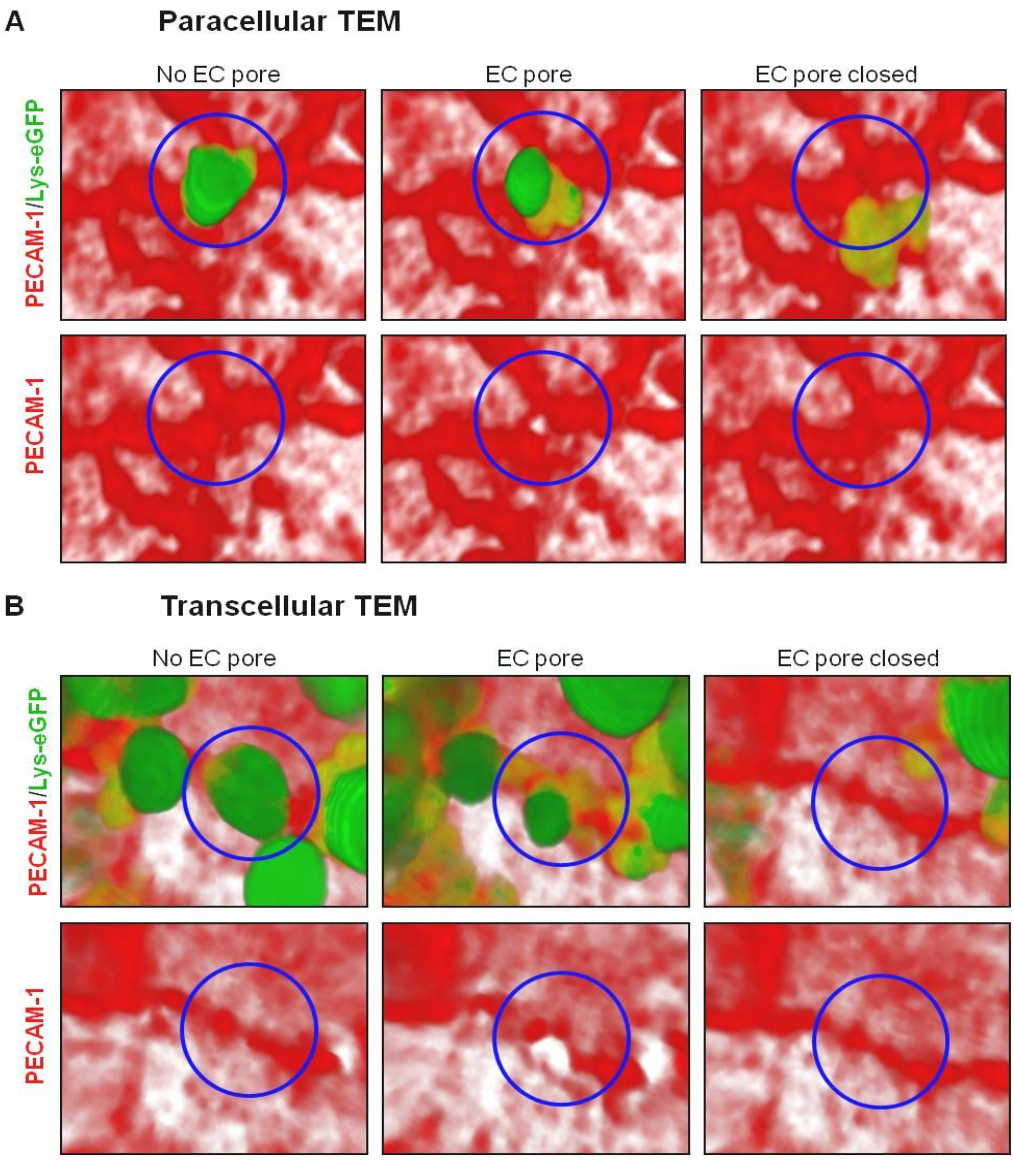

Figure 5.2: Paracellular and transcellular neutrophil TEM as viewed by 4D confocal IVM.

Representative images of cremasteric post-capillary venules from Lys-eGFP-ki mice (neutrophils; green). High magnification images illustrating neutrophil (**A**) paracellular (Movies 7 and 8) and (**B**) transcellular TEM (Movie 9). Individual neutrophil TEM events were tracked and classified as paracellular or transcellular TEM in relation to the location of EC pores (i.e. junctional or non-junctional) (PECAM-1; red). Blue circle indicates the region where the neutrophil breaches the endothelium. Lower panels show the PECAM-1 channel only.

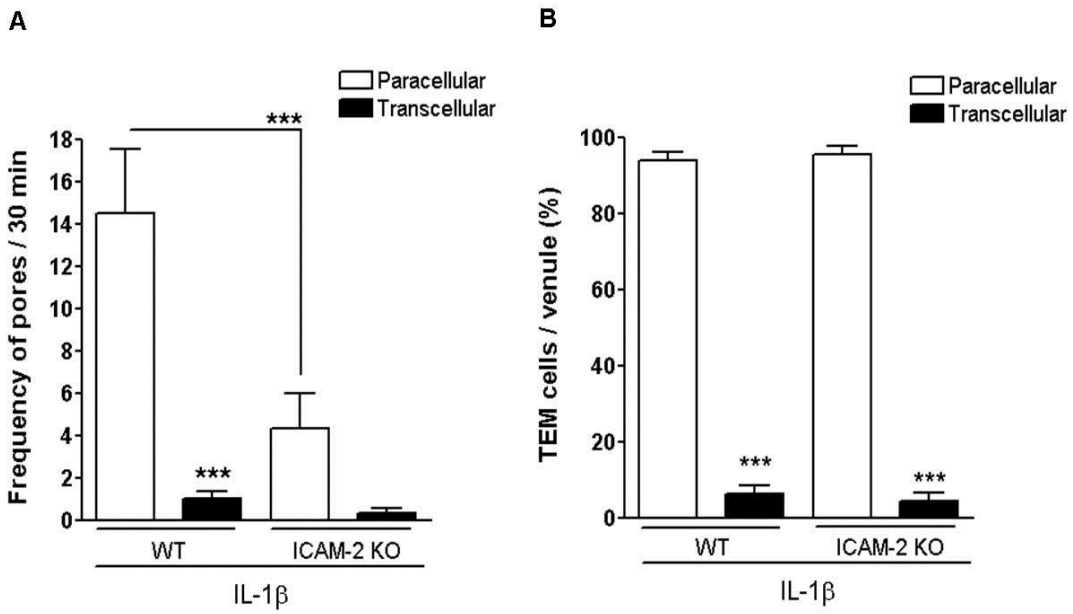

Figure 5.3: IL-1β-stimulated paracellular and transcellular TEM in ICAM-2 KO and WT mice.

Cremasteric confocal IVM of WT or ICAM-2 KO Lys-eGFP-ki mice stimulated with i.s. IL-1β (50 ng/mouse) for 2 hours. (**A**) The frequency at which cells were seen to progress to paracellular or transcellular TEM in each venule was quantified per 30 minutes, the standard period of observation. (**B**) The percentage of paracellular or transcellular TEM events per venule. Bars represent mean ± SEM where n = 10 vessels from 6-7 mice per group. Statistically significant (Anova) differences between paracellular and transcellular data are indicated by asterisks **P< 0.01, ***P <0.001. Differences between WT and ICAM-2 KO mice are indicated with lines.

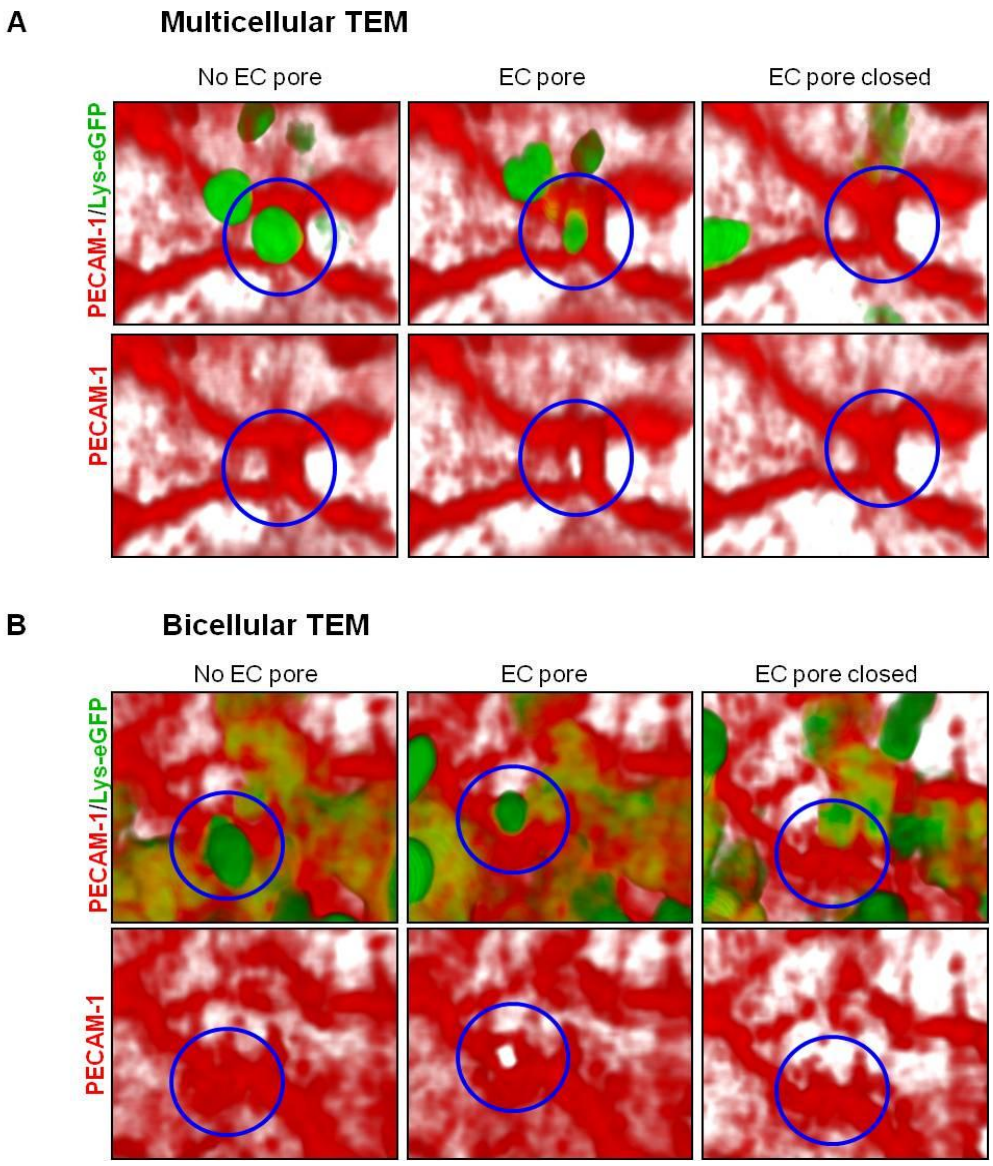

Figure 5.4: Multicellular and bicellular neutrophil TEM as viewed by 4D confocal IVM.

Representative images of cremasteric post-capillary venules from Lys-eGFP-ki mice (neutrophils; green). High magnification images illustrating neutrophil (**A**) multicellular (Movie 8) and (**B**) bicellular (Movie 7) TEM. Individual neutrophil TEM events were tracked and classified as multicellular or bicellular TEM in relation to the location of EC pores (i.e. junctional or non-junctional) (PECAM-1; red). Blue circle indicates the region where the neutrophil breaches the endothelium. Lower panels show the PECAM-1 channel only.

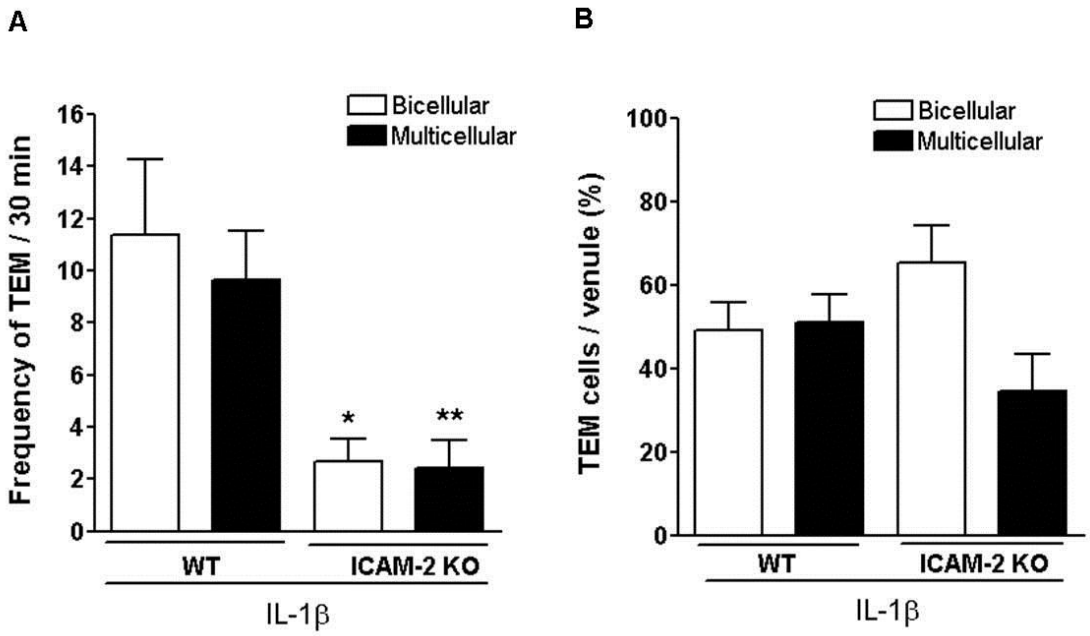

Figure 5.5: IL-1β-stimulated multicellular and bicellular TEM in ICAM-2 KO and WT mice.

Cremasteric confocal IVM of WT or ICAM-2 KO Lys-eGFP-ki mice stimulated with i.s. IL-1β (50 ng/mouse) for 2 hours. (**A**) The frequency at which cells were seen to progress to multicellular or bicellular TEM in each venule was quantified per 30 minutes, the standard period of observation. (**B**) The percentage of multicellular or bicellular TEM events per venule. Bars represent mean ± SEM where n = 10 vessels from 6-7 mice per group. Statistically significant (Anova) differences between multicellular or bicellular data are indicated by asterisks *P< 0.05, **P <0.01. Differences between WT and ICAM-2 KO mice are indicated with lines.

5.2.2 Continuously crawling neutrophils support TEM

Previous studies have identified different crawling characteristics depending on the presence of functional ICAM-2 (Chapter 4) namely, continuous and discontinuous neutrophil crawling. In order to understand the impact of continuous and

discontinuous crawling on TEM, the events leading up to neutrophil TEM and TEM itself were divided into 3 stages (Figure 5.6A). These stages were, neutrophil crawling that was preceded by observed TEM (stage i), the stage at which neutrophils were in contact with EC junctions before being breached (pre-TEM, stage ii) and TEM through EC junctions (stage iii). While the previous analysis of crawling dynamics looked at all luminal crawling cells (Chapter 4), the data here looks only at the crawling behaviour of cells which were seen to progress to TEM (stage i) in isolation from all other crawling cells. When the crawling behaviour of cells which were observed to undergo TEM was examined, 80-90% of this neutrophil population crawled in a continuous rather than discontinuous fashion, and this was irrespective of ICAM-2 deficiency (Figure 5.6B). This suggests that continuously crawling cells, which form the majority in WT vessels, transmigrate more frequently than discontinuously crawling cells. The latter crawling behaviour were more prevalent in the ICAM-2 KO mice (Chapter 4) where a reduction in TEM events were also seen (Figure 5.1). In the KO mice, neutrophil crawling behaviour preceding TEM also had a significantly reduced crawling speed (8.2 ± 0.8 μm/mins, n=34 for WTs vs 5.2 ± 0.5 μm/mins, n=20 for ICAM-2 KOs) and a longer duration of crawling (7.1 ± 1.5 mins, n=34 cells for KOs vs 3.3 ± 0.4 mins, n=20 cells for WTs) in comparison to WT mice (Figure 5.6C). This was in line with previous crawling dynamics data (Chapter 4, Figure 4.8) which was acquired irrespective of the outcome of neutrophil crawling (i.e. whether the neutrophils subsequently de-adhered and returned back into the circulation or progressed to TEM).

The dynamics of the continuous and discontinuous crawling behaviours were also in line with previous data (Chapter 4, Figure 4.15). In WT mice continuously crawling neutrophils to EC junctions had an increase in crawling speed and a trend for a decrease in speed variability and duration when compared to discontinuously crawling cells (Figure 5.7). These characteristics were similar in both WT and ICAM-2 KO mice however, as expected (based on data from Chapter 4, Figure 4.15), continuous crawling speed was significantly reduced in ICAM-2 KO animals in comparison to WTs (Figure 5.7). The duration of crawling was however significantly

increased in discontinuous crawling cells in ICAM-2 KO mice when compared to WTs (Figure 5.7) which is in contrast to previous data where no difference was detected (Chapter 4, Figure 4.15). The reason for this difference is currently unclear however the small number of cells which were observed to crawl and undergo TEM could account for this variation. In line with previous data in Chapter 4, no differences were detected in displacement and straightness parameters between continuous or discontinuous crawling cells or between WT and ICAM-2 KOs (Figure 5.8). Together the results obtained regarding the dynamics of neutrophil crawling preceeding TEM, is in general, in line with neutrophil crawling data from Chapter 4, where all observable crawling behaviour was analysed regardless of whether they progressed to TEM or not. Most importantly continuous crawling neutrophils appeared to progress to TEM more efficiently regardless of genotype and as ICAM-2 KOs have fewer continuously crawling cells this could account for the overall reduction in extravasation seen in these mice.

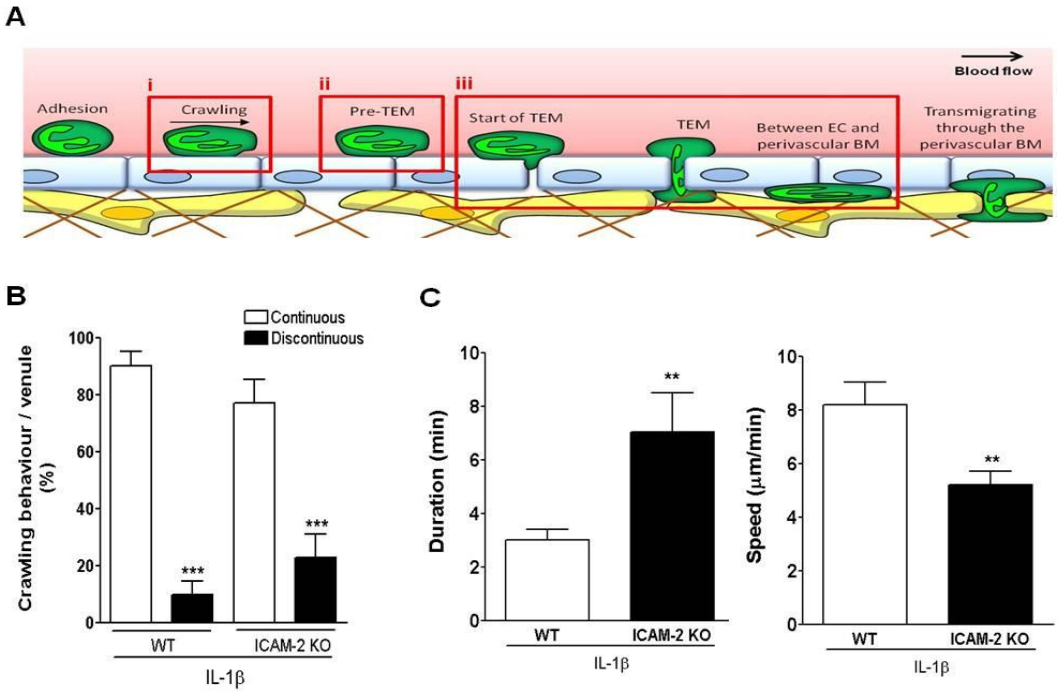

Figure 5.6: Neutrophil crawling behaviors preceding TEM in IL-1β-stimulated cremaster muscles from ICAM-2 KO and WT mice.

Cremasteric confocal IVM of WT or ICAM-2 KO Lys-eGFP-ki mice stimulated with IL-1β (50 ng/mouse, i.s.) for 2 hours. (**A**) The sequence of events from neutrophil crawling through to completion of TEM was divided into three stages as illustrated. (i) Crawling: the period for which a neutrophil is seen to crawl within the lumen prior to reaching it's site of TEM. (ii) Pre-TEM: the period for which a neutrophil is interacting with the endothelial junction at it's TEM location prior to any visible disruption of the junctional integrity. (iii) TEM: the period for which the first visible disruption of junctional PECAM-1 to the completion of migration to the sub-endothelial space. (**B**) The crawling behaviors preceding TEM (stage i) were analysed in isolation and neutrophil crawling behavior (**C**) duration and speed was determined (n = 10 vessels from 6-7 mice per group). Data were obtained from analysis of 14-34 cells observed at stage i. Bars represent mean ± SEM for all events analysed. Statistically significant (T-test) differences between continuous and disrupted crawling data are indicated by asterisks **P <0.01, ***P <0.001.

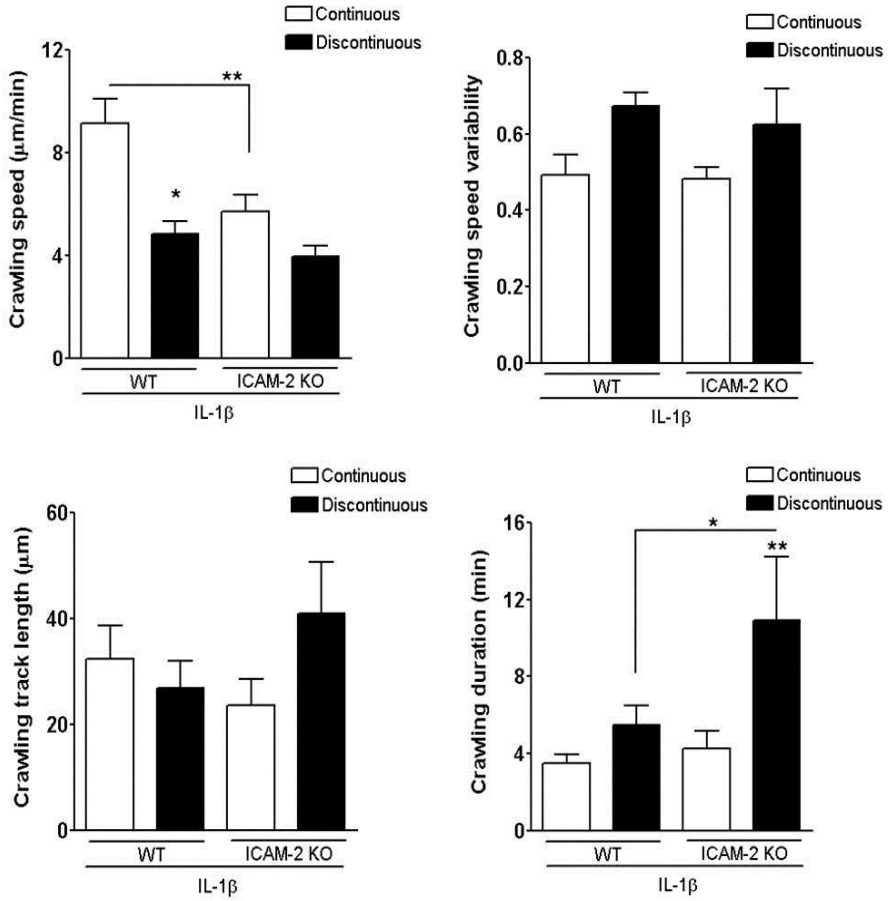

Figure 5.7: Neutrophil continuous and discontinuous crawling dynamics preceding TEM in IL-1β-stimulated cremaster muscles from ICAM-2 KO and WT mice.

Cremasteric confocal IVM of WT or ICAM-2 KO Lys-eGFP-ki mice stimulated with IL-1β (50 ng/mouse, i.s.) for 2 hours. The crawling behavior preceding TEM (stage i) were analysed in isolation and the dynamics of neutrophil continuous and discontinuous crawling behavior was determined. The mean total speed, speed variability, length and duration of crawling in WT and ICAM-2 KO venules was quantified. Data were obtained from analysis of 14-34 cells observed at stage i. Bars represent mean ± SEM for all events analysed. Statistically significant (Anova) differences between continuous and disrupted crawling data are indicated by asterisks *P <0.05, **P <0.01. Differences between WT and ICAM-2 KO mice are indicated by lines.

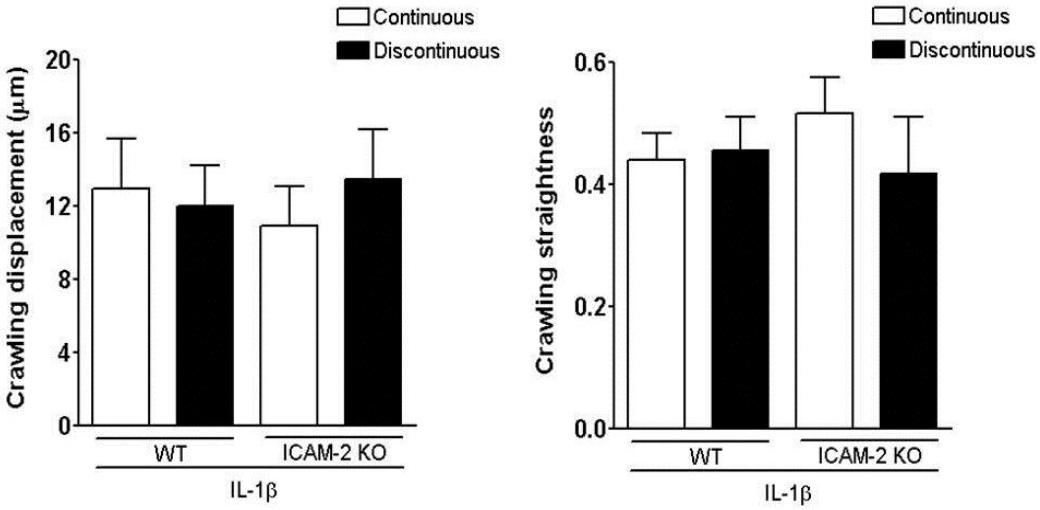

Figure 5.8: Displacement and straightness of crawling preceding TEM in IL-1β-stimulated cremaster muscles from ICAM-2 KO and WT mice.

Cremasteric confocal IVM of WT or ICAM-2 KO Lys-eGFP-ki mice stimulated with IL-1β (50 ng/mouse, i.s.) for 2 hours. The crawling behaviors preceding TEM (stage i) were analysed in isolation and the dynamics of neutrophil continuous and discontinuous crawling behavior was determined. The mean total displacement and straightness of crawling in WT and ICAM-2 KO venules was quantified. Data were obtained from analysis of 14-34 cells observed at stage i. Bars represent mean ± SEM for all events analysed.

5.2.3 ICAM-2 facilitates the initiation of TEM

The results from Chapter 4 suggested that discontinuous neutrophil crawling occurs more frequently in ICAM-2 KOs, and the periods of immobility in this type of crawling were associated with EC junctions, and this was not due to EC morphology. From this data it was hypothesised that the periods of immobility could be due to neutrophils failing to undergo TEM. Of note no EC pore formation or neutrophil protrusions into the EC junctions were observed during these periods. Taking this into account together with the fact that ICAM-2 KO mice stimulated with IL-1β

displayed a significant reduction in TEM events, it is possible that ICAM-2 plays a key role in TEM directly. However as previous data in this chapter has shown no effect of ICAM-2 deficiency on the mode of TEM with respect to transcellular, paracellular, multicellular and bicellular TEM, other TEM dynamics were investigated using the same technique.

The process of TEM was further categorised into 'pre-TEM' and TEM (Figure 5.9A). In stimulated ICAM-2 KO mice, only a few cells were observed to undergo TEM and these cells exhibited a different dynamic profile to that displayed by stimulated WTs. This difference was found once neutrophils were in contact with EC junctions that were later breached (i.e. pre-TEM). ICAM-2 KO mice exhibited a significantly prolonged duration of pre-TEM in comparison to WTs (3.2 ± 0.3 minutes, n=30 cells for ICAM-2 KO mice and 1.1 ± 0.1 minutes, n=76 cells for WT mice) (Figure 5.9B). Interestingly no difference in the duration of TEM was detected, which was approximately 6 minutes in both mouse strains (Figure 5.9C). In conclusion ICAM-2 was found to have a key role in supporting the initiation of TEM, a process which may account for the periods of immobility in discontinuous crawling cells, a phenomenon displayed more frequently in stimulated ICAM-2 KO mice.

The findings presented in the current chapter demonstrates that ICAM-2 KO mice exhibited reduced TEM events in response to IL-1β. Further studies indicated that this could be due to the high frequency of discontinuous crawling cells observed in ICAM-2 KO mice which are unable to support TEM. ICAM-2 was found to have a direct role in the initiation of TEM and this strengthens the possibility that the periods of immobility during discontinuous crawling could reflect the inability of neutrophils-EC junctional interactions to initiate TEM.

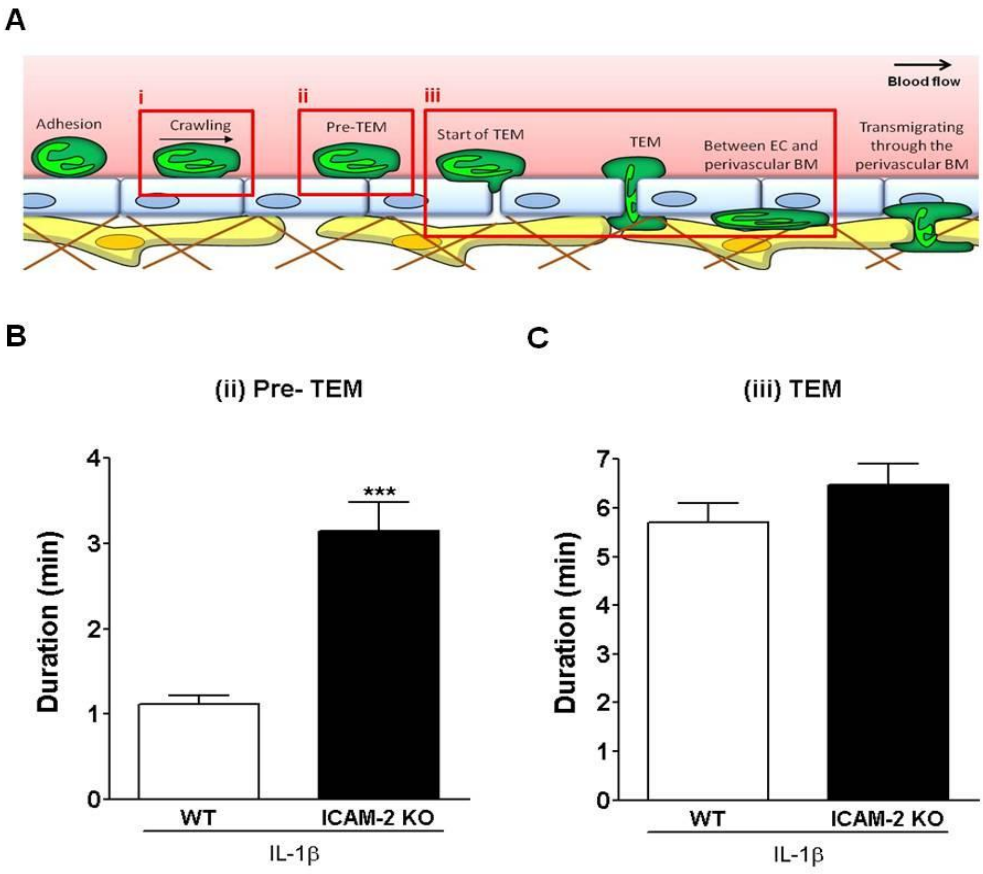

Figure 5.9: Neutrophil TEM dynamics in IL-1β-stimulated cremaster muscles from ICAM-2 KO and WT mice.

Cremasteric confocal IVM of WT or ICAM-2 KO Lys-eGFP-ki mice stimulated with IL-1β (50 ng/mouse, i.s.) for 2 hours. (**A**) The sequence of events from neutrophil crawling through to completion of TEM was divided into three stages as illustrated. Neutrophil crawling preceding TEM (i), Pre-TEM (ii) and TEM (iii). (**B**) The mean duration of pre-TEM (ii) and (**C**) TEM (iii) was determined in both mouse strains. Data were obtained from analysis of 23-76 cells observed at stage ii, and 20-99 cells as observed at stage iii. Bars represent mean ± SEM for all events analysed. Statistically significant (T-test) differences between WT and ICAM-2 KO data is indicated by asterisks ***P <0.001.

5.3 Discussion

The expression and role of ICAM-2 has previously been found to be distinct to that of well-known EC junctional proteins involved in neutrophil TEM (PECAM-1 and JAM-A) (Woodfin et al., 2009). Whist the high luminal ICAM-2 expression was found to be involved in mediating neutrophil crawling speed and continuity, the role of EC junctional ICAM-2 has been linked to the luminal stages of TEM (Woodfin et al., 2009) however the full mechanisms are still unclear. Additionally ICAM-2 KO mice stimulated with IL-1β displayed a high frequency of discontinuous crawling behaviour which had distinct periods of immobility occurring directly on EC junctions (Chapter 4). Based on these findings it was hypothesised that ICAM-2 may have a role in supporting the opening of EC junctions during TEM and therefore the dynamics of neutrophil TEM was examined in more detail in the present chapter.

The route of neutrophil TEM through the EC layer was initially investigated. The frequency at which observed neutrophil TEM events and the formation of EC junctional pores was substantially reduced in stimulated ICAM-2 KO mice, and it is clear that the comparable numbers of adherent and crawling neutrophils were failing to progress to TEM in these mice. In both genotypes the majority (>90%) of TEM events followed the paracellular route and there was no preference for TEM events to occur at multicellular or at bicellular junctions in straight vessels which was in line with previous studies (Sumagin and Sarelius, 2010; Woodfin et al., 2011). These TEM sites were shown to be more prone to TEM due to the enrichment of ICAM-1 which may also increase the likelihood of neutrophil-EC interactions. The TEM events observed in the current study were predominately luminal to abluminal direction and no evidence of ‘disrupted’ TEM consisting of reverse (abluminal to luminal) migration, or disrupted oscillatory movements within the junction was seen (Woodfin et al., 2011).

The process of TEM was divided into several stages for further analysis. Neutrophil crawling behaviour which preceded TEM was initially examined in isolation from other crawling cells in both genotypes. Due to the limitations of this imaging system only a small portion of total neutrophil crawling events were observed to undergo TEM irrespective of mouse strain. However the majority of cells which were observed to successfully progress to TEM had previously crawled in a continuous manner, suggesting that efficient crawling is necessary for the migration to, and/or identification of, sites permissive for TEM. Various crawling dynamics were also analysed in order to fully understand the crawling behaviour prior to TEM, and the results were comparable to the crawling events analysed in Chapter 4 where the neutrophil fate was unknown (i.e. whether they transmigrated or not). More specifically neutrophil crawling that preceded the few cells that transmigrated in ICAM-2 KO vessels crawled for a longer time with a reduced speed. Neutrophil continuous and discontinuous crawling speed and speed variability was also in line with previous data in both mouse strains (Chapter 4). There was however a trend for discontinuously crawling neutrophils in ICAM-2 KO mice to crawl longer distances over a prolonged time period. The reason for this difference in crawling dynamics of all neutrophils (irrespective to fate) with that of neutrophils which were observed to undergo transmigration is unknown but this could be due to fewer cells being observed to crawl and undergo TEM irrespective of mouse strain. The low observable events are likely to be due to the combination of a short time frame and the small field of view (i.e. small section of the cremasteric vasculature) used for analysing neutrophil migration dynamics in this model. Overall these results do however strengthen the data obtained in Chapter 4 where crawling dynamics were analysed irrespective of whether they transmigrated through the EC layer.

Although the cause of discontinuous crawling seen in ICAM-2 KO mice is unclear it is possible that these events are mediated by the impairment of outside-in integrin signalling caused by the lack of ICAM-2 binding. ICAM-2 interactions with LFA-1 (Staunton et al., 1989) and MAC-1 (Xie et al., 1995) has been reported. Of relevance to the current study, the role of EC ICAM-2 in neutrophil migration has been

suggested to occur via neutrophil LFA-1 (Issekutz et al., 1999). The role of ICAM-2 in this context was however only evident when ICAM-1 was also blocked where an additional inhibitory effect was seen relative to ICAM-1 blockade alone. This study was carried out using an *in vitro* HUVECs model, and any differences in the role of ICAM-2 with that presented in the current chapter could be a result of different experimental models used. It is very likely that integrins which are heavily implicated in leukocyte polarisation and crawling (Ridley, 2003) are involved in facilitating the role of ICAM-2 as demonstrated in the present chapter. Specifically integrins are implicated in regulating neutrophil polarity through supporting various signalling pathways linked to Rac, Cdc42 and WAVE/WASP which alter leukocyte locomotive machinery and thus supporting neutrophil crawling (Ridley, 2003).

Within the ICAM-2 KO vessels those cells which did progress to TEM showed significantly prolonged crawling within the lumen before reaching the location of TEM, and exhibited almost a fourfold increase in the time spent interacting with the EC junctions before initiating TEM (pre-TEM). This data supports previous findings from fixed tissue analysis which showed the lack of ICAM-2 leading to arrested cells on the luminal surface of ECs (Woodfin et al., 2009). Collectively these findings indicate that in addition to a role in supporting luminal crawling efficiency, ICAM-2 is also important in the identification of TEM sites and/or the initiation of TEM (opening of the junction). Interestingly however once TEM had been initiated no difference in the duration of TEM itself was detected, indicating that other junctional proteins such as JAM-A, PECAM-1, JAM-C, ESAM, CD99 and/or CD99L2 may support later stages of TEM.

A key aspect of the analysis of TEM in the absence of functional ICAM-2 was that there was a pronounced reduction in the number of TEM events initiated, identified by both observations of transmigrating cells and the formation of a paracellular pores. In the ICAM-2 KO mice while there was a delay in the opening of EC junctional pores in the small number of neutrophils that proceeded to TEM, there

was also a higher number of crawling cells which exhibited periods of immobility (during discontinuous crawling) which may represent failed attempts at entering a junction. The latter hypothesis is strengthened by the fact that immobility periods occurred directly on EC junctions and this was not due to chance (Chapter 4). As mentioned previously, once EC junctional disruption occurred TEM was successfully completed over a normal duration irrespective of the mouse genotype. Together it seems that the greatest defect of the ICAM-2 KO mice in the context of neutrophil transmigration was in the identification or initial opening of EC junctions. The existence of locations particularly permissive to TEM or 'transmigratory portals', have been suggested to exist at tricellular junctions (Burns et al., 1997; Sumagin and Sarelius, 2010), ICAM-1 enriched regions (Sumagin and Sarelius, 2010), or identified by chemotactic gradients (Massena et al., 2010), but there is little information regarding a possible role for ICAM-2 in identifying sites of TEM. No clear gradients of ICAM-2 which might act as guidance towards junctions were observed in studies of EC expression patterns (Chapter 3).

The link between altered crawling characteristics of neutrophils and the formation of EC junctional pores in ICAM-2 KO mice is currently unknown. However, the mechanism by which ICAM-2 exerts its role in TEM is likely to differ from its role in crawling. The C-terminal of ICAM-2 links to the cytoskeleton via binding to α-actinin and ezrin/radixin/moesin proteins (Heiska et al., 1996; Heiska et al., 1998; Helander et al., 1996; Yonemura et al., 1998) so it is possible that ligation of ICAM-2 at EC junctional regions initiates signalling pathways which facilitates opening of the EC junction, similar to that seen with ICAM-1 clustering, VE-PTP activation and VE-cadherin disengagement (Alcaide et al., 2009). Alternatively ICAM-2 may play a role in the formation of protrusive membrane structures which have been observed, primarily *in vitro*, to form at the site of TEM (Barreiro, 2002; Carman and Springer, 2004; Phillipson et al., 2008). Additionally neutrophil protrusions into the EC could also be supported by EC ICAM-2-induced outside-in integrin signalling within the neutrophil which is known to facilitates cytoskeletal rearrangement.

PECAM-1 is an important EC junctional molecule which has many similarities to ICAM-2 in that they both are members of Ig superfamily which are expressed at EC junctions and are both implicated in neutrophil extravasation where they have demonstrated stimulus-specific roles (Huang et al., 2006; Thompson et al., 2001; Woodfin et al., 2009). Interestingly using PECAM-1 KO mice stimulated with IL-1β a delay in neutrophil extravasation was reported rather than a complete inhibition (Thompson et al., 2001), indicating a transient role for PECAM-1 in neutrophil migration. The genetic deletion of ICAM-2 may also result in a delay in neutrophil extravasation rather than a complete inhibition, as demonstrated in an allergic mouse model (Gerwin et al., 1999). Further studies into the role of ICAM-2 in neutrophil extravasation at later time points are required to fully understand the functions and mechanisms of ICAM-2, and to identify other molecules that are capable of supporting TEM in the absence of ICAM-2.

In summary the findings presented in this chapter demonstrate that ICAM-2 has a role in mediating early stages of TEM and it is tempting to speculate that ICAM-2 could be involved in the identification of TEM sites and/or the initiation of TEM by facilitating the opening of EC junctions in IL-1β-stimulated tissues. The data also confirms that once TEM is initiated (i.e. EC junctions opened) neutrophils proceed to TEM normally with respect to the route and duration of TEM. These findings extend previous works on the functional role ICAM-2 by dissecting the precise stage at which ICAM-2 mediates neutrophil TEM *in vivo*.

CHAPTER 6: Potential ligands for ICAM-2 during neutrophil-endothelial interactions

6.1 Introduction

ICAM-2 was originally described as a 'ligand for LFA-1 homologous to ICAM-1' (Staunton et al., 1989). Subsequently numerous other proteins have been demonstrated to have binding capabilities to ICAM-2 such as MAC-1 (Li et al., 1995; Xie et al., 1995), VLA-4 (Seth et al., 1991), DC-SIGN (Geijtenbeek et al., 2000; Wethmar et al., 2006) and homophilic interactions in *trans* can occur (Huang et al., 2005). The latter interaction is unlikely to occur during neutrophil-EC interactions as neutrophil ICAM-2 expression is significantly lower than that on ECs (Chapter 3). The role of ICAM-2 in mediating leukocyte extravasation in general has previously been attributed to EC ICAM-2 (Boscacci et al., 2010; Lehmann et al., 2003; Reiss et al., 1998; Schenkel et al., 2004; Steiner et al., 2010; Woodfin et al., 2009) and for these reasons a possible neutrophil ligand for ICAM-2 was investigated. ICAM-2 interactions with the β_2-integrins, LFA-1 and MAC-1 are widely accepted and have been studied in more detail than its interaction with VLA-4, which has only been reported in one study and DC-SIGN, which is expressed on dendritic cells and macrophages only. Taking all these factors into account as well as the key role for β_2-integrins in the neutrophil transmigration cascade, it was hypothesised that the novel roles of EC ICAM-2 in neutrophil crawling (Chapter 4) and the initiation of TEM (Chapter 5) could be governed by its interactions with neutrophil integrins.

Only a few studies to date have focused specifically on the ligands that bind to ICAM-2 during its role in the recruitment of leukocytes. During dendritic cell migration EC ICAM-2 has been shown to bind to DC-SIGN (Geijtenbeek et al., 2000; Wethmar et al., 2006). In contrast during monocyte crawling EC ICAM-2 has

been shown to bind to both LFA-1 and MAC-1 (Schenkel et al., 2004) whereas during lymphocyte adhesion EC ICAM-2 binds to LFA-1 or VLA-4 (Seth et al., 1991). A recent study looking at neutrophil rolling found the formation of neutrophil 'slings' during this process, and this was demonstrated to be supported via ICAM-2/LFA-1 interactions in *trans* on neutrophils. Of relevance to the current study, the role of EC ICAM-2 in neutrophil migration has been suggested to occur through neutrophil LFA-1 (Issekutz et al., 1999). The role of ICAM-2 in this context was however only evident when ICAM-1 was also blocked where an additional inhibitory effect was seen relative to ICAM-1 blockade alone. This study was carried out using HUVECs, and any differences in the role of ICAM-2 with that presented in Chapter 4 and 5 could be a result of different experimental models used. In line with the latter study however various other groups have also highlighted that ICAM-1 and ICAM-2 have overlapping roles, and can even partially compensate for each other (Boscacci et al., 2010; Lehmann et al., 2003; Reiss et al., 1998; Steiner et al., 2010). Taking these findings into consideration the distinct roles of ICAM-1 and ICAM-2 in neutrophil migration were explored as part of the present chapter.

Integrins are the main leukocyte ligand for ICAMs and have been demonstrated to bind to the argineglycinelaspartic acid (RGD) sequence which is present in various extracellular matrix proteins such as fibronectin and fibrinogen. Interestingly ICAM-2 does not have this motif. LFA-1 and MAC-1 binding sites on ICAM-2 have been mapped to the first 22-amino acid sequence (P1) in first Ig domain on the extracellular portion (Li et al., 1993; Xie et al., 1995). This sequence is recognised by a specific segment called the 'A' or 'I' domain in the extracellular part of the α-subunit in integrins. The 2 Ig domains of ICAM-2 have a 35% homology to ICAM-1, and as these domains are implicated in ligand binding it is not surprising that these two ICAMs have the ability to bind to a similar set of ligands. However as ICAM-2 has a smaller N-terminal than ICAM-1, it is believed to have restricted accessibility for ligands which may limit its roles. For this reason LFA-1 is thought to have much lower affinity for ICAM-2 than ICAM-1, and this is also likely to be the case for MAC-1, although this has not been directly investigated. Both LFA-1, and to a

greater extent MAC-1, have been suggested to be involved in leukocyte polarisation and crawling via activation of numerous signalling pathways within leukocytes (Ley et al., 2007; Phillipson et al., 2006; Sumagin et al., 2010). As the mechanisms underlying these roles are only just beginning to emerge, a potential role for ICAM-2 in these integrin-mediated events cannot be ruled out. Intracellular proteins such as α-actinin (Heiska et al., 1996), ERM (Hamada et al., 2003; Heiska et al., 1998; Helander et al., 1996; Yonemura et al., 1998) and PIP2 (Heiska et al., 1998) are also known to interact with the cytoplasmic domain of ICAM-2, and are involved in intracellular signalling, cell survival (Perez et al., 2002) and ICAM-2 clustering (Helander et al., 1996; Perez et al., 2002). Such events could also be involved in the downstream mechanisms by which ICAM-2 mediates the initiation of neutrophil TEM (Chapter 5).

This chapter focuses on examining the mechanisms underlying the role of ICAM-2 in neutrophil crawling and the initiation of TEM by investigating the potential neutrophil ligands for ICAM-2 in these responses. In general LFA-1 is well accepted to be involved in neutrophil adhesion, whereas MAC-1 is considered to be a key player of neutrophil crawling (Phillipson et al., 2006; Sumagin et al., 2010). For these reasons it was hypothesised that neutrophil MAC-1 interacts with EC ICAM-2 during neutrophil crawling and the initiation of TEM. MAC-1 can also however interact with ICAM-1, and ICAM-1 and ICAM-2 have been shown to have overlapping roles in some inflammatory models. As a result the functions of ICAM-1, ICAM-2 and MAC-1 in neutrophil crawling and the initiation of TEM were analysed using functional blocking mAbs to ICAM-1, ICAM-2 and MAC-1 in the cremasteric confocal IVM model. Collectively the findings of this chapter provide further mechanistic insights into the role of ICAM-2 in neutrophil extravasation.

6.2 Results

6.2.1 ICAM-1 and ICAM-2 have overlapping but distinct expression patterns on venular endothelial cells

A role for ICAM-2 in mediating neutrophil intraluminal crawling and the initiation of TEM has been demonstrated (Chapter 4 and 5), and the identity of the neutrophil ligand for ICAM-2 in these processes was subsequently investigated. Initially the contribution of ICAM-1 in this model was investigated as this protein shares key ligands with ICAM-2 (e.g. LFA-1 and MAC-1), and has been shown to have redundant and/or overlapping roles with ICAM-2 in inflammation (Lehmann et al., 2003; Phillipson et al., 2006; Sumagin et al., 2010). Using *in vivo* immunostaining and confocal analysis of post-capillary venules from the mouse cremaster muscles, the expression pattern of EC ICAM-1 was compared to that of EC ICAM-2 in unstimulated and IL-1β-stimulated tissues. The expression of ICAM-1 in ICAM-2 KO mice was also compared to that in WT animals to determine if any compensatory expression of ICAM-1 was evident in the ICAM-2 KO mice. ICAM-1 was found to be upregulated by IL-1β stimulation in both WT (Figure 6.1 and 6.3) and ICAM-2 KO mice (Figure 6.2 and 6.3), and this up-regulation was found at EC junctions and at EC non-junctional areas (Figure 6.4). No difference in terms of total venular expression or in terms of EC junctional and non-junctional distribution was detected between WT and ICAM-2 KO mice. The distribution of ICAM-1 within individual ECs was distinct from that of PECAM-1. More specifically, whilst PECAM-1 was highly localised at EC junctions with a faint diffuse expression at EC bodies, ICAM-1 was expressed at junctions with a heterogeneous expression at EC bodies (Figure 6.5). In contrast to EC ICAM-2 expression pattern (Chapter 3), junctional EC ICAM-1 expression was higher in comparison to non-junctional areas (Figure 6.4). Isotype control mAb was also used in the place of anti-ICAM-1 mAb to ascertain potential non-specific binding of the anti-ICAM-1 mAb. Tissues treated with this isotype control mAb displayed no specific staining on the vasculature (Figure 6.1 and 6.2).

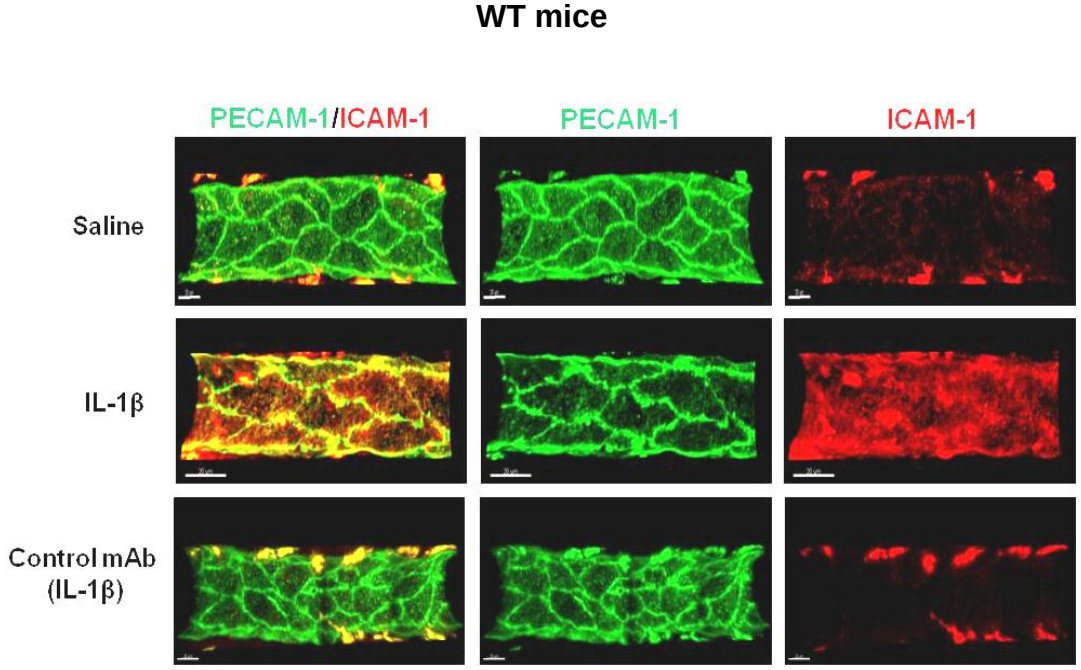

Figure 6.1: PECAM-1 and ICAM-1 expression patterns in WT cremasteric post-capillary venules.

Representative confocal images of venules which were co-injected with saline or IL-1β (50ng/400ul) and fluorescently conjugated mAbs (4μg/mouse) against PECAM-1 (shown in green) and ICAM-1 (shown in red) intrascrotally. Tissues were also labelled with an isotype control mAb to ascertain potential non-specific binding of the anti-ICAM-1 mAb. Scale bar represents 20 μm. NB- In these experiments tissues were also staining for ICAM-1 results are presented in chapter 3.

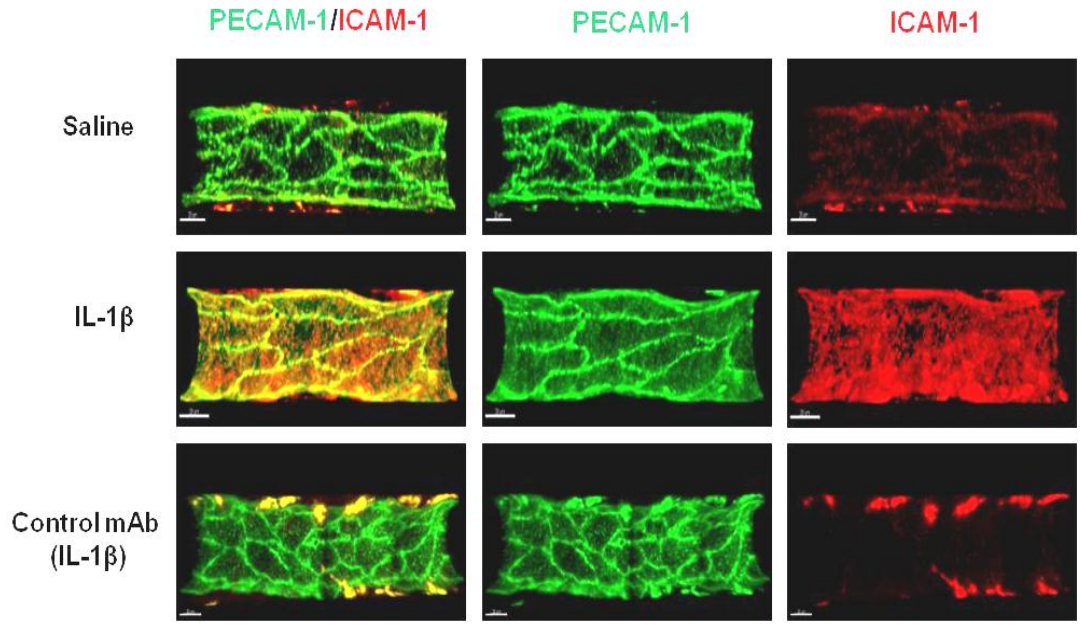

Figure 6.2: PECAM-1 and ICAM-1 expression pattern in ICAM-2 KO cremasteric post-capillary venules.

Representative confocal images of venules which were co-injected with saline or IL-1β (50ng/400ul) and fluorescently conjugated mAbs (4μg/mouse) against PECAM-1 (shown in green) and ICAM-1 (shown in red) intrascrotally. Tissues were also labelled with an isotype control mAb to ascertain potential non-specific binding of the anti-ICAM-1 mAb. Scale bar represents 20 μm. NB- In these experiments tissues were also staining for ICAM-1 results are presented in chapter 3.

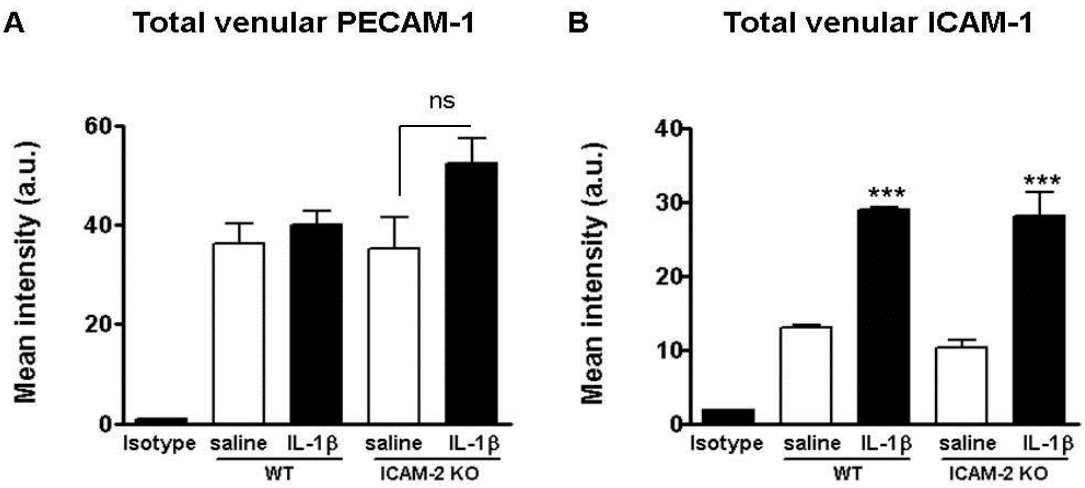

Figure 6.3: Post-capillary venule expression of PECAM-1 and ICAM-1 in IL-1β-stimulated WT and ICAM-2 KO mice.

Venular expression of PECAM-1 and ICAM-1 was investigated in WT and ICAM-2 KO mice. Saline or IL-1β-stimulated (50 ng/mouse, i.s) tissues were analysed by immunofluorescent staining and confocal microscopy 4 hours post-injection. The total post-capillary venule expression of (**A**) PECAM-1 and (**B**) ICAM-1 was quantified using Imaris software to build isosurfaces on whole venules based on PECAM-1 expression (Chapter 2, Figure 2.5). N = 3-5 vessels per mice, 3 mice per group, error bars show SEM. Statistically significant (T-test) differences between saline and IL-1β groups are indicated by asterisks, ***P<0.001, not significant (ns). NB- In these experiments tissues were also staining for ICAM-1 results are presented in chapter 3.

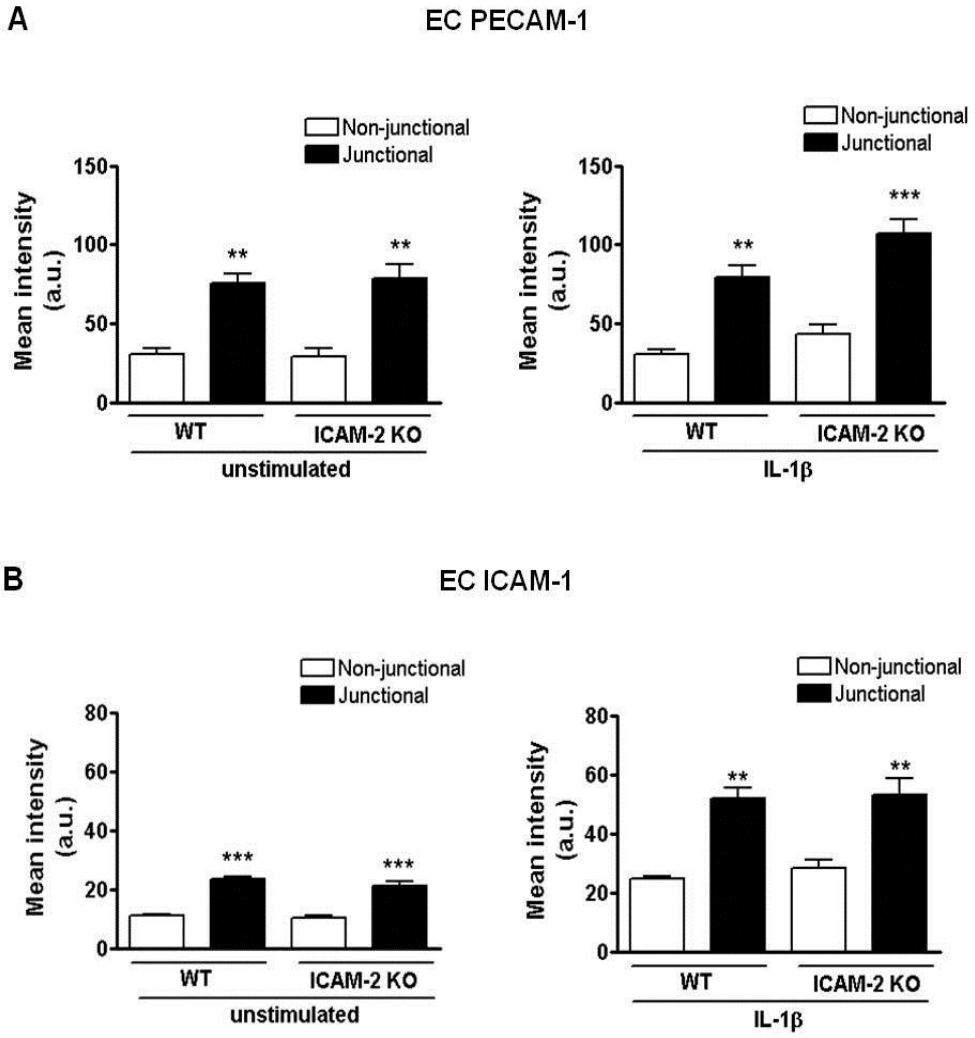

Figure 6.4: Endothelial sub-cellular expression of PECAM-1 and ICAM-1 in WT and ICAM-2 KO mice.

Cremasteric post-capillary venules were stimulated with saline or IL-1β-stimulated (50 ng/mouse, i.s) and analysed by immunofluorescent staining and confocal microscopy 4 hours post-injection. Endothelial junctional and non-junctional expression of (**A**) PECAM-1 and (**B**) ICAM-1 was quantified using Imaris software to build isosurfaces on whole venules based on PECAM-1 expression (Chapter 2, Figure 2.6). N = 3-5 vessels per mice, 3 mice per group, error bars show SEM. Statistically significant (T-test) differences between junctional or non-junctional regions are indicated by asterisks, **P<0.01, ***P<0.001. NB- In these experiments tissues were also staining for ICAM-1 results are presented in chapter 3.

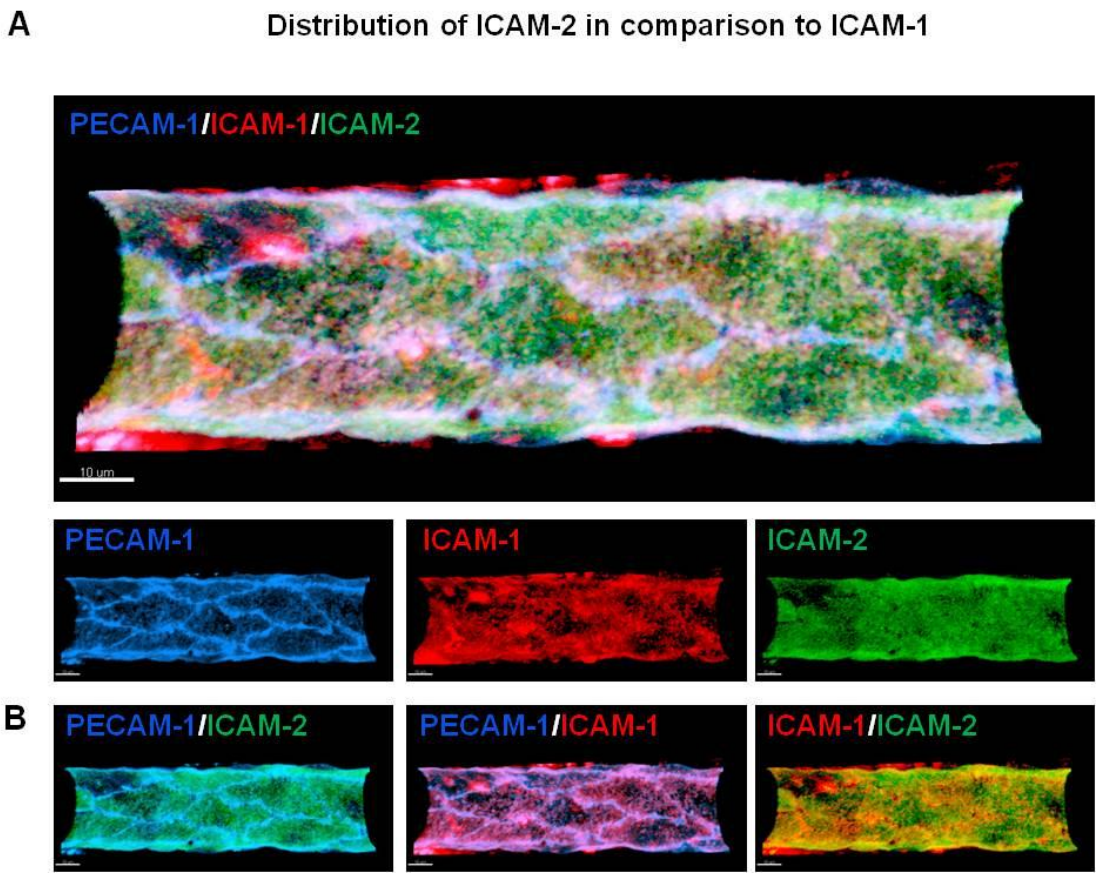

Figure 6.5: ICAM-2 and ICAM-1 co-localisation in the cremasteric post-capillary venules.

Expression of ICAM-1 and ICAM-2 was investigated relative to that of PECAM-1 in WT IL-1β-stimulated tissues by immunostaining and confocal microscopy. (**A**) A representative image of a venule which was co-injected with IL-1β (50ng/400ul) and the fluorescent mAbs (4µg/mouse) to PECAM-1 (shown in blue), ICAM-1 (shown in red) and ICAM-2 (shown in green) intrascrotally. (**B**) Co-localisation of PECAM-1 and ICAM-1 can be seen in light blue, co-localisation of PECAM-1 and ICAM-1 can be seen in pink and co-localisation of ICAM-1 and ICAM-2 can be seen in yellow/orange. Scale bar represents 10 µm.

6.2.2 Low doses of fluorescently conjugated anti-ICAM-1 mAb administered for labelling did not alter neutrophil transmigration responses to IL-1β

Analysis of neutrophil adhesion and transmigration by brightfield microscopy confirmed that a neutrophil response was elicited after IL-1β stimulation in comparison to saline controls (Figure 6.6). Intrascrotal administration of fluorescently labelled anti-PECAM-1, anti-ICAM-2 and anti-ICAM-1 mAbs (Figure 6.5) did not alter leukocyte adhesion or transmigration (Figure 6.6). This was because a non-function blocking mAb to PECAM-1 and very low doses of anti-ICAM-2 and anti-ICAM-1 mAbs were administered. Furthermore ICAM-2 KO mice (which had fluorescently labelled mAb administered) also had normal leukocyte adhesion responses but as expected had a significant reduction in transmigrated leukocytes after IL-1β stimulation in comparison to WT controls.

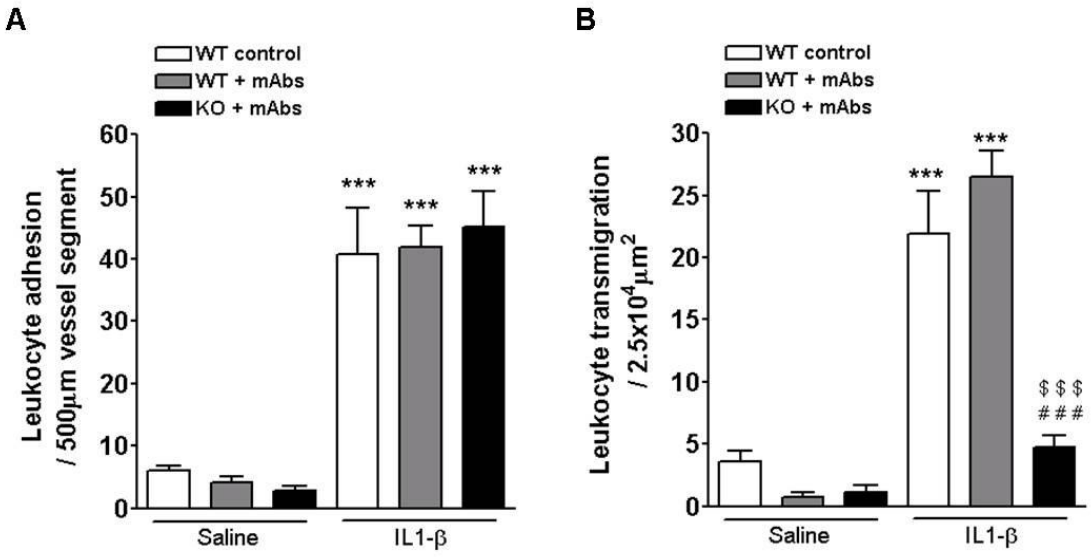

Figure 6.6: Effect of in vivo labelling of ICAM-1 on leukocyte responses in IL-1β-stimulated cremaster muscles.

WT and ICAM-2 KO mice were injected with saline or IL-1β (50ng/400µl, i.s.) for 4 hours. Fluorescently conjugated mAbs to PECAM-1 (2µg/mouse) and ICAM-1 (4µg/mouse) were co administered with the i.s. injection. Cremaster muscles were exteriorised and leukocyte responses were analysed by brightfield IVM. (**A**) Adherent leukocytes per 500 µm vessel segment and (**B**) transmigrated leukocytes per $2.5x10^4\mu m^2$ were analysed. Results are presented as mean ± SEM for each mice (n=3 mice, 3-5 vessels/cremaster). Significant differences (Anova) between saline and IL-1β groups are indicated by asterisks (***P < 0.001). Additional statistical comparisons between WT control and ICAM-2 KO groups are indicated by hash symbols (###P < 0.001). Lastly, comparisons between WT and fluorescent mAb administration and ICAM-2 KO groups are indicated by dollar symbols ($$$P < 0.001).

6.2.3 ICAM-1 and ICAM-2 have distinct roles in regulating intravascular neutrophils

To investigate the relative functional roles of ICAM-1 and ICAM-2 in neutrophil adhesion and extravasation anti-ICAM-1 and anti-ICAM-2 function blocking mAbs were used in the cremaster confocal IVM model. Animals were given 3mg/kg i.v. of blocking mAbs, or matched isotype controls, and cremaster muscles were PECAM-1 labelled and stimulated with IL-1β as previously described. Tissues were exteriorised and intravascular and extravasated neutrophil numbers were quantified from images taken 4 hours post-i.s. injection (Figure 6.7). Previous data using ICAM-2 KO mice could be duplicated using the ICAM-2 blocking mAb administered in WT mice, compared to an appropriate isotype control in terms of both intra- and extravascular neutrophils. The results showed that animals pre-treated with isotype control mAbs had on average 54.6 ± 9.3 intravascular neutrophils in a 500μm vessel segment and 31.9 ± 9.8 extravascular neutrophils in a $2.5x10^4 \mu m^2$ segment. Anti-ICAM-2 mAb did not significantly reduce the number of intravascular cells (37.4 ± 4.0 cells, n=7 mice) but there was a significant suppression in extravasation (8.9 ± 3.0 cells, n=7 mice, $P< 0.001$) as seen in ICAM-2 KO mice (Chapter 4). In contrast, anti-ICAM-1 mAb substantially reduced intravascular neutrophils (8.1 ± 1.6 cells, n=6 mice, $P< 0.001$) and almost totally abrogated numbers of extravasated cells in comparison to controls (Figure 6.7). Anti-ICAM-1 mAb treatment also resulted in a significant ($P< 0.05$, n=4-8 mice) decrease in the number of intravascular neutrophils as compared to anti-ICAM-2 mAb. This data indicates that whilst ICAM-1 has key roles in mediating neutrophil adhesion, ICAM-2 does not and that the reduction in extravasation seen in ICAM-2 KOs after IL-1β stimulation (Chapter 4) could be replicated using a function blocking mAb to ICAM-2 in IL-1β-stimulated WT tissues.

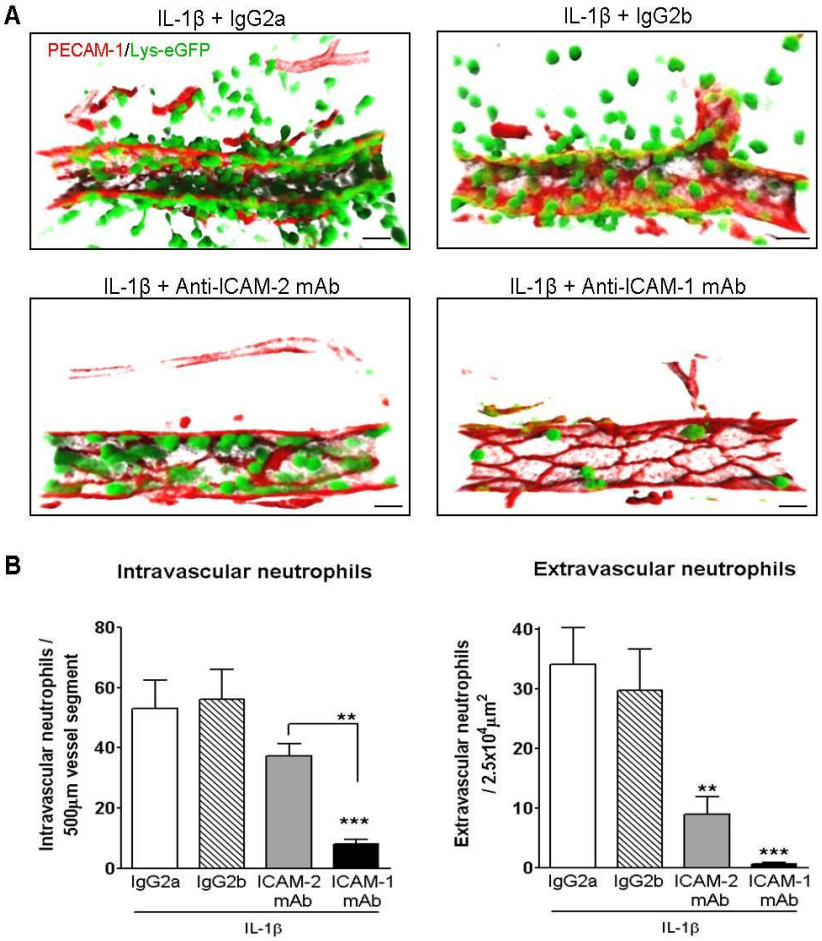

Figure 6.7: Effect of ICAM-1 and ICAM-2 inhibition on neutrophil extravasation in IL-1β-stimulated venules.

Cremasteric confocal IVM of WT Lys-eGFP-ki mice stimulated with i.s. IL-1β (50 ng/mouse). Animals were pre-treated with an i.v. injection of anti-ICAM-1 or anti-ICAM-2 mAb, or isotype control, at 3 mg/kg. (**A**) Representative images of post-capillary venules where PECAM-1 (i.s. labelling *in vivo*) is shown in red and neutrophil (Lys-eGFP-ki mice) are shown in green. (**B**) The mean total intravascular neutrophils per 500µm vessel segment and extravascular neutrophils per $2.5x10^4\mu m^2$ segment were analysed 4 hours post-stimulation. Data were obtained 4-9 vessels in 4-8 mice. Bars represent mean ± SEM for all events analysed. Statistically significant (Anova) differences between isotype control are represented by asterisks **P< 0.01, ***P <0.001. Differences between blocking mAb groups are represented by lines.

6.2.4 ICAM-1 and ICAM-2 have overlapping but distinct roles in regulating crawling

Neutrophil crawling dynamics were also quantified in IL-1β-stimulated WT mice pre-treated with anti-ICAM-1 and anti-ICAM-2 mAbs. The data acquired using ICAM-2 KO mice in Chapter 4 could again be duplicated using the anti-ICAM-2 blocking mAb compared to an appropriate isotype control in terms of neutrophils crawling dynamics (Figure 6.8). Both anti-ICAM-2 and anti-ICAM-1 mAb significantly reduced neutrophil crawling speed (6.7 ± 0.3 μm/min, n=113 for anti-ICAM-2 mAb and 5.1 ± 0.2 μm/min, n=46 for anti-ICAM-1 mAb) in comparison to their respective isotype control mAbs (10.8 ± 0.6 μm/min, n=53 for IgG2a mAb and 9.7 ± 0.5 μm/min, n=66 for IgG2b mAb) (Figure 6.8A). Interestingly the reduction in crawling speed induced by anti-ICAM-1 mAb was significantly greater than that detected after anti-ICAM-2 mAb treatment ($P< 0.05$), although it should be noted that the number of crawling neutrophils analysed per venule after anti-ICAM-1 mAb was fewer than that analysed for anti-ICAM-2, as ICAM-1 has a crucial role in initial adhesion (Figure 6.8A).

While a reduced number of luminal crawling cells were present following anti-ICAM-1 mAb treatment, the few cells that were observed to undergo crawling often exhibited discontinuous crawling behaviour (70.4 ± 8.7%, n=6 mice from 6 vessels), and this was not significantly different from that seen after anti-ICAM-2 mAb treatment (54.9 ± 7.4%, n=8 mice from 9 vessels) (Figure 6.8B). These results were comparable to the frequency of discontinuous crawling in ICAM-2 KO mice in Chapter 4 (Figure 4.13). After mAb treatment discontinuously crawling cells crawled significantly slower than continuously crawling cells (Figure 6.8C). After mAb treatment there was also significant reduction in the speed of continuous crawling cells in comparison to controls ($P<0.001$). This suggests that the overall reduction in speed was not solely due to the high frequency of slow, discontinuous crawling, as continuously crawling cells also crawled significantly slower than in controls (Figure

6.8C). This was in line with previous findings using ICAM-2 KO mice (Chapter 4, Figure 4.14). Additionally anti-ICAM-1 and anti-ICAM-2 mAb treatment had the same level of reduction in the frequency of continuously crawling cells and the speed of continuous crawling. Therefore reasons behind the reduction in the overall crawling speed after anti-ICAM-1 mAb in comparison to anti-ICAM-2 mAb are currently unknown.

The differential effects of blocking ICAM-1 and -2 on the number of intravascular crawling neutrophils, and the mean crawling speed suggest that the roles of ICAM-1 and -2 in this model are not fully overlapping, and maybe a result of differences in ligand binding.

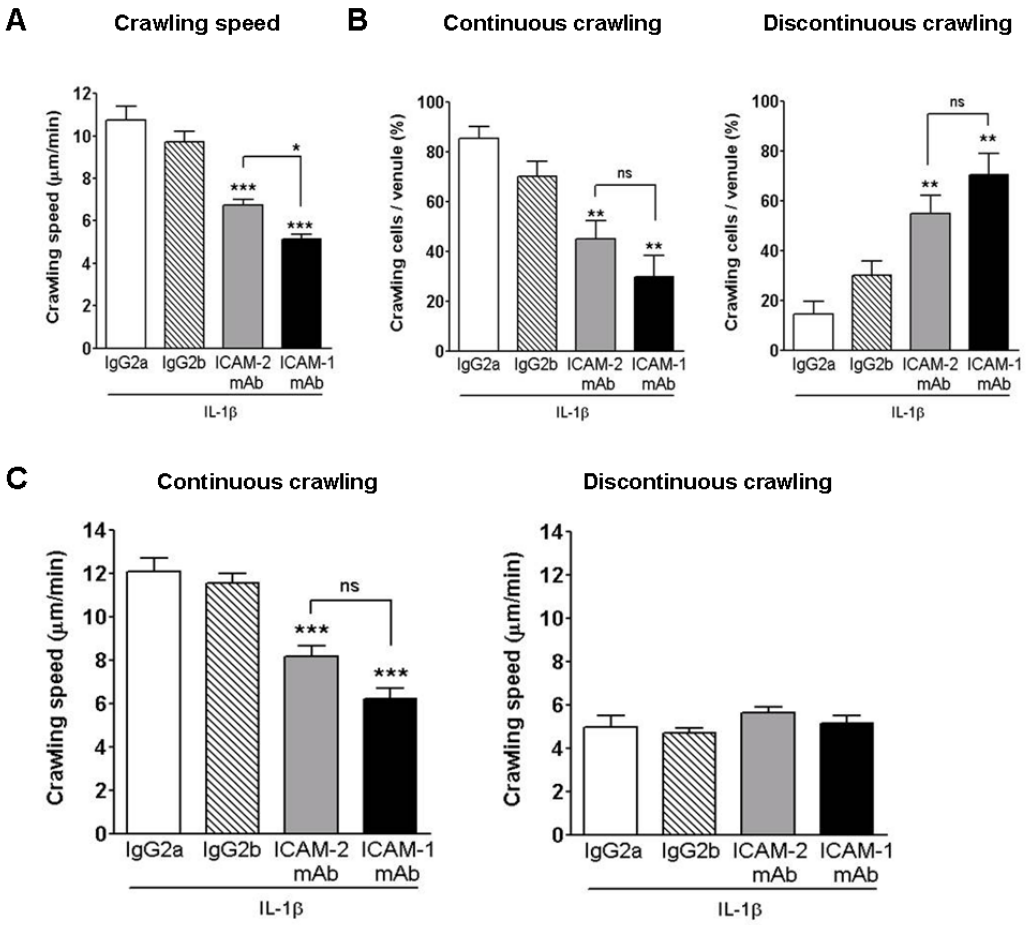

Figure 6.8: Effect of ICAM-1 and ICAM-2 inhibition on neutrophil crawling dynamics in IL-1β-stimulated venules

Cremasteric confocal IVM of WT Lys-eGFP-ki mice stimulated with i.s. IL-1β (50 ng/mouse) for 2 hours. Animals were pre-treated with an i.v. injection of anti-ICAM-1 or anti-ICAM-2 mAb, or isotype control, at 3 mg/kg. (**A**) The mean crawling speed and (**B**) the percentage of continuously and discontinuously crawling neutrophils was determined. (**C**) The mean crawling speed of continuously and discontinuously crawling cells was also determined. Data were obtained from analysis of 46-113 crawling cells from 4-9 vessels in 4-8 mice. Bars represent mean ± SEM for all events analysed. Statistically significant (Anova) differences between isotype control are represented by asterisks *P< 0.05, **P< 0.01, ***P <0.001, ns (not significant). Differences between blocking mAb groups are represented by lines.

6.2.5 Neutrophil MAC-1 does not interact with EC ICAM-2 during neutrophil adhesion

As ICAM-2 and ICAM-1 are known to bind LFA-1 and MAC-1 (Issekutz et al., 1999; Nourshargh et al., 2010; Staunton et al., 1989; Xie et al., 1995), and LFA-1 is thought to support initial leukocyte adhesion, whereas MAC-1 is thought to support crawling (Phillipson et al., 2006; Sumagin et al., 2010), the possibility that ICAM-2/MAC-1 interactions were mediating the role of ICAM-2 in neutrophil crawling was investigated. It is not possible however to discount the possibility that any observed effect of blocking MAC-1 function is related to MAC-1/ICAM-1 interactions, as this integrin is also known to be an ICAM-1 ligand, and using an anti-ICAM-1 mAb in addition to MAC-1 blockade to exclude any effect of this interaction would reduce the number of quantifiable neutrophil crawling events to below viable levels. To this end the effect of a MAC-1 blocking mAb in WT and ICAM-2 KO mice was examined, on the basis that if there is no *cumulative effect* of impairing the function of ICAM-2 and MAC-1, then the observed inhibition represents the function of these two proteins interacting, while a cumulative effect of impairing MAC-1 and ICAM-2 function would represent a possible MAC-1/ICAM-1 interaction.

Images of IL-1β-stimulated vessels treated with i.v. anti-MAC-1 or an isotype control mAb were captured at 4 hours post-IL-1β, and intravascular and extravasated cells were quantified (Figure 6.9A). In WT animals that had been pre-treated with anti-MAC-1 mAb a significant reduction in intravascular cells was seen in comparison to control (56.0 ± 1.0, n=5 mice for control and 22.4 ± 5.4, n=4 mice for anti-MAC-1 mAb) (Figure 6.9B). This effect is not seen following ICAM-2 blockade, indicating that this is a non-ICAM-2 mediated MAC-1 function and is likely to be due to ligation with ICAM-1. Of note, the level of inhibition of intravascular cells was not as complete as that seen following ICAM-1 blockade, suggesting that ICAM-1 has other binding partners that support adhesion namely LFA-1. Additionally it is also possible that the efficacy of anti-ICAM-1 mAb is

higher than that of anti-MAC-1 mAb and hence resulting in a greater reduction. The assertion that this MAC-1 function is not mediated by ICAM-2 is supported by the absence of a reduction in intravascular neutrophils in ICAM-2 KO mice (Figure 6.9B) and in WT mice treated with anti-ICAM-2 mAb (Figure 6.7B). Extravasation is almost totally inhibited by either MAC-1 blockade or in the absence of ICAM-2, so it is not possible to comment on potential cumulative effect (Figure 6.9B).

6.2.6 Neutrophil MAC-1 may interact with EC ICAM-2 during neutrophil crawling

Luminal crawling dynamics in IL-1β-stimulated WT and ICAM-2 KO mice pre-treated with control or anti-MAC-1 mAb were also quantified. WTs treated with isotype control mAb had a similar crawling speed to that detected by WTs in Chapter 4 (9.7 ± 0.7 μm/min, n=66 cells) and as expected this speed was significantly reduced in ICAM-2 KO mice treated with isotype control (6.3 ± 0.3 μm/min, n=36). The number of crawling/intravascular neutrophils in WT and ICAM-2 KO mice were also comparable to that detected previously (Chapter 4). In WT animals the anti-MAC-1 mAb significantly reduced crawling speeds (7.3 ± 0.3 μm/min, n=63, $P<$ 0.01) to a level similar to the mean speed seen in ICAM-2 KO mice treated with control mAb (Figure 6.10A). When ICAM-2 KO mice were pre-treated with the anti-MAC-1 mAb no cumulative effect on crawling speed was seen (6.7 ± 0.7 μm/min, n=72), indicating that this function could be mediated by ICAM-2/MAC-1 interactions (Figure 6.10A).

There was a significant reduction in the frequency of continuously crawling cells in WT mice pre-treated with anti-MAC-1 mAb (50.4 ± 9.1%, n=6 vessels) in comparison to controls and this was in line with that of ICAM-2 KOs treated with anti-MAC-1 mAb. However no significant evidence of cumulative inhibition was

observed when the functions of both ICAM-2 and MAC-1 were impaired (Figure 6.10B). The speed of discontinuous crawling across all groups was approximately 6 μm/min and was in line with previously acquired data (Chapter 4). The speed of continuously crawling cells in WT mice treated with control mAb was 11.5 ± 0.5 μm/min (n=47 cells) and this was significantly reduced after anti-MAC-1 mAb treatment ($P<0.001$), ICAM-2 genetic deficiency ($P<0.05$) and the joint blockade and deletion of MAC-1 and ICAM-2 respectively ($P<0.001$). No additive effects were detected with respect to the speed of continuous crawling cells when MAC-1 and ICAM-2 functions were both impaired. This indicates that the overall reduction in crawling speed was due to the combination of a high frequency of slow, discontinuously crawling cells as well as the reduced crawling speed of continuously crawling cells (Figure 6.10C). This finding is comparable to previous data using ICAM-2 KO mice (Chapter 4) and WT mice treated with anti-ICAM-2 mAb (Figure 6.8).

There was a significant reduction in TEM events in stimulated ICAM-2 KO mice (5 TEM events during a 30 minute period/venule) relative to WT mice as presented in Chapter 5. After MAC-1 inhibition there also appeared to be a reduction in TEM events in line with the reduced number of extravasated neutrophils at the 4 hour time point (Figure 6.7). However only 6 TEM events were observed in animals treated with anti-MAC-1 mAb post-stimulation overall across 7 venules in 5 mice. For this reason TEM dynamics after anti-MAC-1 mAb could not be analysed in detail and hence no comment can be made regarding the potential ligand interactions with ICAM-2 during TEM (i.e. pre-TEM).

Collectively the data indicates that ICAM-1 does not compensate for the genetic deletion of ICAM-2, suggesting that these molecules have distinct roles in this model. Indeed ICAM-1 and ICAM-2 were found to have distinct roles in mediating neutrophil adhesion, however they also have overlapping roles in neutrophil crawling dynamics after IL-1β stimulation. The lack of an additive effect when ICAM-2 and

MAC-1 functions were impaired suggests that ICAM-2 ligation with neutrophil MAC-1 could potentially support the observed roles of ICAM-2 in neutrophil luminal crawling speed and continuity.

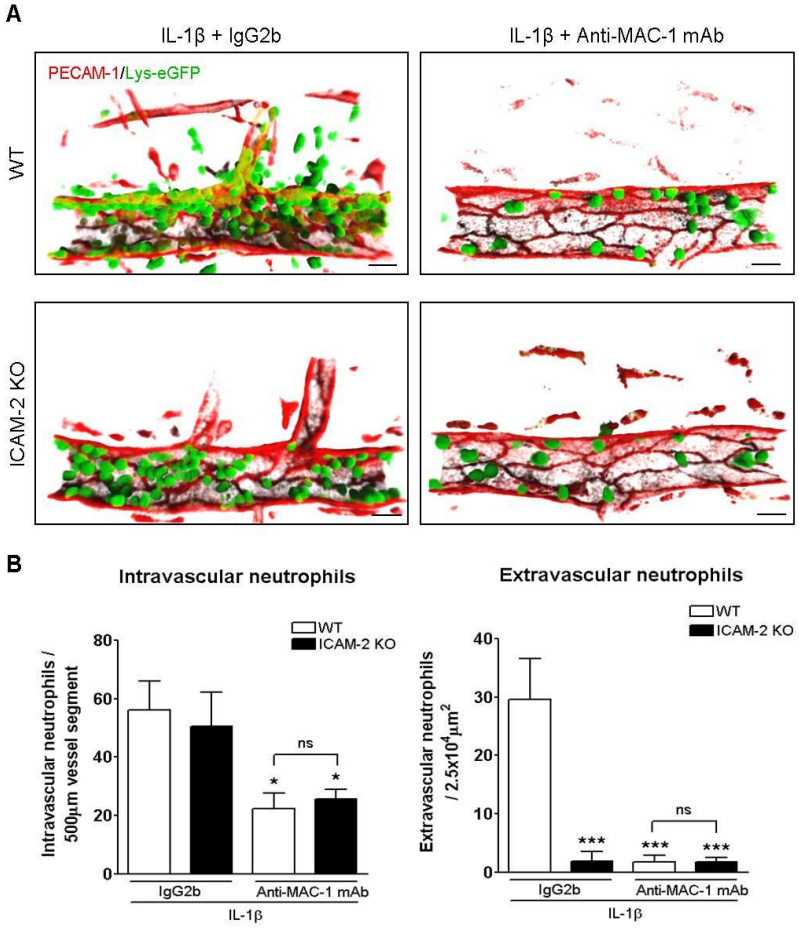

Figure 6.9: Effect of MAC-1 inhibition on neutrophil extravasation in IL-1β-stimulated WT and ICAM-2 KO venules.

Cremasteric confocal IVM of WT and ICAM-2 KO Lys-eGFP-ki mice stimulated with i.s. IL-1β (50 ng/mouse). Animals were pre-treated with an i.v. injection of anti-MAC-1 mAb, or isotype control, at 3 mg/kg. (**A**) Representative images of post-capillary venules where PECAM-1 (i.s. labelling *I*) is shown in red and neutrophil (Lys-eGFP-ki mice) are shown in green. (**B**) The mean total intravascular neutrophils per 500µm vessel segment and extravascular neutrophils per $2.5x10^4\mu m^2$ segment were analysed 4 hours post-stimulation. Data were obtained from 4-7 vessel in 3-5 mice. Bars represent mean ± SEM for all events analysed. Statistically significant (Anova) differences between WT isotype control are represented by asterisks *P< 0.05, ***P < 0.001, ns (not significant).

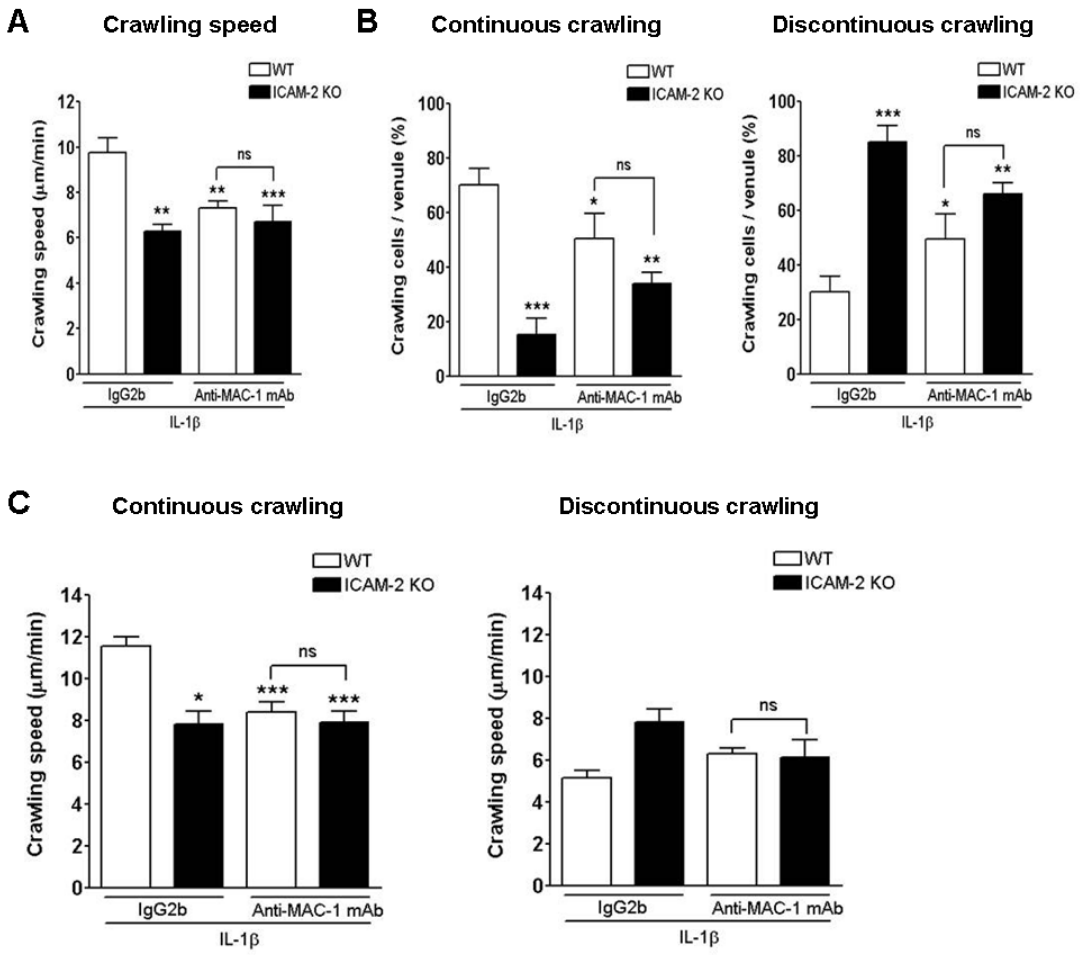

Figure 6.10: Effect of MAC-1 inhibition on neutrophil crawling dynamics in IL-1β-stimulated WT and ICAM-2 KO venules.

Cremasteric confocal IVM of WT and ICAM-2 KO Lys-eGFP-ki mice stimulated with i.s. IL-1β (50 ng/mouse) for 2 hours. Animals were pre-treated with an i.v. injection of anti-MAC-1 mAb, or isotype control, at 3 mg/kg. (**A**) The mean crawling speed and (**B**) the percentage of continuously and discontinuously crawling neutrophils was determined. (**C**) The mean crawling speed of continuous and discontinuous crawling cells was also determined. Data were obtained from analysis of 36-66 crawling cells from 4-7 vessels in 3-5 mice. Bars represent mean ± SEM for all events analysed. Statistically significant (Anova) differences between WT isotype control are represented by asterisks *P< 0.05, **P< 0.01, ***P < 0.001, ns (not significant).

6.3 Discussion

In this chapter the molecular mechanisms underlying the role of ICAM-2 in neutrophil crawling and the initiation of TEM was investigated by examining the ligand interaction for ICAM-2 in this process. ICAM-1 and ICAM-2 share possible key ligands, namely LFA-1 and MAC-1, and there is evidence for these ICAMs to function in a co-operative and/or redundant manner in various models relating to the migration of several leukocyte subsets (Boscacci et al., 2010; Issekutz et al.1999; Lehmann et al., 2003; Steiner et al., 2010), which could be associated with their leukocyte ligands. The complexity of the relationship between these two endothelial proteins, and the overlap between their known ligands and functions, necessitated the consideration of a possible ICAM-1 influence in the current model.

The expression profile of EC ICAM-1 was examined using immunofluorescent labelling and confocal microscopy of the cremasteric vasculature. Whilst ICAM-1 was found to be significantly upregulated after IL-1β expression in both WT and ICAM-2 KO mice, no difference in expression in terms of localisation and fluorescence intensity was found between ICAM-2 KO and WT mice. This suggests that no compensatory up-regulation of ICAM-1 is evident on unstimulated or stimulated cremasteric ECs when ICAM-2 is genetically deleted. In support of this, in ICAM-1 KO ECs, no change in ICAM-2 expression was noted in comparison to WTs even after stimulation (Reiss et al., 1998). Although this observation was *in vitro* using a cell line system, the findings are similar to that noted in the current study. Taking this into account, it is evident that no compensatory up-regulation in ICAM-1 expression was seen in ECs from ICAM-2 KO mice suggesting that they have distinct roles and are not fully redundant proteins.

Functional studies confirmed that mAb blockade of ICAM-1 had a highly inhibitory effect on IL-1β-stimulated neutrophil adhesion, and almost totally abolished

extravasation. These roles are likely to be primarily mediated via its interactions with LFA-1 (Phillipson et al., 2006; Sumagin et al., 2010). Quantification of crawling dynamics of the few remaining adherent neutrophils showed that the anti-ICAM-1 mAb significantly reduced crawling speed and discontinuous crawling was more frequent, similar to that seen after anti-ICAM-2 mAb treatment. Interestingly the reduction in crawling speed after anti-ICAM-1 mAb was significantly more than that detected after anti-ICAM-2 mAb, suggesting that these proteins do not have fully redundant or overlapping roles within this system. It is also possible that the anti-ICAM-1 mAb has a higher binding affinity than that of anti-ICAM-2 mAb and hence resulting in an increased reduction in speed. It should be noted however that the crawling speed detected after anti-ICAM-2 mAb is similar that that detected in the ICAM-2 KOs. Determining the neutrophil crawling dynamics in ICAM-1 KO mice may provide further clarification in regards to this.

The results presented regarding ICAM-1 and ICAM-2, are in contrast to various studies which have reported a co-operative role for ICAM-1 and 2 in the recruitment of leukocytes (Reiss et al. 1998; Reiss and Engelhardt 1999; Lehmann et al. 2003; Steiner et al. 2010; Boscacci et al. 2010 Issekutz et al., 1999). In one particular study when ICAM-1 function was impaired, ICAM-2 was shown to compensate, at least partially, for its absence with respect to T lymphocyte adhesion (Boscacci et al. 2010), however in other models compensation was not evident and a more co-operative role for ICAM-1 and ICAM-2 was seen (Steiner et al. 2010). The compensatory and co-operative roles seem to be largely apparent in the recruitment and homing of T lymphocytes and there is data to suggest that this occurs via LFA-1 interaction (Reiss and Engelhardt, 1999). Studies by Issekutz et al (1999) showed an additive effect on the reduction of neutrophil extravasation when ICAM-1 and ICAM-2 were both blocked, however in contrast to the current study they found no effect on neutrophil extravasation when ICAM-2 alone was inhibited. The occurrence of compensation or co-operation therefore seems to be variable, depending strongly on the subtype of leukocyte being investigated and in the experimental model used. The regulation of ICAM-2 is also dependent on the species

investigated (Cowan et al., 2003) and any inconsistencies seen between models using HUVECs with that of the current murine studies could be due to this reason. The low number of crawling neutrophils per venule analysed could also affect the results obtained (e.g. post-administration of anti-ICAM-1 mAb). The results do however indicate that in the current model, ICAM-1 and ICAM-2 have distinct roles in mediating neutrophil adhesion and have some overlapping functions with respect to neutrophil crawling although the latter process is likely to be governed by different mechanisms.

Anti-MAC-1 blocking mAb elicited a partial reduction in IL-1β mediated adhesion, and this is likely to be a MAC-1/ICAM-1 mediated effect (Smith et al., 1989; Sumagin et al., 2010). This inhibition was not as severe as that seen in the presence of anti-ICAM-1 mAb, and the incomplete inhibition of neutrophil adhesion after anti-MAC-1 mAb administration suggests that ICAM-1/LFA-1 interactions are involved in the initial adhesion of neutrophils in this model (Phillipson et al., 2006; Smith et al., 1989; Sumagin et al., 2010). Previously published findings from TNF-α or MIP-1α stimulated vessels have also found that LFA-1 supports neutrophil adhesion, while in contrast to the current study, a lack of functional MAC-1 had little effect on numbers of adherent cells (Phillipson et al., 2006; Sumagin et al., 2010). The reason for these differences could be a result of the combination of using a different inflammatory stimuli and/or different imaging system. Additionally as mentioned earlier it is also possible that the efficacy of anti-ICAM-1 mAb is higher than that of anti-MAC-1 mAb hence resulting in an incomparable reduction in the number intravascular leukocytes.

After MAC-1 blockade a significant reduction in crawling speed and continuity was noted, which was comparable to that seen when functional ICAM-2 was impaired. There was however no cumulative effect on these parameters when MAC-1 and ICAM-2 were both inhibited simultaneously. This lack of additional effect indicates that ICAM-2 and MAC-1 may be binding partners, and that this interaction supports

efficient leukocyte crawling, which cannot take place without the initial strong adhesive bonds between ICAM-1/LFA-1. As there were low numbers of adherent neutrophils seen after anti-ICAM-1 mAbs treatment, dual inhibition of ICAM-1 and MAC-1 functions to demonstrate ICAM-1 independent roles of MAC-1 was not possible. The effects seen in neutrophil crawling dynamics after anti-MAC-1 mAb therefore does not directly or completely rule out the possibility of MAC-1/ICAM-1 interactions. The lack of additive effects after impairing MAC-1 and ICAM-2 functions does however indirectly indicate that ICAM-2 may potentially be interacting with MAC-1. An interaction of MAC-1 with other known ligands such as fibrinogen, fibronectin, Factor X or other RGD-containing proteins are highly unlikely in this context (Issekutz et al., 1999).

The intracellular mechanism by which MAC-1/ICAM-2 ligation may promote neutrophil motility is currently unclear. MAC-1 is homogenously expressed on the cell surface and its activity is more pronounced at the leading edge of the cell (Hidalgo et al., 2009), suggesting a role in mediating dynamic adhesions and de-adhesions between leukocytes and ECs during leukocyte crawling. Changes in integrin conformation have been linked to inside-out signalling via linkage proteins such as talin, which provide communication between the cell membrane and the cytoskeleton. These events together with that of outside-in integrin signalling are tightly regulated through Rac and Rho signalling pathways as well as through WASP/WAVE, PI3K and Cdc42 which are implicated downstream of integrin activation during crawling (Ridley, 2003). It is therefore possible that these pathways could be impaired when ICAM-2 function is blocked hence resulting in inefficient crawling. It is important to note that the mechanism proposed here is that of ICAM-2 interacting with MAC-1 during neutrophil crawling only. Due to the low frequency of observable TEM events after MAC-1 treatment, no comment can be made regarding the role of MAC-1/ICAM-2 interactions in the initiation of TEM.

ICAM-2 is also expressed on neutrophils (Chapter 3) and the possibility that ICAM-2 expressed on neutrophils could be contributing to the effects reported in the current

study has not been fully disproved although it does seem unlikely. Neutrophillic ICAM-2 has recently been linked to stabilisation of neutrophil rolling through intracellular *trans* interactions with LFA-1 expressed on the same cell (Sundd et al., 2012). No defects in the progression from rolling to adhesion were observed in this model however. The role of EC ICAM-2 (as oppose to neutrophil ICAM-2) as suggested in the current study is supported by previous work within our group which showed that WT bone marrow leukocytes transferred into ICAM-2 KO animals did not restore the observed reduction in IL-1β-stimulated extravasation (Woodfin et al., 2009). Additionally numerous other studies have also demonstrated a key role of EC ICAM-2 in neutrophil (Issekutz et al., 1999), T cell (Boscacci et al., 2010; Lehmann et al., 2003; Steiner et al., 2010) and monocyte (Schenkel et al., 2004) recruitment. Interestingly lymphocytes and monocytes have significantly more cells that express ICAM-2 and at higher levels than that of neutrophils (Chapter 3) and the expression of ICAM-2 on the lymphocytes and monocytes are still considered to have minimal roles in EC-leukocyte interactions. However these studies still cannot rule out the possibility that the effects seen could be due to the impairment of ICAM-2 homophilic interactions. The relatively low ICAM-2 expression on neutrophils strongly indicates that the mechanisms demonstrated here relate to a heterophilic binding and homophillic interactions are highly unlikely.

In conclusion results in the present chapter demonstrate that in the absence of ICAM-2 the expression of ICAM-1 is not altered. This is possibly due to the fact that ICAM-1 and ICAM-2 have distinct roles with respect to neutrophil adhesion however these ICAMs also have some overlapping functions in neutrophil crawling. The role of ICAM-1 in mediating neutrophil crawling speed and continuity is likely to be through a distinct mechanism possibly involving LFA-1. The results also show that the novel role for ICAM-2 in supporting efficient neutrophil luminal crawling could potentially be mediated through the ligation of neutrophil MAC-1. It is not currently known if the defects in speed and continuity of crawling, and the identification or opening of endothelial junctions reflect several distinct roles for ICAM-2. However it is tempting to speculate that crawling is supported by activation

of neutrophil locomotive machinery, while EC junctional opening may be facilitated by signalling within the ECs leading to junctional and/or cytoskeletal rearrangement. Further *in vitro* and *in vivo* investigations are required to shed light on these questions.

CHAPTER 7: Development of a pathological model of inflammation

7.1 Introduction

A key role for ICAM-2 in luminal neutrophil crawling and the initiation of TEM has been demonstrated in this study using an acute inflammatory reaction induced by IL-1β. To extend these findings, it would be of value to investigate the role of ICAM-2 in more complex disease mimicking inflammatory reaction. This chapter describes the development of a pathological cremasteric model of inflammation.

Previous data within our group has shown stimulus-specific functions of ICAM-2 in neutrophil transmigration, in that it mediates responses by IL-1β but not as induced by TNF-α, thioglycolate or LTB_4 (Huang et al., 2006; Woodfin et al., 2009). The stimulus-specific effects of ICAM-2 in these studies have been linked to the ability of the stimulus to predominately activate the ECs directly as in the case for IL-1β (Woodfin et al., 2009). These results however question the importance of ICAM-2 in pathological inflammatory reactions where several mediators are involved simultaneously and thus may bypass the need for ICAM-2 in leukocyte recruitment. There have been numerous pathologically relevant studies which do however provide evidence for a role of ICAM-2 in leukocyte recruitment. These include a cremasteric model of I/R injury (unpublished work by Woodfin et al), a bacterial induced murine model of ocular inflammation (Hobden, 2003), and a murine model of allergic airway inflammation (Gerwin et al., 1999). Despite the above there exist very few studies that have investigated the role of ICAM-2 in neutrophil extravasation in inflammatory disease models and therefore a more pathologically relevant reaction in the confocal IVM model was established as part of this work. This reaction could be used for investigating the role of ICAM-2 and indeed other components of the neutrophil adhesion cascade.

The Shwartzman reaction (SR) is a phenomena named after Gregory Shwartzman in the 1920s. It is a process which describes the body's reaction to particular toxic reagents and has been likened to, and claimed to manifest in, various clinical disorders such as septicaemia, acute pancreatitis and hypersensitivity reactions (Hjort and Rapaport, 1965). Classically it is elicited experimentally via two LPS doses 24 hours apart, however other reagents such as TNF-α and zymozan have also shown to induce similar characteristics and hence have been termed to stimulate a 'Shwartzman-like reaction' (Movat et al., 1987). A general SR is classed as a response affecting the circulation and is evoked by two i.v. injections which represents a model of sepsis. A local SR is induced when the initial injection is administered into specific areas and is then followed by an i.v. injection (or vice versa), or alternatively can be stimulated by two local injections (Brozna, 1990). Local SR is commonly known to represent a model of vasculitis. The first administration is usually a low dose which prepares the site for a reaction through up-regulating various inflammatory mediators. 24 hours later a higher dose is injected which then provokes the reaction (Brozna, 1990). The prepared site undergoes hemorrhagic necrosis which is fully developed within 24 hours of the provoking injection. Key vascular responses noted in the SR include leukocyte transmigration peaking at 2 hours (Brozna, 1990), thrombosis of capillaries and veins with thrombi consisting of platelets, leukocytes and fibrin, and haemorrhage.

SR is predominately stimulated in dermal models (Argenbright & Barton, 1992; Brozna, 1990; Pepys MB, 1982) and to date this reaction has not been established and investigated in the mouse cremaster muscle by IVM, a technique that provides detailed insight into the dynamics of vascular processes such as leukocyte recruitment, thrombosis, hemodynamics, vascular tone and oedema in real time, *in vivo*. Interestingly ICAM-2 is expressed on vascular ECs (de Fougerolles et al., 1991), neutrophils (Sundd et al., 2012) and platelets (Diacovo et al., 1994; Kuijper et al., 1998), all of which may play a significant role in vascular processes that occur during a SR. The cremasteric SR model may therefore provide a valuable tool to gain additional insights into the role of ICAM-2 not only in the dynamics of leukocyte

extravasation (i.e. neutrophil crawling and initiation of TEM in pathological inflammation), but also other vascular processes such as the formation of thrombus and haemorrhage in real time.

This chapter describes a series of studies aimed at the development of a cremasteric SR model. Although due to lack of time the model was not used for investigations into the functional role of ICAM-2, the findings indicate its potential value for such future experiments.

7.2 Results

7.2.1 Leukocyte responses in the cremasteric Shwartzman Reaction model

A classical local SR was elicited in the cremaster muscle by two LPS injections 24 hours apart. The initial injection was administered i.s. followed 24 hours later by an i.v. dose. 2 hours after the i.v. injection the cremaster muscle was exteriorised and analysed by brightfield IVM (Figure 7.1A). Tissues stimulated with this SR protocol showed no significant difference in leukocyte adhesion in comparison to controls (27.5 ± 4.3 leukocytes, n=5 mice for SR tissues and 21.1 ± 3.4 leukocytes, n=7 mice for controls) (Figure 7.1). The reason for this is currently unclear but as the control tissues (two saline injections) had a high numbers of adherent leukocytes it is possible that the initial i.s. injection of saline 24 hours prior to quantification may have induced a leukocyte response. Nevertheless SR stimulation did induce a response above that of controls with respect to the number of leukocytes in the extravascular tissue (22.1 ± 3.4 leukocytes, n=5 for SR tissues and 10.1 ± 2.2 leukocytes, n=7) (Figure 7.1B).

Live confocal IVM using Lys-eGFP-ki mice, which express eGFP in neutrophils and monocytes, and CX3CR1-eGFP-ki mice which express eGFP in monocytes and dendritic cells (Jung et al., 2000), confirmed that the SR elicited in the cremaster muscle stimulated a neutrophil mediated response as the Lys-eGFP-ki mice had significantly higher number of eGFP positive cells in the intravascular and extravascular tissue, in comparison to CX3CR1-eGFP mice (Figure 7.2 and 7.3). A slightly higher number of neutrophils were detected in the intravascular regions of SR-stimulated tissues using this method compared to that noted with brightfield IVM, possibly due to the greater resolution of the confocal method. This resulted in a significant increase in this parameter in SR tissues compared to controls (Figure 7.2 and 7.3). After SR stimulation a higher number of neutrophils migrated to the extravascular tissue in comparison to both controls and CX3CR1-eGFP mice and this was in line with previous data (Figure 7.1). Additionally as neutrophils were observed to migrate further into the extravascular tissue, the number of transmigrated neutrophils 50-100μm away from the vessel was also quantified. This data also showed a high number of neutrophils within the extravascular tissue in comparison to both controls and CX3CR1-eGFP mice (Figure 7.2 and 7.3). Overall the high number of neutrophil infiltration in SR-stimulated cremaster muscles was in line with previous dermal models.

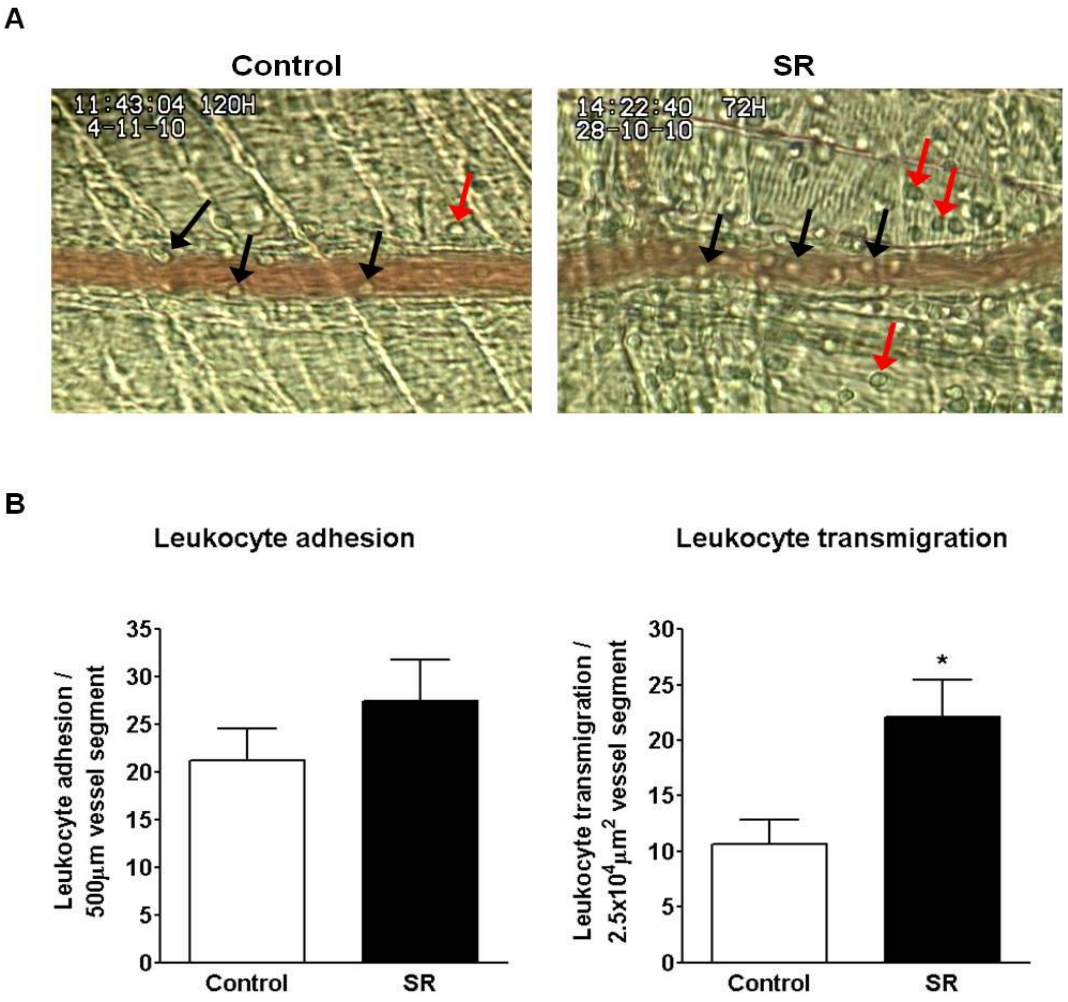

Figure 7.1: SR-induced leukocyte recruitment in cremasteric post-capillary venules.

(**A**) Representative brightfield images of leukocytes responses in control and SR (30µg LPS i.s. 24 hours later 150µg LPS i.v.) -stimulated venules. Leukocyte adhesion and transmigration was quantified 2 hours later using brightfield IVM. Black arrows show adherent leukocytes and red arrows show leukocytes in the extravascular region. (**B**) Adherent leukocytes per 500µm vessel segment (left panel) and transmigrated leukocytes in the perivascular tissue $2.5x10^4\mu m^2$ segment were quantified (right panel) in SR and control tissues. N = 5-7 vessels per cremaster, 5-8 mice per group, error bars show SEM. Statistically significant (T-test) differences are indicated by asterisks, *P<0.05.

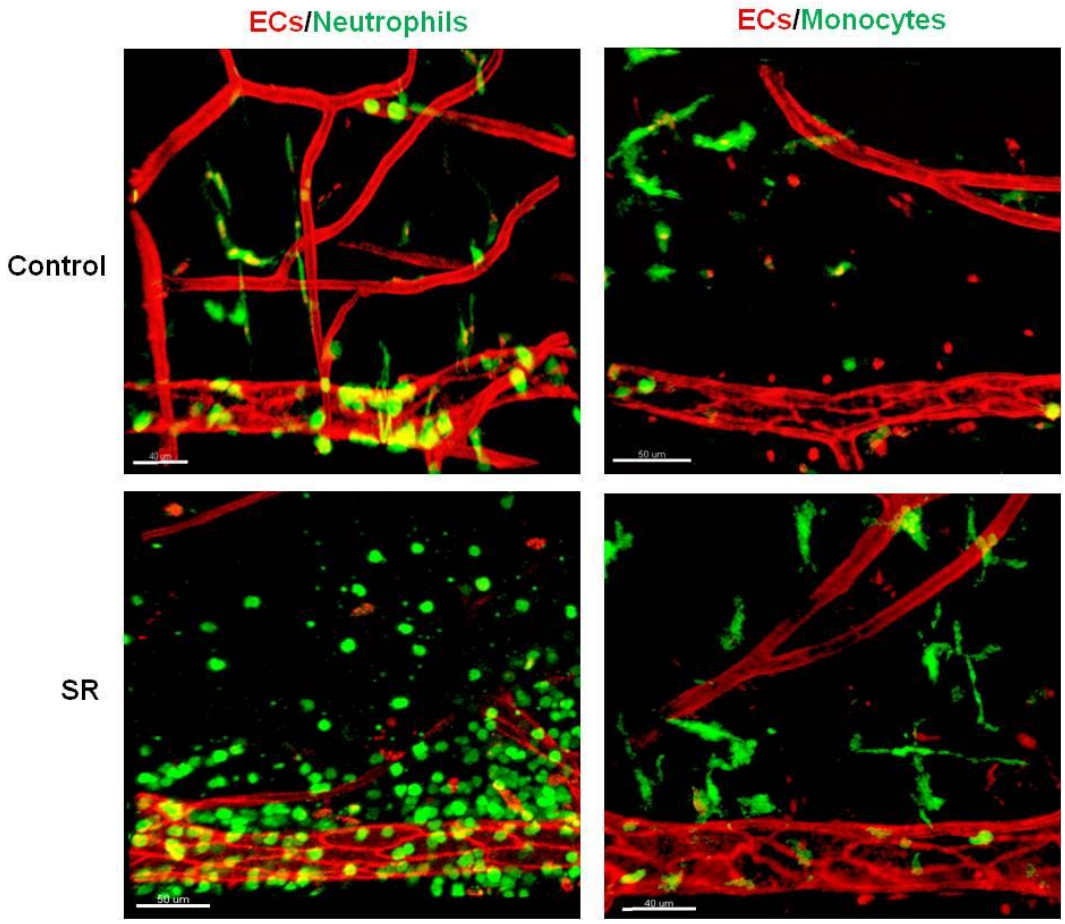

Figure 7.2: Confocal images of SR-induced neutrophil and monocyte recruitment in cremasteric post-capillary venules.

Representative images of leukocytes responses in control and SR (30µg LPS i.s. 24 hours later 150µg LPS i.v.) -stimulated venules from Lys-eGFP-ki mice (neutrophils shown in green, left panels) and CX3CR1-eGFP-ki (monocytes shown in green, right panels). PECAM-1 (red) was labelled *in vivo* as a marker for venules. Scale bar represents 40-50µm**.**

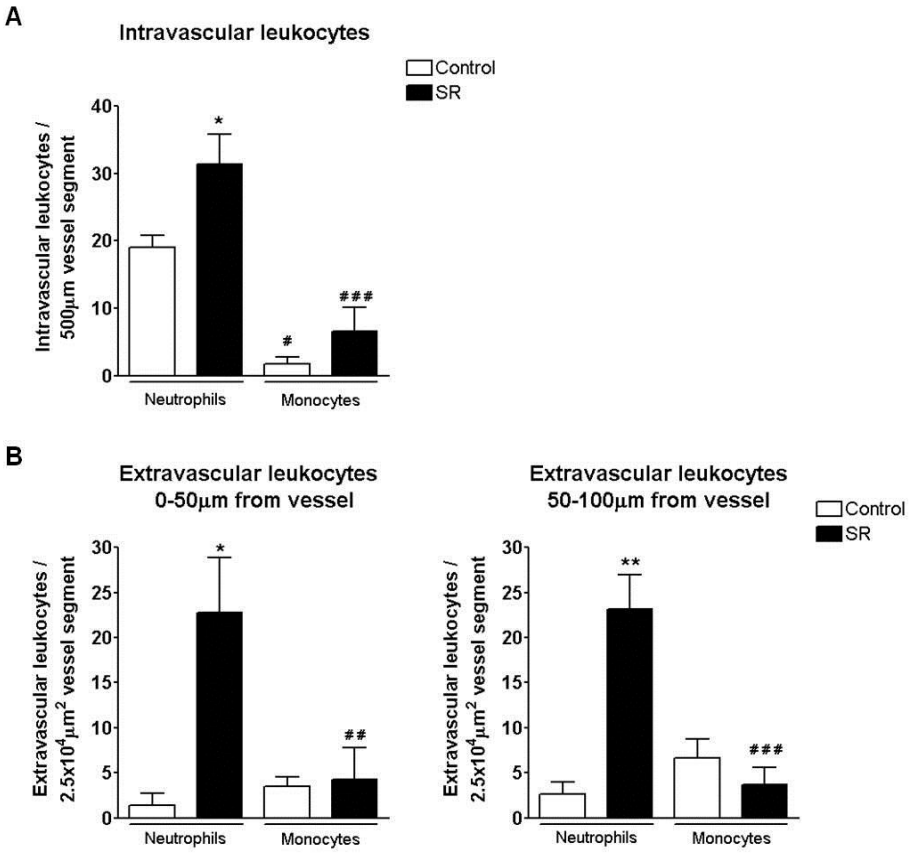

Figure 7.3: SR-induced neutrophil and monocytes recruitment in cremasteric post-capillary venules.

A SR was induced and vessels were labelled as previously described in Lys-eGFP-ki mice (GFP neutrophils and monocytes) and CX3CR1-eGFP-ki (GFP monocytes) mice. Tissues were viewed under a confocal microscope where live images of venules 20-40µm in diameter was taken and analysed in 3D using Imaris software. (**A**) Quantification of intravascular leukocytes in a 500µm vessel segment and (**B**) extravascular leukocytes in a $2.5x10^4\mu m^2$ segment 0-50µm and 50-100µm away from the vessel was quantified in both mouse strains in control or SR-stimulated tissues. N = 3-5 vessels per mice, 3-7 mice per group, error bars show SEM. Statistically significant (Anova) differences between control and SR-stimulated tissues are indicated by asterisks (*P<0.05, **P<0.01). Differences between neutrophil and monocyte groups are indicated by hash symbols (#P < 0.05, ##P < 0.01, ###P < 0.001).

7.2.2 Hemodynamic responses in the cremasteric Shwartzman Reaction model

Current dermal models of the SR are known to produce sites of haemorrhage and microthrombi, and these characteristics were examined in the current cremasteric SR model. In brightfield experiments a reduction in vascular perfusion and sites corresponding to the formation of microthrombi and haemorrhage were observed in SR tissues (Figure 7.4) and some of these events were further quantified using immunostaining and confocal IVM.

To quantitatively determine if there was any evidence of microthrombi and/or platelet-EC interactions in this model, platelets were fluorescently labelled using anti-CD41-PE mAb. Live confocal microscopy analysis of SR-stimulated tissues were carried out and the abundance of labelled platelets was examined. SR-stimulated tissues had higher ratio of anti-CD41-PE to AlexaFluor-647 conjugated anti-CD31 fluorescent intensity, indicating that more platelets interacting with the ECs were detected in comparison to control tissues (Figure 7.5). This may not reflect microthrombi or platelet-EC interaction completely as slower blood flow was also observed in SR-induced tissues which would make labelled platelets more visible. In conclusion, further investigations are required to establish whether SR-induced in the cremaster muscle stimulates microthrombi and/or platelet-EC interactions.

Having directly visualised SR-induced tissues in real time, there appeared to be a distinct decrease in the number of perfused vessels (Figure 7.4). These findings were extended by fluorescently labelling perfused vessels with dextran-FITC and analysing tissues using live confocal microscopy. SR-induced tissues showed a trend towards lower ratio of dextran-FITC to AlexaFluor-647 conjugated anti-CD31 fluorescent intensity in comparison to control tissues (Figure 7.6). Future studies are however required to explore the loss of vascular perfusion post-induction of SR in terms of magnitude.

Taken together, the established model of the SR in the cremaster muscle is characterised by neutrophil extravasation, a possible increase in platelet-EC interaction and a trend towards reduced vascular perfusion. Further work is required to fully characterise and quantify these vascular responses.

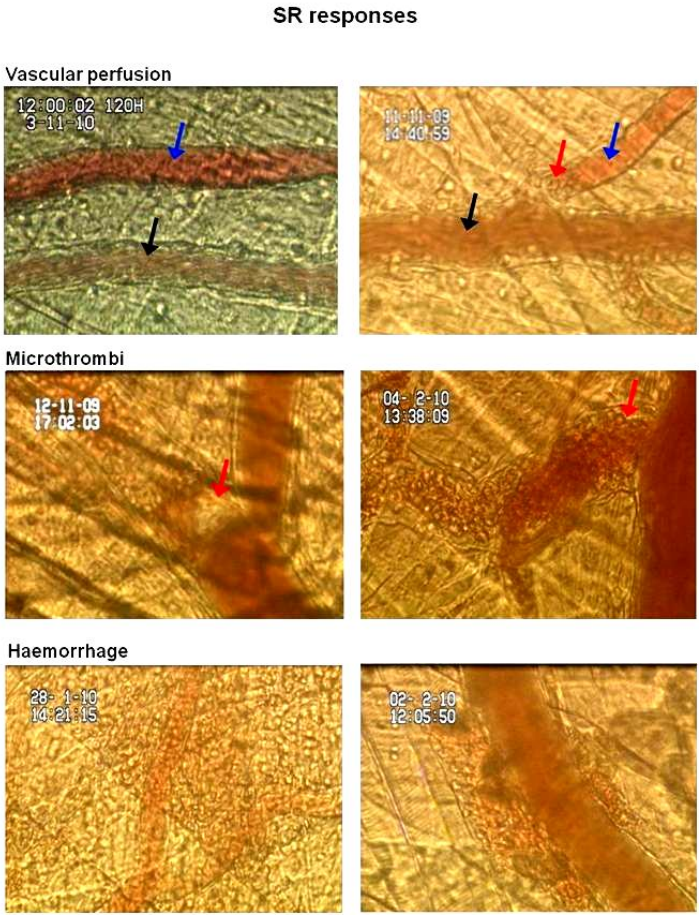

Figure 7.4: Brightfield images of SR-induced vascular responses in cremasteric post-capillary venules.

Representative images of vascular perfusion, microthrombi and haemorrhage in the cremaster muscle SR (30µg LPS (i.s.) 24 hours later 150µg LPS (i.v.)). Black arrows show perfused vessels, blue arrows show non-perfused vessels and red arrows show microthrombi.

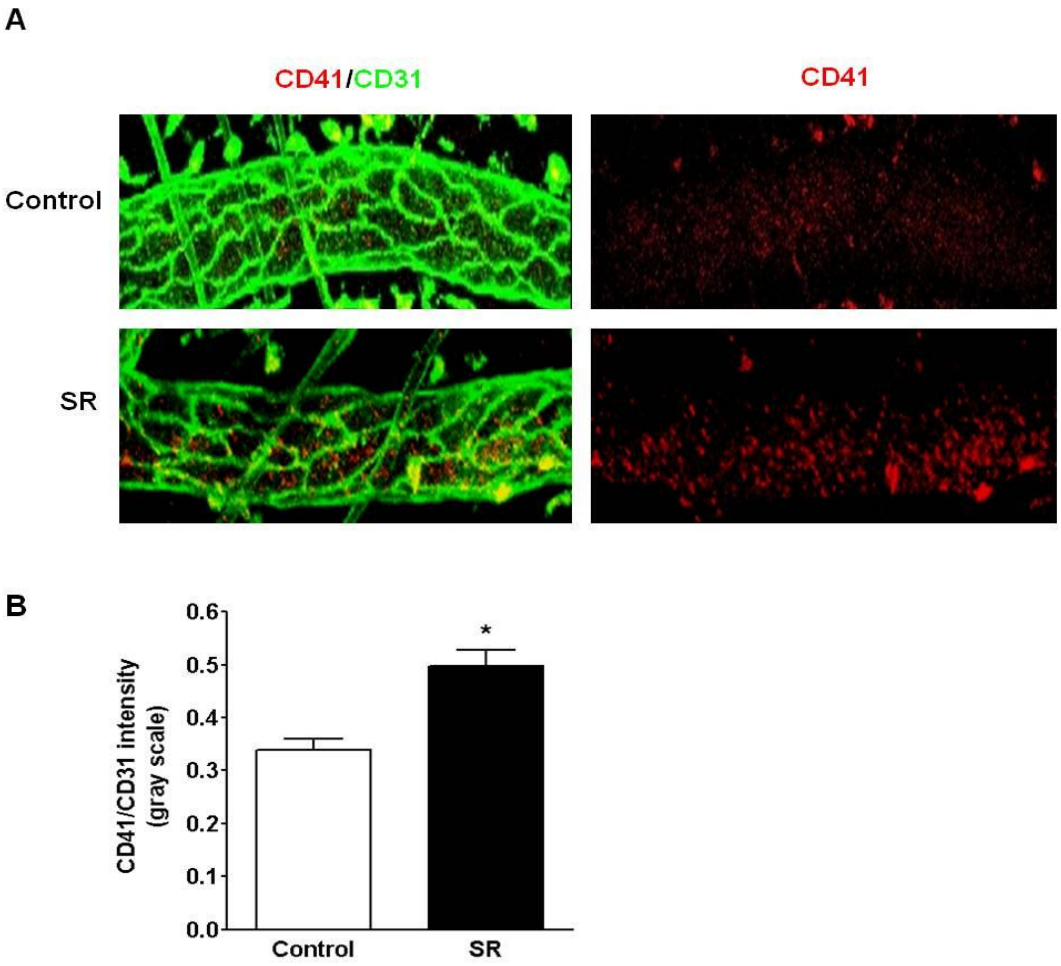

Figure 7.5: SR-induced platelet-endothelial interaction in cremasteric post-capillary venules.

A SR was induced in the cremaster muscle and vessels were labelled (PECAM-1, green) *in vivo* as previously described (Chapter 2). Platelets were labelled using anti-CD41-PE i.v. (red) and the cremaster muscle was viewed under a confocal microscope where live images of venules were taken. (**A**) Representative confocal images of venules from control and SR-stimulated tissues where platelets and endothelial cell interactions can be seen. (**B**) Anti-CD41-PE to AlexaFluor-647 conjugated anti-PECAM-1 ratio intensity in control and SR-induced tissues was analysed using Leica LAS AF Lite (2.1.1 build) software. N = 3-4 mice, 4-8 vessels per cremaster, error bars show SEM. Statistically significant (T-test) differences are indicated by asterisks, *P<0.05.

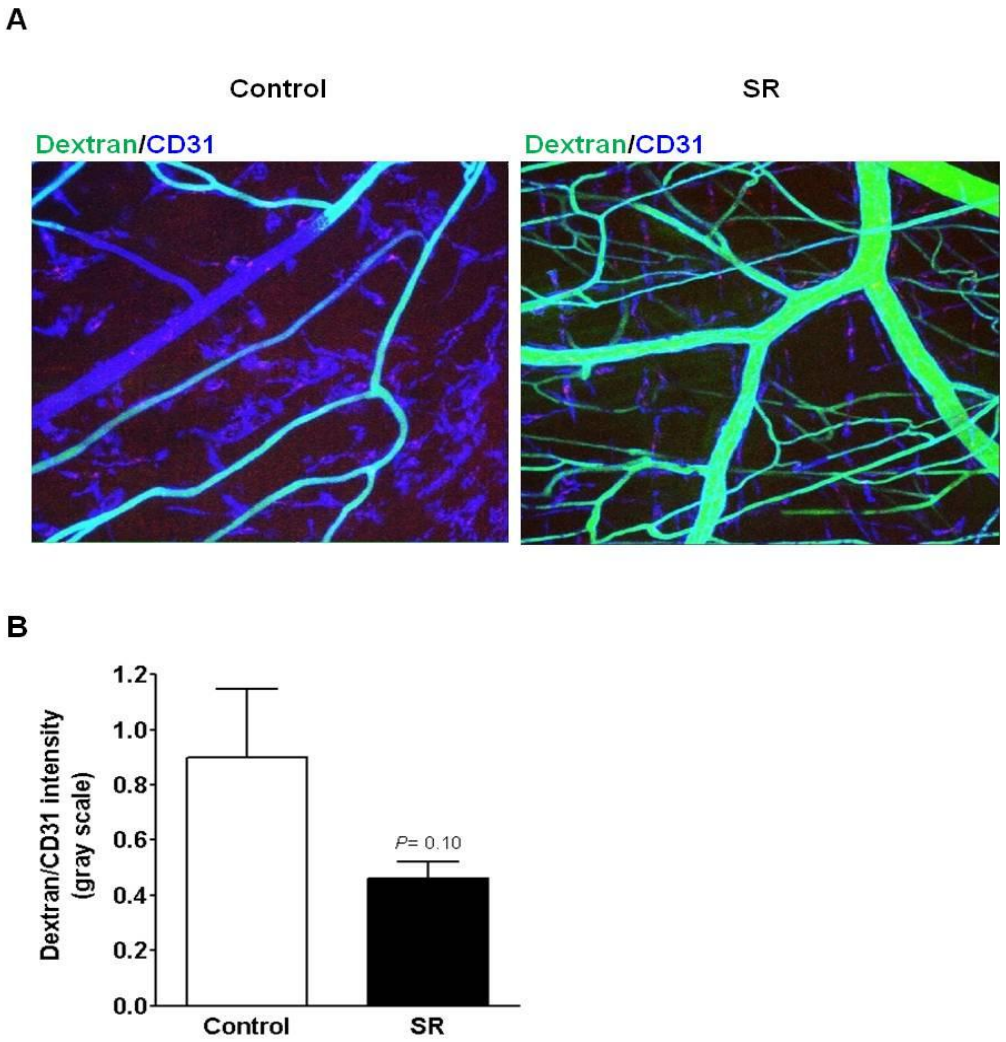

Figure 7.6: Vascular perfusion in SR-stimulated post-capillary venules.

A SR was induced and vessels were labelled (PECAM-1, blue) *in vivo* as previously described (Chapter 2). Perfused vessels were labelled using FITC-dextran (green) and the cremaster muscle was viewed under a confocal microscope where live images of venules were taken. (**A**) Representative confocal images of specific regions from control and SR-stimulated tissues where perfused vessels (green and blue) and all vessels (blue) can be seen. Scale bar represents 50µm. (**B**) FITC-dextran to AlexaFluor-647 conjugated anti-anti-PECAM-1 ratio intensity in control and SR-induced tissues was analysed using Leica LAS AF Lite (2.1.1 build) software. N = 3-4 mice, 5 regions per cremaster, error bars show SEM.

7.3 Discussion

In this chapter a cremasteric SR IVM model was developed that could be used for investigations into the functional role of ICAM-2 and other adhesion molecules in a vascular injury model of inflammation. The SR was selected due to the hemorrhagic and microthrombotic characteristics that occur in conjunction with leukocyte recruitment and hence represents features often noted in severe pathological inflammatory scenarios. As the SR is predominately stimulated in dermal models (Argenbright and Barton, 1992; Brozna, 1990; Pepys MB, 1982) and had not previously been studied in the cremasteric model of IVM, the latter was established as a technique that could provide detailed insights into numerous vascular responses in real time *in vivo*.

For the present project a classical SR-stimulated by an initial local LPS dose (i.s.) followed by an i.v. dose 24 hours after was used. The results demonstrated that a SR-stimulated in the cremaster muscle resulted in neutrophil extravasation, low frequency of haemorrhage and a possible increase in platelet-EC interactions. Current literature suggests that these vascular processes occur in the SR due to the first dose of LPS priming the EC by up-regulating various inflammatory mediators (e.g. IL-1β and TNF-α) and adhesion molecules (e.g. E-selectin and ICAM-1) (Brozna, 1990). The second dose of LPS primarily induces a thrombohemorrhagic response (Brozna, 1990). SR-stimulated in the cremaster muscle did not completely reflect responses as observed in dermal models in terms of the severity of thrombus and haemorrhage formation, however leukocyte extravasation was clearly evident.

A high number of neutrophils were found in the intra and extravascular tissue of SR-stimulated cremaster muscles although no differences in the number of adherent leukocytes was detected by brightfield IVM. The reason for the lack of difference in neutrophil adhesion between control and SR tissues in this model is currently

unknown however using confocal IVM a significant increase in intravascular and extravascular neutrophils was seen. This could be due to the fact that confocal IVM enables analysis of tissue sections deeper within the muscle therefore a more complete representation of the recruitment of leukocytes in that vessel can be acquired. It is also likely that as the leukocytes were fluorescently tagged in confocal IVM experiments they were seen with greater clarity and hence higher numbers of intravascular neutrophils could be quantified.

As the SR is known to incorporate thrombosis, platelets were also fluorescently labelled using anti-CD41-PE mAb, in order to analyse EC-platelet interactions in this model. A high fluorescent intensity of anti-CD41-PE mAb was detected in SR tissues implying that there could be an increase in platelet-EC interactions. In the present study the blood velocity of SR-induced tissues also appeared to be reduced, and this would have influenced the high fluorescent intensity of anti-CD41-PE mAb detected. Therefore no conclusions on this parameter in the cremasteric SR model can be made using the current data. Interestingly the reduction in blood pressure is a characteristic of sepsis and as LPS was administered i.v. this could have led to various systemic effects which were not analysed in these experiments. Local vascular perfusion was however analysed and the results indicated that the SR-induced a trend towards reduced vascular perfusion. It is also possible that the local systemic effects observed could be a result of leukocyte plugs and/or EC-platelet interactions.

The characteristics displayed in the cremasteric SR model is in agreement with numerous literature reports using dermal models of the SR although dermal models have shown a much higher frequency of microthrombi and haemorrhage formation (Brozna, 1990; Pepys MB, 1982). The differences between cremasteric and dermal models could be due to the reactivity of the two tissues to local inflammatory mediators, in line with their different physiological roles. The cremaster muscle is located deep within the body relative to that of the skin vasculature and is therefore less susceptible to thrombus and haemorrhage formation in response to local trauma

in comparison to the dermis. The skin is a tissue on the outer surface and acts as a protective barrier and hence maybe more sensitive to locally applied stimuli making it more prone to thrombus and haemorrhage formation. In contrast the cremaster muscles primary function is to regulate the temperature of the testis and it may therefore not be highly responsive to locally applied LPS.

In summary a SR-stimulated in the cremaster muscle produced neutrophil transmigration, low frequency of haemorrhage formation, a possible increase in EC-platelet interactions and reduced vascular perfusion. Further studies are however required to fully characterise these parameters and this response in more detail before extending it to investigations of the functional roles of molecules such as ICAM-2.

CHAPTER 8: General discussion

8.1 Project overview

The recruitment of leukocytes from the circulation to the site of inflammation is crucial for physiological and pathological processes involving the innate and adaptive immune system. Although a lot of progress has been made in identifying the molecular mechanisms involved during leukocyte extravasation there are still many unanswered questions particularly with respect to specific functions of individual adhesion molecules. This study aimed to investigate the role of the largely neglected adhesion molecule ICAM-2 at specific stages of the leukocyte transmigration cascade. In order to address this, the expression profile, functional role and the possible ligand interactions of ICAM-2 were examined in an acute IL-1β-induced inflammatory model. To extend these findings to a more complex pathological scenario, a cremasteric SR was also developed as part of this project.

Using immunostaining and confocal microscopy of the mouse cremasteric vasculature, the expression profile of EC ICAM-2 was examined under basal and IL-1β-stimulated conditions. Detailed analysis of the distribution of EC ICAM-2 expression within post-capillary venules showed that this molecule is expressed at non-junctional regions of ECs in addition to junctional sites, under both basal and IL-1β-stimulated conditions. As a result of this finding it was hypothesised that ICAM-2 could be involved in luminal neutrophil-EC interactions post-adhesion, in addition to TEM, and these possible roles of ICAM-2 were investigated.

Using the cremasteric confocal IVM model neutrophil-EC interactions were examined in IL-1β-stimulated tissues. A functional blocking mAb to ICAM-2 as well as an ICAM-2 KO mouse strain, which also exhibited Lys-eGFP-ki, were utilised.

The results indicated that neutrophil adhesion was unaffected by the impairment of ICAM-2 function in inflamed tissues, however a reduced number of neutrophils were detected in the extravascular tissue, confirming previous work (Huang et al., 2006; Woodfin et al., 2009). The precise mechanisms by which ICAM-2 mediates extravasation is currently unknown, and the present study focused on investigating the role of ICAM-2-mediated mechanisms at specific stages of the neutrophil transmigration cascade. Detailed analysis of IL-1β-induced neutrophil crawling and TEM dynamics were carried out using confocal IVM. Overall the results indicated a role for ICAM-2 in facilitating efficient neutrophil crawling, as well as supporting the initiation of TEM. The former role, at least in part, was found to be potentially mediated by EC ICAM-2 interacting with neutrophil MAC-1.

This study provides the first direct *in vivo* evidence that ICAM-2 can support neutrophil intraluminal crawling and the initiation of TEM in IL-1β-induced neutrophil extravasation. This discussion gives a critical overview of the functions attributed to ICAM-2 during neutrophil extravasation in the present study, and suggests potential mechanisms that may underlie these roles.

8.2 The distribution of EC ICAM-2 during neutrophil recruitment

Initial experiments focused on examining the expression pattern of ICAM-2 in order to gain further insights into it's functions during neutrophil extravasation. These studies expanded on previous observations that ICAM-2 is heterogeneously distributed on the surface of venular ECs (Woodfin et al., 2009). More specifically ICAM-2 was found to be expressed at both EC non-junctional and junctional areas as shown by immunofluorescent staining and confocal microscopy. This expression pattern was seen in venules of the mouse cremaster muscle as well as venules of the ear dermis, suggesting that the distribution of EC ICAM-2 expression found in the cremaster muscle was not tissue-specific.

The overall venular EC ICAM-2 expression, in terms of total levels, was found to be unaffected by IL-1β-stimulation which is in line with the majority of previous reports (de Fougerolles et al., 1991; Hobden, 2003). Studies using IL-1β-stimulated HUVECs and human mammary arteries have however reported a down regulation in ICAM-2 (McLaughlin et al., 1999; McLaughlin et al., 1998). The differences seen between the findings of the present work and the work of Mc Laughlin and colleagues maybe due to the latter study being carried out with human cells in *in vitro* and *ex vivo* contexts, suggesting possible differences between species and/or influences of the experimental conditions used. The reason why ICAM-2 is down regulated on human and not mouse ECs is currently unknown. Although human ICAM-2 expression in ECs has been linked to the binding of Sp1 and GATA-2 transcription factors (Cowan et al., 1998), there is currently little information with respect to the transcriptional regulation of ICAM-2 in mice. For these reasons further studies are required to understand the regulation of ICAM-2 expression on a transcriptional level in a range of different species.

While the total venular EC expression of ICAM-2 remained unchanged under inflamed conditions, it is possible that ICAM-2 may redistribute within ECs in order to support neutrophil extravasation. For this reason the EC non-junctional and junctional expression of ICAM-2 was determined in control and in IL-1β stimulated conditions. The results however indicated no significant re-distribution of ICAM-2 following IL-1β stimulation. Interestingly a previous study found that on NK cells ICAM-2 was localised at uropods where its function was linked to cytoskeletal redistribution via erzin binding to the C-terminal of ICAM-2 (Helander et al., 1996). The differences in the ability of ICAM-2 to re-distribute on NK cells and not on ECs, is most likely to be a direct consequence of the individual function of ICAM-2 in the two cell types. It must be noted that other stimuli or processes such as angiogenesis, which ICAM-2 has been linked to, may induce redistribution.

ICAM-2 is known to have a role in neutrophil extravasation into the tissue but no roles in earlier stages of adhesion have been described, similar to that reported for PECAM-1 and JAM-A (Woodfin et al., 2009). The expression pattern of EC ICAM-2 on post-capillary venules was however found to be distinct to these junctional proteins (PECAM-1 and JAM-A) implicated in leukocyte transmigration. Whilst PECAM-1 was found to be highly localised at EC junctions with a faint and diffuse cell-body expression, ICAM-2 was expressed equally at these areas as previously described. The distinct expression of ICAM-2 compared to that of PECAM-1 suggests that these molecules may have different functional roles. It was therefore hypothesised that ICAM-2 may have a role in luminal leukocyte-EC interactions post-adhesion, as well as in TEM during neutrophil recruitment and this hypothesis was examined.

8.3 The role of ICAM-2 in IL-1β-induced neutrophil crawling

The present study confirmed that ICAM-2 supports neutrophil extravasation and not initial adhesion using 4D confocal IVM of IL-1β-stimulated cremaster muscles from WT and ICAM-2 KO mice. The mechanism by which ICAM-2 mediates extravasation was subsequently investigated by analysing luminal neutrophil-EC interactions post-adhesion using the same high resolution imaging system. Using this technique various neutrophil crawling dynamics were analysed. It was found that in ICAM-2 KO mice, neutrophils crawled slower, for longer time periods and in a discontinuous manner, where distinct periods of immobility were seen (Figure 8.1). Discontinuous crawling behaviour was more frequently observed in stimulated ICAM-2 KO mice and further analysis into the dynamics of discontinuous crawling revealed that this behaviour had a slower crawling speed in comparison to continuously crawling cells in both mouse strains. The high frequency of discontinuously crawling cells in ICAM-2 KO mice however only partially accounted for the overall reduction in crawling speed as continuously crawling cells, in this mouse strain, also crawled more slowly (Figure 8.1). This indicates that

ICAM-2 supports both speed and continuity of crawling. Neutrophils crawling dynamics observed in IL-1β-induced tissues from ICAM-2 KO mice were comparable to that observed in stimulated WT mice treated with an anti-ICAM-2 mAb. This confirms the affinity and efficacy of the anti-ICAM-2 mAb used and more importantly discounts the possibility of any compensatory mechanisms occurring in the ICAM-2 KO mice as a result of the genetic deletion of ICAM-2 with respect to neutrophil recruitment. Collectively these results indicate that neutrophil crawling is supported by ICAM-2. This process maybe regulated through its interactions with its neutrophil ligand thus inducing various signalling pathways within the neutrophil which is associated with crawling and polarisation.

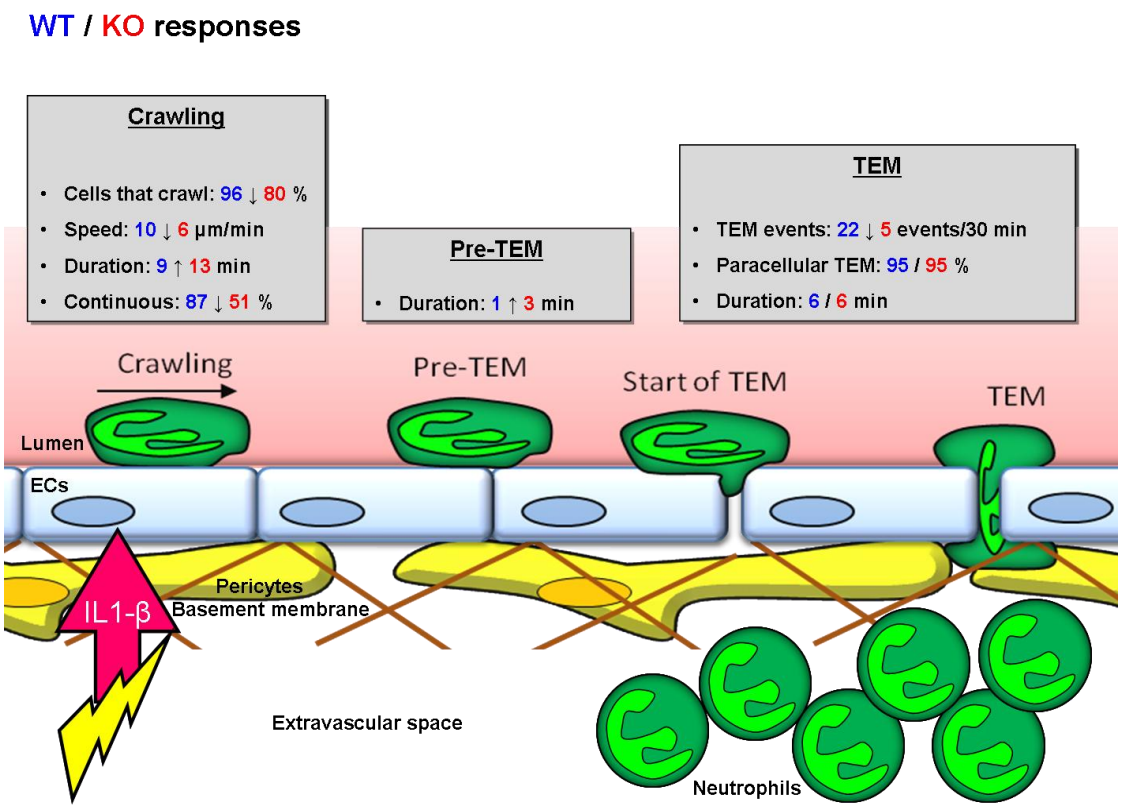

Figure 8.1: IL-1β-induced neutrophil recruitment dynamics in WT and KOs.

A summary diagram depicting neutrophil crawling and TEM dynamics in response to IL1-β in the presence (blue) and absence (red) of ICAM-2 in the mouse cremaster muscles. In ICAM-2 KO mice changes occur in the dynamics of neutrophil recruitment in comparison to WT mice. More specifically in ICAM-2 KOs the efficiency of neutrophil crawling and the initiation of TEM are impaired, leading to a reduction in the number of extravascular neutrophils. Arrows indicate an increase or decrease in each parameter in the KO mice in comparison to WTs.

The neutrophil ligand for EC ICAM-2 during neutrophil crawling was investigated in order to gain some insights into the mechanisms involved. MAC-1 has been shown to interact with ICAM-2 (Xie et al., 1995) and it has also been implicated in neutrophil crawling, but not adhesion (Phillipson et al., 2006; Sumagin et al., 2010). These findings collectively suggest a role for MAC-1/ICAM-2 pathway in neutrophil

crawling. To test this hypothesis a MAC-1 blocking mAb was administered in WT and ICAM-2 KO mice, and the dynamics of neutrophil-EC interactions were examined. If there was no evidence of a *cumulative effect* of deletion/inhibition of ICAM-2 and MAC-1 respectively, then the findings could suggest an interaction between these two proteins. Alternatively a cumulative effect could suggest a MAC-1 function independent of ICAM-2, and hence may indicate a role for MAC-1 interacting with other ligands, possibly ICAM-1. ICAM-1 mediated influences in the current model were also investigated for this reason. Distinct differences between the role of MAC-1 and ICAM-1 in neutrophil adhesion and crawling dynamics were noted suggesting some ICAM-1-independent MAC-1 functions (some of which could be mediated via ICAM-2). Neutrophil crawling dynamics in ICAM-2 KO mice after anti-MAC-1 mAb inhibition were therefore investigated. The results were comparable to that detected in ICAM-2 KO mice without mAb treatment, showing no cumulative effect. The lack of additive effects when both molecules were functionally impaired suggests that these two molecules could potentially be interacting during neutrophil crawling. It should be noted that although this was not directly confirmed, it is possible that this interaction would induce intracellular signalling within neutrophils resulting in polarisation and cytoskeletal contraction required for efficient crawling of neutrophils (Ridley, 2003).

The specific intracellular mechanism by which MAC-1/ICAM-2 ligation may promote neutrophil crawling is currently unclear, however there is a lot of information available regarding the signalling mechanisms downstream of integrins. The interaction of ICAM-2 with MAC-1 is known to occur via the first Ig domain of ICAM-2, located on the extracellular N-terminal (Staunton et al., 1989) with the β subunit on the extracellular N-terminal of MAC-1 (Xie et al., 1995). This could stimulate neutrophil MAC-1 outside-in integrin signalling which is known to cause structural rearrangement of the actin cytoskeleton and cell polarisation (Figure 8.2) (Ridley, 2003). Cell polarisation is required for crawling, and occurs when the front of the cell nearest to the chemokine gradient forms a leading edge, and the opposite side forms a trailing edge. Rapid, transient and adhesive interaction of protrusions to

the EC is followed by de-adhesion (Rottner and Stradal, 2011). The differential distribution of proteins at either end of the cell regulates adhesion. When adhesion occurs at the leading edge de-adhesion occurs at the trailing edge which induces a millipede-like motion facilitating neutrophil crawling (Ridley, 2003; Rohlena, 2009; Rottner and Stradal, 2011).

MAC-1 is known to be homogenously expressed on the cell surface, and its activity is more pronounced at the leading edge of the cell (Hidalgo et al., 2009), and could have a role in mediating dynamic adhesions and de-adhesions between neutrophil and ECs during crawling. Integrin conformational changes have been linked to inside-out signalling via proteins such as talin, which provide communication between the cell membrane and the cytoskeleton (Figure 8.2). These events are tightly regulated through Rac and Rho signalling pathways as well as through VAV-1, WASP/WAVE, PI3K and Cdc42 (Ridley, 2003). In ICAM-2 KO mice neutrophils crawled more slowly than neutrophils in WT mice therefore de-adhesion maybe partially impaired, hence reducing the mobility of the neutrophil resulting in slower neutrophil crawling. ICAM-2 induced outside-in MAC-1 signalling within neutrophils may therefore specifically support transient de-adhesion required for efficient crawling.

The possibility of ICAM-2/LFA-1 and/or ICAM-2/ICAM-2 interactions occurring during crawling are not fully discounted, however analysis of ICAM-2 expression on whole mouse blood indicated that this protein is expressed on a small percentage of neutrophils at very low levels. Additionally earlier studies in which WT bone marrow leukocytes were transferred into ICAM-2 KO animals did not restore the observed defect in IL-1β-stimulated extravasation (Woodfin et al., 2009). These facts, coupled with the absence of the CD18 integrins, which are the primary ICAM-2 ligands, on the endothelium, strongly indicate that mechanisms demonstrated here relate to EC expressed ICAM-2. Collectively these findings, along with previously published studies, suggest that in this model both ICAM-1/LFA-1 and ICAM-

1/MAC-1 binding (Phillipson et al., 2006; Smith et al., 1989) supports initial adhesion, while MAC-1 interactions with ICAM-2 contributes to the speed and continuity of luminal crawling. Further studies are required in order to fully conclude that the observed roles for ICAM-2 are mediated largely by MAC-1.

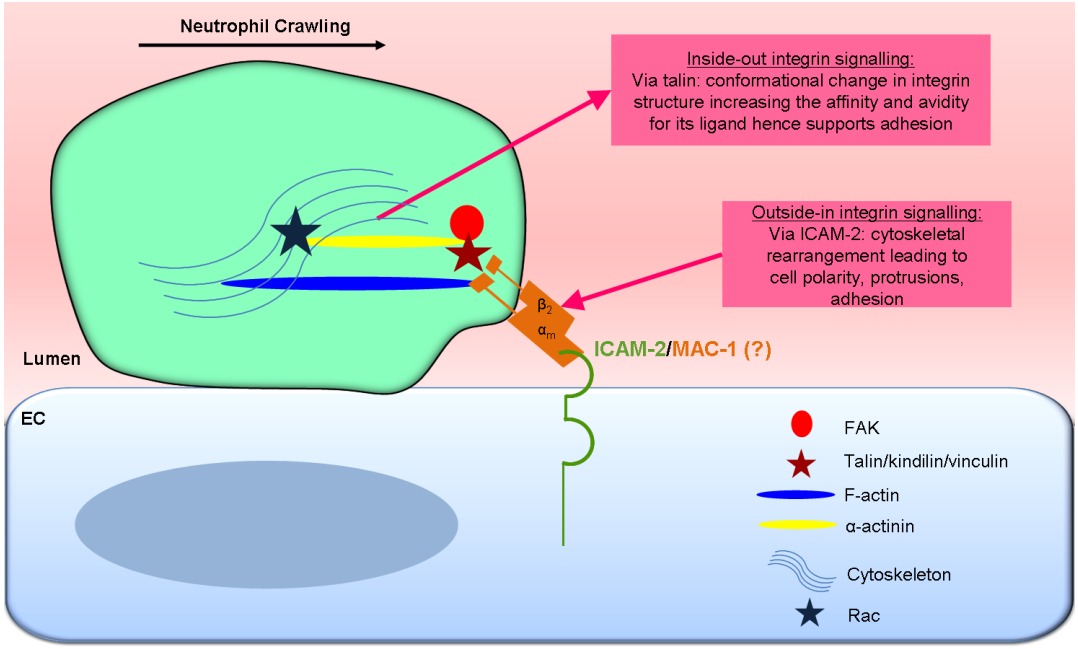

Figure 8.2: Suggested mechanisms associated with EC ICAM-2 during neutrophil crawling.

A summary diagram depicting possible mechanisms for the role of EC ICAM-2 in neutrophil crawling. EC ICAM-2 is suggested to interact with neutrophil MAC-1 during neutrophil crawling. Inside-out MAC-1 signalling induces conformational change in the structure of MAC-1 allowing this protein to interact with ICAM-2 and support neutrophil adhesion. Signalling events within the neutrophil as a result of ICAM-2 ligation to MAC-1 could stimulate outside-in integrin signalling collectively resulting in neutrophil cytoskeletal rearrangement, neutrophil polarity and the formation of protrusions facilitating neutrophil crawling.

8.4 The role of ICAM-2 in IL-1β-induced neutrophil TEM

The periods of immobility during discontinuous crawling were associated with EC junctions, suggesting that these periods may be a result of failed attempts to initiate TEM. The role of ICAM-2 in mediating crawling speed and continuity of crawling may therefore be a result of two distinct mechanisms. For this reason togather with the finding that ICAM-2 is expressed at EC junctions the dynamics of neutrophil TEM was analysed in more detail. Neutrophil TEM through the EC layer was investigated in IL-1β-stimulated WT and ICAM-2 KO mice. The frequency at which TEM was observed to occur was substantially reduced in the ICAM-2 KO mice, and WT mice treated with anti-ICAM-2 mAb, and it is clear that the comparable numbers of adherent and crawling neutrophils were failing to progress to TEM (Figure 8.1). In both these groups TEM primarily followed the paracellular route. The crawling behaviour which preceded TEM was analysed, and in both genotypes the majority of cells which successfully progressed to TEM had previously crawled in a continuous manner (Figure 8.1), suggesting that efficient crawling is necessary for the migration to, and/or identification of, sites permissive for TEM.

The process of TEM was divided into two stages, pre-TEM (neutrophil-EC junctional interactions preceding TEM) and TEM (classified by neutrophil protrusions into EC junctions) for further analysis. In the ICAM-2 KO vessel the few cells which did progress to TEM spent significantly longer time periods migrating within the lumen before reaching the location of TEM. These cells also displayed a fourfold increase in the time spent interacting with the junction before initiating TEM (pre-TEM). These findings are in line with previous data from our group using fixed tissue analysis of inflamed vessels from ICAM-2 KO mice (Woodfin et al., 2009). These studies collectively suggest that ICAM-2 deficiency leads to prolonged/arrested luminal neutrophil junctional interactions and that discontinuous crawling may also represent failed attempts of neutrophils to undergo TEM. These data indicate that in addition to a role in supporting luminal crawling efficiency,

ICAM-2 is also important in the identification of TEM sites and/or the initiation of TEM (opening of the junction) (Figure 8.3).

A striking feature of the analysis of TEM in the absence of functional ICAM-2 was once any disruption of the junction had been achieved the TEM was successfully completed over a normal time frame. It therefore seems that the greatest defect lies in the identification or initial opening of the junctions and that other junctional proteins such as JAM-A, PECAM-1 and JAM-C may support the latter stages of TEM (Dangerfield et al., 2002; Woodfin et al., 2009; Woodfin et al., 2011). No comment can be made in regards to the ligand interaction of EC junctional ICAM-2 during the initiation of TEM in this study as very few events were observed after anti-MAC-1 mAb treatment in comparison to TEM events following anti-ICAM-2 mAb treatment.

ICAM-2 was found to support the migration of neutrophils to specific sites to undergo TEM and/or support the opening of the EC junctions, however the precise mechanism is currently unclear. The existence of locations particularly permissive to neutrophil TEM have previously been suggested to be at EC tricellular junctions (Burns et al., 1997; Sumagin and Sarelius, 2010), ICAM-1 enriched regions (Sumagin and Sarelius, 2010) and determined by chemotactic gradients (Massena et al., 2010). There is little information however, regarding a possible role for ICAM-2 in identifying sites of TEM, and no gradients of ICAM-2 which might act as haptotactic guidance towards junctions have been reported. As TEM occurs at multiple sites even around an individual EC it seems highly unlikely that the inefficient crawling seen in ICAM-2 KO mice resulted in neutrophils being unable to find sites permissive for TEM. It seems more plausible that the biggest defect in stimulated ICAM-2 KO mice was the failed attempts to initiate TEM. This may also be the underlying reason for the high frequency of discontinuously crawling cells observed in the in the ICAM-2 KO mice. More specifically, the periods of immobility displayed during discontinuous crawling could reflect failed attempts to

initiate TEM. This is supported by the fact that the periods of immobility were associated to occur directly on EC junctions. Additionally crawling cells which were observed to undergo TEM were found to crawl in a continuous fashion confirming that discontinuous crawling is less able to support TEM in this reaction, at this time point. The impaired ability to initiate TEM in the KOs could be a result of the lack of strong adhesive interactions with the EC junctions in the ICAM-2 KOs however further studies are required to fully understand this process in more depth.

Interestingly, the C-terminal of ICAM-2 links to the cytoskeleton via α-actinin and ezrin/radixin/moesin proteins (Heiska et al., 1996; Heiska et al., 1998; Helander et al., 1996; Yonemura et al., 1998), so it is possible that ligation of ICAM-2 at junctional regions initiates signalling pathways which facilitate opening of the EC junctions, similar to that seen with ICAM-1 clustering, VE-PTP activation and VE-cadherin disengagement (Figure 8.3) (Alcaide et al., 2009). ICAM-2 has also been shown to mediate downstream Rac signalling which is known to regulate the phosphorylation status of VE-cadherin and thus cause EC-EC junctional disruption (Figure 8.3). A lack of neutrophil protrusions into the EC was also observed in ICAM-2 KO mice and therefore the impairment of ICAM-2/integrin interaction may also cause defects in the formation of protrusion within the neutrophil into the EC junction which occurs during TEM through outside-in integrin signalling (Figure 8.3). Alternatively ICAM-2 may play a role in the formation of docking structures within the EC layer which has been observed, primarily *in vitro*, to form at the site of TEM (Barreiro et al., 2002; Carman and Springer, 2004; Phillipson et al., 2008). Other molecules such as ICAM-1 and VCAM-1 have also been previously demonstrated to have key roles in supporting TEM at preferred sites via the formation of docking structures and could also be involved in opening EC junctions together with numerous other molecules (Barreiro et al., 2002) in conjunction with ICAM-2.

Collectively the current study demonstrates that ICAM-2 is directly involved in neutrophil crawling and the initiation of TEM *in vivo*. It is likely that these roles represent two distinct mechanisms associated with EC ICAM-2 binding to its neutrophil ligand. Firstly, efficient neutrophil crawling may potentially be mediated by neutrophil MAC-1, and hence induce outside-in MAC-1 signalling within the neutrophil to support crawling. Secondly EC ICAM-2 signalling may strengthen neutrophil-EC junctional interactions and/or activate EC signalling pathways to open junctions and hence initiate EC junctional pore formation. Together this provides further insights into the role of ICAM-2 in neutrophil extravasation during IL-1β-stimulated inflammation.

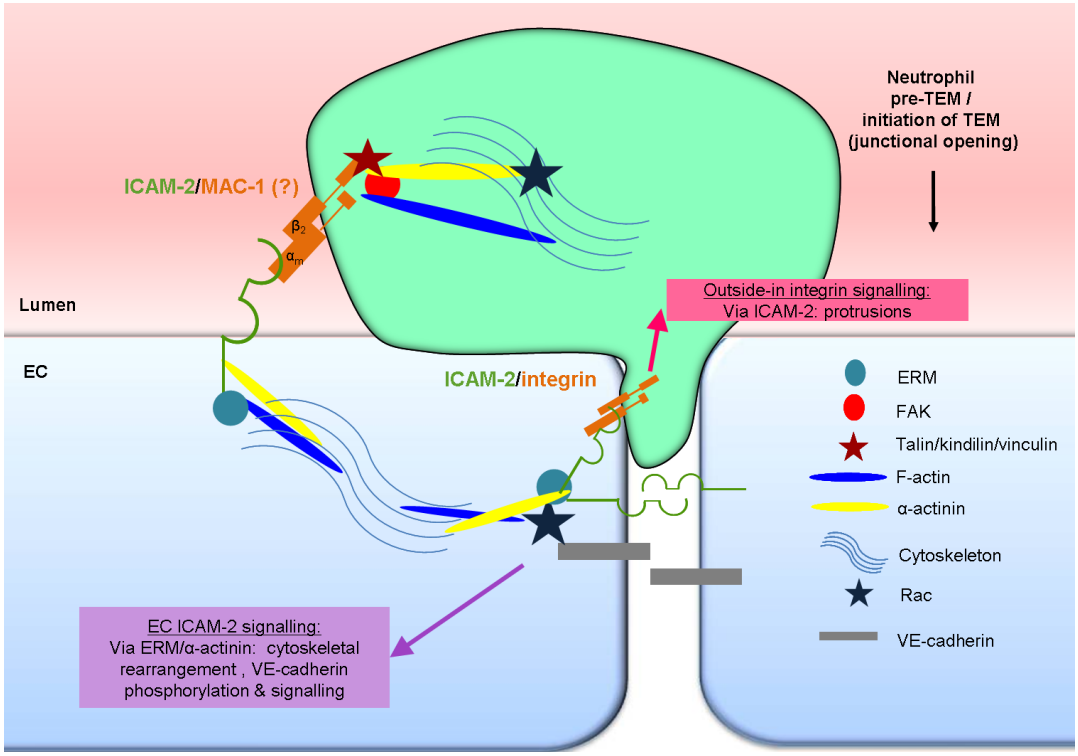

Figure 8.3: Suggested mechanisms associated with EC ICAM-2 during neutrophil TEM.

A summary diagram depicting possible mechanisms for the role of EC ICAM-2 in the initiation of neutrophil TEM. EC ICAM-2 is suggested to interact with neutrophil integrins during the neutrophil transmigration cascade. Inside-out integrin signalling induces conformational change in the structure of integrins allowing this protein to interact with ICAM-2 and support neutrophil adhesion. Signalling events within the EC as a result of ICAM-2 ligation with integrins could stimulate the interaction of the C-terminal of ICAM-2 with intracellular proteins (e.g. ERM, α-actinin) which are linked to the EC cytoskeleton. This may consequently induce Rac mediated phosphorylation of VE-cadherin. Thus EC-EC junctional contacts are dissociated resulting in the opening of EC junctions allowing the neutrophil to transmigrate through it. Outside-in and/or inside-out integrin signalling within the neutrophil may collectively result in cytoskeletal rearrangement, neutrophil polarity and thus support the formation of neutrophil protrusions into EC junctions which is required during TEM.

8.5 Development of a cremasteric SR model

To extend the findings for role of key molecules in neutrophil extravasation a more complex, disease mimicking inflammatory reaction was developed as part of this project. Although due to lack of time the model was not used for investigations into the functional role of key molecules (i.e. ICAM-2), the findings indicate its potential value for such future experiments. SR stimulated in the cremaster muscle produced neutrophil transmigration, low frequency of haemorrhage formation, a possible increase in EC-platelet interactions and reduced vascular perfusion. Further studies are however required to fully characterise these parameters and this response in more detail before extending it to investigations of the functional roles of molecules such as ICAM-2.

8.6 Future directions and unanswered questions

8.6.1 Does ICAM-2 bind to ligands other than MAC-1 during its role in neutrophil extravasation?

MAC-1 and LFA-1 both exhibit binding affinity to ICAM-2 and have been shown to have distinct and overlapping functions. During monocyte crawling EC ICAM-2 has been shown to bind to both LFA-1 and MAC-1 (Schenkel et al., 2004) whereas during lymphocyte adhesion EC ICAM-2 binds to LFA-1 or VLA-4 (Seth et al., 1991). Whether ICAM-2 binds to LFA-1 during neutrophil crawling and/or the initiation of TEM during extravasation in the current model, as well as MAC-1 is unknown. Although the present study provides evidence for the potential interaction of ICAM-2/MAC-1 during neutrophil crawling, it does not exclude a possible interaction of ICAM-2 with LFA-1. Investigating the contribution of ICAM-2/LFA-1 interaction in this model using anti-LFA-1 mAb was not conducted as LFA-1 has a profound role in supporting neutrophil adhesion. Based on the results obtained using

anti-ICAM-1 mAb which is the key ligand for LFA-1 in adhesion, inhibiting LFA-1 would result in more than 90% reduction in neutrophil adhesion, and hence a very low frequency of crawling events. Additionally the ligand for ICAM-2 during the initiation of TEM has not been determined in the present study again due to the low frequency of events following anti-MAC-1 mAb treatment. Further studies are therefore required to understand these concepts in more detail.

Administering anti-LFA-1, anti-MAC-1, anti-ICAM-1 or anti-ICAM-2 mAbs post-adhesion during the crawling stage in the cremasteric confocal IVM model could provide further details in regards to this. After anti-LFA-1 and anti-ICAM-1 mAb treatment post-adhesion, neutrophils could however deattach from the EC and go back into the circulation as ICAM-1/LFA-1 interactions could be crucial to the maintenance of adhesion. It is however also possible that other interactions involving ICAM-2 are sufficient to keep the neutrophils in contact with the ECs during crawling, in which case various crawling dynamics could be analysed post-adhesion and the contribution of LFA-1/ICAM-1, LFA-1/ICAM-2, MAC-1/ICAM-1 and MAC-1/ICAM-2 interactions could be determined. Depending on the frequency of TEM events, various TEM parameters could then be analysed in order to further understand ICAM-2 ligand interactions during its role in the initiation of TEM.

Another technique such as fluorescence resonance energy transfer (FRET) may be required to understand the contribution of these interactions at specific stages of the neutrophil transmigration cascade. Using this technique the function of ICAM-1 interactions with LFA-1 or MAC-1, and ICAM-2 interactions with LFA-1 or MAC-1 during neutrophil crawling and the initiation of TEM could be determined in more detail. Of note this technique could also be used to examine the downstream signalling events that occur within ECs upon ICAM-2 ligation which could provide further detail into the mechanisms underlying the role of ICAM-2 as suggested in the current study (Section 8.2 and 8.3). This latter area of investigation is also currently understudied and further information regarding the intracellular signalling pathways

involved is required to fully appreciate the role of ICAM-2 in neutrophil crawling and the initiation of TEM.

8.6.2 Is there a delay or a total inhibition in neutrophil TEM in the absence of functional ICAM-2?

In the absence of functional ICAM-2 a reduction in neutrophil extravasation is seen at 4 hours post IL-1β stimulation. This effect was attributed to the involvement of ICAM-2 in supporting neutrophil crawling speed, continuity of crawling and the initiation of TEM. Whether these effects persist at later time points (> 4 hours) after IL-1β stimulation is currently unknown. It is possible that the slow, discontinuously crawling cells in IL-1β-stimulated ICAM-2 KO vessels do undergo TEM at a later point, thus resulting in a delay in neutrophil extravasation as opposed to a complete inhibition. Analysis of neutrophil dynamics for longer and/or at later time periods would provide further insights into the role of ICAM-2 in supporting neutrophil extravasation. More specifically its key functions in mediating crawling speed, continuity and the initiation of TEM can be further examined to understand the fate of discontinuously crawling cells. Of note a delayed response in ICAM-2 KO mice has been reported in the recruitment of eosinophils to the lungs in a hyperresponsive allergic model (Gerwin et al., 1999) and thus requires further studies with respect to neutrophil recruitment.

8.6.3 Does ICAM-2 support crawling and the initiation of TEM in a stimulus-specific manner?

Previous data within our group has shown stimulus-specific functions of ICAM-2, indicating a role for ICAM-2 in IL-1β-stimulated responses but not in response to TNF-α or thioglycolate (Huang et al., 2006). This was demonstrated in both the cremasteric IVM model as well as in the peritonitis model (Huang et al., 2006), findings that were subsequently linked to the ability of the stimulus to predominately activate ECs directly (Woodfin et al., 2009). It would therefore be of interest to

investigate the role of ICAM-2 in the dynamics of neutrophil recruitment in several inflammatory models in order to gain further insights into the factors that influence ICAM-2 functions.

8.6.4 Does ICAM-2 support crawling and the initiation of TEM in disease models?

The stimulus-specific roles of ICAM-2 as described previously, also questions the pathological relevance of ICAM-2 in the recruitment of neutrophils in inflammation. A number of studies have used disease models to demonstrate the role of ICAM-2. This includes a murine bacterial induced inflammatory model (Hobden, 2003), a murine allergic hypperresponsive airway model (Gerwin et al., 1999), a human pancreatic carcinogenesis model (Hiraoka et al., 2011) and a study using tissue samples from patients with Crohn's disease (Bernstein et al., 1998) although the latter three are likely to be due to ICAM-2 expression on epithelium rather than on EC and therefore the function of ICAM-2 may differ. Collectively there are very few studies published which have investigated the role of EC ICAM-2 in neutrophil extravasation in pathological inflammation where a more complex reaction takes place. Previous work in our group has however indicated a role for ICAM-2 in a cremasteric ischemia-reperfusion (I-R) injury model (unpublished work by Woodfin et al) and the results were in line with inflammatory responses induced by IL-1β, where a role for ICAM-2 in neutrophil extravasation, but not adhesion was demonstrated. Further examination of the dynamics of neutrophil crawling and TEM in a cremasteric I-R injury model would be valuable to understand the roles of ICAM-2 in more pathologically relevant models.

The present study describes a series of studies aimed at the development of a cremasteric SR model. This model was developed in order to extend our current understanding of endothelial junctional molecules in a more complex disease mimicking reaction (Chapter 7). However, due to time restrictions this reaction was not used for investigations into the role of endothelial junctional molecules. This

model could therefore be used in order to gain further insights into the role of ICAM-2 in numerous vascular processes such as thrombosis and vascular damage simultaneously alongside neutrophil recruitment in real time which is more clinically relevant to conditions such as vacuities. The cremasteric SR response induced neutrophil extravasation, few sites of thrombi and haemorrhage formation. Further studies are now required to fully characterise the later two processes in more detail before investigating the role of ICAM-2 in this model. Understanding the role of this molecule as well as other junctional molecules such as PECAM-1 and JAM-A would be of great interest due to the key role of platelets in this model together with the fact that these molecules are also expressed on platelets where there function is currently unknown.

8.6.5 Do different leukocyte subtypes use different mechanisms to undergo crawling and initiation of TEM during leukocyte extravasation?

In this study the role of ICAM-2 in leukocyte migration dynamics was restricted to neutrophils. A key function for ICAM-2 in monocyte crawling *in vitro* has been demonstrated however dynamics of this response in relation to ICAM-2 expression was not investigated (Schenkel et al., 2004). Understanding whether ICAM-2 is involved in the regulation of monocyte crawling speed, continuity and the initiation of TEM, as reported for neutrophils, would provide further insight into the role of ICAM-2 in the recruitment of leukocytes as a whole and may shed further light into the general mechanisms associated with this process. Using the Lys-eGFP-ki mice monocytes can be distinguished from neutrophils due to their lower GFP intensity and hence provides a model to investigate monocyte responses. Alternatively cross breeding the ICAM-2 KO mice with CX3CR-1-eGFP mice (mice which endogenously express GFP in monocytes and dendritic cells) would also provide a key tool to investigate the role of ICAM-2 in the dynamics of monocyte recruitment. Anti-ICAM-2 mAb administration in the CX3CR-1-eGFP mice would also be useful in conjunction with the ICAM-2 KO mice studies to eliminate the possibility of compensatory mechanisms occurring as a result of the genetic deficiency of ICAM-2. These experiments could be carried out by using a monocytic stimulus such as

CCL2 where various monocyte-EC dynamics can be determined using confocal IVM. This will be based on the assumption that ICAM-2 is involved in CCL2 induced monocyte recruitment which is currently unknown. The stimulus-specific roles of ICAM-2 previously demonstrated (Woodfin et al., 2009) however suggest that CCL2 may bypass the need for EC ICAM-2 in this reaction as it can directly activate monocytes. Alternatively IL-1β- or LPS-induced inflammation could be examined at time points when monocyte recruitment is at its peak.

8.6.6 What is the function of ICAM-2 on platelets in inflammation?

ICAM-2 is known to be expressed on platelets (Diacovo et al., 1994) and to date its function in this cell type is largely unknown. Since platelets are involved in the recruitment of leukocytes (Gawaz et al., 2005) it is possible that platelet ICAM-2 could mediate adhesive interactions with integrins found on leukocytes. ICAM-2 expressed on platelets could also interact homophillically with ECs and/or platelets and/or leukocytes. Additionally it is also possible that these cellular interactions could occur through a ligand which is yet to be discovered. It would therefore also be interesting to see if ICAM-2 has a role in leukocyte-platelet and/or platelet-EC interactions during leukocyte extravasation. This could be carried out using confocal IVM in WT and ICAM-2 KO Lys-eGFP-ki mice under conditions where platelets and ECs have also been labelled by appropriate fluorescently labelled mAbs.

8.6.7 Does ICAM-2 support vascular integrity?

ICAM-2 has been previously found to support EC-EC interactions via homophilic interactions (Huang et al., 2005). Taking this into account together with the fact that ICAM-2 is highly expressed on ECs under basal conditions, it is possible that ICAM-2 could be involved in supporting junctional integrity. Numerous other related molecules such as JAMs (Dejana, 2004) and PECAM-1 (Privratsky et al., 2011) have also being studied in this respect and have demonstrated to have key roles in regulating the permeability of the EC layer. To date there exist no information on the

potential role of ICAM-2 in vascular permeability during inflammation, an issue that requires further investigation. A simple and direct way of investigating this would be through experiments addressing vascular leakage of i.v. Evans blue in the mouse dorsal skin inflammatory model in WT and ICAM-2 KO mice. Alternatively using small fluorescent dextran or microspheres in the confocal IVM model as described in the present study can also be used to answer this question.

8.6.8 What are the translational implictaions of the findings?

Leukocyte migration from the blood into in the site of infection or injury is a crucial component of both physiological and pathological inflammation. Uncontrollable and excessive recruitment of leukocytes contribute to the progression of many pathogical disorders such as atherosclerosis and ischemia-reperfusion injury. Further understanding of the mechanisms of leukocyte recruitment would facilitate identification of potential therapeutic targets. Through the use of rigorous *in vivo* imaging methods this study has provided significant insight into the role of a key EC adhesion molecule ICAM-2 in leukocyte recruitment. Future translational benefits to healthcare may take in the form of novel therapeutics that specifically target ICAM-2. ICAM-2 blocking therapies may be able to specifically target pathological neutrophil accumulation, without causing more widespread immunosupression. This of course requires futher comprehensive understanding of the role of ICAM-2 specifically in disease models to see the therapeutic value in individual inflammatory reactions. The strong emphasis of this work on understanding of fundamental cellular mechanisms of inflammation could lead to novel drug targets but the time-scale of this will not be easy to predict.

8.7 Concluding remarks

This study has demonstrated for the first time a role for ICAM-2 in neutrophil crawling and the initiation of TEM during IL-1β-induced extravasation *in vivo*. It was found that ICAM-2 facilitates neutrophil crawling speed and continuity, as well as neutrophil-EC junctional interactions preceding TEM. The results also suggest that some of these roles maybe mediated through the ligation of EC ICAM-2 with neutrophil MAC-1, adding an additional molecular interaction to the neutrophil transmigration cascade. It is not currently known if the defects in speed and continuity of crawling and the identification and/or opening of endothelial junctions reflect several distinct roles for ICAM-2, although it is tempting to speculate that crawling is supported by activation of neutrophil locomotive machinery, while junctional opening may be facilitated by signalling within the ECs leading to junctional and/or cytoskeletal rearrangement. ICAM-2 is therefore a molecule that should be added to the list of proteins crucial for neutrophil crawling and the initiation of TEM. Collectively the findings of the present study provide further insights into the biological mechanisms of neutrophil extravasation *in vivo*.

References

1. **Albelda, S. M., Smith, C. W. and Ward, P. A.** (1994). Adhesion molecules and inflammatory injury. *The FASEB Journal* **8,** 504-512.

2. **Alcaide, P., Auerbach, S. and Luscinskas, F. W.** (2009). Neutrophil recruitment under shear flow: it's all about endothelial cell rings and gaps. *Microcirculation* **16,** 43-57.

3. **Alizadeh, A. A., Eisen, M. B., Davis, R. E., Ma, C., Lossos, I. S., Rosenwald, A., Boldrick, J. C., Sabet, H., Tran, T., Yu, X. et al.** (2000). Distinct types of diffuse large B-cell lymphoma identified by gene expression profiling. *Nature* **403,** 503-511.

4. **Argenbright, L. W. and Barton, R. W.** (1992). Interactions of leukocyte integrins with intercellular adhesion molecule 1 in the production of inflammatory vascular injury in vivo. The Shwartzman reaction revisited. *J Clin Invest* **89,** 259-272.

5. **Barreiro, O., Yanez-Mo, M., Serrador, J. M., Montoya, M., Vicente-Manzanares, M., Tejedor, R., Furthmayr, H. and Sanchez-Madrid, F.** (2002). Dynamic interaction of VCAM-1 and ICAM-1 with moesin and ezrin in a novel endothelial docking structure for adherent leukocytes. *J. Cell Biol.* **157,** 1233-1245.

6. **Bernstein, C. N., Sargent, M. and Gallatin, W. M.** (1998). β_2 integrin/ICAM expression in Crohn's Disease. *Clinical Immunology and Immunopathology* **86,** 147-160.

7. **Bevilacqua, M. P. and Nelson, R. M.** (1993). Selectins. *J Clin Invest* **91,** 379-387.

8. **Bixel, M. G., Li, H., Petri, B., Khandoga, A. G., Khandoga, A., Zarbock, A., Wolburg-Buchholz, K., Wolburg, H., Sorokin, L., Zeuschner, D. et al.** (2010). CD99 and CD99L2 act at the same site as, but independently of, PECAM-1 during leukocyte diapedesis. *Blood* **116,** 1172-1184.

9. **Boscacci, R. T., Pfeiffer, F., Gollmer, K., Sevilla, A. I. C., Martin, A. M., Soriano, S. F., Natale, D., Henrickson, S., von Andrian, U. H., Fukui, Y. et al.** (2010). Comprehensive analysis of lymph node stroma-expressed Ig superfamily members reveals redundant and nonredundant roles for ICAM-1, ICAM-2, and VCAM-1 in lymphocyte homing. *Blood* **116,** 915-925.

10. **Brain, S. D.** (1997). Sensory neuropeptides: their role in inflammation and wound healing. *Immunopharmacology* **37,** 133-152.

11. **Brinkmann, V., Reichard, U., Goosmann, C., Fauler, B., Uhlemann, Y., Weiss, D. S., Weinrauch, Y. and Zychlinsky, A.** (2004). Neutrophil Extracellular Traps Kill Bacteria. *Science* **303,** 1532-1535.

12. **Brozna, J. P.** (1990). Shwartzman Reaction. *Semin Thromb Hemost* **16,** 326-332.

13. **Burns, A. R., Walker, D. C., Brown, E. S., Thurmon, L. T., Bowden, R. A., Keese, C. R., Simon, S. I., Entman, M. L. and Smith, C. W.** (1997). Neutrophil transendothelial migration is independent of tight junctions and occurs preferentially at tricellular corners. *J Immunol* **159,** 2893-2903.

14. **Carman, C. V. and Springer, T. A.** (2004). A transmigratory cup in leukocyte diapedesis both through individual vascular endothelial cells and between them. *J. Cell Biol.* **167,** 377-388.

15. **Carman, C. V. and Springer, T. A.** (2008). Trans-cellular migration: cell-cell contacts get intimate. *Curr. Opin. Cell Biol.* **20,** 533-540.

16. **Carpenito, C., Pyszniak, A. M. and Takei, F.** (1997). ICAM–2 Provides a Costimulatory Signal for T Cell Stimulation by Allogeneic Class II MHC. *Scandinavian journal of immunology* **45,** 248-254.

17. **Carpenito.C, Pyszniak, A. and Takei, F.** (1997). ICAM-2 provides a costimulatory signal for T cell stimulation by allogeneic class II MHC. *Scand J Immunol.* **45(3),** 248-254.

18. **Carreno, M. P., Chomont, N., Kazatchkine, M. D., Irinopoulou, T., Krief, C., Mohamed, A. S., Andreoletti, L., Matta, M. and Belec, L.** (2002). Binding of LFA-1 (CD11a) to Intercellular Adhesion Molecule 3 (ICAM-3; CD50) and ICAM-2 (CD102) Triggers Transmigration of Human Immunodeficiency Virus Type 1-Infected Monocytes through Mucosal Epithelial Cells. *Journal of Virology* **76,** 32-40.

19. **Casasnovas, J. M., Springer, T. A., Liu, J. h., Harrison, S. C. and Wang, J. h.** (1997). Crystal structure of ICAM-2 reveals a distinctive integrin recognition surface. *Nature* **387,** 312-315.

20. **Cowan, P. J., Shinkel, T. A., Fisicaro, N., Godwin, J. W., Bernab+®u, C., Almendro, N., Rius, C., Lonie, A. J., Nottle, M. B., Wigley, P. L. et al.** (2003). Targeting gene expression to endothelium in transgenic animals: a comparison of the human ICAM-2, PECAM-1 and endoglin promoters. *Xenotransplantation* **10,** 223-231.

21. **Cowan, P. J., Tsang, D., Pedic, C. M., Abbott, L. R., Shinkel, T. A., Anthony J.F. and Pearse, M. J.** (1998). The human ICAM-2 promoter is endothelial cell-specific in vitro and in vivo and contains

critical Sp1 and GATA binding sites. *Journal of Biological Chemistry* **273,** 11737-11744.

22. **Cunningham, S. A., Rodriguez, J. M., Arrate, M. P., Tran, T. M. and Brock, T. A.** (2002). JAM2 Interacts with $\alpha_4\beta_1$. *Journal of Biological Chemistry* **277,** 27589-27592.

23. **Dangerfield, J., Larbi, K. Y., Huang, M. T., Dewar, A. and Nourshargh, S.** (2002). PECAM-1 (CD31) homophilic interaction up-regulates $\alpha_6\beta_1$ on transmigrated neutrophils in vivo and plays a functional role in the ability of α_6 integrins to mediate leukocyte migration through the perivascular basement membrane. *The Journal of Experimental Medicine* **196,** 1201-1212.

24. **de Fougerolles, A. R., Stacker, S. A., Schwarting, R. and Springer, T. A.** (1991). Characterization of ICAM-2 and evidence for a third counter-receptor for LFA-1. *The Journal of Experimental Medicine* **174,** 253-267.

25. **Dejana, E.** (2004). Endothelial cell-cell junctions: happy together. *Nat Rev Mol Cell Biol* **5,** 261-270.

26. **DeLisser, H. M., Baldwin, H. S. and Albelda, S. M.** (1997). Platelet Endothelial Cell Adhesion Molecule 1 (PECAM-1/CD31): A Multifunctional Vascular Cell Adhesion Molecule. *Trends in Cardiovascular Medicine* **7,** 203-210.

27. **Diacovo, T. G., deFougerolles, A. R., Bainton, D. F. and Springer, T. A.** (1994). A functional integrin ligand on the surface of platelets: intercellular adhesion molecule-2. *J Clin Invest* **94,** 1243-1251.

28. **Ebnet, K., Suzuki, A., Ohno, S. and Vestweber, D.** (2004). Junctional adhesion molecules (JAMs): more molecules with dual functions? *J Cell Sci* **117,** 19-29.

29. **Faust, N., Varas, F., Kelly, L. M., Heck, S. and Graf, T.** (2000). Insertion of enhanced green fluorescent protein into the lysozyme gene creates mice with green fluorescent granulocytes and macrophages 28. *Blood* **96,** 719-726.

30. **Feduska, J., Garcia, P., Brennan, S., Bu, S., Council, L. and Yoon, K.** (2013). N-glycosylation of ICAM-2 is required for ICAM-2-mediated complete suppression of metastatic potential of SK-N-AS neuroblastoma cells. *BMC Cancer* **13,** 261.

31. **Feng, D., Nagy, J. A., Dvorak, H. F. and Dvorak, A. M.** (2002). Ultrastructural studies define soluble macromolecular, particulate, and cellular transendothelial cell pathways in venules, lymphatic vessels,

and tumor-associated microvessels in man and animals. *Microsc. Res. Tech.* **57,** 289-326.

32. **Feng, D., Nagy, J. A., Pyne, K., Dvorak, H. F. and Dvorak, A. M.** (1998). Neutrophils emigrate from venules by a transendothelial cell pathway in response to FMLP. *J. Exp. Med.* **187,** 903-915.

33. **Gawaz, M., Langer, H. and May, A. E.** (2005). Platelets in inflammation and atherogenesis. *J Clin Invest* **115,** 3378-3384.

34. **Geijtenbeek, T. B., Krooshoop, D. J., Bleijs, D. A., van Vliet, S. J., van Duijnhoven, G. C., Grabovsky, V., Alon, R., Figdor, C. G. and van, K. Y.** (2000). DC-SIGN-ICAM-2 interaction mediates dendritic cell trafficking. *Nat. Immunol.* **1,** 353-357.

35. **Geissmann, F., Auffray, C., Palframan, R., Wirrig, C., Ciocca, A., Campisi, L., Narni-Mancinelli, E. and Lauvau, G.** (2008). Blood monocytes: distinct subsets, how they relate to dendritic cells, and their possible roles in the regulation of T-cell responses. *Immunol Cell Biol* **86,** 398-408.

36. **Gerwin, N., Gonzalo, J. A., Lloyd, C., Coyle, A. J., Reiss, Y., Banu, N., Wang, B., Xu, H., Avraham, H., Engelhardt, B. et al.** (1999). Prolonged eosinophil accumulation in allergic lung interstitium of ICAM-2-deficient mice results in extended hyperresponsiveness. *Immunity* **10,** 9-19.

37. **Glogowska-Ligus, J., Dàbek, J., Zych-Twardowska, E. and Tkacz, M.** (2012). Expression analysis of intercellular adhesion molecule-2 (ICAM-2) in the context of classical cardiovascular risk factors in acute coronary syndrome patients. *Arch Med Sci*.

38. **Godwin, J. W., d'Apice, A. J. and Cowan, P. J.** (2004). Characterization of pig intercellular adhesion molecule-2 and its interaction with human LFA-1. *Am. J. Transplant.* **4,** 515-525.

39. **Hamada, K., Shimizu, T., Yonemura, S., Tsukita, S., Tsukita, S. and Hakoshima, T.** (2003). Structural basis of adhesion-molecule recognition by ERM proteins revealed by the crystal structure of the radixin–ICAM-2 complex. *EMBO J* **22,** 502-514.

40. **Hayflick, J., Kilgannon, P. and Gallatin, W. M.** (1998). The intercellular adhesion molecule (ICAM) family of proteins. *Immunol Res* **17,** 313-327.

41. **Heiska, L., Kantor, C., Parr, T., Critchley, D. R., Vilja, P., Gahmberg, C. G. and Carpen, O.** (1996). Binding of the cytoplasmic domain of intercellular adhesion molecule-2 (ICAM-2) to α-actinin. *J. Biol. Chem.* **271,** 26214-26219.

42. **Heiska, L., Alfthan, K., Gronholm, M., Vilja, P., Vaheri, A. and Carpen, O.** (1998). Association of ezrin with intercellular adhesion molecule-1 and -2 (ICAM-1 and ICAM-2). *Journal of Biological Chemistry* **273,** 21893-21900.

43. **Helander, T. S., Carpen, O., Turunen, O., Kovanen, P. E., Vaheri, A. and Timonen, T.** (1996). ICAM-2 redistributed by ezrin as a target for killer cells. *Nature* **382,** 265-268.

44. **Heping Yang**. (2012). Structure, Expression, and Function of ICAM-5. p. 11.

45. **Hidalgo, A. s., Peired, A. J., Wild, M. K., Vestweber, D. and Frenette, P. S.** (2007). Complete Identification of E-Selectin Ligands on Neutrophils Reveals Distinct Functions of PSGL-1, ESL-1, and CD44. *Immunity* **26,** 477-489.

46. **Hidalgo, A., Chang, J., Jang, J. E., Peired, A. J., Chiang, E. Y. and Frenette, P. S.** (2009). Heterotypic interactions enabled by polarized neutrophil microdomains mediate thromboinflammatory injury. *Nat Med* **15,** 384-391.

47. **Hiraoka, N., YamazakiΓÇôItoh, R., Ino, Y., Mizuguchi, Y., Yamada, T., Hirohashi, S. and Kanai, Y.** (2011). CXCL17 and ICAM2 are associated with a potential anti-tumor immune response in early intraepithelial stages of human pancreatic carcinogenesis. *Gastroenterology* **140,** 310-321.

48. **Hjort, P. F. and Rapaport, S. I.** (1965). The Shwartzman Reaction: pathogenetic mechanisms and clinical manifestations. *Annu. Rev. Med.* **16,** 135-168.

49. **Hobden, J. A.** (2003). Intercellular adhesion molecule-2 (ICAM-2) and Pseudomonas aeruginosa ocular Infection. *DNA and Cell Biology* **22,** 649-655.

50. **Hogg, N., Patzak, I. and Willenbrock, F.** (2011). The insider's guide to leukocyte integrin signalling and function. *Nat Rev Immunol* **11,** 416-426.

51. **Horley, K. J., Carpenito, C., Baker, B. and Takei, F.** (1989). Molecular cloning of murine intercellular adhesion molecule (ICAM-1). *EMBO J* **8,** 2889-2896.

52. **Huang, M. T.** (2004). The roles of intercellular adhesion molecule (ICAM-2) in leukocyte migration and angiogenesis.

53. **Huang, M. T., Larbi, K. Y., Scheiermann, C., Woodfin, A., Gerwin, N., Haskard, D. O. and Nourshargh, S.** (2006). ICAM-2 mediates

neutrophil transmigration in vivo: evidence for stimulus specificity and a role in PECAM-1-independent transmigration. *Blood* **107,** 4721-4727.

54. **Huang, M. T., Mason, J. C., Birdsey, G. M., Amsellem, V., Gerwin, N., Haskard, D. O., Ridley, A. J. and Randi, A. M.** (2005). Endothelial intercellular adhesion molecule (ICAM)-2 regulates angiogenesis. *Blood* **106,** 1636-1643.

55. **Huttenlocher, A. and Horwitz, A. R.** (2011). Integrins in cell migration. *Cold Spring Harbor Perspectives in Biology* **3**.

56. **Issekutz, A. C., Rowter, D. and Springer, T. A.** (1999). Role of ICAM-1 and ICAM-2 and alternate CD11/CD18 ligands in neutrophil transendothelial migration. *J. Leukoc. Biol.* **65,** 117-126.

57. **Jung, S., Aliberti, J., Graemmel, P., Sunshine, M. J., Kreutzberg, G. W., Sher, A. and Littman, D. R.** (2000). Analysis of Fractalkine Receptor CX3CR1 Function by Targeted Deletion and Green Fluorescent Protein Reporter Gene Insertion 29. *Mol. Cell. Biol.* **20,** 4106-4114.

58. **Kinashi, T.** (2005). Intracellular signalling controlling integrin activation in lymphocytes. *Nat Rev Immunol* **5,** 546-559.

59. **Kuijper, P. H., Gallardo Tores, H. I., Lammers, J. W., Sixma, J. J., Koenderman, L. and Zwaginga, J. J.** (1998). Platelet associated fibrinogen and ICAM-2 induce firm adhesion of neutrophils under flow conditions. *Thromb Haemost* **80,** 443-448.

60. **Lamagna, C., Meda, P., Mandicourt, G., Brown, J., Gilbert, R. J. C., Jones, E. Y., Kiefer, F., Ruga, P., Imhof, B. A. and urrand-Lions, M.** (2005). Dual interaction of JAM-C with JAM-B and $\alpha_M\beta_2$ integrin: function in junctional complexes and leukocyte adhesion. *Mol. Biol. Cell* **16,** 4992-5003.

61. **Lawson, C. and Wolf, S.** (2009). ICAM-1 signaling in endothelial cells. *Pharmacological Reports* **61,** 22-32.

62. **Lehmann, J. C. U., Jablonski-Westrich, D., Haubold, U., Gutierrez-Ramos, J. C., Springer, T. and Hamann, A.** (2003). Overlapping and selective roles of endothelial intercellular adhesion molecule-1 (ICAM-1) and ICAM-2 in lymphocyte trafficking. *J Immunol* **171,** 2588-2593.

63. **Ley, K., Laudanna, C., Cybulsky, M. I. and Nourshargh, S.** (2007). Getting to the site of inflammation: the leukocyte adhesion cascade updated. *Nature Rev. Immunol.* **7,** 678-689.

64. **Li, R., Nortamo, P., Valmu, L., Tolvanen, M., Huuskonen, J., Kantor, C. and Gahmberg, C. G.** (1993). A peptide from ICAM-2 binds to the leukocyte integrin CD11a/CD18 and inhibits endothelial cell adhesion. *Journal of Biological Chemistry* **268,** 17513-17518.

65. **Li, R., Xie, J., Kantor, C., Koistinen, V., Altieri, D. C., Nortamo, P. and Gahmberg, C. G.** (1995). A peptide derived from the intercellular adhesion molecule-2 regulates the avidity of the leukocyte integrins CD11b/CD18 and CD11c/CD18. *The Journal of Cell Biology* **129,** 1143-1153.

66. **Li, X., Akiyama, M., Nakahama, K. i., Koshiishi, T., Takeda, S. and Morita, I.** (2012). Role of intercellular adhesion molecule-2 in osteoclastogenesis. *Genes Cells* **17,** 568-575.

67. **Ludwig, R. J., Hardt, K., Hatting, M., Bistrian, R., Diehl, S., Radeke, H. H., Podda, M., Schaan, M. P., Kaufmann, R., Henschler, R. et al.** (2009). Junctional adhesion molecule (JAM)-B supports lymphocyte rolling and adhesion through interaction with $\alpha_4\beta_1$ integrin. *Immunology* **128,** 196-205.

68. **Ludwig, R. J., Zollner, T. M., Santoso, S., Hardt, K., Gille, J., Baatz, H., Johann, P. S., Pfeffer, J., Radeke, H. H., Schon, M. P. et al.** (2005). Junctional adhesion molecules (JAM)-B and -C contribute to leukocyte extravasation to the skin and mediate cutaneous inflammation. *J Investig Dermatol* **125,** 969-976.

69. **Lyck, R., Reiss, Y., Gerwin, N., Greenwood, J., Adamson, P. and Engelhardt, B.** (2003). T-cell interaction with ICAM-1/ICAM-2 double-deficient brain endothelium in vitro: the cytoplasmic tail of endothelial ICAM-1 is necessary for transendothelial migration of T cells. *Blood* **102,** 3675-3683.

70. **Mamdouh, Z., Mikhailov, A. and Muller, W. A.** (2009). Transcellular migration of leukocytes is mediated by the endothelial lateral border recycling compartment. *J. Exp. Med.* **206,** 2795-2808.

71. **Mamdouh, Z., Chen, X., Pierini, L. M., Maxfield, F. R. and Muller, W. A.** (2003). Targeted recycling of PECAM from endothelial surface-connected compartments during diapedesis. *Nature* **421,** 748-753.

72. **Mamdouh, Z., Kreitzer, G. E. and Muller, W. A.** (2008). Leukocyte transmigration requires kinesin-mediated microtubule-dependent membrane trafficking from the lateral border recycling compartment. *The Journal of Experimental Medicine* **205,** 951-966.

73. **Mantovani, A., Cassatella, M. A., Costantini, C. and Jaillon, S. +.** (2011). Neutrophils in the activation and regulation of innate and adaptive immunity. *Nat Rev Immunol* **11,** 519-531.

74. **Massena, S., Christoffersson, G., Hjertstrom, E., Zcharia, E., Vlodavsky, I., Ausmees, N., Rolny, C., Li, J. P. and Phillipson, M.** (2010). A chemotactic gradient sequestered on endothelial heparan sulfate induces directional intraluminal crawling of neutrophils. *Blood* **116,** 1924-1931.

75. **McLaughlin, F., Ludbrook, V. J., Kola, I., Campbell, C. J. and Randi, A. M.** (1999). Characterisation of the tumour necrosis factor (TNF)-α response elements in the human ICAM-2 promoter. *J Cell Sci* **112,** 4695-4703.

76. **McLaughlin, F., Hayes, B. P., Horgan, C. M. T., Beesley, J. E., Campbell, C. J. and Randi, A. M.** (1998). αTumor necrosis factor (TNF)-α and Interleukin (IL)-1β down-regulate intercellular adhesion molecule (ICAM)-2 expression on the endothelium. *Cell Commun Adhes* **6,** 381-400.

77. **Movat, H. Z., Burrowes, C. E., Cybulsky, M. I. and Dinarello, C. A.** (1987). Acute inflammation and a Shwartzman-like reaction induced by interleukin-1 and tumor necrosis factor. Synergistic action of the cytokines in the induction of inflammation and microvascular injury. *Am J Pathol* **129,** 463-476.

78. **Nourshargh, S., Hordijk, P. L. and Sixt, M.** (2010). Breaching multiple barriers: leukocyte motility through venular walls and the interstitium. *Nat Rev Mol Cell Biol* **11,** 366-378.

79. **Pepys MB**. (1982). Role of the acute phase response in the Shwartzman phenomenon
21. *Clinical Experimental Immunology* **47,** 289-295.

80. **Perez, O. D., Kinoshita, S., Hitoshi, Y., Payan, D. G., Kitamura, T., Nolan, G. P. and Lorens, J. B.** (2002). Activation of the PKB/AKT Pathway by ICAM-2. *Immunity* **16,** 51-65.

81. **Phillipson, M., Heit, B., Colarusso, P., Liu, L., Ballantyne, C. and Kubes, P.** (2006). Intraluminal crawling of neutrophils to emigration sites: a molecularly distinct process from adhesion in the recruitment cascade. *J. Exp. Med.* **203,** 2569-2575.

82. **Phillipson, M., Heit, B., Parsons S, Petri, B., Mullay S, Colarusso, P., Gower M, Neely S and Kubes, P.** (2009). Vav1 is essential for mechanotactic crawling and migration of neutrophils out of the inflamed microvasculature. *J. Immunol.* **182,** 6870-6878.

83. **Phillipson, M., Kaur, J., Colarusso, P., Ballantyne, C. M. and Kubes, P.** (2008). Endothelial domes encapsulate adherent neutrophils and minimize increases in vascular permeability in paracellular and transcellular emigration. *PLoS One* **3,** e1649.

84. **Porter, J. C. and Hall, A.** (2009). Epithelial ICAM-1 and ICAM-2 regulate the egression of human T cells across the bronchial epithelium. *The FASEB Journal* **23,** 492-502.

85. **Privratsky, J. R., Newman, D. K. and Newman, P. J.** (2010). PECAM-1: Conflicts of interest in inflammation. *Life Sciences* **87,** 69-82.

86. **Privratsky, J. R., Paddock, C. M., Florey, O., Newman, D. K., Muller, W. A. and Newman, P. J.** (2011). Relative contribution of PECAM-1 adhesion and signaling to the maintenance of vascular integrity. *J Cell Sci***,** jcs.

87. **Proebstl, D., Voisin, M. B., Woodfin, A., Whiteford, J., Acquisto, F., Jones, G. E., Rowe, D. and Nourshargh, S.** (2012). Pericytes support neutrophil subendothelial cell crawling and breaching of venular walls in vivo. *The Journal of Experimental Medicine*.

88. **Reiss, Y., Hoch, G., Deutsch, U. and Engelhardt, B.** (1998). T cell interaction with ICAM-1-deficient endothelium in vitro: essential role for ICAM-1 and ICAM-2 in transendothelial migration of T cells. *Eur. J. Immunol.* **28,** 3086-3099.

89. **Reiss, Y. and Engelhardt, B.** (1999). T cell interaction with ICAM-1-deficient endothelium in vitro: transendothelial migration of different T cell populations is mediated by endothelial ICAM-1 and ICAM-2. *International Immunology* **11,** 1527-1539.

90. **Renkonen, R., Paavonen, T., Nortamo, P. and Gahmberg, C. G.** (1992). Expression of endothelial adhesion molecules in vivo: Increased endothelial ICAM-2 expression in lymphoid malignancies. *American Journal of Pathology* **140,** 763-767.

91. **Ridger, V., Krams, R., Carpi, A. and Evans, P. C.** (2008). Hemodynamic parameters regulating vascular inflammation and atherosclerosis: A brief update. *Biomedicine & Pharmacotherapy* **62,** 536-540.

92. **Ridger, V. C., Hellewell, P. G. and Norman, K. E.** (2005). L- and P-Selectins Collaborate to Support Leukocyte Rolling in Vivo When High-Affinity P-Selectin-P-Selectin Glycoprotein Ligand-1 Interaction Is Inhibited. *Am J Pathol* **166,** 945-952.

93. **Ridley, A. J.** (2003). Cell migration: integrating signals from front to back. *Science* **302,** 1704-1709.

94. **Rohlena, J.** (2009). Endothelial CD81 is a marker of early human atherosclerotic plaques and facilitates monocyte adhesion. *Cardiovasc. Res.* **81,** 187-196.

95. **Rottner, K. and Stradal, T. E.** (2011). Actin dynamics and turnover in cell motility. *Current Opinion in Cell Biology* **23,** 569-578.

96. **Sachs, U. J. H., ndrei-Selmer, C. L., Maniar, A., Weiss, T., Paddock, C., Orlova, V. V., Choi, E. Y., Newman, P. J., Preissner, K. T., Chavakis, T. et al.** (2007). The Neutrophil-specific Antigen CD177 Is a Counter-receptor for Platelet Endothelial Cell Adhesion Molecule-1 (CD31). *Journal of Biological Chemistry* **282,** 23603-23612.

97. **Scheiermann, C., Colom, B., Meda, P., Patel, N. S. A., Voisin, M. B., Marrelli, A., Woodfin, A., Pitzalis, C., Thiemermann, C., urrand-Lions, M. et al.** (2009). Junctional adhesion molecule-C mediates leukocyte infiltration in response to ischemia reperfusion injury. *Arterioscler Thromb Vasc Biol* **29,** 1509-1515.

98. **Schenkel, A., Mamdouh, Z. and Muller, W. A.** (2004). Locomotion of monocytes on endothelium is a criticial step during extravasation. *Nature Immunol.* **5,** 393-400.

99. **Serhan, C. N., Brain, S. D., Buckley, C. D., Gilroy, D. W., Haslett, C., O'Neill, L. A. J., Perretti, M., Rossi, A. G. and Wallace, J. L.** (2007). Resolution of inflammation: state of the art, definitions and terms. *The FASEB Journal* **21,** 325-332.

100. **Serhan, C. N., Chiang, N. and Van Dyke, T. E.** (2008). Resolving inflammation: dual anti-inflammatory and pro-resolution lipid mediators. *Nat Rev Immunol* **8,** 349-361.

101. **Seth, R., Salcedo, R., Patarroyo, M. and Makgoba, M. W.** (1991). ICAM-2 peptides mediate lymphocyte adhesion by binding to CD11a/CD18 and CD49d/CD29 integrins. *FEBS Letters* **282,** 193-196.

102. **Shattil, S. J., Kim, C. and Ginsberg, M. H.** (2010). The final steps of integrin activation: the end game. *Nat Rev Mol Cell Biol* **11,** 288-300.

103. **Shulman, Z., Shinder, V., Klein, E., Grabovsky, V., Yeger, O., Geron, E., Montresor, A., Bolomini-Vittori, M., Feigelson, S. W., Kirchhausen, T. et al.** (2009). Lymphocyte crawling and transendothelial migration require chemokine triggering of high-affinity LFA-1 integrin. *Immunity* **30,** 384-396.

104. **Singh, S. K., Baar, V., Morbach, H. and Girschick, H. J.** (2006). Expression of ICAM-1, ICAM-2, NCAM-1 and VCAM-1 by human synovial cells exposed to Borrelia burgdorferi in vitro. *Rheumatol. Int.* **26,** 818-827.

105. **Somersalo, K., Carpren, O., Saksela, E., Gahmberg, C. G., Nortamo, P. and Timonen, T.** (1995). Activation of natural killer cell migration

by leukocyte integrin-binding peptide from intracellular adhesion molecule-2 (ICAM-2). *Journal of Biological Chemistry* **270,** 8629-8636.

106. **Staunton, D. E., Dustin, M. L. and Springer, T. A.** (1989). Functional cloning of ICAM-2, a cell adhesion ligand for LFA-1 homologous to ICAM-1. *Nature* **339,** 61-64.

107. **Steiner, O., Coisne, C., Cecchelli, R., Boscacci, R., Deutsch, U., Engelhardt, B. and Lyck, R.** (2010). Differential roles for endothelial ICAM-1, ICAM-2, and VCAM-1 in shear-resistant T cell arrest, polarization, and directed crawling on blood brain barrier endothelium. *J Immunol* **185,** 4846-4855.

108. **Sumagin, R. and Sarelius, I. H.** (2010). Intercellular adhesion molecule-1 enrichment near tricellular endothelial junctions is preferentially associated with leukocyte transmigration and signals for reorganization of these junctions to accommodate leukocyte passage. *J. Immunol.* **184,** 5242-5252.

109. **Sumagin, R., Prizant, H., Lomakina, E., Waugh, R. E. and Sarelius, I. H.** (2010). LFA-1 and Mac-1 define characteristically different intralumenal crawling and emigration patterns for monocytes and neutrophils in situ. *J Immunol* **185,** 7057-7066.

110. **Sundd, P., Gutierrez, E., Koltsova, E. K., Kuwano, Y., Fukuda, S., Pospieszalska, M. K., Groisman, A. and Ley, K.** (2012). `Slings' enable neutrophil rolling at high shear. *Nature* **488,** 399-403.

111. **Tanaka, H., Yashiro, M., Sunami, T., Sakate, Y., Kosaka, K. and Hirakawa, K.** (2004). ICAM-2 gene therapy for peritoneal dissemination of scirrhous gastric carcinoma. *Clinical Cancer Research* **10,** 4885-4892.

112. **Thompson, R. D., Noble, K. E., Larbi, K. Y., Dewar, A., Duncan, G. S., Mak, T. W. and Nourshargh, S.** (2001). Platelet-endothelial cell adhesion molecule-1 (PECAM-1)-deficient mice demonstrate a transient and cytokine-specific role for PECAM-1 in leukocyte migration through the perivascular basement membrane 7. *Blood* **97,** 1854-1860.

113. **Toivanen, A., Ihanus, E., Mattila, M., Lutz, H. U. and Gahmberg, C. G.** (2008). Importance of molecular studies on major blood groups intercellular adhesion molecule-4, a blood group antigen involved in multiple cellular interactions. *Biochimica et Biophysica Acta (BBA) - General Subjects* **1780,** 456-466.

114. **Vaporciyan, A. A., DeLisser, H. M., Yan, H. C., Mendiguren, Thom, Jones, M. L., Ward, P. A. and Albelda, S. M.** (1993). Involvement

of platelet-endothelial cell adhesion molecule-1 in neutrophil recruitment in vivo. *Science* **262,** 1580-1582.

115. **Voisin, M. B., Proebstl, D. and Nourshargh, S.** (2010). Venular basement membranes ubiquitously express matrix protein low expression regions: characterisation in multiple tissues and remodelling during inflammation. *Am. J. Pathol.* **176,** 482-495.

116. **Wakelin, M. W., Sanz, M. J., Dewar, A., Albelda, S. M., Larkin, S. W., Boughton-Smith, N., Williams, T. J. and Nourshargh, S.** (1996). An anti-platelet-endothelial cell adhesion molecule-1 antibody inhibits leukocyte extravasation from mesenteric microvessels in vivo by blocking the passage through the basement membrane. *The Journal of Experimental Medicine* **184,** 229-239.

117. **Weber, C., Fraemohs, L. and Dejana, E.** (2007). The role of junctional adhesion molecules in vascular inflammation
10. *Nat Rev Immunol* **7,** 467-477.

118. **Wethmar, K., Helmus, Y., Luhn, K., Jones, C., Laskowska, A., Varga, G., Grabbe, S., Lyck, R., Engelhardt, B., Bixel, M. G. et al.** (2006). Migration of immature mouse DC across resting endothelium is mediated by ICAM-2 but independent of beta2-integrins and murine DC-SIGN homologues. *Eur. J. Immunol.* **36,** 2781-2794.

119. **Woodfin, A., Voisin, M. B., Beyrau, M., Colom, B., Caille, D., Diapouli, F. M., Nash, G. B., Chavakis, T., Albelda, S. M., Rainger, G. E. et al.** (2011). The junctional adhesion molecule JAM-C regulates polarized transendothelial migration of neutrophils in vivo. *Nat Immunol* **12,** 761-769.

120. **Woodfin, A., Voisin, M. B., Imhof, B. A., Dejana, E., Engelhardt, B. and Nourshargh, S.** (2009). Endothelial cell activation leads to neutrophil transmigration as supported by the sequential roles of ICAM-2, JAM-A, and PECAM-1. *Blood* **113,** 6246-6257.

121. **Woodfin, A., Voisin, M. B. and Nourshargh, S.** (2007). PECAM-1: A multi-functional molecule in inflammation and vascular biology. *Arterioscler Thromb Vasc Biol* **27,** 2514-2523.

122. **Xie, J., Li, R., Kotovuori, P., Vermot-Desroches, C., Wijdenes, J., Arnaout, M. A., Nortamo, P. and Gahmberg, C. G.** (1995). Intercellular adhesion molecule-2 (CD102) binds to the leukocyte integrin CD11b/CD18 through the A domain. *J Immunol* **155,** 3619-3628.

123. **Yonemura, S., Hirao, M., Doi, Y., Takahashi, N., Kondo, T., Tsukita, S. and Tsukita, S.** (1998). Ezrin/Radixin/Moesin (ERM) proteins bind to a positively charged amino acid cluster in the juxta-membrane

cytoplasmic domain of CD44, CD43, and ICAM-2. *The Journal of Cell Biology* **140,** 885-895.

124. **Zarbock, A. and Ley, K.** (2008). Mechanisms and Consequences of Neutrophil Interaction with the Endothelium. *Am J Pathol* **172,** 1-7.

125. **Zarbock, A., Ley, K., McEver, R. P. and Hidalgo, A.** (2011). Leukocyte ligands for endothelial selectins: specialized glycoconjugates that mediate rolling and signaling under flow. *Blood* **118,** 6743-6751.